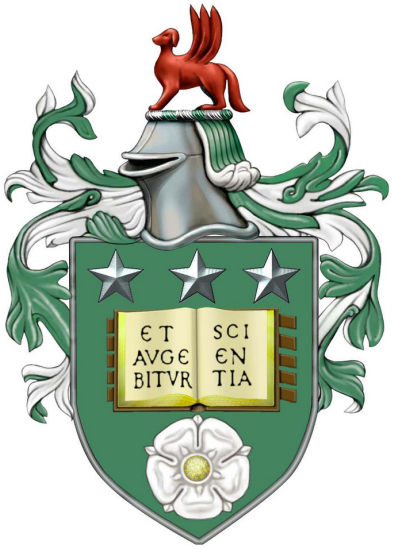


# Proteomic Investigation of the Cellular Interactors of $\alpha$-Synuclein Fibrils

by

Michael James Davies

Astbury Centre for Structural Molecular Biology

Submitted in accordance with the requirements for the degree of Doctor of Philosophy

March 2021

# Declaration of Authorship

The candidate confirms that the work submitted is her own and that appropriate credit has been given where reference has been made to the work of others.

# *Acknowledgements*

I would like to thank my supervisors Dr. Eric Hewitt and Prof. Sheena Radford without whom this work would not have been possible. Your unwavering support, especially over what has been a difficult final year, means a great deal to me. Thanks also go to my funders; BBSRC White Rose and the University of Leeds and to all members of the Radford and Hewitt labs who have helped me along the way. In particular, a great deal of thanks is owed to Nasir, the lynch pin of the Radford lab. I'm incredibly grateful to you for all the help you have given me over the last four years, not to mention the ever present supply of biscuits and seemingly unquenchable enthusiasm. You have made completing this PhD far more enjoyable than it would otherwise have been.

I'd also like to thank several other members of the Radford lab who have provided endless advice, support, and a significant quantity of tea. Thanks are due in particular to Dr. Matt Jackson for all the help he gave me in the lab, you always believed I could do it. I'm also very grateful to Dr. Lucy Barber for all those cups of teas, and those long, work related, chats, and to Romany Mclure for all those times you encouraged me to study rather than go out drinking or stealing cats.

Thanks also to my family for all your support in everything that has lead up to this. Mother, you've always been there to help me through the tough times with a hug and a discussion of a problematic nature; and Dad, I've got to say, words of encouragement #157 really got me through this, although #89 definitely deserves an honorable mention. Dan and Hal, let's be honest you didn't do jack, but etiquette demands that I mention you here, so here you go – enjoy.

Finally I'd like to thank Sammy for all her love and silliness not to mention averting my death by scurvy. Without you and your wonderful methods keeping me sane, this thesis wouldn't have been written.

*The time has come,' the Walrus said,*
*To speak of many things:*
*Of shoes – and ships – and sealing wax –*
*Of cabbages – and kings –*
*And why the sea is boiling hot –*
*And whether pigs have wings.'*

**Lewis Carroll**

# *Abstract*

$\alpha$-Synuclein is an intrinsically disordered protein that is commonly expressed in neuronal cells where it is thought to play a role in neurotransmitter recycling. Aggregation of $\alpha$-synuclein into amyloid fibrils has been linked to the development of a number of neurodegenerative diseases including Parkinson's disease and dementia with Lewy bodies. Transmission of $\alpha$-synuclein fibrils between neurons has been linked to the progression of $\alpha$-synuclein associated diseases. Moreover, exposure of cells to $\alpha$-synuclein fibrils has been shown to induce cellular dysfunction and ultimately cell death following internalisation. Therefore, in order to better understand the mechanisms by which $\alpha$-synuclein fibrils disrupt cellular function, the identity of the protein interactors of $\alpha$-synuclein fibrils, following cellular internalisation, is of considerable interest.

Herein, a system was developed by which $\alpha$-synuclein fibrils can be assembled from recombinant monomer, internalised by a neuronal-like cell line, and isolated – both following internalisation and from cell lysate – using a magnetic biotin-streptavidin isolation system. Proteins that co-isolated with $\alpha$-synuclein fibrils were then identified and separated from background binding proteins by quantitative mass spectrometry, to define the $\alpha$-synuclein fibril interactome. Cellular pathways as well as protein complexes that were overrepresented in the $\alpha$-synuclein fibril interactome were then characterised by a variety of bioinformatic techniques.

By this method a number of pathways were identified that may link $\alpha$-synuclein fibril internalisation to cellular dysfunction. These included interference with the nucleo-cytoplasmic transport machinery, sequestration of translational proteins including entire ribosomal complexes, disruption of the cellular trafficking – particularly of the endoplasmic reticulum to the Golgi – and potentially inducing mitochondrial dysfunction. This work demonstrates the application of unbiased proteomic study to the characterisation of an $\alpha$-synuclein fibril interactome, and highlights a number of avenues for future research.

# CONTENTS

# LIST OF FIGURES

# ABBREVIATIONS

| | |
|---|---|
| **Aβ** | amyloid-β. |
| **AFM** | atomic force microscopy. |
| **ALS** | amyotrophic lateral sclerosis. |
| **AMP** | antimicrobial peptides. |
| **APP** | amyloid precursor protein. |
| **ATF6** | activating transcription factor 6. |
| **ATP** | adenosine triphosphate. |
| | |
| **BAP** | biofilm associated protein. |
| **BCA** | bicinchoninic acid. |
| **$\beta_2$M** | $\beta_2$-microglobulin. |
| **BSA** | bovine serum albumin. |
| | |
| **CD** | circular dichroism. |
| **CID** | collision-induced dissociation. |
| **CMA** | chaperone mediated autophagy. |
| | |
| **DLB** | dementia with Lewy bodies. |
| **DNA** | deoxyribonucleic acid. |
| **DTT** | dithiothreitol. |
| | |
| ***E.coli*** | *Escherichia coli*. |
| **eEF** | eukaryotic elongation factor. |
| **eEF2K** | eukaryotic elongation factor (eEF)2 kinase. |
| **eIF** | eukaryotic initiation factor. |
| **4E-BP1** | eukaryotic initiation factor (eIF)4E binding protein. |
| **EM** | electron microscopy. |
| **ER** | endoplasmic reticulum. |
| **ERAD** | endoplasmic reticulum (ER)-associated degradation. |

**ESI** electrospray ionisation.

**FAP** functional amyloid in pseudomonas.
**FBS** foetal bovine serum.
**FDR** false discovery rate.
**FTD** frontotemporal dementia disease spectrum.
**FTIR** Fourier transform infra-red.

**GAG** glycosaminoglycan.
**GDP** guanosine diphosphate.
**GFP** green flourescent protein.
**GO** gene ontology.
**GTP** guanosine triphosphate.

**HFIP** hexafluoro-2-propanol.
**HRP** horseradish peroxidase.
**HSC** heat shock cognate.
**HSP** heat shock protein.

**IAPP** islet amyloid polypeptide.
**IPOD** insoluble protein deposit.
**IPTG** isopropyl β-D-1-thiogalactopyranoside.
**IRE1** inositol-requireing enzyme 1.
**iTRAQ** isobaric tag for relative and absolute quantification.

**JUNQ** juxtanuclear quality control.

**KEGG** kyoto encyclopedia of genes and genomes.

**LAG3** leukocyte activation gene 3.
**LAMP1** lysosomal-associated membrane protein 1.
**LAMP2** lysosomal-associated membrane protein 2.
**LB** Lewy body.
**LC** liquid chromatography.
**LCR** low complexity region.

**MALDI** matrix-assisted laser desorption ionization.
**MCL** Markov clustering.
**MLKL** mixed-lineage kinase domain-like.

**MS** mass spectrometry.
**MW** molecular weight.

**NAC** non-amyloid component.
**NADH** reduced nicotinamide adenine dinucleotide (NAD).
**NHS** N-hydroxysuccinimide.
**NMR** nuclear magnetic resonance.

**PBS** phosphate buffered saline.
**PERK** protein kinase RNA (PKR)-like endoplasmic reticulum (ER) kinase.

**RIPK** receptor serine/threonine protein kinase.
**RNA** ribonucleic acid.
**ROS** reactive oxygen species.

**SDS** sodium dodecyl sulfate.
**SDS-PAGE** sodium dodecyl sulfate (SDS) - polyacrylamide gel electrophoresis (PAGE).
**SEC** size exclusion chromatography.
**SEM** standard error of the mean.
**SILAC** stable isotope labelling by amino acids in cell culture.

**TAMRA** 5-carboxytetramethylrhodamine.
**TAP** tandem affinity purification.
**TEMED** tetramethylethylenediamine.
**THOC** Tho complex subunit.
**ThT** thioflavin T.
**TMT** tandem mass tagging.
**TNT** tunnelling nanotubes.
**TOMM** translocase of outer mitochondrial membrane.

**UPR** unfolded protein response.
**UV** ultra violet.

**VDAC1** voltage-dependent anion-selective channel.

**WT** wild type.

# 1

# Introduction

## 1.1 Amyloid: A Historical Perspective

Amyloid is a term classically used to refer to abnormal fibrous, extracellular structures formed of proteins or peptides. It was coined in the mid 19th century by Rudolph Virchow to describe a tissue abnormality in the cerebral *corpora amylacea*, that exhibited positive iodine staining [1]. The macroscopic description of the cerebral abnormality was similar to an abnormality previously described in the liver and spleen. Due to the blue staining upon the addition of iodine and subsequent violet staining when treated with sulfuric acid, Virchow concluded that the deposit consisted of starch, and derived the term amyloid from the latin term for the same [1].

However, shortly thereafter it was shown by Friedreich and Kekulé [2] that amyloid deposits in the liver predominantly contained protein. Furthermore the study showed limited presence of detectable carbohydrate associated with the deposits [2], switching the focus of future studies of amyloid deposits from carbohydrate to protein. Later investigations into the tinctorial properties of these deposits further revealed specific binding to the birefringent dye Congo Red, producing an "apple green" birefringence under a polarising light microscope [3], a finding that indicated the presence of a highly ordered subunit structure [4, 5]. Later transmission electron micrographs demonstrated that the inclusions contained fibril like protein structures [6] while studies using X-Ray fibre diffraction technology revealed a 4.7 Å cross-β repeating

feature down the fibril axis [5, 7, 8](Fig. 1.1), establishing a structural footprint for amyloid. At the same time, the identification of an amyloid prone protein in several disease related plaques including amyloid A [9], antibody light-chains [10] and transthyretin [11], demonstrated that amyloid fibrils could be formed by a number of protein precursors.

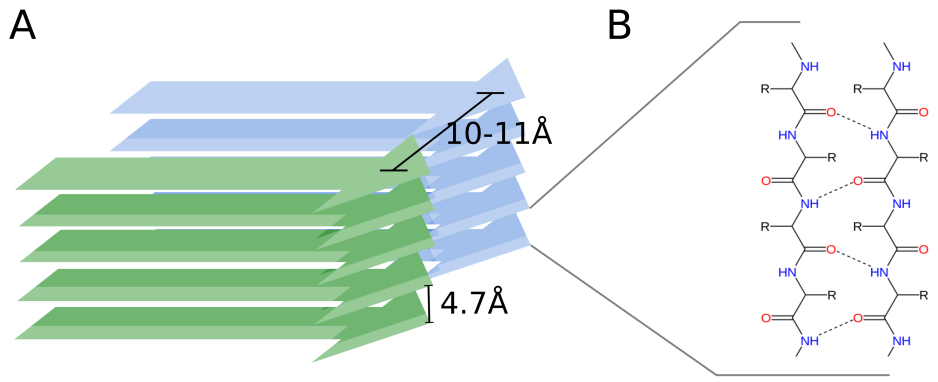


***Figure 1.1:*** *Arrangement of cross β fibril structure. A) representation of parallel cross-β sheet structure, in which the N and C terminals of strands within a β sheet are aligned. In each sheet cross-β strands are aligned perpendicular to the fibril axis, stabilised by hydrogen bonds with a spacing of* 4.7 Å*. Cross-β sheets associate with an inter-sheet distance of 10-*11 Å*. B) Hydrogen bonds that stabilise the cross-β structure of the β-sheet, in a parallel cross-β structure.*

Since the identification of the cross-β structure of amyloid fibres a cornucopia of techniques have been leveraged to investigate the amyloid fold [5] including: (i) X-ray fibre diffraction, often used as an orthoginal validation technique in which simulated diffraction patterns are compared with experimental data [12]; (ii) X-ray crystallography and micro-electron diffraction of microcrystals, especially useful for determining the structure of small amyloidogenic peptides [13–15]; (iii) solid state nuclear magnetic resonance (NMR), capable of determining the dihedral angles and inter-atomic distances between the fibril subunits, facilitating the building of atomic models based on these constraints [16–19]; and (iv) cryo-electron microscopy (EM), a technology that has been in use for decades but has only recently become able to resolve fibrils at atomic detail [20, 21], an advancement that represents a step change in the field of structural biology. Utilising these techniques it has been possible to identify how individual protein subunits can form the stereotypical cross-β structure.

## 1.2 Formation of Amyloid

The formation of the amyloid fibril from the diverse protein subunits is an ongoing field of discovery, and there is keen interest in understanding the molecular mechanisms by which this can occur, since discoveries in made here may shine a light on a potential treatment for one or more amyloid related diseases [5, 22]. In order to understand how a wide variety of protein subunits with highly divergent amino acid sequences can self assemble into the highly-ordered cross-β structure stereotypical of amyloid fibres, it is important to understand the manner by which these proteins can adopt different structures as well as what can induce them to undergo structural changes [22, 23]. Furthermore, it is important to understand how unwanted amyloid formation is prevented in a physiological system thereby preventing the development of an amyloid related disease.

### 1.2.1 Assembly of Amyloid Fibrils

Protein function depends upon its three dimensional structure which in turn depends upon protein folding. An early hypothesis for protein folding suggested that all the information required for a protein to reach its native fold was encoded in its amino acid sequence [24] and involved a systematic search of all possible conformations. However, it was soon realised that this could not occur in a physiologically relevant time scale [25, 26] a problem that became known as the Levinthal paradox [25, 26].

Further studies have, however, provided a resolution for this paradox. It has demonstrated that *in vitro* protein folding occurs by a stochastic search of the conformations available to the polypeptide chain, eventually arriving at a thermodynamically stable conformer [27]. The protein then begins a search of the conformations available to this conformer. Since it is unfavorable for a protein to move away from a stable state to an unfolded state, folding progresses in a fashion that can be described conceptually as a folding tunnel Fig. 1.2. It can be envisioned as the protein "falling" down the energy landscape, moving from one stable conformer to another conformer with greater stability [25].

Amyloid proteins are proteins that can fold to adopt β-sheet rich, oligomeric and fibrillar conformers [27]. Many biologically active proteins such as curli (a major extra-cellular matrix protein produced by many *Enterobacteriaceae* [28]) adopt these conformations physiologically. However for other proteins this conformation represents the occurrence of a misfolding event. In such proteins, the native state of a protein is not the most thermodynamically stable conformer, rather it remains in this state due to an energy barrier preventing it from adopting the more stable conformation. Misfolding events can allow the protein to overcome this barrier to

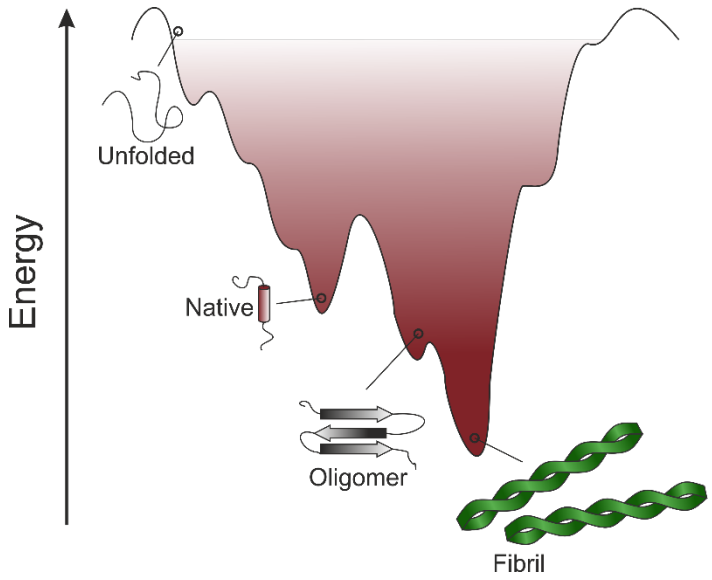


***Figure 1.2:*** *Energy landscape scheme of protein folding and aggregation showing the movement of the unfolded protein at the high energy state through lower energy states to the native conformation and the energy barrier that separates the native conformation from the lower energy oligomeric and fibrillar conformations.*

adopt oligomeric and fibrillar structures [27]. Many *in vivo* proteins require the assistance of molecular chaperones to reach their native conformation and the failure of this process can lead to a number of amyloid related diseases. Other amyloidogenic proteins such as $\beta_2$-microglobulin ($\beta_2$M), can become unfolded and aggregation prone following dissociation from a folded protein complex.

Amyloid consists of straight, unbranching peptide fibrils. Aggregation of proteins to an amyloid fibril occurs broadly in two stages, the first is nucleation where misfolded protein monomers reversibly bind to one and other to form β-sheet rich oligomeric species [29]. In a simplified kinetic model, this oligomeric core eventually reaches a critical mass at which time monomers begin to bind irreversibly [30], leading to the formation of amyloid fibrils (Fig. 1.3). Each amyloid related disease predominantly involves the aggregation of a specific protein, although many other components can be found incorporated into the in vivo deposits. Although the soluble species of the many amyloidogenic proteins can be very disparate in structure, amyloid fibrils have many common characteristics regardless of their protein backbone [31]. Through the use of X-ray diffraction it was demonstrated that amyloid fibrils are composed of polypeptide chains stacked in cross- β conformation, running perpendicular to the fibril axis. The core structure of the fibril is stabilised primarily by interactions of the peptide main chain, explaining the similarity of fibril structures arising from proteins with very different amino acid sequences.

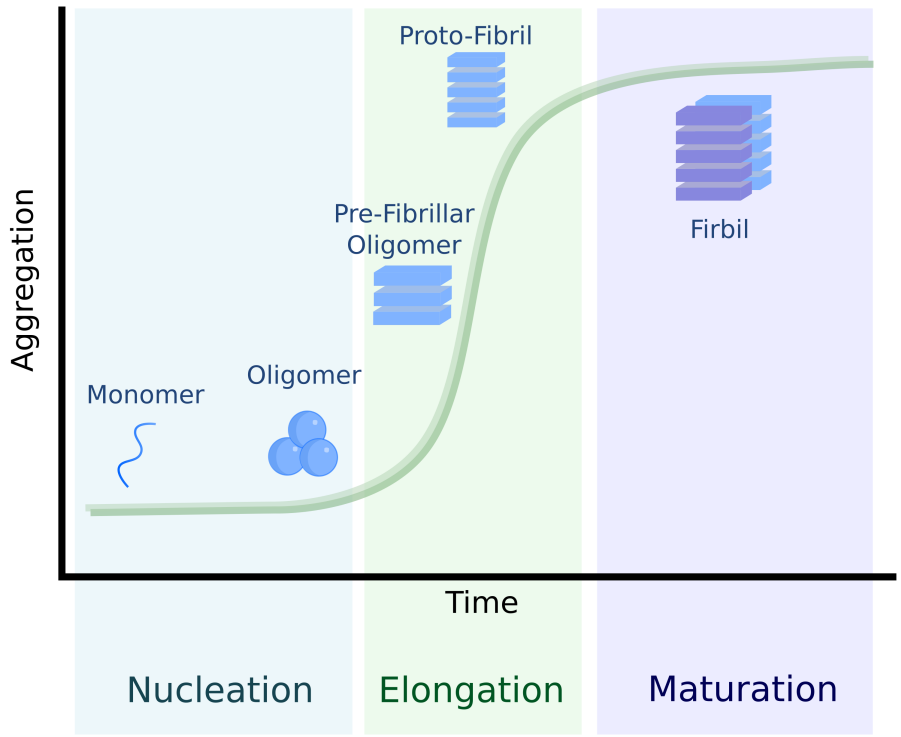


***Figure 1.3:*** *Fibril growth curve illustrating kinetics of amyloid formation. Monomeric subunits first misfold to form an oligomeric conformation that then undergoes a conformational shift to an elongation competent prefibrillar nucleus. The time taken to reach this nucleus is known as the lag phase. Elongation of the nucleus then occurs by monomer addition onto the fibril. Finally the proto-fibrillar amyloid associates with another proto-fibril during a process known as fibril maturation.*

## 1.3 Functional Amyloid

Although amyloid formation is typically associated with misfolding and disease, there is a growing body of evidence identifying several cases of beneficial amyloid or amyloid-like proteins. In 2000 the term "functional amyloid" was coined to describe such proteins and distinguish them from their pathogenic cousins [32]. These functional amyloids utilise the intrinsic properties of a key structural element of amyloid proteins, the cross-β fold, to facilitate important cellular tasks [33–36]. The thermodynamically stable structure of the amyloid fibril facilitates their use as cellular scaffolds while their compact size lends them to use as protein storage systems [37–41]. Indeed, the diversity of uses of this structure, shown to have functions in both eukaryotic and prokaryotic organisms [34, 41], suggests that the functional amyloid may represent an essential protein folding state.

The presence of functional amyloid in bacteria is widespread, and was the initial focus of functional amyloid studies [36]. Since then, functional amyloids have been identified in both Gram negative and Gram positive bacteria with roles ranging from survival to increased pathogenicity [42]. An early example of a bacterial functional amyloid was the discovery of their importance to the structural congruency of a bacterial biofilm [36]; a form of bacterial community in which bacteria are contained within an extracellular matrix of proteins, saccharides and other organic molecules [43].

These structural amyloids of the bacterial biofilm include the curli family of proteins [36, 44], known to be essential for the formation of the effective formation of biofilms in a large number of bacteria [28]. Curli proteins act as a scaffold within the extracellular matrix, for which the stability conferred by the β-sheet nature of amyloid fibrils is of significant benefit. It was shown that curli proteins form amyloid fibrils within this matrix via a highly regulated process, in order to avoid toxic, off-pathway effects [36]. The formation of curli occurs through the regulated aggregation of the protein CsgA into β-sheet rich fibrils, based on the nucleation capabilities of the protein CsgB, which remains anchored to the bacterial outer membrane and serves as a seed for CsgA aggregation [45]. In addition to curli, many other amyloid proteins have been shown to form important structural components of various bacterial biofilms including: functional amyloid in pseudomonas (FAP) [46], enabling the adhesion of *Pseudomonas* colonies to surfaces; TasA from Bacillus [47], involved in cell-to-cell adhesion as well as spore dispersal and motility [48]; and biofilm associated protein (BAP)s from Staphylococcus [49], crucial in Staphylococcal infectivity.

Other functions performed by functional bacterial amyloids include protein storage and anti-toxic functions [50], pathogenic activity [51, 52], and cell defence through

host-cell lysis [53, 54]. For example, the bacterial toxin microcin E492, produced by the *Klebsiella pneumoniae* bacteria, is reversibly sequestered into non-toxic amyloid fibrils [50]. This fibre can then dissociate under certain environmental conditions, including changes in pH [55], releasing a pore-forming oligomeric conformer of the protein capable of killing other competing Enterobacteria [55]. Conversely, the phenol-soluble modulins of *Staphylococcus aureus*, rely on an amyloid-like structure to induce toxicity in human T-cells [54].

The first evidence of functional amyloid in humans came in 2006 [34] with the discovery of amyloid-like, thioflavin T (ThT) positive, fibrils of the Pmel17 protein forming within melanin synthesis and storage organelles, known as melanosomes [34]. It was shown that the purpose of these structures was the sequestration of toxic biosynthetic intermediates, produced during the synthesis of melanin [34]. This discovery was soon followed by evidence of a heteromeric amyloid signalling complex comprised of receptor serine/threonine protein kinase (RIPK)-1 and RIPK-3, identified as a key component of a inflammation-driven programmed cell-death pathway, necroptosis [56, 57]. This occurs through the amyloidogenic co-assembly of RIPK subunits into necrosome signalling complex [58], the necrosome then recruits and phosphorylates mixed-lineage kinase domain-like (MLKL) a downstream effector in necroptosis [58].

Another method by which functional amyloids modulate human cell function can be seen in amyloid-bodies, which, in cells subject to external stressors, act as storage units for proteins [37]. Stressors capable of inducing the formation of amyloid bodies in the nucleus include heat shock and acidosis [37] which can induce multiple proteins (>180), including those involved cell cycle progression and deoxyribonucleic acid (DNA) synthesis, to assemble into amyloid-bodies, resulting in the cell entering a "dormant" state [37]. Within these amyloid bodies proteins can be found sequestered as fibrils that exhibit a cross-β X-ray fibre diffraction pattern characteristic of amyloid fibrils [37]. In a similar manner to that seen in bacterial examples of sequestration via amyloid fibril formation [50], this aggregation is reversible and monomeric protein is released following the removal of the stressor [37].

Similarly, several peptide hormones have been shown to be stored intracellularly as amyloid fibrils, within the acidic environment of endocrine secretory granules [38]. However, this aggregation is pH dependent, with the amyloid fibre dissociating into monomeric peptides upon the release of the secretory granule into the pH neutral environment of the extracellular matrix [38].

Furthermore, functional amyloids have potentially been identified in the innate immune response to infection. Antimicrobial peptides (AMP)s are key effector proteins in the innate immune response to microbial infection, functioning to induce cell death in invading microorganisms through channel forming mechanisms [59, 60].

It has been demonstrated that AMP peptides exhibit a cross-β structure similar to that seen in amyloid fibrils [61]. Furthermore, generic amyloidogenic peptides containing β-sheet rich regions will form channels in lipid bilayers [62, 63] while the AMPs LL-37 and protegrin-1 have been shown to be capable of assembly into amyloid-like fibrils [64, 65], data that together is suggestive of a functional amyloid.

In cases of functional amyloids, there must be stringent controls on fibril assembly and localisation in order to prevent amyloid formation from becoming toxic. Indeed several functional amyloids have been shown to display toxic side effects when mislocalised or fibril assembly is perturbed [38, 66–68]. Interestingly, the archetypal amyloid protein, amyloid-β (Aβ) (linked to the development of the neurodegenerative disease Alzheimer's disease), may be a functional amyloid itself, functioning as an AMP to target pathogenic bacteria and fungi [69, 70] with amyloid aggregation of Aβ central to its anti-microbial function [69–71].

Cells utilising functional amyloids may prevent off target toxicity through a variety of mechanisms including: regulating the level of amyloidogenic proteins in the cell [72, 73]; minimising the levels of potentially toxic [74–76] pre-fibrillar oligomers [34, 72]; sequestering amyloid assembly reactions within membrane bounded compartments [34, 38, 72]; only inducing amyloid formation as required, via molecules that induce the formation of amyloid fibrils by otherwise stable proteins/peptides [37, 38, 72]. In cases where unwanted amyloid formation occurs the deleterious side effects seen in classical amyloid diseases can be found.

## 1.4 Disease Related Amyloid

From the first discovery of what came to be termed amyloid there was a close association with disease, with Virchow's discovery being made in a patient autopsy sample [1]. One of the early diseases to be associated with the presence of amyloid plaques, and the disease perhaps the disease most commonly associated with amyloid pathology was Alzheimer's disease. This disease was first documented by Alois Alzheimer in 1906 [77], where it was demonstrated that the post-mortem plaques of the afflicted patient exhibited iodine staining, classically associated with amyloid fibres. Since that time over 50 proteins or peptides all with dissimilar primary amino acid sequences, have been shown to assemble into amyloid fibrils that are associated with one or more human diseases [5, 78].

These diseases straddle many medical fields, from neurodegenerative disorders, such as the aforementioned Alzheimer's disease involving the amyloid proteins Aβ [79] and tau [80], Parkinson's disease linked to the amyloid protein $\alpha$-synuclein [81] and Huntington's Disease (amyloid protein huntingtin [82]), to disorders affecting the pancreas such as the Type-II diabetes typified by islet amyloid polypeptide (IAPP) aggregation in the Islets of Langerhans [83]; and disorders of the kidney and heart resulting from antibody light chain deposition [84], to name but a few. Amyloid proteins also play a role in treatment related illnesses such as with dialysis related amyloidosis, caused by the accumulation of aggregated $\beta_2$M in osteo-articular tissues [85].

Moreover, it has been noted that there exists a degree of cross-talk between amyloid fibrils and their associated diseases, a good example being the presence of amyloid protein $\alpha$-synuclein found in Alzheimer's disease patients [86]. In Parkinson's disease and other related conditions such as dementia with Lewy bodies (DLB), $\alpha$-synuclein and tau inclusions have been identified in the same cell and even co-locate to the same inclusion body [87]. Similarly in familial Danish dementia, co-localisation of Aβ and another amyloidogenic peptide Dan-amyloid has been described [88]. These data have been further substantiated with in vitro evidence demonstrating the ability of Aβ and IAPP to interact with one and other, co-aggregating into hybrid amyloid fibrils [89]. This extends to the diseases themselves with patients suffering from IAPP associated type-II diabetes are at significantly higher risk of developing Alzheimer's disease [90].

Although it is not altogether clear what drives the onset of amyloid disease, it has been noted that in many cases age is a factor, and many of the most common amyloid diseases involve the aggregation of physiological proteins [91]. In rarer cases a mutation in the wild-type protein can increase the aggregation propensity of the precursor [92–94] thereby increasing the likelihood of amyloid deposition.

In other cases an increase in concentration of the wild-type amyloidogenic protein through gene multiplication is sufficient cause the onset of an amyloidogenic disease [95, 96]. In these rarer genetic cases the age of disease onset is often significantly lower, and the progression of the disease faster, than in cases involving the wild-type protein. However, in some cases of sporadic amyloid disease, the causative factor may be similar to the widespread increase in concentration seen in cases of gene multiplication. Spatially limited increases in concentration, driven by liquid phase separation [97], are capable of inducing aggregation in the amyloidogenic tau protein [98].

In some instances of amyloidogenic disease, the development of the amyloid-associated disease is reliant on the expansion of an amino acid sequence in the amyloid precursor protein [82]. This sequence, often one prone to aggregation, increases the aggregation propensity of the amyloid protein, such as is the case in tri-nucleotide repeat diseases [99]. These diseases include poly-glutamine (poly-Q) associated diseases such as Huntington's disease, in which a poly-Q repeat sequence is expanded within the huntingtin protein [82, 100], as well as poly-alanine (polyA) expansions in polyadenylate-binding protein 2 (PABPN1) [101] associated with oculopharyngeal muscular dystrophy [102].

In other cases, the onset of amyloid aggregation and progression into a disease state may be the result of an increased level of amyloidogenic sequences through a disruption to post translational processing. In Alzheimer's disease, for example, two paths exist for the cleavage of amyloid precursor protein (APP) : under normal conditions most APP is cleaved by $\alpha$ secretase, releasing non-amyloidogenic peptides, under disease conditions however, cleavage by $\gamma$ secretase is elevated, releasing the amyloidogenic peptide Aβ[103]. Increases in the amyloidogenic protein Aβ have been proposed as a possible mechanism for disease development [103]. Furthermore, there is evidence that even minor modifications in a protein's primary sequence, such as truncation, can dramatically alter amyloidogenicity: for example, an increased ratio of Aβ40 to Aβ42 is associated with a greatly reduced the risk of Alzheimer's disease [104], while shortening of the amyloidogenic apolipoprotein A1 greatly increases the risk of systemic amyloidosis [105].

### 1.4.1 Maintaining Protein Homeostasis

Under normal conditions cells have a multiplicity of mechanisms at their disposal to prevent the unwanted aggregation of endogenous proteins, and deposition of fibrils in amyloid plaques or inclusions [106]. This cellular quality control system responsible for maintaining cellular protein homeostasis involves coordinating several pathways, including protein biogenesis, folding, trafficking and degradation. Failure of any one

of these processes can lead to runaway accumulation and misfolding of endogenous protein [106].

### 1.4.2 Molecular Chaperones

One mechanism used to manage the risk of protein misfolding is the molecular chaperone; a protein that stabilises or assists in the proper folding of another protein in a catalytic manner [107]. One key group of molecular chaperones is the family of heat shock protein (HSP)s, named as such for their upregulation during cellular stress [107, 108]. These proteins are responsible for folding newly synthesised and misfolded proteins [109] as well as the trans-membrane transport of proteins [110] and performing protein degradation functions, targeting non-repairable proteins to the ubiquitin proteasomal pathway [108, 111]. Classically molecular chaperones prevent self-association and aggregation by binding exposed hydrophobic regions of the target protein [112].

Molecular chaperones are closely entwined with amyloid diseases, with several members of the HSP family of chaperones capable of suppressing the aggregation [113] and reducing the cellular toxicity of poly-glutamine amyloid [114]. Likewise HSP-70 can prevent $\alpha$-synuclein induced toxicity in a model system of disease by binding aggregation intermediates [115–118]. Molecular chaperones have also been shown to play a role in preventing the development of Alzheimer's disease, where activation of the HSP chaperone system significantly reduced the levels of soluble Aβ while multiple HSPs [119] alleviate tau toxicity when overexpressed in cells [120].

In transgenic mice it has been demonstrated that the upregulation of HSP70, a major protein in the HSP chaperone network, reduces the aggregation load and significantly improves survival [116, 121]. HSP70 achieves this by co-operating with a co-chaperone that transfers misfolding proteins to HSP70 [122]. When incubated *in vitro* with amyloidogenic peptides, HSP70 can prevent the formation of oligomeric intermediates [123]. As such chaperones appear to be most effective when introduced during the lag phase of amyloid fibril aggregation [124] and are thus focused on preventing aggregation before it occurs.

However, in addition to this primary function, molecular chaperones have also been shown to possess a degree of disaggregase activity, and have been shown to be capable of disassembling a number of amyloid aggregates. Several HSP proteins including HSP-110, HSP-40 and HSP-70 have been shown to cooperate in metazoan cells, to rapidly and effectively disassemble amorphous misfolded protein aggregates and return them to an active state [125–127], while the same system can exploit slow monomer exchange dynamics of amyloid fibrils to gradually depolymerise ordered amyloid aggregates [125, 126, 128]. Furthermore, a trimeric chaperone complex of

HSP-110, HSP-70 and J-protein, another class of molecular chaperones, has been shown capable of complete depolymerisation of huntingtin fibrils [129] and $\alpha$-synuclein fibrils in an adenosine triphosphate (ATP) dependent manner.

Indeed, though there is no direct ortholog in metazoan cells, yeast cells can leverage the HSP104 protein that has been shown to effectively disassemble a number of amyloid fibrils [130–133]. To disaggregate amyloid fibrils, the hexameric subunits of HSP104 cooperatively engage the substrate, and in an ATP dependent manner disaggregate the amyloid fibril by threading through a central pore [134, 135]

It is therefore clear that chaperones play an important role in preventing amyloid deposition both by attenuating initial aggregation, and potentially by aiding in the depolymerisation of mature aggregates.

### 1.4.3 Unfolded Protein Response

The unfolded protein response (UPR) is a system that operates in the endoplasmic reticulum (ER) that is induced during periods of cellular and ER stress. By reducing repressing translation, the UPR attempts to reduce the unfolded protein load on the cell [136, 137]. Stressors that can induce the activation of the UPR include, among others, amino acid deprivation, viral replication, and the presence of unfolded proteins. In order to rectify these stressors the UPR upregulates molecular chaperones [138], transcription and translation is down-regulated [139] and ER-associated degradation (ERAD) increased [140] to accelerate clearance of slowly folding or misfolded proteins. Should the cell be unable to resolve the protein-folding defect, the UPR is capable of triggering the cell-death signalling pathways [136, 137].

The UPR can be activated from three major kinases acting as sensors for the UPR. These kinases are: protein kinase ribonucleic acid (RNA) (PKR)-like ER kinase (PERK), inositol-requireing enzyme 1 (IRE1) and activating transcription factor 6 (ATF6) [141]. In cases of amyloid related diseases activation of many of these UPR sensors has been demonstrated [142]. In tissue samples of Alzheimer's disease patients an increase in phosphorylated PERK which associated with hyperphosphorylated tau protein, indicative of fibrillar tau tangles [142, 143]. Likewise phosphorylated PERK has been identified in Parkinson's disease and multiple system atrophy tissue samples where it associates with $\alpha$-synuclein [144], while in Huntington's disease increased levels of phosphorylated IRE1 were detected [145]. These data suggest that the UPR plays a role in attempting to prevent amyloid aggregation.

### 1.4.4 Compartmentalisation

Another mechanism by which the cell can prevent the unwanted aggregation of amyloidogenic proteins is the sequestration of misfolded proteins into distinct control

compartments. Such compartments can act as storage facilities until such time as the protein can be refolded or degraded as appropriate. Several such compartmentalisation mechanisms exist: insoluble proteins may be sequestered near the periphery of the cell in structures known as insoluble protein deposit (IPOD)s [146], whereas misfolded but soluble proteins accumulate in a juxtanuclear quality control (JUNQ) compartment [146] for degradation, or into an ER-anchored Q-body [147]. Insoluble proteins may also be sequestered into compartments known as aggresomes should the proteasome be impaired [148].

The JUNQ and Q-bodies contain chaperones and clearance factors, facilitating a more efficient processing of misfolded proteins [146], while the IPOD and aggresomes contain disaggregases and autophagy related proteins to protect the cell from toxic misfolded species [146]. It is noteworthy that poly-Q expanded huntingtin and prion protein intermediaries and aggregates are directed to and accumulate within IPODs [146, 149] where they await further degradation by downstream pathways. Furthermore, when poly-Q expanded huntingtin is expressed in tissues, aggresome formation can be observed [150]. These aggresomes appear to be protective to the cells they appear in with such cells still capable of undergoing mitosis [150].

### 1.4.5 Protein Degradation

Finally, should it not be possible to recover the misfolded protein to an active state the cell has several protein degradation pathways available [151]. The first is the ubiquitin proteasome system which is called on for the removal of soluble misfolded proteins. The system is dependent on a cascade of three enzyme ligases that conjugate the protein ubiquitin to the misfolded protein. The ubiquitinated protein can then be identified by chaperones and transported to the proteolytic system, where it is unfolded and cleaved into shorter peptides [152].

The second pathway available to the cell for protein degradation is chaperone mediated autophagy (CMA). CMA target and degrade proteins expressing a KFERQ-like motif recognised by the chaperone heat shock cognate (HSC) 70, a constitutively expressed variant of HSP70. HSC70 delivers matching proteins to the lysosome for degradation by lysosomal hydrolases [153, 154].

Should misfolded or aggregated proteins avoid degradation by the first two pathways they are subject to macroautophagy. Here proteins targeted for removal are segregated into autophagosomes which then fuse with lysosomes where degradation proceeds as with CMA [155]

There is evidence that CMA and ubiquitin proteasome are activated in the brains of Parkinson's disease patients [156, 157]. Furthermore CMA has been shown to target APP, tau and $\alpha$-synuclein via one or more KFERQ-like motifs [156, 158,

159]. Deletion of this motif in APP resulted in the failure of APP transport to the lysosome and an accumulation of C-terminal fragments and phosphorylated tau [158]. Similarly inhibition of the ubiquitin proteasome system has been reported to induce pathology in a mouse model of Parkinson's disease [160, 161].

### 1.4.6 Amyloid Diseases and Ageing

A noteworthy risk factor of sporadic amyloid-related diseases, as mentioned previously, is aging [91]. It has been proposed that during aging or under an environment of continuous cellular stress, the cell becomes unable to maintain cellular protein homeostasis [106]. This failure increases levels of misfolded proteins in the cell thereby further straining the quality control system, compounding the failure and eventually leading to the deposition of protein aggregates [106, 162]. The number of reasons age may reduce the protein quality control system of a cell are myriad and complex however some key events have been elucidated.

In aged cells there appears to be an impairment of the upregulation of molecular chaperones [155]. This includes HSP70 which, when measured in cells taken from aged rats, is no longer induced to the same extent following heat shock as when measured in cells taken from younger rats [163–165]. Such a reduction in activity may result from accumulation of oxidative damage [166, 167]. This is accompanied by a reduction in the absolute levels of these chaperones with age [168], further reducing protein folding capacity of the cell.

Furthermore, since many molecular chaperones require ATP for proper function, it may be that age dependent depletion of ATP levels may contribute to the reduction in their activity [169–171]. This may result from an age dependent reduction in mitochondrial function [169, 170]. This is reflected by induction of ATP independent chaperones in the aging brain [172]. The loss of these chaperones will not only impact the ability of the cell to maintain proper protein folding, but also attenuate the CMA pathway, thereby additionally reducing the cell's degradation capacity.

An increase in misfolding proteins as a result of reduced chaperone capacity should be managed by the activation of the UPR. However, elements of the UPR have also been shown to decline with age including PERK levels [173] and IRE1 activation [174]. Thus age appears to play an important role in priming cells for misfolding and amyloid aggregation.

## 1.5 The Synucleinopathies: Parkinson's Disease and Dementia With Lewy Bodies

Parkinson's disease and DLB are among the most common neurological disorders associated with aging [175]. Parkinson's disease was first described in 1817 by James Parkinson, [176] a description of the disease that was later revised and refined by Jean-Martin Charcot in the mid-1800s [177]. The symptoms of Parkinsonism are now well defined and include bradykinesia (slowness of movement), tremor when at rest, and muscular rigidity [178]. Several non-motor symptoms of the disease have also been described including olfactory dysfunction and sleep disorders [179] some of which are present before the onset of typical motor symptoms [180]. DLB is characterised by a progressive and disabling cognitive impairment that progresses rapidly to dementia. Attention deficit and problem solving difficulties often mark the onset of the disease [181]. However, presentation between the diseases is not clear cut and many symptoms are shared between DLB and Parkinson's disease.

A feature of Parkinson's disease, thought to be the major cause of disease related symptoms, is the loss of dopaminergic neurons within the *substantia nigra*. Loss of neurons specifically in the ventrolateral tier of the substantia nigra where the loss is most severe (91% neuronal loss per decade) [182] has been demonstrated to have a strong negative correlation with the appearance of motor related features of the disease, bradykinesia and rigidity in particular [183]. The loss of dopaminergic neurons is a feature present in early stages of the disease with a 50-90% loss of dopamine neurons in the substantia nigra at the time when symptoms emerge [184], with little change occurring thereafter. DLB symptoms however, are related to the loss of cholinergic neurons in the basal forebrain [185]. The feature that links both diseases is the presence of intracellular inclusion bodies known as Lewy bodies.

### 1.5.1 Lewy Bodies and $\alpha$-Synuclein

First identified in 1912 by Dr Fritz Heinrich Lewy, Lewy bodies appear as a semi-spherical mass displacing cellular contents. The presence of Lewy bodies has often been used for the identification of Parkinson's disease and DLB post mortem, with its presence of Lewy bodies in the substantia nigra defining Parkinson's disease. In Parkinson's disease Lewy pathology is hypothesised to progress through the brain in a defined manner; put forward by Braak et al (2003) the model describes six stages in which the lesions first appear in the peripheral nervous system and then progress into the central nervous system (Fig. 1.4).

The model of Lewy progression [187] corresponds well to the clinical course of Parkinson's disease, beginning with the onset of pre-motor symptoms progressing

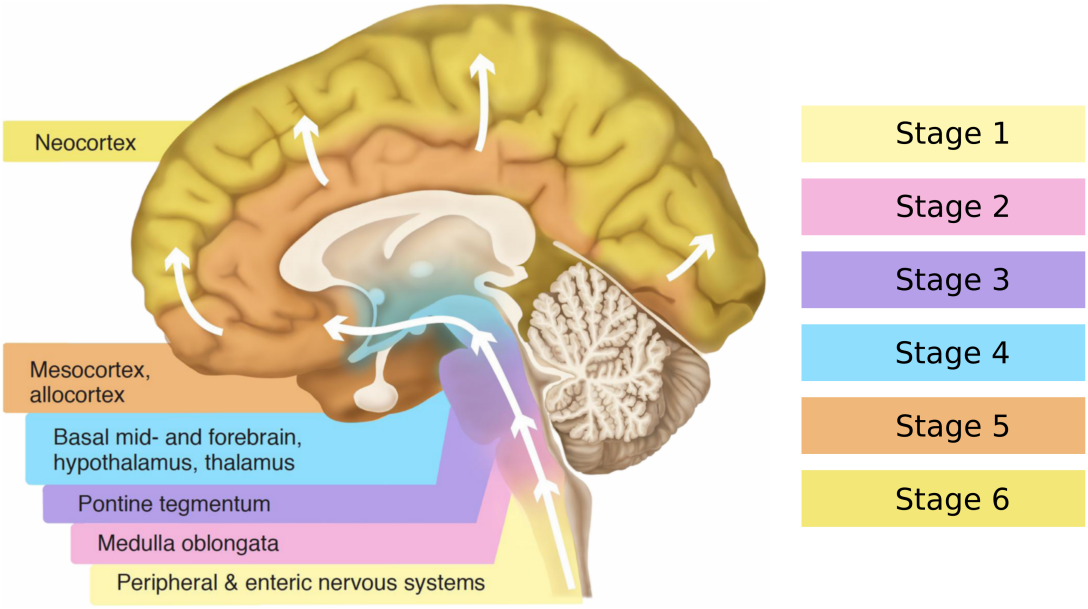


***Figure 1.4:*** *Braak stages of Parkinson's disease progression showing the spread of Parkinson's disease pathology through the brain. Adapted from [186].*

into loss of motor function with a loss of neurons in the substantia nigra. However it is worth noting that the relevance of Lewy pathology in Parkinson's disease is a subject of some debate. While studies have identified strong correlations between Lewy body (LB) pathology and dementia symptoms in Parkinson's disease [188], there is little correlation between LB load and dopaminergic neuronal loss in the substantia nigra [189]. However, another study has identified LBs as toxic to cells in the substantia nigra, with the appearance of inclusions apparently leading to nuclear degradation [190]. It was shown that in human brain tissue of Parkinson's disease and DLB patients, the presence of LB pathology in a cell was strongly associated with the presence of microtubule regression and mitochondrial and neuronal degradation [190].

LBs were initially shown to be composed of several proteins including ubiquitin and neurofilament protein. In 1997 it was shown that LBs taken from the brains of idiopathic Parkinson's disease patients also display a strong immunoreactivity for the full length presynaptic protein, $\alpha$-synuclein [191] and the number of $\alpha$-synuclein stained structures exceeded the number stained by ubiquitin, suggesting that $\alpha$-synuclein is indeed the principal component of these inclusions [192]. Furthermore, detailed study of LBs by electron microscopy has revealed that the $\alpha$-synuclein component is present as long unbranched fibrillar structures, with lengths in the range of 200-600nm and a width of 5-10nm [192]. These results marked $\alpha$-synuclein as a potential contributor to the development of Parkinson's disease.

## 1.6 Physiological Function of $\alpha$-Synuclein

$\alpha$-Synuclein is protein 140 amino acids long, that is found in high abundance in the brain, estimated to be around 1 µM in cells [193, 194]. $\alpha$-synuclein is a neuron specific protein that is localised to nerve terminals by N-terminal dependent membrane interaction [195–197] where it has been found at local concentrations of 50 µM [198]. The precise physiological function of $\alpha$-synuclein is uncertain, however it is thought to play a role in synaptic neurotransmitter trafficking and release [199–201]. Studies have demonstrated that in mice lacking $\alpha$-synuclein there is a significant reduction in the number of undocked vesicles present in hippocampal synapses [200] and that knockdown of $\alpha$-synuclein reduces the synaptic vesicle reserve pool of primary hippocampal neurons [202].

In contrast, moderate overexpression of $\alpha$-synuclein, such that overt toxicity is not apparent, impairs synaptic vesicle exocytosis and thereby reduces the release of neurotransmitter [201]. Using a synaptic protein bound to a pH dependent florescent tag that becomes fluorescent upon exocytosis, the effect of $\alpha$-synuclein on synaptic vesicle trafficking was directly examined. It was shown that when overexpressed $\alpha$-synuclein inhibited vesicle exocytosis with no effect on compensatory endocytosis [201]. In cultured hippocampal slices, $\alpha$-synuclein overexpression resulted in less synaptic baseline transmission as the result of a presynaptic deficiency. This defect in transmitter release occurs because of a reduction in the presynaptic recycling pool, resulting from a failure of synaptic vesicles to recluster following endocytosis, rather than a reduction in the rate of vesicle fusion [201].

The function of $\alpha$-synuclein to mediate synaptic vesicle transport may be related to the ability of $\alpha$-synuclein to act as chaperone for proteins of the soluble N-ethylmaleimide–sensitive factor attachment protein receptor (SNARE) complex [199], responsible for the membrane fusion of synaptic vesicles [203]. $\alpha$-synuclein overexpression recovers lethal neurodegeneration caused by a knockout of the chaperone cysteine string protein-$\alpha$ (CSP$\alpha$) [204]. $\alpha$-Synuclein directly binds component proteins of the SNARE complex, both in *ex vivo* samples and when co-expressed in a human cell line, and promotes SNARE complex assembly in a concentration, C-terminal dependent manner [199]. Furthermore it was demonstrated that in triple synuclein knockout ($\alpha$, $\beta$ and $\gamma$ synuclein) mice severe neurological defects and a reduction in SNARE complex assembly developed during aging, and that reintroduction of $\alpha$-synuclein produced a dose-dependent recovery in SNARE complex assembly [199]. Further work has demonstrated that the enhancement of SNARE complex assembly by $\alpha$-synuclein required $\alpha$-synuclein to bind to a membrane [205].

Overexpression of $\alpha$-synuclein also significantly increased the level of apoptosis detectable in embryonic in rat hippocampal cells and the N27 dopaminergic cell

line [206]. Moreover, it was shown that $\alpha$-synuclein abundance correlated with a reduction in the dopamine capacity of nigral neurons [207], and $\alpha$-synuclein presence was found to increase in such neurons in an age dependent manner. When imaged by confocal microscopy the loss of dopaminergic neurons was significantly higher in neurons that costained with elevated levels of $\alpha$-synuclein [207]. These results suggest that $\alpha$-synuclein possesses several important roles in the physiological function of neuronal cells.

## 1.7 Structure of Physiological $\alpha$-Synuclein

The native conformational state of $\alpha$-synuclein is somewhat debated. It has long been thought that the protein exists as a natively unfolded protein [208, 209]. Initial studies demonstrated by mass spectrometry, that natively purified $\alpha$-synuclein had a mass close to its predicted molecular weight of 14460Da. However, the Stokes radius of purified $\alpha$-synuclein, as observed by size exclusion chromatography, was significantly larger than expected for a protein of that weight. Together these data indicate that $\alpha$-synuclein exists natively as a monomeric unfolded protein [208]. However, it was determined that in the presence of lipids, such as would be the case in a physiological environment, $\alpha$-synuclein adopted an alpha helical state upon interaction [209, 210] (Fig. 1.5).

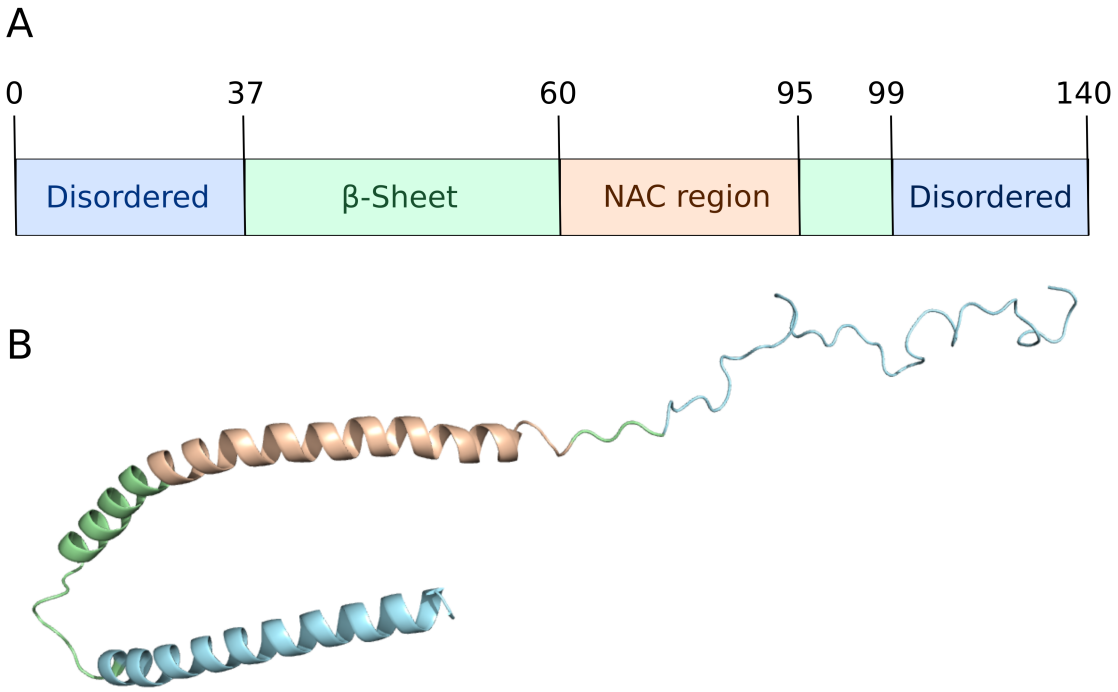


***Figure 1.5:*** *Structure of monomeric $\alpha$-synuclein. A) The domain structure of full length $\alpha$-synuclein showing the major regions of the protein. NAC refers to non amyloid component, named for its presence in A$\beta$ plaques and the region of $\alpha$-synuclein most associated with fibril formation. B) The lipid bound structure of monomeric $\alpha$-synuclein [211]*

However, questions have been raised about the methods used to purify $\alpha$-synuclein; it has been argued that the boiling step used in the purification may artificially reduce $\alpha$-synuclein to an unfolded state. It has been demonstrated that following non-denaturing purification $\alpha$-synuclein from a neuroblastoma cell line, ran as a 55-60kDa protein on native PAGE [212, 213], corresponding to the weight of a tetrameric form of the protein. The tetrameric conformation of $\alpha$-synuclein was further corroborated

by AUC, deriving a molecular mass of 57.8kDa and single particle electron microscopy, showing four 'v' shaped structures arranged in a symmetric configuration [212, 213]. Furthermore, the native conformer was determined to have an alpha helical secondary structure irrespective of lipid interaction [212, 213].

Further study utilising *in vivo* crosslinking techniques showed that purified crosslinked $\alpha$-synuclein ran as a single 60kDa band on native PAGE and four bands on denaturing PAGE, bands that were subsequently shown to have masses of monomeric to tetrameric $\alpha$-synuclein [212–214]. Furthermore cleavage of cross linkers in the crosslinked tetramer resulted in the release of monomeric $\alpha$-synuclein. Importantly, crosslinking occurred under conditions that crosslinked known dimers but did not affect known monomeric proteins [214]. This finding was further confirmed by fluorescence complementation in which a functional yellow fluorescent protein (YFP) fluorophore is split between two proteins and only becomes fluorescent upon interaction [214, 215]. These data suggest a functional oligomeric conformation of $\alpha$-synuclein that was dependent on the pseudo repeat region in the N terminal domain of the protein [212, 216].

However, other studies have demonstrated findings contradictory to that of Bartels, Choi and Selkoe [212], and Wang et al. [216]. Fauvet et al. [217] found that the method of purification of $\alpha$-synuclein from neuronal cells did not affect the mass of the purified protein, which was consistently shown to be around 14kDa, the weight of monomeric $\alpha$-synuclein. Likewise, the multiple techniques used by the study failed to detect any ordered secondary structure in the purified protein [217]. Furthermore, in-cell nuclear magnetic resonance (NMR) imaging showed the presence of natively disordered monomeric $\alpha$-synuclein in neuronal cell lines [218]. However it is worth noting that the $\alpha$-synuclein examined by this study was not endogenous $\alpha$-synuclein but rather recombinant purified monomer that was delivered into the cells by electroporation. The conformation may therefore differ in endogenous proteins which have been exposed to chaperone mediated folding from the moment of translation.

It is thought that the pathological effects of $\alpha$-synuclein are the result of monomeric misfolding and aggregation into cross-$\beta$ amyloid fibrils. Interestingly, tetrameric $\alpha$-synuclein was strongly resistant to fibrillization [212], while disease associated, familial mutants of $\alpha$-synuclein showed limited tetramer formation were linked to increased aggregation and a high propensity for inclusions and neurotoxicity [219]. These results demonstrated that the disease associated $\alpha$-synuclein mutation significantly decreased the ratio of tetrameric to monomeric protein [219].

Together these data suggest that under physiological conditions $\alpha$-synuclein exists as an alpha helical tetramer that must undergo unfolding to a disordered monomer before aggregation can occur. In the case of disease linked mutants $\alpha$-synuclein

fails to form the ordered tetramer, existing physiologically as a disordered monomer. Therefore, such mutant proteins are predisposed to fibril formation and the resultant toxicity.

## 1.8 The Aggregation of $\alpha$-Synuclein Into Amyloid Fibrils

The pathological aggregation of $\alpha$-synuclein in Parkinson's disease is hypothesised to be due, in part, to an intracellular accumulation of the protein. Many diseases featuring widespread aggregation, including a number of other neurodegenerative diseases have been found to be associated with supersaturated proteins [220]. Furthermore, in some familial forms of Parkinson's disease, multiplication of the SNCA gene – the gene encoding $\alpha$-synuclein – results in increased expression and concomitant aggregation of $\alpha$-synuclein [81]. Indeed, certain conditions are thought to accelerate $\alpha$-synuclein aggregation by providing a high local concentration of the protein [221].

Increased protein concentrations can occur as a result of a breakdown in protein homeostasis. Under normal conditions $\alpha$-synuclein is degraded by CMA within cellular lysosomes. Inhibition of lysosomal function or the blockade of specific lysosomal receptors inhibited the degradation of $\alpha$-synuclein [222]. Inhibition of CMA dependent $\alpha$-synuclein degradation, by deletion of the CMA targeting sequence on $\alpha$-synuclein, strongly correlated with the loss of intact nuclei, suggestive of enhanced toxicity [223]. Interestingly, the disease linked $\alpha$-synuclein mutants A53T and A30P were both found on the surface of, but were poorly internalised into, lysosomes [222]. This interaction with the lysosomal receptor lysosomal-associated membrane protein 2 (LAMP2), functioned as a blockade, impairing the degradation of all proteins using lysosomal autophagy via CMA. These data suggest a mechanism by which disease linked mutants may further bias their propensity for aggregation by increasing their intracellular concentrations.

*In vitro*, during fibrillization, synthetic $\alpha$-synuclein undergoes a conformational change from a largely disordered monomeric structure to a cross β-polymeric structure, typical of other amyloid fibrils [224]. Such fibrillization requires a hydrophobic stretch of amino acids in the middle of $\alpha$-synuclein, known as the non-amyloid component (NAC) region [225] (Fig. 1.5), so named following its identification in Aβ plaques of Alzheimer's disease patients. $\alpha$-synuclein, a protein with high homology to $\alpha$-synuclein but lacking the NAC region, or an $\alpha$-synuclein mutant lacking the region, fails to assemble into amyloid fibrils under the same conditions [225]. Furthermore the region taken alone is capable of assembling into structures resembling the classical amyloid fibril and possessing the cross-β secondary structure.

The formation of many amyloid fibrils first involves the formation of a loosely ordered oligomeric nucleus that undergoes a shift to a cross-β structure, after which the fibril grows by monomer addition [226, 227]. $\alpha$-Synuclein is no different in this respect; the formation of $\alpha$-synuclein fibrils is dependent upon the initial formation

of an oligomeric nucleus [228, 229]. Initial disperse oligomer formation is followed by a conversion to a compact cross-β structure that rapidly lengthens by monomer addition [230]. The effect of nucleation dependence is apparent in the lag phase of fibril formation. In the presence of monomer alone there is an initial period during which there is no apparent fibril formation followed by a period of sudden, exponential growth. In the presence of existing fibrils however, fibril growth begins immediately due to monomer addition to existing fibril ends. The rate limiting effect of nucleation on fibrillization is thought to be due to the time taken for oligomers to switch to the compact cross-β structure [230].

Several conditions can affect the formation of a fibrillar nucleus. A common property of disease linked α-synuclein mutants, for example, is the acceleration of nucleation as opposed to the acceleration of fibrillization [231]. Another condition shown to accelerate the rate of nucleation is the presence of lipid vesicles. [221]. This occurs at a lipid to monomer ratio lower than that required for the formation of an α-helical structure in α-synuclein, and is thought to be due to the lipid vesicles providing a high local concentration of α-synuclein.

The structure of the mature α-synuclein fibril has been studied on many occasions. On a number of structural aspects there is good agreement between studies. All structural studies have shown monomeric subunits running perpendicular to the fibril axis in a parallel, cross-β structure. Most studies have further shown that within the fibril core monomeric subunits adopt a configuration resembling a 'Greek key', in which residues 30-95 form the fibril core, while the N and C terminal residues remain largely unstructured [18] Fig. 1.6. Early NMR studies were unable to accurately identify the inter-protofibril interface [18]. However, recent advancements with cryo-EM have permitted high resolution structures of this interface to be obtained [232–234]. By this method it was shown that α-synuclein can aggregate into a number of fibril polymorphs with distinct fibrillar structures (Fig. 1.6).

In one such α-synuclein fibril structure obtained by cryo-EM, the interface between cross-β sheets was found to encompass residues 50 to 57 [233], a stretch encompassing the mutation sites associated with three forms of familial Parkinson's disease. However, this interaction site is not conserved in other fibril polymorphs [232, 234]. These polymorphs can be seen to differ in the location of protofilament interaction site though maintain the same structural kernel [232]. This is consistent with evidence from Parkinson's disease patient brains, where a number of polymorphic α-synuclein fibrils have been identified [235]. Moreover, there is some evidence to suggest that the polymorphs identified in the diseased brain are different in structure to any produced *in vitro* [236].

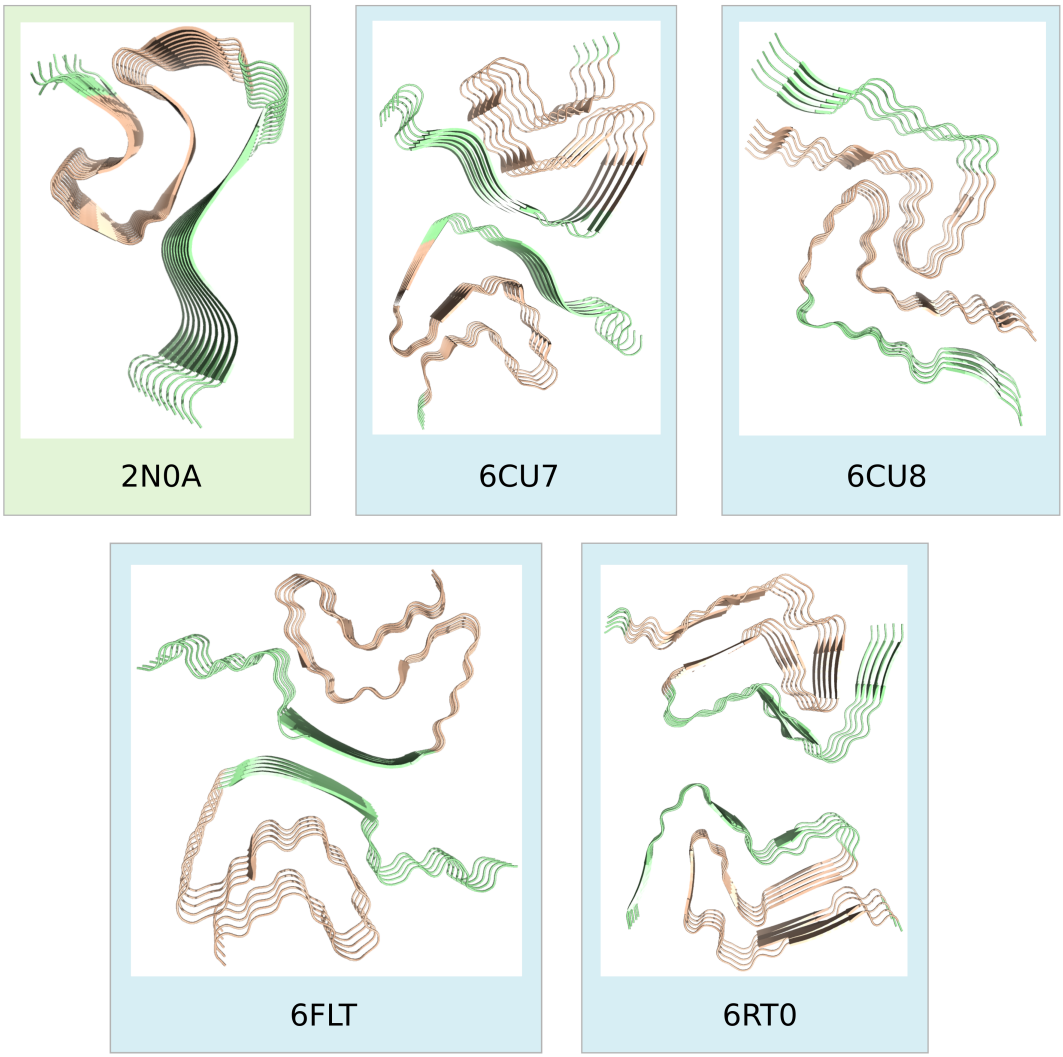


***Figure 1.6:*** *The structures of full length α-synuclein in a fibrillar structure. Each panel depicts a structure of α-synuclein fibril identified either by solid-state NMR (green) or cryo-EM (blue). The Protein Data Bank ID of each structure is shown below the image. For each structure the NAC region (residues 60-95) is highlighted (orange).*

## 1.9 Mechanisms of the Toxicity of $\alpha$-Synuclein Aggregates

The precise mechanism by which $\alpha$-synuclein misfolding and aggregation causes toxicity and cell loss is still unclear, although it is thought that aggregates may disrupt several cellular processes, all of which contribute to the final disease state. It has been demonstrated that in a GFP-tagged $\alpha$-synuclein over-expressing cell line, synaptic release was significantly impaired [237]. The study also demonstrated a clear reduction in the ability of overexpressing cells to internalise, by endocytosis, a dye specifically taken up into vesicle recycling pools, in cells overexpressing $\alpha$-synuclein. This result suggests that a failure or endocytosis occurs following the accumulation $\alpha$-synuclein [237]. It was noted that these results were reminiscent of the phenotypes observed following the knockout of SNARE complex components. Indeed, when cells were stained for the presence of such components, it was found that in overexpressing cells they were significantly reduced, with some 'ghost' cells lacking their presence altogether [237].

Another study, looking to investigate the early stages of toxicity identified an impairment to the ER associated degradation pathway [238]. Researchers demonstrated that four hours after induction of $\alpha$-synuclein overexpression in a yeast model of $\alpha$-synuclein aggregation, a significant reduction in the degradation of select proteins by this pathway as well as a generalised decrease in ER to Golgi traffic [238]. Furthermore, using a genome wide screen for toxicity inhibitors, proteins involved in membrane traffic were identified as the largest, most potent group of inhibitors. Specifically, overexpression of ypt1, a protein involved in the docking of the transport vesicle to the Golgi, both recovered ER to Golgi traffic and reduced dopaminergic neuronal loss. Interestingly, it has since been shown that toxic $\alpha$-synuclein species are formed within the ER in overexpressing cells [239]. Together, these data suggest disruption to membrane trafficking may represent an early event in $\alpha$-synuclein induced toxicity.

Another mechanism, suggested to be responsible for the toxicity of $\alpha$-synuclein, is membrane permeabilization by oligomeric species. Under physiological conditions molecular traffic through the cell membrane is tightly controlled; loss of this control by membrane permeabilization has the potential to markedly affect cell viability, ultimately threatening cell survival [240]. Several studies have identified a ring like structure of oligomeric species [241] that could potentially have pore forming properties. Indeed, oligomers bind to synthetic lipid vesicles with high affinity and induce dye release, though the vesicle itself is not lysed [242]. This pore formation appears to be dependent on the C-terminal region of $\alpha$-synuclein and can be inhibited

by reducing the flexibility of this region [239].

Indeed, there is a body of evidence to suggest that cellular toxicity is the result of soluble oligomeric species of $\alpha$-synuclein which form on pathway to fibril formation rather than the fibrils themselves [243]. Using mutants of $\alpha$-synuclein that even following one year of agitated incubation failed to form fibrillar material, but did successfully form ring-like oligomeric species, one study identified oligomers of $\alpha$-synuclein as a highly toxic species of aggregate. In contrast, a truncation mutant of $\alpha$-synuclein, in which amino acids 30-110 were retained, rapidly formed fibrils failed to produce any toxicity in cells [243]. Furthermore, when wild type (WT) and disease associated mutants of $\alpha$-synuclein were investigated it was found that the speed at which they formed fibrils was inversely correlated with their toxicity [243]. It is also of note that dopamine adducts can inhibit the formation of $\alpha$-synuclein fibrils by stabilising the pre-fibrillar oligomer, suggestive of a mechanism by which $\alpha$-synuclein toxicity can selectively target dopaminergic neurons [244].

Though much evidence appears to suggest that oligomeric $\alpha$-synuclein represents the toxic species with some studies going as far as to suggest that fibrils may represent an inert end product [243], a number of studies have equally demonstrated toxic properties of fibrillar $\alpha$-synuclein. Treatment of neuronal-like cells with pre-formed $\alpha$-synuclein fibrils has been shown to be far more toxic, via permeabilization of lipid vesicles and altered calcium homeostasis, than pre-fibrillar oligomeric species [245]. This is supported by evidence from studies into $\beta_2$M fibril toxicity, wherein it was demonstrated that internalisation of the $\beta_2$M amyloid fibril resulted in the cell displaying evidence of cytotoxicity [246]. Moreover, there is evidence to suggest that $\alpha$-synuclein fibril toxicity is highly dependent on the fibril structure, with some polymorphs of $\alpha$-synuclein fibrils displaying far greater cytotoxicity than others when applied to neuronal cell cultures [247]. Indeed, this variation in toxicity may explain the lack of fibrillar toxicity seen by Winner et al. [243].

Furthermore, there is some evidence to suggest that the conversion event, between oligomeric to fibrillar conformations, plays a role in the development of cytotoxicity. $\alpha$-synuclein mutants that are unable to form fibrils in vivo either due to fibrillization disrupting phosphorylation mimicry [243] or by proline disruption of the $\beta$-sheet core [248, 249], but nevertheless form oligomeric species, fail to show the prolonged neurodegeneration of fibrillization competent $\alpha$-synuclein. These data suggest that fibrillization is required for prolonged $\alpha$-synuclein toxicity. This is consistent with data from the A$\beta$ field that demonstrated that purified oligomers that failed to form fibrils displayed much lower toxicity than crude preparations capable of forming fibrils [250]. The requirement for fibril formation in prolonged degeneration may be related to the ability of fibrillar material to seed aggregation and to spread from cell to cell in a prion like manner.

## 1.10 Cellular Transmission of $\alpha$-Synuclein Fibrils

The concept of $\alpha$-synuclein transmissibility was first evident in the disease progression seen by Braak et al. (2003) (Fig. 1.4) in which the ascending Lewy body pathology in synucleinopathies can be interpreted as a spreading aggregation from a single point of origin. Further evidence is to be found in the spread of Lewy body pathology into the disease free striatum grafts into patients with Parkinson's disease [251, 252], highly suggestive of host to graft transmission. Equally, in a mouse model of Parkinson's disease, $\alpha$-synuclein positive inclusions spread into stem cell grafts [253]. When the brain homogenates from diseased mice were injected into the cerebellum of young, healthy mice, neurological symptoms and Lewy body pathology were accelerated in that area and pathology propagated to regions far beyond the site of injection [254].

Although $\alpha$-synuclein is an intracellular protein forming intracellular inclusion bodies, toxic species of $\alpha$-synuclein can be expelled from cells under pathological conditions including mitochondrial and lysosomal stress [255, 256]. In cells overexpressing $\alpha$-synuclein, the aggregated protein is found in the lumen of intracellular vesicles and is released by exocytosis into culture medium [257, 258]. The released aggregates are found associated with exosomes in the culture media and were toxic to neuroblastomas [257].

Released fibrils can be internalised by a number of methods including endocytosis following membrane receptor binding, internalisation of fibril containing exosomes and via cell-to-cell tunnelling nanotubes (TNT)s. $\alpha$-synuclein fibrils have been shown to be taken up directly from the culture media, via receptor mediated endocytosis [259, 260]. One such receptor, known to mediate the internalisation of $\alpha$-synuclein fibrils by endocytosis is the transmembrane receptor protein, lymphocyte activation gene 3 (LAG3) [260]. Inhibition of this receptor significantly attenuated the internalisation of $\alpha$-synuclein fibril and prevented the associated pathology [260]. Another method by which fibrils may enter cells is via the internalisation of fibril containing exosomes released by cells showing evidence of $\alpha$-synuclein aggregation [256]. Finally the transfer of $\alpha$-synuclein fibrils between donor and acceptor cells has also been shown to occur through cell-to-cell TNTs, that facilitate traffic between neurons [261].

Following endocytosis, aggregative pathology spreads through the neuron from the point of entry [262]. Internalised fibrils have been shown to pass through the endolysosomal pathway of acceptor cells following internalisation [256] before escaping (the method by which this occurs is as yet unknown) into the cytoplasm. Upon entry into the cytoplasm, internalised $\alpha$-synuclein fibrils seed further aggregation of endogenous $\alpha$-synuclein [259]. Fibrils labelled with a fluorescent dye added to the media of a neuronal like cell culture formed punctate structures within the cells over a period of 24-48hrs [259]. The majority of the aggregated protein

following this incubation period is present in the insoluble fraction, suggesting the formation of mature fibrils. The formation of such punctate structures was blocked by low temperature or expression of a dominant negative form of dynamin, both well characterised inhibitors of endocytosis [259]. The resultant intracellular inclusions display properties of Lewy body disease including hyper-phosphorylation and ubiquitination, and included endogenous $\alpha$-synuclein surrounding a core of internalised fibrils [263].

In addition to the seeding properties of $\alpha$-synuclein fibrils, fibrils of other amyloid proteins have been shown to disrupt lysosomal function, the endpoint of the endolysosomal pathway by which $\alpha$-synuclein fibrils are internalised, following endocytosis [264]. Amyloid fibrils co-localise with lysosomes and disrupt their ability to degrade cellular proteins that commonly enter the lysosomal pathway. The disruption to lysosomal function may in turn feedback to increase the exocytosis of $\alpha$-synuclein, known to exacerbate such release [255]. Despite what is known about the endocytosis of $\alpha$-synuclein, little is known about the proteins that interact with the fibrils following endocytosis that may lead to cellular dysfunction. The aim of this study is to investigate such interactions, following endocytosis, using proteomic based techniques to enable unbiased identification of protein binders, followed by characterisation of the pathways affected by these interactions.

## 1.11 Proteomics and its Use in the Study of Amyloid Disease

The proteome is a term coined in 1995 by Dr. Marc Wilkins to describe the entire complement of proteins expressed by the genome of an organism [265]. The term proteomics refers to the study of the proteome. Proteomics represents a useful approach for the study of amyloid disease as it has enabled large scale, unbiased study of proteome changes in as well as the identification of protein interactors (so called interactomes) of amyloid proteins, allowing for unbiased study of disease mechanisms.

Though there are many techniques used in the study of proteins, the most commonly used proteomic tool in the detection of proteins is mass spectrometry (MS). Identification of proteins through MS is possible via a technique known as tandem MS (also known as MS/MS). Early proteomic investigations were primarily qualitative, being used to identify proteins and potential post-translational modifications; however, advancements in methodologies have enabled the introduction of quantitative proteomics, where the levels of a protein can be compared between multiple sample conditions.

Such techniques have enabled large scale investigation into many aspects of amyloid diseases, from the expression and modification of amyloid *in vivo* [266] to the protein interactors of amyloid fibrils *in vitro* [267, 268]. The major techniques used by studies of this nature include stable isotope labelling by amino acids in cell culture (SILAC), isobaric tag for relative and absolute quantification (iTRAQ) and the related technique of tandem mass tagging (TMT), along with label free methods. Such methods enable the quantification, both relative and absolute, of protein levels in a sample [269].

### 1.11.1 Peptide Identification Via Tandem MS

The term shotgun proteomics refers to a bottom up, unbiased identification of all proteins within a sample [270] and forms the basis of many proteomic studies of amyloid disease. For identification of these proteins from a tissue or cell derived sample, proteins are first digested into peptides via proteases such as trypsin [271]. Peptides are then separated using liquid chromatography (LC) and directly enter the mass spectrometer.

Within the MS, a voltage between the LC elution capillary and the MS itself leads to a process of electrospray ionisation (ESI); positively charged peptides concentrate within eluting droplets as they undergo evaporation [272]. This occurs until coulombic repulsion between peptides exceeds surface tension and the droplet

releases the peptides into the gas phase [272]. Different peptides ionize with radically different efficiencies [273] and therefore the number of ions detectable by the MS cannot be used as a readout of protein concentrations within the sample [269]. MS is therefore inherently non-quantitative.

The ionised peptides can now be separated based on their mass to charge (m/z) ratio. With the resolving power of current mass analysers the mass of a peptide alone is not sufficient to perform identification [269]. The mass separated peptides are therefore subject to fragmentation via collision with inert gases in a process known as collision-induced dissociation (CID). This collision causes the fragmentation of the peptide at the weakest bonds, typically a peptide bond [269, 274]. Usually there is only a single fragmentation event for any given peptide passing through the CID, resulting in pairs of complementary fragments termed b and y ions. b ions refer to ions containing the peptides N terminus and y ions to fragments containing the peptides c terminus [269, 275](Fig. 1.7 bottom center panel). The mass to charge ratio of these fragment ions are then recorded by a second mass analyser MS-2. The resulting spectrum can then be used to identify the peptide as well as any post-translational modifications [269, 274] (Fig. 1.7).

The method by which a peptide can be identified from the spectrum of its fragment ions is as follows. Where all possible b or y ions are present for a given peptide then the peptide sequence can be calculated based on the mass differences between ion peaks, each difference representing the mass of a single amino acid. In other words the mass of the b1 peak represents the N-terminal amino acid (Fig. 1.7 bottom right panel, leftmost peak), b2 the N-terminal amino acid plus the next amino acid, and so on. As might be expected however, it is rarely the case that all ions can be identified, especially in complex samples such as those from whole cell lysate. Instead peptides are typically identified by their "fingerprint", their experimentally derived spectra, that is compared to theoretical spectra of all possible peptides resulting from the organism under study [276] to identify the most likely peptide. Multiple search algorithms have been developed to automate this search [277–280] greatly simplifying the process.

Identification of peptides is a core tool of proteomic study. However, identification alone is often not enough. It is often desired to quantify the level peptide in a sample in order to compare the effects of different conditions on the cellular proteome. Over the years several techniques have been developed to enable MS, a technique that is inherently unreliable for quantification, to deliver accurate quantitative results.

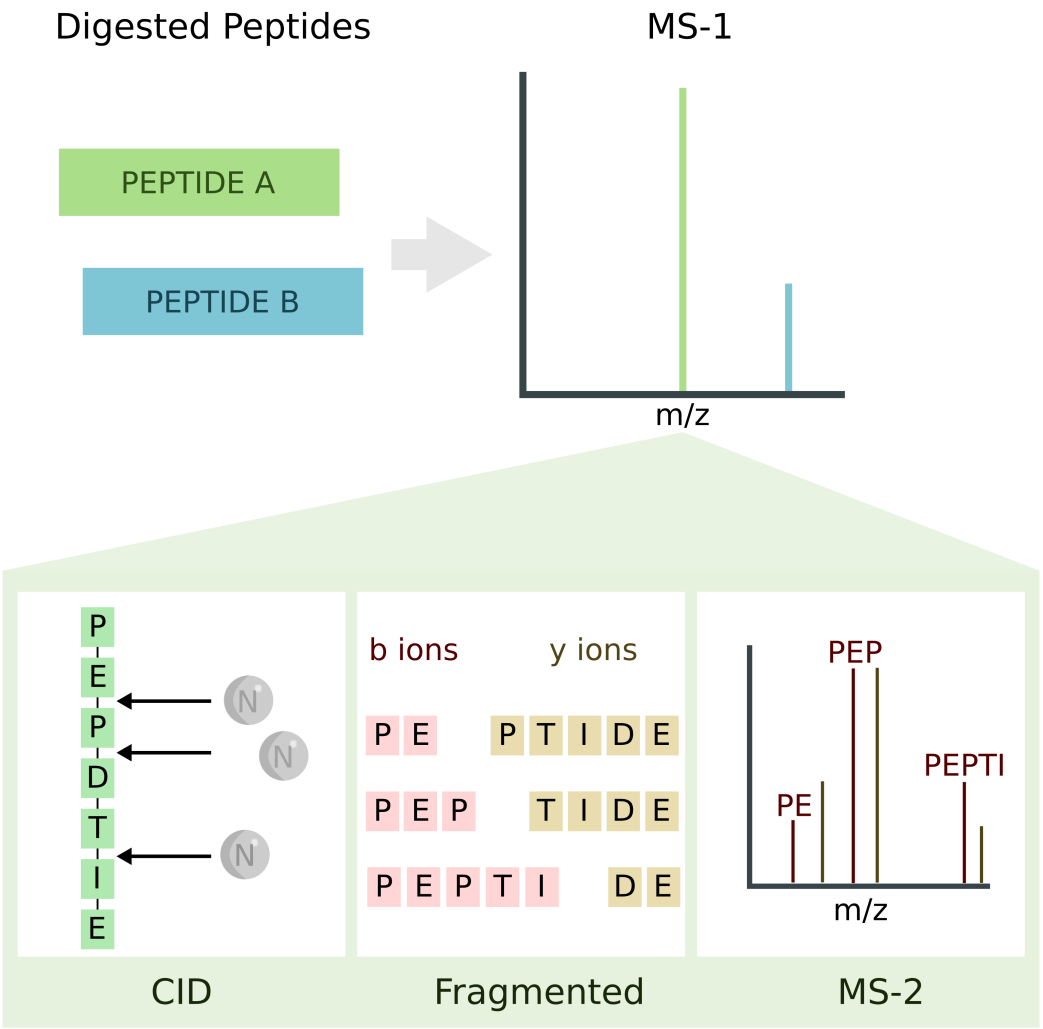


***Figure 1.7:*** *Schematic showing the process of tandem MS. Proteins are first digested by protease to form peptides which are ionized and their mass to charge calculated by the first mass analyser, MS-1. Each of these ions are then selected and fragmented via collision with an inert gas in a process known as CID. Typically this process breaks a peptide once at an amine bond, resulting in complementary b and y ions. By measuring the mass to charge values of these b and y ions via a second mass analyser, MS-2, it is possible to reconstruct the peptide by calculating the mass change between the peaks. In an ideal case all peptide fragments would be represented (ie. P, PE, PEP, PEPT, etc.) enabling straightforward calculation. Here, for simplicity, only a subset of possible b and y ions are shown.*

### 1.11.2 Quantitative Proteomics

Within the field of quantitative proteomics there are two methods of quantification, relative quantification (determining protein concentration relative to another sample) and absolute quantification (determining the absolute concentration of the protein in the sample). However, as mentioned previously, there is an intrinsic limitation on using MS for protein quantification, that is the variation on peptide ESI efficiencies [269]. Although ESI has been shown to produce signals that scale linearly with peptide concentration [281, 282], nonlinearity and ion suppression effects are a legitimate concern in complex biological samples [283, 284]. Absolute quantification is therefore often an extension of relative quantification, where proteins are quantified relative to a spiked standard with a known absolute concentration [285]. Forms of absolute quantification exist that leverage a relation of a protein's total ion count to the absolute protein concentration [286] however, the error with this technique is often too high to be practicable [287].

Relative quantification involves the comparison of protein abundance between two samples. In order to do this the relative abundance of their peptides are individually quantified, the individual abundances being calculated from the peak area of the peptide, and the data of multiple peptides integrated to calculate the relative abundance for the protein [288]. For accurate quantification, peptide abundances from distinct samples are typically measured from a mixed sample population. Therefore, in order to compare peptides from different samples, it must be possible to distinguish the sample origin of the peptide being quantified.

There are a number of ways to achieve this, one common approach is based on the theory of stable isotope dilution which states that a stable isotope-labelled peptide is chemically identical to its unmodified counterpart and will behave in a identical manner during LC and ESI [288]. The MS is then able to distinguish between the labelled and unlabelled form of the peptide based on its m/z ratio. Thus the same peptide originating in separate samples can be isotopically labelled in a sample dependent manner, and the relative abundance of that peptide directly compared [288]. The relative abundance of a protein can then be calculated from the relative abundances of all peptides identified for that protein.

Another approach relies only on quantifying the MS1 signal of a peptide obtained from tryptic digestion, before fragmentation, and involves no isotopic labels. In this label free approach samples are not combined prior to analysis. In order to prevent some differences in ESI between samples affecting the calculated concentration, some form of correction is then applied to the peptide abundance before relative quantification [283, 289].

Some of the most common techniques for quantitative proteomics are explored in

more detail below.

### 1.11.3 Label-Free Quantification

A method of relative quantification that avoids some of the shortcomings of label based methods, including cost and increased complexity of the experimental workflow, is label-free quantification. In label-free proteomic quantification all samples are analysed in separate MS/MS experiments and the peptide abundances compared between samples. Protein quantification is then conducted by one of two methods, peptide peak area quantification, or spectral counting.

Abundance calculation by peptide peak area quantification relies on the correlation of the sum of peptide peak areas with the concentration of the protein in the sample [281, 282]. This method of quantification is further improved by normalising the calculated peak areas to a constant reference protein or spiked internal control [282, 289]. Although theoretically sound, this approach was initially complicated by a number of practical factors resulting in poor chromatographic peak alignment, leading to large variability and inaccurate quantification. However, advances in computational algorithms have somewhat mitigated these issues [290, 291].

Spectral counting, conversely, calculates relative protein quantification by comparing the number of MS/MS spectra from the same protein in each sample dataset. This relies on the fact that protein abundance typically correlates to the number of proteolytic peptides generated by tryptic digestion [292]. This in turn correlates with the number of identified MS/MS spectra (spectral count) a protein produces [292, 293]. This correlation of spectral count to protein concentration is linear with a dynamic range of $10^2$ [293]. Normalisation to total spectral counts can then be applied to account for inter-run variance [294, 295]. An advantage of this method lies in its simplicity. Whereas chromatographic peak intensity based quantification relies on complex and delicate algorithms to prevent an misalignment of chromatographic peaks between samples, spectral counting requires no such complexity.

Label-free techniques are among the most popular in the proteomic field [296]. This is largely because of the many advantages offered by the technique including; low experimental cost, as the experiment requires no reagents other than the samples themselves; largely automated data analysis; shorter experimental process as no peptide labelling is required; and the feasibility of running hundreds or even thousands of samples, there are several important limitations [296–299]. Although label-free techniques appear to be more sensitive, detecting a far greater proportion of the proteome than label based techniques, the label free approach suffers from larger technical variability and lower quantitative accuracy than label based techniques [296–299]. Furthermore, quantitative reproducibility was lower in label-free quantification-

based techniques [298, 299].

### 1.11.4 SILAC Based Proteomics

Several label-based approaches to quantitative proteomics exist. As discussed above, all rely on the combination of samples prior to MS analysis. The first major label-based quantitative proteomics approach, known as SILAC, involves protein labelling with heavy non-radioactive isotopes Fig. 1.8. Proteins are labelled though the culture of cells or tissue in media containing only heavy isotopes of one or more essential amino acids [300]. Most commonly this amino acid is Leucine or Arginine due to their relatively high abundance in proteins, therefore enabling good coverage of the cell or tissue proteome [300]. Since these heavy isotopes have identical chemical characteristics to their light counterparts, proteins produced by these tissues will gradually be replaced by higher molecular weight versions. MS can then be used to separate proteins originating from heavy and light samples [300]. By using no (light), 1 (medium) or 2 (heavy) heavy amino acid isotopes, it is possible to compare three samples simultaneously.

Proteins can then be quantified based on the integrated signal intensity of the peptide peaks identified at MS1, prior to peptide fragmentation [300]. Using this approach peptides from different samples are co-analysed in the MS, thereby reducing the potential for experimental variation between MS runs to affect quantitative accuracy, and inherently leads to much higher reproducibility [300]. Similar strategies include the labelling of peptides following digestion with isotope-coded affinity tags [301, 302]. This post-digestion strategy requires the cross-linking of peptides to affinity beads and subsequent affinity purification prior to MS/MS analysis.

A major limitation of techniques that utilise MS1 peptide intensity to quantify protein abundance however, is the increase in MS1 spectrum complexity with sample number [298]. Therefore, though theoretically possible to simultaneously compare a large number of samples, such techniques are practically limited to at most three simultaneous comparisons [298]. There has been innovation attempting to bypass this limit by incorporating heavy amino acids differing by only a few daltons [303]. This advancement has shown remarkable promise, offering the quantitative accuracy offered by SILAC with the multiplexing capabilities of MS2 quantification based techniques such as TMT and iTRAQ [303]. However such multiplexing leverages high-resolution MS, and is therefore not yet widely available [269]. A further limitation of MS1-based quantification is that should low-abundance peptides co-elute with a high abundance peptide on the LC, precision of quantification of the low-abundance peptide can be dramatically reduced. This is due to a limitation on the number of ions that can be collected by the MS high-resolution analyser (the Orbitrap); ions of

low-abundance peptides can be masked in the above scenario, resulting in poor ion statistics [269].

A further limitation of this technique is the need to culture cells in labelled media for multiple passages in order to incorporate sufficient heavy isotopes into the proteome of the cell Fig. 1.8. Not only is this expensive it also increases the complexity of experiments involving tissue samples.

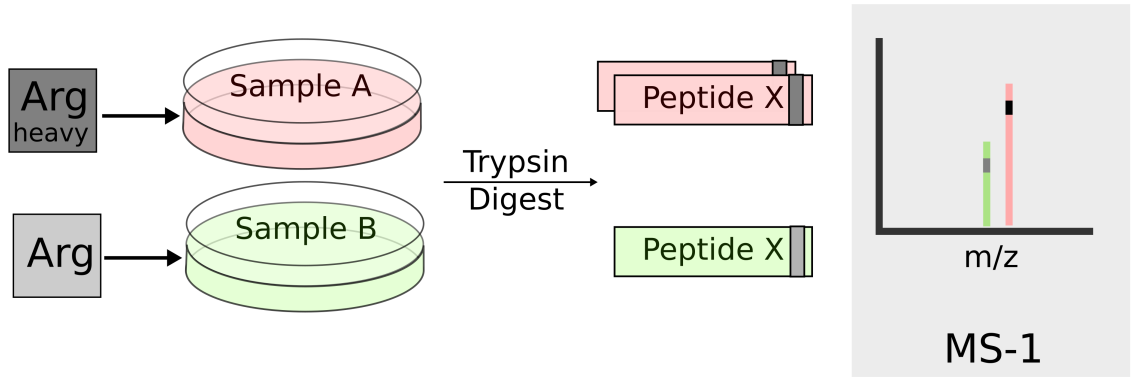


***Figure 1.8:*** *Diagrammatic representation of the quantitative proteomics by SILAC. Heavy or light isotopes of the amino acid Arginine (Arg) are added to the cell culture medium. Proteins incorporating the amino acid isotopes are then digested to form peptides, peptides from different samples are mixed and the mixed samples undergo tandem-MS to perform identification and quantification. Quantification by this method is performed at MS-1. Peptide peaks originating from the sample containing the heavy isotope will appear to have a higher mass than those originating from the light isotope sample. Quantification can then be made by comparing the abundances of these peaks.*

### 1.11.5 Quantitative Proteomics with Isobaric Labelling

The use of isobaric labelling in quantitative proteomics overcomes the several of the major issues faced by label-free and SILAC based techniques. Namely the low accuracy and repeatability of label-free proteomics and the low sample number of SILAC and related techniques. Furthermore, as with SILAC, samples are combined prior to analysis by MS meaning that although the sample preparation time is increased the instrument time is dramatically shorter, especially for large sample sets [304].

The principle of quantitative proteomics by isobaric labelling is to label digested sample peptides such that peptide quantification can be made alongside peptide identification in MS2, following peptide fragmentation in the MS1 Fig. 1.9. This alleviates the problem faced by SILAC and other MS1-based quantification techniques

of complex MS1 spectra at high sample numbers, as quantification can be performed on m/z separated peptides [304, 305]. In order for this to be possible the mass of peptides originating from separate samples must be identical at MS1 but their origin be identifiable at MS2. Were the label to affect MS1 m/z the problem of MS1 spectra complexity would once again arise. This problem is solved through the use of isobaric tags.

Similarly to other isotopic labelling techniques such as SILAC isobaric tags utilise heavy isotopes to maintain chemical similarity. This ensures that peptides from different samples elute at the same time from the LC. However, unlike other isotopic-based labelling, isobaric labels have identical total weights. The difference between tags is rather in the distribution of heavy isotopes within the label Fig. 1.9. Finally, to enable separation in MS2 the tags contain a region designed to fragment under CID, generating reporter ions with different masses depending on the sample origin of the peptide. Such reporter ions are low molecular weight ions, enabling straightforward separation of ions for quantification and the b and y ions required for peptide identification. Identical peptides from different samples labelled in this manner will appear as a single peak in MS1, thus ensuring spectrum complexity is minimised. Quantification can instead be made from the reporter ion intensity in MS2. As a result the number of conditions that can be compared by this technique is much higher than that of SILAC, the current limit being 11 concurrent comparisons.

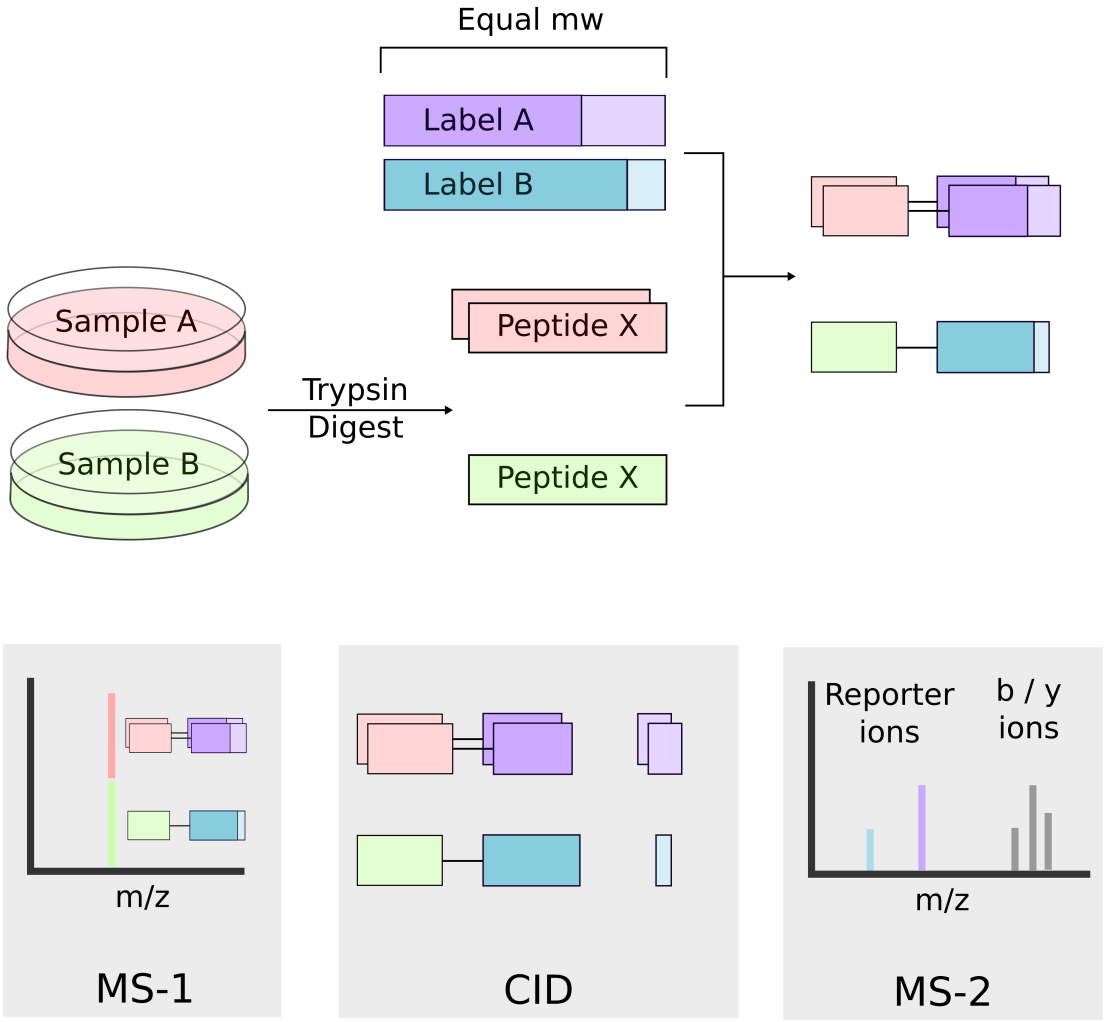


***Figure 1.9:*** *Diagrammatic representation of peptide quantitation by TMT proteomics. Peptides are generated by digesting proteins originating from 2 or more samples (2 shown here). Peptides are then labelled with isobaric tags (labels) of equivalent molecular weight. A different label is used for each sample. labelled peptides are then mixed and identified/quantified by tandem-MS. During detection in the first mass analyser MS-1 (bottom left panel) both samples appear at the same mass to charge due to the identical weight of the isobaric labels. During CID (center panel) reporter ions are fragmented from the isobaric labels. These reporter ions appear at different mass to charge ratios in the second mass analyser, enabling relative quantification to be performed based on the abundance of each reporter ion.*

## 1.12 Proteomics Based Study of Parkinson's Disease

Proteomics has been used in a number of ways to study the events and proteins related to the development of Parkinson's disease. One such example is the identification of key post-translational modifications of $\alpha$-synuclein, associated with pathogenic inclusions in cells. There are many reports that indicate $\alpha$-synuclein can undergo a variety of post-translational modifications, including phosphorylation [266], truncation [306] and nitration [307], in the brain tissue of Parkinson's disease patients. Several of these modifications have been linked to accelerated $\alpha$-synuclein aggregation and enhanced neurotoxicity [308, 309]. One seminal study in the field of $\alpha$-synuclein research identified Ser129 phosphorylation in Lewy bodies through proteomic based methods.

Fujiwara et al. (2002) employed matrix-assisted laser desorption ionization (MALDI) MS to identify such post-translational modifications in amyloid lesions extracted from the cortices of Parkinson's disease patients. MALDI is an MS technique that permits the analysis of biomolecules such as peptides which tend to fragment when ionised by conventional MS techniques. One species, identified by MALDI MS as corresponding to residues 128-140, differed between monomeric and Parkinson's disease associated $\alpha$-synuclein, by the weight of one phosphate group, indicating the presence of a post-translational phosphorylation associated with synucleinopathic lesions [266].

Further analysis identified the phosphopeptide as Ser129. Antibodies raised specifically against phosphorylated Ser129 revealed that roughly 90% of the LB associated $\alpha$-synuclein recovered from cortices of Parkinson's disease patients is phosphorylated at Ser129. Staining of brain tissue revealed specific identification LBs, in contrast to staining with a phosphorylation independent antibody that also displayed labelling of presynaptic termini [266]. This specificity has enabled researchers to better describe LB formation in early disease states [310]. The increased specificity and sensitivity of anti-phosphorylated Ser129 enabled the identification of pathology linked to DLB in apparently pre-symptomatic cases [310] Ser129 as a particularly good biomarker of disease, and importantly, may enable pre-symptomatic identification of the disease.

Another more recent study demonstrated a method for quantitative analysis of intact $\alpha$-synuclein proteoforms in Parkinson's disease brain tissue by ESI MS. ESI-MS enables the analysis of macromolecules such as intact proteins by mass spectrometry, earlier mass spectrometry techniques, including the previously described MALDI, relied on digestion of the protein into peptides. This technique enables intact protein

mass determination, and when coupled with tandem mass spectrometry represents a robust top down approach to proteomics. This technique enabled the identification and quantification of several, previously unreported, $\alpha$-synuclein proteoforms [311].

## 1.13 Proteomic Analysis of Amyloid Fibril Interactomes

The interaction of amyloid aggregates with cellular proteins is important, as it is thought that many of the pathogenic effects of amyloidogenic proteins are the result of a toxic gain of function and or disruption of normal cellular function [312, 313]. Proteomics has enabled the large scale, unbiased, identification of protein interactors with several amyloid proteins including artificial amyloid proteins and the amyloidogenic poly-Q expanded huntingtin protein.

### 1.13.1 Investigating the Interactions of Artificial Amyloid

In order to investigate the gain-of-function toxicity of amyloidogenic proteins a study utilised artificial amyloid-like proteins, designed with a β-sheet structure and shown to self-assemble into amyloid fibrils [312]. By expressing the artificial protein in cells, the aberrant interactions of such amyloid-like proteins with cellular components was investigated. The advantage of using several artificial amyloid-like peptides over a known pathogenic amyloid is that the interactions observed would likely represent those made specifically by the aggregate rather than amplified physiological interactions made by the pathogenic protein. By this method researchers hoped to identify proteins binding to the fibrillar conformation of amyloid proteins.

The artificial amyloid-like proteins were shown to have a cytotoxicity profile and aggregation properties similar to those of known amyloidogenic proteins, suggesting that the artificial proteins functioned in a similar fashion to their non-artificial counterparts [312]. By utilising SILAC the interactomes of the three artificial proteins, relative to a fourth protein known to remain as a monomer, were identified. Olzscha et al. (2011) identified many proteins throughout the nucleus, cytoplasm and mitochondria as interactors of the artificial amyloid proteins, including proteins involved in RNA processing, transcription, translation and protein quality control. It was found that common features of the amyloid protein interactors included a high molecular weight and reduced hydrophobicity. Furthermore, amyloid protein interactomes are preferentially rich in intrinsically disordered regions, many of which contain low complexity region (LCR)s [312]. LCRs are regions of the protein consisting of repetitive sequences of 1-4 amino acids and are proposed to mediate protein-protein interactions [314]. The length of the LCRs are also increased in the interactomes of amyloid proteins relative to the cellular proteome, indicating that amyloid protein aggregates preferentially sequester proteins containing such sequences.

Following the identification of artificial amyloid protein interactors, further studies

were undertaken to investigate the implications of these interactions. Proteins involved in nuclear transport were one of the protein groups found to be enriched in the interactomes of the artificial amyloid proteins [315]. Additional study demonstrated that cytoplasmic aggregates of artificial amyloid prevented the nuclear transport of several key proteins and the export of mRNA. Indeed proteins involved in mRNA export were found to mislocalise to the cytoplasm in the presence of cytoplasmic amyloid proteins, where they formed punctate structures [315]. These findings provide an insight into the mechanisms which may contribute to the toxicity of amyloid aggregates; by causing aggregation of nuclear transport machinery, containing low complexity regions, amyloid aggregates prevent nuclear export of mRNA and thereby protein synthesis [315].

### 1.13.2 Investigating the Interactions of Poly-Q Expanded Huntingtin

Huntington's disease is a dominantly inherited condition, associated with the aggregation of the protein huntingtin, and neuronal death and is thought to be caused by the expansion of a poly-Q repeat sequence found in exon 1 [316]. The propensity of the protein to form aggregates increases dramatically with extension of the poly-Q repeat beyond 36 residues [317]. Furthermore, extension of the repeat correlates with the severity of the disease and negatively with the age of disease onset, indicating that increased aggregation propensity leads to a faster depletion of the cell's quality control machinery [318].

A recent study [267] investigated the aberrant interactions of a poly-Q expanded huntingtin fragment. Three huntingtin mutants were used in the study with varying sizes of poly-Q repeats; Q18 was monomeric when expressed in cells while Q64 and Q150 both produced soluble and insoluble aggregates. Using SILAC the interactomes of the huntingtin variants were identified and quantified; proteins enriched in the interactomes of the aggregation prone peptides, relative to the monomeric protein, were proposed to be involved in mediating the toxic effects of the poly-Q expanded aggregates. The study identified proteins involved in RNA binding, ribosome biogenesis and intracellular transport as highly enriched in the interactomes of soluble aggregates.

These findings are in agreement with another study, which utilised tandem affinity purification (TAP) and iTRAQ to identify aberrant interactions [268]. TAP allows for purification under mild native conditions to preserve interactions [319]; furthermore, interactomes were identified in a striatal cell line, a cell line that more closely models HD. Ratovitski et al. [268] demonstrated that expanded huntingtin aberrantly interacts with proteins involved in gene expression, protein synthesis

and molecular transport. In addition, this study identified proteins involved in DNA replication, RNA transport and modification, energy production and cell death, to bind monomeric huntingtin, but to be enriched in the interactome of expanded huntingtin. Such findings indicate that expanded huntingtin interferes with physiological interaction pathways of huntingtin, (indicated by the enrichment of proteins found to bind non-expanded, monomeric, huntingtin) in addition to aberrant interactions with proteins not found in the interactomes of non-expanded huntingtin. Interestingly, both Ratovitski et al. [268] and Kim et al. [320] are in agreement with the findings of artificial amyloid protein, found that proteins containing large LCRs were highly enriched in the interactomes of soluble huntingtin aggregates. These data would appear to suggest that enrichment of LCRs is a common feature of amyloid aggregates. As with artificial amyloid, confocal imaging study of cells expressing poly-Q mutants, demonstrated that proteins involved in ribosome biogenesis and RNA transport mislocalised in the presence of soluble aggregates [267]. RNA binding proteins were another group common of proteins found in the interactome of expanded huntingtin [267, 268].

### 1.13.3 Investigating the Interactions of $\alpha$-Synuclein

There have been a number of studies seeking to identify the interactome of $\alpha$-synuclein in the past. Notable studies include several that have utilised the yeast two-hybrid approach to investigate protein-protein interactions of the amyloid protein. This method is based on the principle that in many eukaryotic transcription factors the activating and binding domains can function in proximity without direct binding, meaning the expression of a reporter gene can be used to infer the interaction of a bait and prey protein [321]. Technically, this method involves the hybridisation of the protein of interest (the prey protein) with the DNA binding domain of the reporter gene. High throughput bait protein screening can then be conducted by hybridising the bait proteins to the activation domain of the reporter gene [322].

This method has been used previously to identify a number of peptides that exhibit aggregation inhibiting behavior when exposed to $\alpha$-synuclein [323], providing possible therapeutic avenues of study. Moreover, this method has been used to elucidate the protein-protein interactions of 500 neurodegenerative-associated proteins, including $\alpha$-synuclein and huntingtin [324]. This study identified, among other findings, a role for the protein ARF in preventing a number of amyloid proteins from misfolding, including $\alpha$-synuclein [324]. The protein ARF has previously been shown to play a role in phagocytosis, again pointing to the possibility of immune system involvement in the development of Parkinson's disease.

## 1.14 Project Aims

The aim of this work was to identify the intracellular interactome of $\alpha$-synuclein fibrils. Since the exogenous $\alpha$-synuclein fibrils are internalized by cells, as part of their transmission between cells, the work was proposed to identify proteins that interact with $\alpha$-synuclein fibrils following internalisation. Proteomics was used to enable an unbiased identification of interacting proteins and potentially identify novel pathways by which $\alpha$-synuclein fibrils can disrupt normal cellular function.

In Chapter 3 an experimental system whereby $\alpha$-synuclein fibrils, once internalised by cells, could be isolated and interactors identified needed was developed. For this purpose recombinantly expressed $\alpha$-synuclein was used to synthesise $\alpha$-synuclein fibrils *in vitro*. These fibrils were then labelled with biotin to enable isolation with streptavidin coated magnetic beads. Secondly it was necessary to ensure that the labelled fibrils were internalised by cultured cells. The cells that were chosen for this study were SH-SY5Y cells, a neuronal-like neuroblastoma cell line commonly used in the study of neurodegenerative diseases. The steps involved in the development of this system are covered in the first results chapter.

In Chapter 4, proteins that interacted with $\alpha$-synuclein fibrils from SH-SY5Y cell lysate were identified. This provided both a proof of concept for the method of proteomic identification of a fibril interactome. Furthermore, by comparing the interactome of fibrillar $\alpha$-synuclein to that of monomeric $\alpha$-synuclein, it enabled fibril specific interactions to be elucidated. Due to the rapid clearance of monomeric $\alpha$-synuclein by cells this comparison could only be made in the cell lysate. A quantitative proteomic method was chosen to conduct this identification, both to enable comparison between monomeric and fibrillar $\alpha$-synuclein and to identify proteins that bound non-specifically to the beads used to isolate the fibrils. The quantitative proteomic method chosen was TMT as it offers the advantage of high sensitivity, lacking in label free techniques without the cost and time required to conduct a SILAC experiment. Chapter 4 describes the proteins identified as interactors of fibrillar and monomeric $\alpha$-synuclein when exposed to cell lysate. Furthermore it displays the result of bioinformatic analyses performed on these interactomes and identifies key pathways and cellular processes potentially affected by fibrillar $\alpha$-synuclein.

In Chapter 5 proteins that interacted with $\alpha$-synuclein fibrils following incubation and internalisation by SH-SY5Y cells, were identified. $\alpha$-synuclein fibrils were incubated with SH-SY5Y cells for 24hrs to enable internalisation. Cells were then lysed and the $\alpha$-synuclein fibrils isolated by the methodology developed in Chapter 3. Proteins interacting with $\alpha$-synuclein fibrils following incubation with SH-SY5Y cells, were then identified by TMT proteomics. By utilising similar bioinformatic

techniques as those used in Chapter 4, Chapter 5 characterises the interactomes of cells exposed to $\alpha$-synuclein fibrils and identifies a number of cellular pathways, shown to interact with internalised $\alpha$-synuclein fibrils, that warrant further investigation.

# 2

# Materials and Methods

## 2.1 Technical Equipment

| Centrifuges | |
|---|---|
| ***Avanti J-26 XP Centrifuge*** | (Beckman Coulter, Brea, CA, USA) |
| ***Eppendorf 5810R Centrifuge*** | (Fisher Scientific, Loughborough, UK) |
| ***Eppendorf 5804R Refrigerated Benchtop Centrifuge*** | (Fisher Scientific, Loughborough, UK) |
| **Incubators, Shakers and Mixers** | |
| ***Innova 43 Shaker Incubator*** | (New Brunswick Scientific, USA) |
| ***Innova 44 Shaker Incubator*** | (New Brunswick Scientific, USA) |

| | |
|---|---|
| ***SI500 orbital incubator*** | (Stuart, Staffordshire, UK) |
| ***SI600 orbital incubator*** | (Stuart, Staffordshire, UK) |

**Spectrophotometers**

| | |
|---|---|
| ***UltroSpex 2100 Pro UV/Visible Spectrophotometer*** | GE Healthcare, Little Chalfont, UK |
| ***NanoDrop 2000 Spectrophotometer*** | Thermo Scientific, Surrey, UK |

**Protein Purification**

| | |
|---|---|
| ***Büchi Vac V-500 Vacuum Pump*** | (Sigma Life Sciences, St. Louis, MO, USA) |
| ***ÄKTAprime*** | (GE Healthcare, Little Chalfont, UK) |
| ***ÄKTApure*** | (GE Healthcare, Little Chalfont, UK) |
| ***Superdex™ 75 Hiload 26/60 gel filtration column*** | (GE Healthcare, Little Chalfont, UK) |
| ***Superloop 50 mL ÄKTA*** | (GE Healthcare, Little Chalfont, UK) |

**Gel Electrophoresis Equipment**

| | |
|---|---|
| ***Slab Gel Electrophoresis Chamber AE-6200*** | (ATTO, Tokyo, Japan) |
| ***Powerpac Basic*** | (Bio-Rad Lab., Hercules, CA, USA) |
| ***Alliance Q9 chemiluminescence and spectral fluorescence imager*** | (Uvitec Cambridge, Cambridge, UK) |
| ***ChemiDoc XRS+*** | (Bio-Rad, CA, USA) |

**Electron Microscope**

| | |
|---|---|
| ***JEOL JEM-1400 transmission electron microscope*** | (JEOL USA Inc., Peabody, USA) |
| | **Microplates and Readers** |
| ***FLUOstar Omega*** | (BMG Labtech, Ortenburg, Germany) |
| ***FLUOstar Optima*** | (BMG Labtech, Ortenburg, Germany) |
| | **Other Equipment** |
| ***Grant JB1 Unstirred Waterbath*** | (Grant Instruments, Shepreth, UK) |
| ***T 18 digital ULTRA-TURRAX homogenizer*** | (IKA Dispersers, Staufen, Germany) |
| ***Jenway 3020 Bench pH Meter*** | (Bibby Scientific, Stone, UK) |

## 2.2 Protein Expression, Purification Labelling and Fibril Formation

### 2.2.1 *Escherichia coli* transformation and starter culture

*Escherichia coli* (*E.coli*) BL21 (DE3) cells (Agilent technologies, Berkshire, UK) were freshly transformed with the pET23a vector encoding $\alpha$-synuclein and spread onto an ampicillin selection plate and grown at 37 °C, 16 hours. The pET23a plasmid encoding $\alpha$-synuclein (expression under control of T7 promoter) was provided by Prof Jean Baum (Department of Chemistry and Chemical Biology, Rutgers University, NJ, USA). The pET23a plasmid encoding A18C $\alpha$-synuclein (expression under control of T7 promoter) was provided by Dr Ciaran Docherty (Faculty of Biological Science, University of Leeds, UK). The Starter culture was created by inoculating 200 mL of sterile LB medium containing 100 $\mu$g/mL ampicillin with a single colony. The inoculated medium was incubated at 37 °C, 200 rpm, 16 hours.

### 2.2.2 Preparation and purification of monomeric $\alpha$-Synuclein

10 X 1L LB medium cultures containing 100 $\mu$g/mL carbenicillin were each inoculated with 10 mL starter culture. The cells were grown at 37 °C to an OD600 of 0.6. Expression of $\alpha$-synuclein was induced with final concentration 1 mM isopropyl β-D-1-thiogalactopyranoside (IPTG) for 4 h post-induction, before harvesting by centrifugation at 4 °C, 6000 x g, 30min. Supernatant was discarded and pellets were resuspended in lysis buffer (20 mM Tris-HCl, 1 mM EDTA, 5 mM DTT, 1 mM PMSF, 2 mM benzamidine, 100 $\mu$g/ml lysozyme, 20 $\mu$g/ml DNase, pH 8.0). The pellet was homogenised and then heated to 80 °C for 10min. The homogenate was then centrifuged at 4 °C, 35,000 x g, 30min. The soluble fraction containing soluble $\alpha$-synuclein was precipitated by incubation with 50 % (w/v) ammonium sulphate at 4 °C, 30min. The suspension was centrifuged at 4 °C, 35,000 x g, 30min, and the pellet resuspended and precipitated again in 50% (w/v) ammonium sulphate, 4 °C, 30min. After a second centrifugation (4 °C, 35,000 x g, 30min) the pellet was resuspended in 20 mM Tris-HCl, pH 8.0 for anion exchange. The partially purified $\alpha$-synuclein was loaded onto a Q-Sepharose anion exchange column with a 20 mM Tris-HCl, pH 8.0 mobile phase. Elution was triggered with a linear gradient of 0-500 mM NaCl and protein elution was monitored by absorbance at 280 nm. Fractions containing $\alpha$-synuclein were analysed by SDS-PAGE, dialysed against 50 mM ammonium bicarbonate and lyophilised by snap freezing in liquid $N_2$ and drying on a lyophilizer.

Protein was resuspended in 20 mM sodium phosphate, pH 7.5, and loaded onto a HiLoad 26/60 Superdex 75 gel filtration column. $\alpha$-synuclein was eluted from the column with 20 mM sodium phosphate, pH 7.5 at a flow rate of 3 mL/min. The protein was dialysed against 50 mM ammonium bicarbonate and lyophilised. Purified protein was stored at – 20 °C. The purity of $\alpha$-synuclein was confirmed by intact mass measurement (processed through the Mass Spectrometry facility, University of Leeds).

### 2.2.3 Preparation of $\alpha$-Synuclein Fibrils

*De novo* fibrils, henceforth termed fibril seeds, were produced from $\alpha$-synuclein monomer in phosphate buffered saline (PBS). The following method is based on that described by Buell et al. [227]. Monomeric $\alpha$-synuclein was first filtered under sterile conditions by syringe-driven 0.22µm filter (Merck Millipore and Jet Biofil). $\alpha$-synuclein fibril seeds were then generated by incubation of 600µM (600µl) monomeric $\alpha$-synuclein for 3 days, at 42°C, under constant agitation by magnetic stirrer bar (1500rpm) to promote fibril fracture. Following aggregation fibrils were pelleted by centrifugation at 16000×g for 40min in a benchtop microfuge, resuspended at 100µM, flash frozen in liquid $N_2$ and stored at -80°C until use. PBS was used as a buffer for all steps. Elongated fibrils were produced by incubation of 100µM $\alpha$-synuclein monomer with $\alpha$-synuclein fibril seeds (10% v/v unless otherwise stated) for 5 days at 37°C. 1 30 second period of shaking (300rpm) was applied every 10min to ensure fibrils remained in suspension.

### 2.2.4 Labelling of $\alpha$-Synuclein

#### N-hydroxysuccinimide (NHS) labelling of $\alpha$-Synuclein monomer

Lyophilised $\alpha$-synuclein monomer was resuspended in PBS at a concentration of 100µM. Monomeric $\alpha$-synuclein was incubated in 10× NHS-Biotin (Sigma-Aldrich, Germany) or NHS-5-carboxytetramethylrhodamine (TAMRA) at 4°C for 16hrs. Unbound label was then removed by Zeba™ spin desalting column 7kDa molecular weight (MW) cutoff (Thermo Fisher Scientific, USA).

#### Maleimide Labelling of A18C $\alpha$-Synuclein Monomer

Lyophilised $\alpha$-synuclein monomer was resuspended in PBS at a concentration of 100µM. Dithiothreitol (DTT) was added to a final concentration of 5mM and incubated for 30min to reduce the disulphide bonds. DTT was removed by Zeba spin desalting column <7kDa MW cutoff. Monomeric $\alpha$-synuclein was then immediately incubated in 10× Biotin Maleimide (Sigma-Aldrich, Germany) at 4°C for 16hrs.

Unbound label was then removed by Zeba™ spin desalting column 7kDa MW cutoff (Thermo Fisher Scientific, USA).

#### Maleimide Labelling of A18C $\alpha$-Synuclein Fibril Seeds

Fibril seeds were generated from A18C $\alpha$-synuclein monomer as described in Section 2.2.3. Fibril seeds were diluted to a concentration of 100µM (monomer equivalent) and DTT was added to a final concentration of 5mM. $\alpha$-synuclein Fibril seeds were incubated in DTT for 30min to reduce the disulphide bonds. $\alpha$-synuclein Fibril seeds were then pelleted by centrifugation at 16000$\times g$ for 40min. The soluble fraction was aspirated and replaced with PBS. Pelleting was repeated three times to remove DTT. $\alpha$-synuclein fibrils were then incubated with 10× Biotin Maleimide (Sigma-Aldrich, Germany) or Alexa Flour® 594 Maleimide (Invitrogen USA), at 4°C for 16hrs. Unbound label was then removed by repeated pelleting of $\alpha$-synuclein fibrils as for removal of DTT.

### 2.2.5 Negative Staining TEM

Imaging by negative staining TEM was done to validate fibril formation. Imaging was done in a JEOL 1400 electron microscope operating at 100 kV. Micrographs were taken at 5000 X - 15000 X magnification and captured with an AMT 2k CCD camera (AMT Corp., MA) in the Astbury BioStructure laboratory at the University of Leeds. For fibril TEM, 10 uL aliquots of $\alpha$-synuclein fibril were adsorbed for 40 seconds on to carbon coated glow discharged copper grids. They were then washed twice with water and subsequently stained with 2% uranyl acetate for 40 seconds. Grids were left to dry at room temperature and stored until used.

### 2.2.6 Fibril Pelleting Assay

Fibrils were pelleted by centrifugation in a bench-top microfuge at 16000 $\times$ $g$ for 40min. The soluble fraction (Supernatant) was carefully removed so as not to disturb the pellet. The pellet was resuspended in an equal volume of buffer. To determine fibril yields, sample buffer was then added to both fractions and the relative presence of $\alpha$-synuclein in each sample assessed by sodium dodecyl sulfate (SDS) - polyacrylamide gel electrophoresis (PAGE) (SDS-PAGE) (Section 2.3.1). Densitometry analysis on experiments conducted in triplicate was conducted in the Fiji image analysis software. The normalised data in this thesis is a product of processing using the plate reader software and normalised (after buffer subtraction) between 0 and 100.

### 2.2.7 ThT Aggregation Assay

$\alpha$-synuclein fibril reaction was prepared as per elongated fibrils (Section 2.2.3) and ThT added to a final concentration of 20 $\mu$M and and dispensed into Corning 96-well flat bottom assay plates. The plate was incubated at 37 °C. The samples were excited at 444 nm and the fluorescence emission was monitored at 480 nm on a BMG Labtech FLUOstar optima plate reader. The gain was set at 350.

### 2.2.8 Streptavidin Magnetic Bead Pull-Down

Streptavidin coated magnetic DynaBeads™ C1 (Thermo Scientific, USA), were washed of storage solution by applying a magnet to the side of a 1.5ml eppendorf to pellet the beads, removing the storage buffer and applying an equal volume of pull-down wash buffer (PBS + 0.1% Tween 20). Beads were resuspended by gentle pipetting. This washing step was repeated 3 times. The washed magnetic beads were then added to the samples in 1.5ml eppendorfs at the concentrations described below. Pull-down suspensions were incubated for 1hr at RT (or 4 °C if cell lysate present) with constant agitation on rotator disk to ensure beads remain in suspension. A magnet was then applied to the edge of the eppendorf to pellet the DynaBeads™ and the solution (termed Flow Through) was removed. The beads were then washed in 3 times by gently resuspending beads in pull-down wash buffer pull-down wash buffer. Wash buffer was then removed by applying a magnet to the side of eppendorf to pellet the beads and the wash buffer was aspirated. The DynaBead™ bead pellet was then transferred to a new eppendorf and termed the Pull-Down fraction.

## 2.3 Biochemistry Techniques

| Buffers | |
|---|---|
| ***SDS-PAGE resolving gel buffer*** | 1 M Tris-HCl pH 8.45, 0.1 % (w/v) SDS, 15 % (v/v) acrylamide, 13 % (v/v) glycerol, 0.7 % (w/v) TEMED, 0.07 % (v/v) TEMED |
| ***SDS-PAGE stacking gel buffer*** | 750 mM Tris-HCl pH 8.45, 0.07 % (w/v) SDS, 4 % (v/v) acrylamide, 0.32 % (w/v) APS, 0.16 % (v/v) TEMED |
| ***SDS-PAGE loading buffer (×2 concentrated stock)*** | 2 % (w/v) SDS, 10 % (v/v) glycerol, 0.1 % bromophenol blue, 100 mM DTT |
| ***SDS-PAGE cathode buffer (×10 concentrated stock)*** | 1 M Tris, 1 M Tricine, 1 % (w/v) SDS (pH 8.25) |
| ***SDS-PAGE anode buffer (×10 concentrated stock)*** | 2 M Tris-HCl (pH 8.8) |
| ***Tris Buffered Saline + Tween 20 (TBST)*** | 0.1% (v/v) tween (TBS-T), 20 mM Tris-HCl, 150 mM NaCl, pH 7.2 |

| Antibodies | |
|---|---|
| ***Anti-Biotin (Streptavidin-HRP)*** | (Termo Fisher Scientific, NY, USA) |
| ***Anti-Alpha-synuclein antibody [syn211] (ab80627)*** | Abcam, Cambridge, UK |
| ***Rabbit Anti-Mouse IgG H&L (HRP) (ab6728)*** | Abcam, Cambridge, UK |

### 2.3.1 SDS-PAGE

Tris-tricine buffered SDS-PAGE was used for confirming the purification of $\alpha$-synuclein and to separate according to molecular weight. Two glass plates were assembled to set a gel of 1.5 mm thickness. Resolving and stacking gel solutions were freshly prepared and APS and TEMED added immediately before casting. 12-well combs were inserted into the stacking gel at the point of pouring to create sample loading wells and gels were set for 1 hr. Electrophoresis 1x cathode and 1x anode buffers were added to the inner and outer reservoirs of the gel tanks respectively. Sample was diluted in SDS-PAGE loading buffer to a final concentration of 1x, and boiled for 5min prior to loading 15 µL per lane.

5µl of Precision Plus Protein Dual Xtra Prestained protein standard (Bio-Rad Laboratories) was loaded into one lane of the gel for molecular weight determination. Gels were electrophoresed at a constant current of 30 mA until samples entered the resolving gel, and then the current was increased to 60 mA until the dye front left the gel.

### 2.3.2 Staining of SDS-PAGE gels

Gels were removed from the glass casts and stained with Instant Blue (Abcam, Cambridge, UK) or Silver Stain (Thermo Fisher, USA). For Instant Blue staining, the stain was added to the protein gel for a minimum of 1hr on a rocking table until bands developed. Silver staining was conducted per the manufacturer's instructions.

### 2.3.3 Western Blot

Samples were run by SDS-PAGE (Section 2.3.1) and unstained gels transferred to an methanol-activated PVDF membrane (0.45 $\mu$m pore size, Amersham, GE Healthcare) using a BioRad semi-dry transfer blotter for 1hr, 12 V. The protein was fixed onto the membrane with 4% formaldehyde, and then blocked with 5% (w/v) bovine serum albumin (BSA), in TBST for 1hr, RT. Following blocking, membranes were incubated overnight, 4 °C, in desired primary antibody stocks, both stocks in 5% (w/v) BSA TBS-T solution). The membrane was subsequently washed twice in TBS-T and then left incubating 1 h, RT, in desired secondary antibody stocks (anti-mouse HRP or anti-rabbit HRP secondary antibodies in TBS-T (1:2000)). For detection, the membrane was washed twice in TBS-T and twice in TBS and chemiluminescence was detected using the SupersSignal West Pico PLUS substrate (Thermo Fisher) following the manufacturer's instructions.

## 2.4 Cell Culture and Imaging

| Antibodies and Cell Dyes | |
|---|---|
| ***Anti-LAMP1*** | H4A3 mouse monoclonal (Abcam, UK) |
| ***Lysotracker™ Green*** | Lysosomal dye (ThermoFisher Scientific, USA) |
| ***CellMask™*** | Cell membrane dye (ThermoFisher Scientific, USA) |
| ***Anti-Mouse Alexa Flour® 488*** | (Invitrogen, CA, USA) |
| ***NeutrAvidin™ Texas Red™*** | (Invitrogen, CA, USA) |
| ***HRP Conjugated Streptavidin*** | (Thermo Scientific, USA) |
| ***Hoechst 33342*** | Nuclear stain (Invitrogen, CA, USA) |
| **Cells** | |
| ***SH-SY5Y Cells*** | (American Type Culture Collection (ATTC), Virginia, USA) |
| **Media** | |
| ***Full Media*** | (Gibco Dulbecco's Modified Eagle Medium (DMEM) (Thermo Scientific, UK) 5% supplemented with 10% FBS (Sigma-Aldrich), 1% (v/v) GlutaMAX (Gibco), 20 units/ml penicillin, 20 mg/ml streptomycin (Penn-Strep, Gibco)) |

### 2.4.1 Recovery of cells from frozen stocks and cell maintenance

Frozen SH-SY5Y cells were removed from liquid $N_2$ storage and quick-thawed by briefly placing cryovials in a water bath, 37°C. Cells were then resuspended in Full Media and grown in 75 cm2 culture flasks. Cells were incubated at 37°C, 5% CO2. After 24 h, medium was replaced with fresh full media. To maintain, cells were passaged using a 0.25% Trypsin-EDTA solution (Sigma-Aldrich) to lift the cells when they reached 80% confluency.

### 2.4.2 Confocal Microscopy

Confocal images were acquired on an LSM700 confocal microscope at 40x magnification using an oil immersion lens unless otherwise stated. The individual laser gain was adjusted such that the image was as bright as possible without introducing noise in the negative control. Acquired images were processed using the Fiji image editing software to apply false color and a scale bar.

### 2.4.3 Cellular Internalisation of $\alpha$-Synuclein

SH-SY5Y cells were plated into individual FluoroDishes 35mm (World Precision Instruments) at 300 000 cells per well and cultured as above for 24hrs to allow cells to adhere to the base of the dish. Fibrillar $\alpha$-synuclein was then added to the culture media to a final concentration of 1µM (monomer equivalent concentration). Prior to addition fibrils were sonicated in a bath sonicator for 10min to reduce clumping and increase fibril length homogeneity. Fibrils were then incubated with the cells for 24hrs. Culture media was removed and cells were washed 3 times in PBS.

For live cell imaging cells were at this point incubated with Lysotracker™ Green (ThermoFisher Scientific) for lysosome visualisation and CellMask™ for visualisation of the cell membrane, per manufacturer's instructions. For fixed cell imaging cells were then fixed in fixative buffer (PBS, 4% formaldehyde, 1% sucrose) for 15minutes. Cells were then permeabilised with permeabilization buffer (PBS, 3% BSA, 0.1% Saponin) for 1hr at RT. Cells were then probed with anti-LAMP1 antibody in permeabilization buffer for 1hr at RT. Fixed cells were then washed 3 times in PBS for 5min each. Cells were then probed with anti-mouse conjugated Alexa-Flour™ 488 and, when probing biotin, Neutravidin conjugated Texas Red for 1hr at RT. Finally cells were washed 3 times in PBS and 5mM Hoechst 33342 added to visualise the nuclei 5min prior to imaging by confocal microscopy Section 2.4.2.

### 2.4.4 Intracellular $\alpha$-Synuclein Seeding with exogenous $\alpha$-Synuclein Fibrils

SH-SY5Y cells overexpressing a green flourescent protein (GFP)-$\alpha$-synuclein construct cells (kindly gifted by Dr. Eric Hewitt) were plated into individual FluoroDishes 35mm (World Precision Instruments) at 100 000 cells per well and cultured as described in Section 2.4.1 for 24hrs to allow cells to adhere to the base of the dish. Fibrillar $\alpha$-synuclein was then added to the culture media to a final concentration of 1µM. Prior to addition fibrils were sonicated in a bath sonicator for 10min to reduce clumping and increase fibril length homogeneity. Fibrils were then incubated with the cells for 5 days. Culture media was removed and cells were washed 3 times in

PBS. Cells were gently permeabilised in permeabilization buffer for 15min and then washed in PBS, to remove soluble $\alpha$-synuclein-GFP. Great care was taken not to detach the cells from the plate. Cells were then incubated with fixative buffer for 15min and finally 5mM Hoechst 33342 added to visualise the nuclei 5min prior to imaging by confocal microscopy Section 2.4.2.

## 2.5 Proteomic Experiments

### 2.5.1 Pull-Down of Biotinylated A18C $\alpha$-Synuclein Fibril Seeds From SH-SY5Y Cell Lysate

SH-SY5Y cells were plated into 35mm 6 well plates (Corning, NY, USA) at a concentration of 300k cells per well and maintained in cell culture media for 24hrs. 1× 6 well plate was used per experimental repeat for a total of 1800k cells per experimental repeat. Cells were detached from plates using plastic cell scrapers (Nunc, NY, USA) . For each experimental repeat, detached cells were pelleted at $300 \times g$ for 5min, the cell media was aspirated and the pellet resuspended in PBS. Pelleting and resuspension was repeated three times to remove cell media.

Pelleted Cells were resuspended in lysis buffer (PBS + Triton X 100 + mixed protease inhibitors (Pierce)) and incubated at 4°C for 1hr. Lysate then underwent centrifugation ($2000 \times g$, 5min) to remove cellular debris. The concentration of lysate was then determined by bicinchoninic acid (BCA) assay (Pierce) using provided BSA standards per manufacturer's instructions.

For fibril added condition, 1mg of lysate (by protein concentration) was incubated with $1 \times 10^{-9}$µ mols of biotinylated A18C $\alpha$-synuclein fibril seeds for 1hr at 4°C. For the control (no fibrils added) condition lysate was incubated at 4°C for 1hr. Pull down by streptavidin coated magnetic DynaBeads™ was performed on both fibril added and control samples. For pull-down experiments 100µg of streptavidin coated magnetic DynaBeads were added to each sample and processed as described in Section 2.2.8.

### 2.5.2 Pull-Down of Biotinylated A18C $\alpha$-Synuclein Fibril Seeds and Biotinylated A18C $\alpha$-Synuclein Monomer From SH-SY5Y Cell Lysate

SH-SY5Y cells were plated into 35mm 6 well plates (Corning, NY, USA) at a concentration of 300k cells per well and maintained in cell culture media for 24hrs. 1× 6 well plate was used per experimental repeat for a total of 1800k cells per experimental repeat. Cells were detached from plates using plastic cell scrapers (Nunc, NY, USA). For each experimental repeat, detached cells were pelleted at $300 \times g$ for 5min, the cell media was aspirated and the pellet resuspended in PBS. Pelleting and resuspension was repeated three times to remove cell media.

Pelleted Cells were resuspended in lysis buffer (PBS + Triton X 100 + mixed protease inhibitors (Pierce)) and incubated at 4°C for 1hr. Lysate then underwent centrifugation ($2000 \times g$, 5min) to remove cellular debris. The concentration of

lysate was then determined by BCA assay (Pierce) using provided BSA standards per manufacturer's instructions.

For fibril and monomer added conditions, 1mg of lysate (by protein concentration) was incubated with $1 \times 10^{-9}$µmols (monomer equivalent) of biotinylated A18C $\alpha$-synuclein fibril seeds or biotinylated A18C $\alpha$-synuclein monomer respectively, for 1hr at 4°C. For the control (no $\alpha$-synuclein fibrils or monomer added) condition, lysate was incubated at 4°C for 1hr. Pull down by streptavidin coated magnetic DynaBeads™ was performed on both fibril added and control samples. For pull-down experiments 2.5mg of streptavidin coated magnetic DynaBeads were added to each sample and processed as described in Section 2.2.8.

### 2.5.3 Pull-Down of Biotinylated A18C $\alpha$-Synuclein Fibril Seeds Following Incubation With SH-SY5Y Cells

SH-SY5Y cells were plated into 35mm 6 well plates (Corning, NY, USA) at a concentration of 300k cells per well and maintained in cell culture media for 24hrs. 1× 6 well plate was used per experimental repeat for a total of 1800k cells per experimental repeat. For the fibril added condition, biotinylated A18C fibril seeds were added to each of the six wells to a final concentration of 1µM. For the control condition, an equivalent volume of PBS was added. The cells were then incubated for 24hrs under standard cell culture conditions. Following incubation the cells were detached from plates using plastic cell scrapers (Nunc, NY, USA).Detached cells were then pelleted at $300 \times g$ for 5min, the cell media was aspirated and the pellet resuspended in PBS. Pelleting and resuspension was repeated three times to remove cell media.

Pelleted Cells were resuspended in lysis buffer (PBS + Triton X 100 + mixed protease inhibitors (Pierce)) and incubated at 4°C for 1hr. Lysate then underwent centrifugation ($2000 \times g$, 5min) to remove cellular debris. The concentration of lysate was then determined by BCA assay (Pierce) using provided BSA standards per manufacturer's instructions.

Protein concentrations were then normalised between the samples. Pull down by streptavidin coated magnetic DynaBeads™ was performed on both fibril added and control samples. For pull-down experiments 100µg of streptavidin coated magnetic DynaBeads were added to each sample and processed as described in Section 2.2.8.

### 2.5.4 Proteomics

Following isolation by streptavidin coated magnetic DynaBeads, samples were shipped to the proteomics facility at Bristol University, where TMT analysis of the samples was conducted.

### 2.5.5 Bioinformatic Analysis

For analysis of TMT proteomic data, the data was first filtered by removing any fibrils that were identified in the database of contaminants during peptide identification. Next proteins with fewer than 3 peptide identifications were eliminated as were proteins with an false discovery rate (FDR) (the probability that the identification could be made by chance) $< 0.01$. The FDR was calculated using the method described by Benjamini and Hochberg [325]. The abundance of each protein in an experimental sample was then compared with its abundance in its matched control sample. The mean fold change in abundance between the control sample and the experimental samples was then calculated for each experimental condition (e.g. $\alpha$-synuclein Fibril added vs no fibril added), and the p-value of that fold change calculated. Proteins with a fold change of $> 1.5$ and a p-value of $< 0.01$ were considered specific to the experimental condition (i.e. belonged to the $\alpha$-synuclein fibrillar or monomeric interactome).

#### Gene ontology (GO) term overrepresentation

GO term overrepresentation analysis (identification of protein associated GO terms that appear more frequently in the interactome than would be predicted by chance given a background proteome) of $\alpha$-synuclein monomeric and fibrillar interactomes was conducted using the BiNGO [326] and ClueGO [327] plugins for Cytoscape. GO terms were mapped from the protein accession numbers (Uniprot) identified by proteomic analysis. The proteomic background for the analysis was set to that of SH-SY5Y cells and the FDR required for a GO term to be considered overrepresented was to be less than 0.01.

StringDB network analysis of proteins present in an interactome was conducted via the StringApp Cytoscape plugin. StringDB IDs were mapped from the interactome protein accession numbers (Uniprot) identified by proteomic analysis. Protein protein interactions (edges in the network) were considered if their score, calculated by StringDB based on the evidence for the interaction, was greater than 0.6. Clustering analysis of the network was performed in Cytoscape via the Markov clustering (MCL) algorithm. The inflation parameter for MCL clustering was set to 2.0 and the edges were weighted by the protein-protein interaction score calculated by StringDB.

#### Comparison with other proteomic studies

Interactomes identified by other studies were drawn from the supplementary data of the papers indicated. The gene names for each protein in both external interactomes and the interactomes identified herein were mapped via the Uniprot ID mapping service or from the file describing the interactome, if available. The Jaccard Coefficient

(a measure of set similarity) is defined as:

$$J(A, B) = \frac{|A \cap B|}{|A \cup B|}$$

Where A is the set representing proteins identified in one interactome and B is a set representing proteins identified in another. The calculated value, a number between 1 and 0, is a measure of the similarity of the sets with 1 representing two identical sets and 0 representing two unique sets.

### Solubility and LCR analysis

The solubility and LCR analysis of each protein in the given interactome was conducted by CamSol [328] and fLPS [329] software respectively. The protein sequences required for this analysis were mapped from the interactome protein accession numbers (Uniprot) using the Uniprot service.

# 3

# Developing the Methodology for Synthesising and Isolating $\alpha$-synuclein Fibrils

## 3.1 Aims

The overall aim of the project was to identify interaction of $\alpha$-synuclein following internalisation by neuronal like cells. Therefore, in this chapter, a method was developed by which $\alpha$-synuclein fibrils can be synthesised and labelled in such a way that it is possible to extract them from a buffer or protein mixture. It was then demonstrated that these fibrils are internalised by SH-SY5Y cells, a neuronal like cell line commonly used in the study of $\alpha$-synuclein and other neurodegenerative amyloid conditions.

## 3.2 Introduction

### 3.2.1 Production of $\alpha$-Synuclein *in vitro*

#### Recombinant $\alpha$-Synuclein

The use of recombinant $\alpha$-synuclein in the study of synucleinopathies has enabled the study of both *in vivo* and *in vitro* properties of $\alpha$-synuclein monomeric, oligomeric and fibrillar conformations [330, 331]. For example, recombinant $\alpha$-synuclein has been used extensively to study the fibril morphology, giving rise to multiple fibril structures by a number of methodologies [18, 232, 233]. Moreover, investigation into the kinetics of $\alpha$-synuclein fibril formation has relied exclusively on recombinant protein to provide the required purity of sample for study [230, 330]. Meanwhile, recombinant protein has likewise been used to study the cellular effects and toxicity of fibrillar and oligomeric species [262, 332, 333]. The extracellular application of pre-characterised conformations of $\alpha$-synuclein, has not only enabled such studies to elucidate several methods by which $\alpha$-synuclein may be responsible for synaptic deficiency and neuronal loss, but further to attribute the cause of this damage to defined species [262, 332, 333].

#### *In vitro* fibril synthesis

There are several methods for synthesis of fibrils from recombinant $\alpha$-synuclein protein many of which have been highly characterised, including the generation of high resolution structures of fibril morphology, and the characterisation of fibril growth kinetics [18, 232–234]. The aggregation propensity of $\alpha$-synuclein is lower than that of other amyloid proteins such as A$\beta$, though under the right conditions $\alpha$-synuclein can be driven to aggregate [331]. *De novo* (i.e. unseeded aggregation of monomeric $\alpha$-synuclein) aggregation of $\alpha$-synuclein typically requires high monomer concentrations and constant agitation [224]. A number of other solution conditions may also affect the rate of aggregation [227]. As different fibril morphologies produced under different conditions may exert differing biological effects [247, 332], ensuring a consistent fibril morphology is important for understanding how $\alpha$-synuclein fibril structure relates to function.

**Monomer concentration** The concentration of $\alpha$-synuclein monomer used in the assembly reaction is a key factor in determining the kinetics of fibril formation [334]. The minimum concentration of $\alpha$-synuclein required for fibril formation is estimated to be approximately $0.2\,\mathrm{mg\,ml^{-1}}$ [335]. Above this concentration, fibril length has been found to directly correlate with initial monomer concentration [335],

though this concentration dependance disappears in the presence of high monomeric concentrations [335, 336]. Typically, concentrations in the range of 0.5 to 7 mg ml$^{-1}$ are used [334]. Herein a concentration of 500 µM was used to synthesise *de novo* $\alpha$-synuclein fibrils (henceforth termed $\alpha$-synuclein fibril seeds), while 100 µM was used for elongation reactions, consistent with those used elsewhere [227, 337].

**Agitation** Another major condition that can dramatically effect the kinetics and morphology of *in vitro* fibrils is the presence of agitation [227, 334]. Under quiescent conditions the lag phase of $\alpha$-synuclein fibril formation lasts for several weeks, however, agitation of the monomeric solution can shorten this to hours [338]. This increase in aggregation rate may be the result of an increase in the air-water interface, thereby inducing a partial folding of $\alpha$-synuclein and promoting the formation of an aggregation intermediate [339]. Furthermore, agitation of can induce fibril breakage [340] leading to an increase in elongation ends and an acceleration of fibril formation [341].

Furthermore, fragmentation of fibrils by agitation during fibrillation produces fibrils of relatively homogeneous length and height [337, 340, 342]. Several common methods of agitation exist including agitation by mini stir bar, resulting in greater fragmentation [337, 340, 342], or in microplates on an orbital shaker [334]. It has been shown that a reduction in the lag time of fibril formation greatly improves reproducibility of fibril synthesis [343]. Therefore, this combined with the reduction in fibril length variability, marks agitation as an effective way of reducing variability between fibrils. In order to generate $\alpha$-synuclein fibril seeds that demonstrated reproducible elongation kinetics, monomeric $\alpha$-synuclein was aggregated under constant agitation by magnetic stir bar [227].

**Solution conditions** Several other conditions are highly important to the kinetics of $\alpha$-synuclein fibril formation including: temperature, pH and ionic strength. Several studies have reported that decreasing the pH at which the fibrillation reaction occurs, substantially increases the rate of fibril formation [227, 344]. Furthermore, although $\alpha$-synuclein fibrils can form under a wide variety of pH conditions, rapid growth only occurs under acidic pHs approximating those found in endosomes and other organelles [227]. In addition to the speed at which fibrillation occurs, changes in pH also affect the rate of secondary nucleation [227]. At neutral pH fibril elongation dominates the fibril growth reaction however, at pH values below pH 7 dramatically increasing the rate of secondary nucleation [227].

Increasing the temperature at which the fibrillation reaction occurs is likewise capable of increasing the rate of fibril formation [344]. The increase in temperature induces structural changes in $\alpha$-synuclein monomer, as measured by far-UV

circular dichroism (CD) and Fourier transform infra-red (FTIR). This contributes to a reversible transformation of the $\alpha$-synuclein monomer into a partially folded conformation, which predisposes the monomer to fibril formation [344]. The assembly of $\alpha$-synuclein fibrils herein, was conducted in PBS (pH 7.4) and 42°C in order to generate reproducible fibril morphologies [227].

### 3.2.2 Cellular Models of Amyloid Disease

#### SH-SY5Y cells as a disease model in synucleinopathies

The SH-SY5Y cell line is a human derived neuroblastoma cell line isolated from a bone marrow biopsy [345, 346]. The cell line is commonly used in the study of neurodegenerative diseases as a model system including in the study of $\alpha$-synuclein pathogenicity and Parkinson's disease [347]. This cell line displays many characteristics of a dopaminergic neuron. Characterisation of the cell line has shown it has tyrosine hydroxylase activity [348], the rate-limiting enzyme of the catecholamine synthesis pathway responsible for the conversion of tyrosine to L-dopa the precursor to dopamine and dopamine-β-hydroxylase [346], responsible for converting dopamine to noradrenaline. Although the SH-SY5Y cell line cannot be considered purely dopaminergic, its capability to sythesise the neurotransmitter is important as Parkinson's disease is classically considered a disease of dopaminergic neuron. Furthermore, although the cancer derived cell line has a number of genetic abnormalities, most of the pathways found to be dysregulated in Parkinson's disease are unaffected in SH-SY5Y cells [349].

#### Cellular internalisation of $\alpha$-Synuclein fibrils

There is evidence to suggest that the spread within the brain occurs due to the transmission of $\alpha$-synuclein aggregates between cells [187, 251–253, 259]. There is clinical evidence of spread of LB pathology from diseased regions of the brain into healthy transplanted mesencephalic dopaminergic neurons, suggesting propagation of $\alpha$-synuclein aggregates into the grafted cells [251, 252]. Secondly, *in vitro* evidence has demonstrated transmission of $\alpha$-synuclein fibrils between cultured cells overexpressing $\alpha$-synuclein: these fibrils are capable of seeding new inclusions in healthy cells in a prion-like manner [253].

Furthermore, cells were shown to internalise recombinant pre-formed fibrillar $\alpha$-synuclein from the cell media [262, 263], thus providing a model for cell to cell transmission of LB pathology. This internalisation was seen as early as 24hrs after incubation with the exogenous $\alpha$-synuclein fibril seeds [259]. Cellular internalisation of fibrils is commonly demonstrated through the use of antibodies against $\alpha$-synuclein,

or through fluorescent labelling of $\alpha$-synuclein fibrils prior to addition [253, 259, 262, 263].

#### Seeding of intracellular inclusions

It has been demonstrated that in addition to internalisation by SH-SY5Y cells, $\alpha$-synuclein fibrils can induce LB like pathology in cells. It was shown that the addition of pre-formed fibrils to the media of cultured neurons was capable of inducing the formation of insoluble $\alpha$-synuclein aggregates within cells, an event that occurred at around 5-10 days [262]. Soluble or oligomeric species of $\alpha$-synuclein however, were incapable of inducing inclusion formation [262]

The intracellular inclusions, formed as the result of exogenous fibril application, display similar properties to those of disease related LB [263], being both reactive to antibodies against misfolded $\alpha$-synuclein, and to antibodies against ubiquitinated $\alpha$-synuclein and $\alpha$-synuclein phosphorylated at S129 [263], post-translational modifications strongly linked with pathological LB inclusions [266]. Furthermore, it has been demonstrated that endogenous $\alpha$-synuclein protein is recruited into the inclusion bodies, following internalisation indicating that this is true "seeding" of intracellular aggregation [262, 263].

Detection of these inclusion bodies has been shown by a number of methods. One method is via the use of antibodies against pathological forms of $\alpha$-synuclein [263]. This includes the use of antibodies against phosphorylated, ubiquitinated and aggregated $\alpha$-synuclein [253, 263]. Alternatively the use of a transfected GFP-tagged variant of $\alpha$-synuclein, reproduces many of the same findings [350]. Therein, intracellular seeding was demonstrated by the formation of GFP puncta within the cell following prolonged incubation with $\alpha$-synuclein [350].

### 3.2.3 Isolation of fibrils for proteomics analysis

The aim of this project was to identify the cellular, protein-protein, interactions of $\alpha$-synuclein with the goal of potentially identifying pathways or intracellular complexes that are disrupted during amyloid aggregation. Several studies have previously investigated the intracellular interactions of a number of amyloid proteins including poly-Q expanded huntingtin [267], the A$\beta$ precursor APP [351], as well as 'artificial' amyloid proteins, designed proteins that mimic pathogenic amyloid proteins with a capacity for forming cross-$\beta$ fibrillar structures *in vitro*. In order to facilitate the identification of intracellular proteins interacting with amyloid fibrils these studies similarly required a method of isolation, and likewise chose to leverage magnetic pull-downs for this purpose.

Several methods for isolating a protein of interest from a cell extract exist.

These methods can be broadly divided into antibody based isolation methods and tag based isolation methods. The aforementioned studies investigating proteome interactions, looked to investigate the interactions of fibrils within mammalian systems, overexpressing a tagged form of the amyloid protein under investigation. In the case of elucidating the poly-Q expanded Huntingtin interactome, the protein was expressed as a GFP conjugate to enable visualisation, with the added benefit of antibody based isolation of the GFP tag [267]. By this method, cells overexpressing a variety of huntingtin poly-Q expansions, mapping to monomeric, oligomeric and fibrillar conformers of protein, could be analysed to identify the cellular interactomes of these conformations. Futhermore the addition of the GFP tag enabled intracellular tracking and puncta identification, facilitating classification of the expressed protein into monomeric, oligomeric and fibrillar subtypes [267].

Though this technique proved effective, identifying several key pathways affected by the aggregation of poly-Q expanded huntingtin, there are a number of caveats to using GFP tagged proteins for this purpose. Firstly, the size of GFP is significant, increasing the number of intracellular proteins that will interact with the GFP tag rather than the protein of interest. Though this is mitigated when comparing conditions via quantitative proteomics [267], it nonetheless increases the background interactions which can lead to false positive identification of protein interactions. Secondly, this method of tagging limits the investigation of the interactome to that of the cell overexpressing the construct. Identification of the interactions that occur during fibrillar internalisation by a cell, could not be achieved. Finally, *in vivo* expression of amyloid proteins, though capable of forming fibril like structures, does not permit the fine-grain control over amyloid conformations that is available to fibrils synthesised *in vitro*. Therefore, the interactomes of amyloid proteins expressed intracellularly is likely to represent the interactomes of multiple conformations [267].

Another methodology available for the isolation of fibrils is the conjugation of fibrils with a small molecule such as biotin. Biotin interacts with the homotetramer streptavidin, and is commonly used in applications requiring protein isolation due to the strength and specificity of this interaction [352]. Indeed, the use of biotinylated fibrils has been used to identify potential cell surface interactors of $\alpha$-synuclein fibrils that may be responsible for cellular internalisation [260]. Importantly, it was shown that the addition of biotin did not significantly alter $\alpha$-synuclein fibril morphology [260].

For the study described in this chapter, biotinylation was chosen as the method for enabling fibril isolation as it is straightforward to perform, and was likely to be minimally disruptive to $\alpha$-synuclein fibril formation.

### 3.2.4 Overview

Using recombinantly expressed $\alpha$-synuclein monomer, $\alpha$-synuclein fibrils were generated *in vitro*. These fibrils were then labelled with biotin and it was shown that fibrils could be isolated from storage buffer by use of streptavidin coated magnetic beads. Moreover, $\alpha$-synuclein fibrils generated herein were shown to be internalised by the neuronal-like SH-SY5Y cell line.

## 3.3 Results

### 3.3.1 Purification of $\alpha$-Synuclein

The investigation of cellular interactions by fibrillar $\alpha$-synuclein following endocytic internalisation, required the generation of $\alpha$-synuclein fibrils. The decision was made to synthesise fibrils from recombinant $\alpha$-synuclein in a similar manner to other studies investigating the internalisation of $\alpha$-synuclein [253, 259, 262]. Spiking of biotinylated monomeric $\alpha$-synuclein into elongated $\alpha$-synuclein fibrils via the fibril growth reaction, would in theory enable internalised fibril to be isolated, by means of streptavidin coated Dynabeads, enabling analysis of protein-protein interactions in a cellular context. Furthermore, this approach would enable the use of fluorescently labelled monomer to be spiked into the fibrillation reaction, enabling monitoring of fibril location by fluorescence microscopy as previously described [253, 259, 262, 263].

Therefore, for this purpose, recombinant $\alpha$-synuclein monomer was produced and purified from *E.coli* (as described in Section 2.2.2). Briefly this involved the transfection of *E.coli* BL21 DE3 with a plasmid containing the gene encoding full length human $\alpha$-synuclein, under the T7 promoter. $\alpha$-synuclein expression was induced by addition of IPTG and the cells harvested and lysed to release intracellular protein. $\alpha$-synuclein monomer was then purified first by ammonium sulphate precipitation then by anion exchange chromatography. Finally, the protein was subjected to size exclusion chromatography (SEC) dialysed into ammonium bicarbonate and lyophilized for storage at -20°C. The purity of the purified monomer was determined by analysis of the SEC purification trace and by subsequent MS analysis of the lyophilized protein.

The SEC purification trace confirmed that the sample eluted largely as a monomeric protein, showing only a small secondary peak, eluting at a lower volume (Fig. 3.1A). SDS-PAGE analysis of protein eluting in this peak showed a single band at 14.5 kDa (Fig. 3.1B). The presence of $\alpha$-synuclein in the sample was further confirmed by MS analysis of the purified protein, demonstrating a single high intensity peak at 14 460.40 Da (Fig. 3.1C), within 1 Da of the theoretical mass of $\alpha$-synuclein (14460.16). This discrepancy is within the margin of error for the instrument in use. It was therefore determined that the purified protein was of the correct molecular weight for monomeric $\alpha$-synuclein, and showed minimal oligomeric impurities.

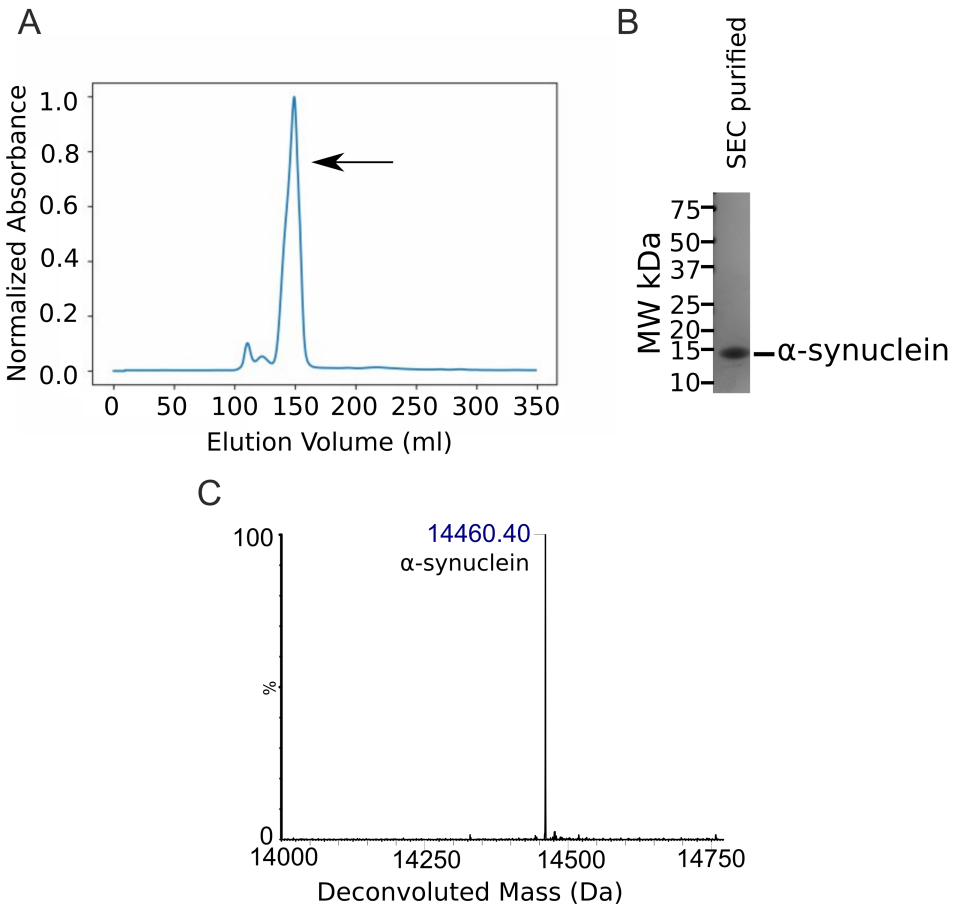


***Figure 3.1:*** *Recombinant WT α-synuclein is purified as monomeric protein. A) SEC trace of WT α-synuclein purification showing largely monomeric conformation. Only the protein from the large peak at 150ml was collected and lyophilized. Arrow denotes collected peak. B) Coomassie stained, SDS-PAGE gel of the collected SEC peak showing a protein with the predicted MW of α-synuclein. C) Deconvoluted MS spectrum showing the molecular weight of the purified protein. This closely matches the theoretical weight of monomeric α-synuclein (14460.16 Da)*

.

### 3.3.2 Synthesis of Fibrils from $\alpha$-Synuclein Monomer

Having purified $\alpha$-synuclein monomer the next step was to generate the fibrils that could be used to identify cellular proteins that interact with fibrils. There are many methods in common use for generating *de novo* $\alpha$-synuclein fibrils from recombinant $\alpha$-synuclein monomer. Due to the polymorphic nature of $\alpha$-synuclein fibrils when generated under different conditions [247, 353], and the demonstration that different fibril structures display divergent cellular effects [247], a reliable and well defined method of fibril formation was required. Here the decision was made to follow a protocol set out in Buell et al. [227]. This method was chosen as, at the time of developing this system, the fibrils produced were well characterised both structurally and functionally. Fibrils produced by this protocol have been used both

to demonstrate cellular internalisation of fibrils [337] and to characterise fibril growth kinetics [342].

Briefly, the protocol first involves generation of short *de novo* synthesised fibrils, henceforth termed fibril seeds, by incubating $\alpha$-synuclein in a heated glass vial under constant agitation by magnetic stir bar [337] (Fig. 3.2). It was demonstrated that the fibril seeds generated by this method were found in the insoluble fraction of the pelleting assay (>95% by densitometry) (Fig. 3.2 A and B) and appeared to have fibrillar morphology when observed under EM (Fig. 3.2C). Fibril seeds generated in this manner have an average length of  75nm as calculated from EM micrographs (Fig. 3.2D).

Elongation of fibrils, by the addition of $\alpha$-synuclein fibril seeds to monomeric $\alpha$-synuclein (10% Seed w/w), appeared to progress in a similar manner to that show elsewhere [227]. Fibril growth curves obtained by monitoring the elongation reaction by ThT fluorescence appeared similar to those previously described [227] (Fig. 3.3). Furthermore seeds elongated in this manner were found to be largely insoluble (>95% by densitometry) (Fig. 3.4).

Moreover, elongated fibrils possessed physical and morphological properties matching those previously described for $\alpha$-synuclein fibrils (Fig. 3.5) [227]. Atomic force microscopy (AFM) analysis of elongated fibrils showed that the fibrils were unbranching with a median height of 8nm (Fig. 3.5A and B). EM micrographs further confirmed the fibrillar morphology of the elongated $\alpha$-synuclein fibrils (Fig. 3.5 C). Taken together these data indicate that elongated $\alpha$-synuclein amyloid fibrils can be generated by extending $\alpha$-synuclein fibril seeds with recombinant $\alpha$-synuclein monomer and the resultant fibrils have properties close to those previously described [227, 337, 342].

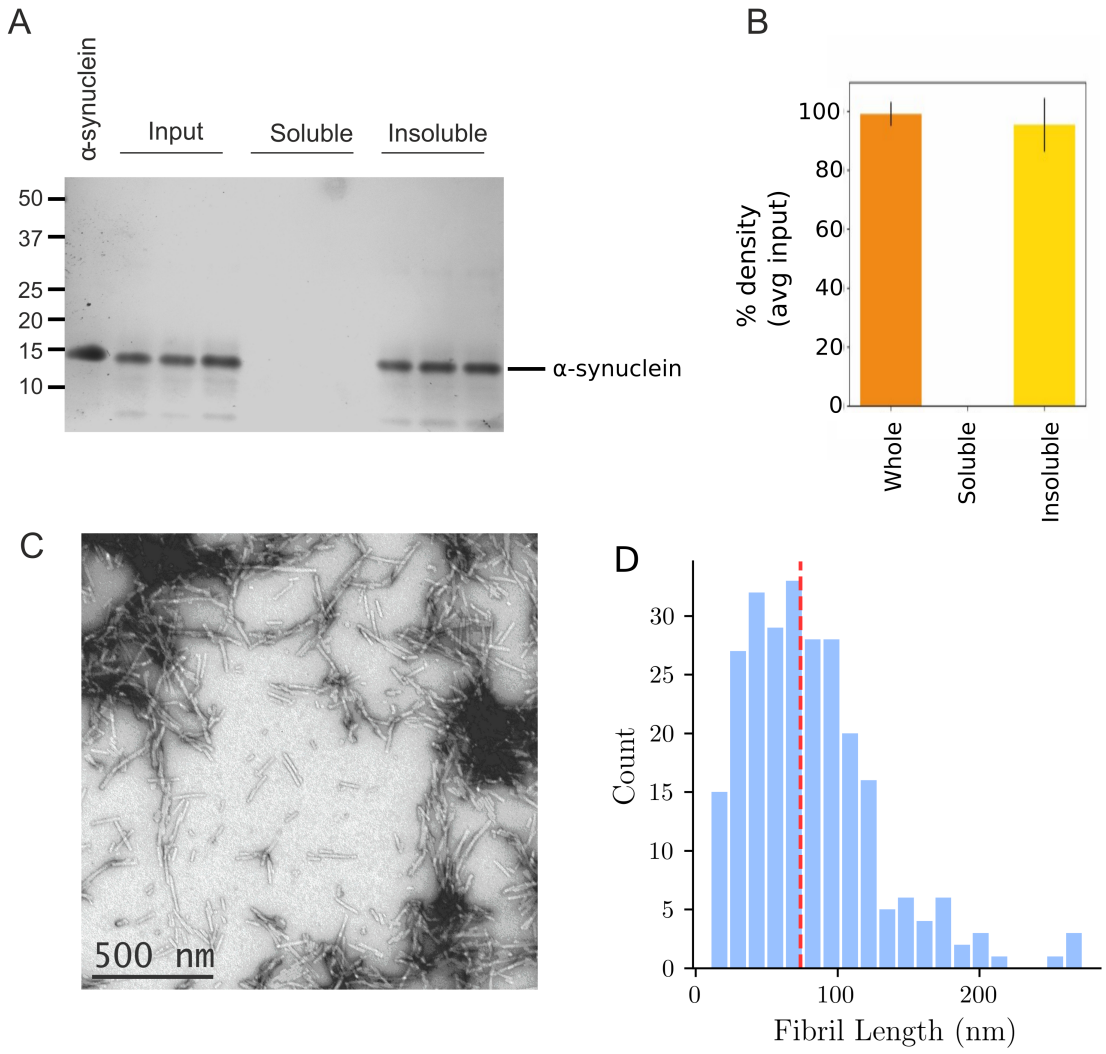


***Figure 3.2:*** *Characterisation of α-synuclein fibril seeds. Fibril seeds were produced from 500μM α-synuclein monomer incubated for 3 days at 42°C under constant agitation by magnetic stir bar. A) Pelleting assay (centrifugation at 16400×g for* 40 min*) of α-synuclein fibril seeds indicating presence of insoluble aggregates. Input denotes the lanes prior to centrifugation. α-synuclein denotes monomeric protein. Experiment was performed in triplicate to enable densitometry analysis. B) Bar chart showing the densitometry analysis of A. Error bars denote standard error of the mean (SEM) C) negative stain EM image obtained from α-synuclein fibril seeds showing fibrillar morphology. D) Lengths of fibril seeds calculated from EM micrographs. Lengths were measured manually via an ImageJ plugin. Red line denotes median median length. n=259.*

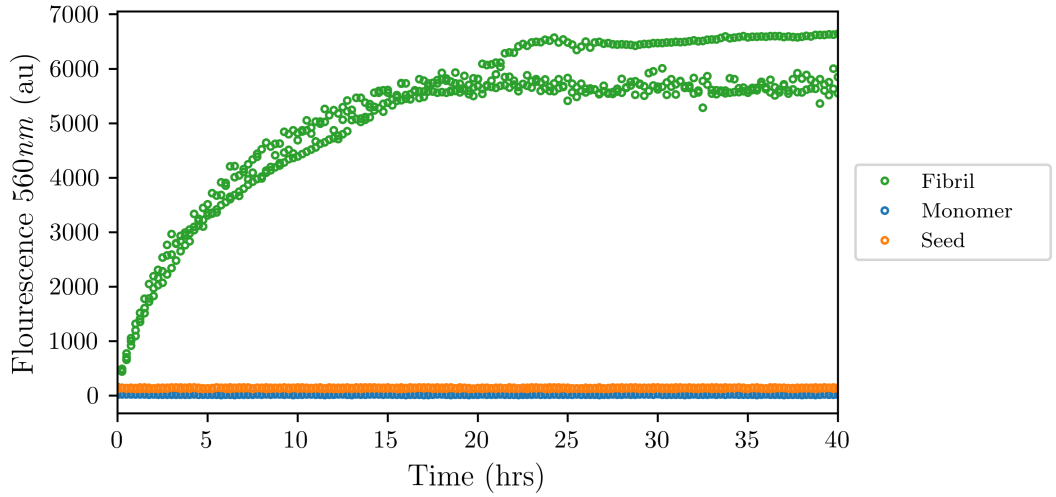


***Figure 3.3:*** *Elongation kinetics of α-synuclein fibril seeds. α-synuclein fibril seeds were elongated by addition of fibril seeds (10% w/w) to 100μM monomeric α-synuclein under quiescent conditions. 20μM ThT was added and fibril growth monitored by reading the fluorescence every 10 seconds. Plot showing the ThT fluorescence over time for triplicates of elongating fibrils (Fibril), seed alone (Seed), and monomer alone (Monomer).*

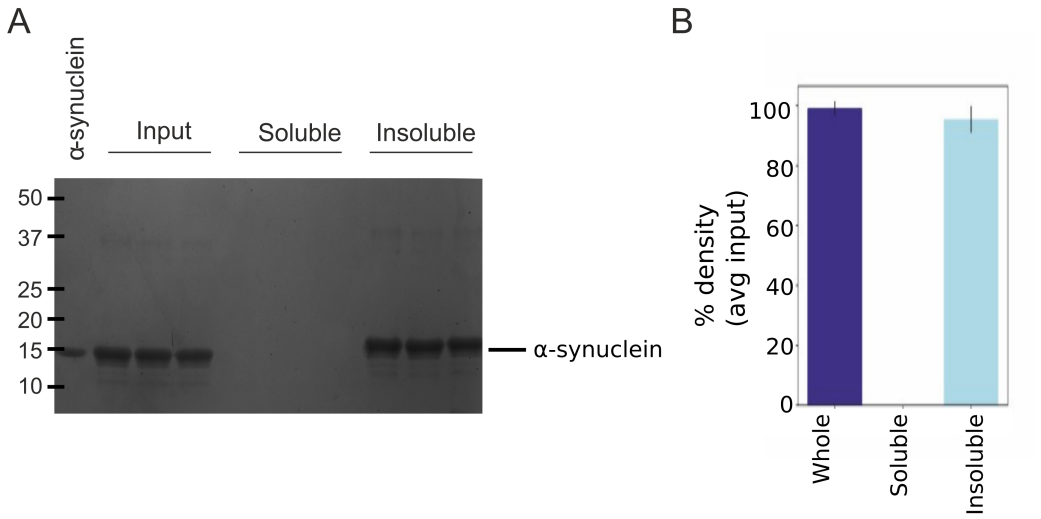


***Figure 3.4:*** *Characterisation of elongated α-synuclein fibrils. Fibrils were produced by elongation of α-synuclein fibril seeds (10% w/w) with monomeric α-synuclein under quiescent conditions. A) Pelleting assay (centrifugation at 16400×g for* 40 min*) of α-synuclein fibril seeds indicating presence of insoluble aggregates. Input denotes the lanes prior to centrifugation. α-synuclein denotes monomeric protein. Experiment was performed in triplicate to enable densitometry analysis. B) Bar chart showing the densitometry analysis of A. Error Bars denote SEM*

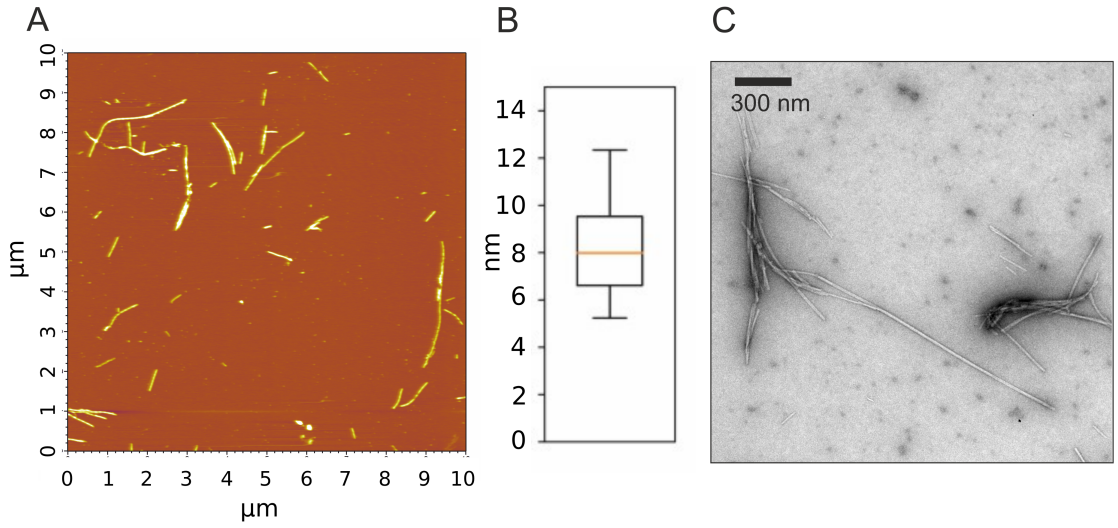


***Figure 3.5:*** *Elongated fibrils display fibrillar morphology by EM and AFM. Elongated fibrils were produced by incubation of 10% fibril seed with monomeric protein for 5 days under quiescent conditions. Elongated fibrils were then analysed by AFM (A) and the height distribution of fibrils calculated (B). Calculated heights are shown as a box and whisker diagram (median* 8.3 nm*) n=75. C) EM negative stain micrograph of elongated fibrils.*

### 3.3.3 Labelling of Monomeric $\alpha$-Synuclein with Biotin

In order to identify the cellular protein interactors of $\alpha$-synuclein fibrils following internalisation into cells and from cell lysates, a method for affinity isolation was required. It was determined that the use of a Biotin-Streptavidin affinity isolation system would be an effective method for capturing fibrils and their cellular interactions due, to the high specificity and sensitivity of biotin to Streptavidin [352]. Therefore, in order to make use of this biotin based isolation system it was necessary to label the fibrils with biotin. It was determined that this could be done through the labelling of monomeric $\alpha$-synuclein with biotin and then spiking a small percentage of the labelled $\alpha$-synuclein monomer into the fibril growth reaction. This method has been used previously to introduce a fluorescent label for the purpose of monitoring $\alpha$-synuclein internalisation by cells [253, 262, 337].

Labelling of monomeric $\alpha$-synuclein could, in this instance, be performed via biotin linked to an NHS ester (Fig. 3.6). The NHS ester is an amine reactive compound and will covalently conjugate the biotin molecule with the protein via exposed lysine residues and the N-terminus of the protein. At these locations NHS reacts with the primary amine group (-$NH_2$) leading to the covalent modification with biotin of the protein. Due to the distribution of lysines present in $\alpha$-synuclein this would result in the conjugation of biotin at a variety of points along the polypeptide chain. It was hypothesised that this would reduce the possibility of the label being inaccessible when monomers were incorporated into fibrils.

Using this method monomeric $\alpha$-synuclein was labelled with biotin and successful labelling was demonstrated by MS. MS spectra showed several distinct peaks differing by the weight of a conjugated biotin molecule. When analysed it showed that that every $\alpha$-synuclein monomer was labelled between five and nine times (median of 7) (Fig. 3.7). Incomplete labelling of all lysine residues on the monomer (of which there are 15) is important as it has previously been demonstrated that occlusion of all lysine residues can inhibit the formation of $\alpha$-synuclein fibrils [354].

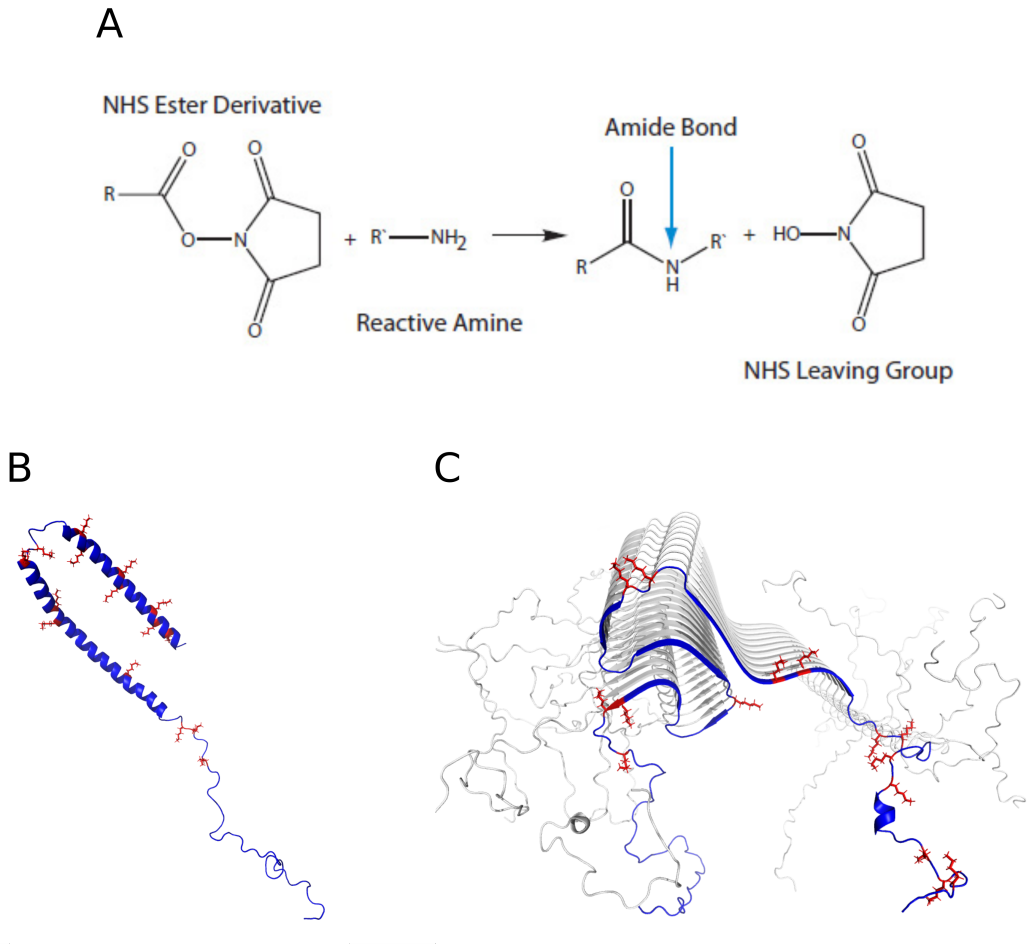


***Figure 3.6:*** *Lysine labelling of α-synuclein with NHS-biotin. A) The chemical reaction by which an NHS ester attaches a label to a lysine side chain. B and C) A monomeric [211] (PDB 1XQ8) and fibrillar [18] (PDB 2N0A) structure of α-synuclein with the locations of the lysine residues shown in red. The monomeric structure (B) was obtained for lipid bound α-synuclein.*

.

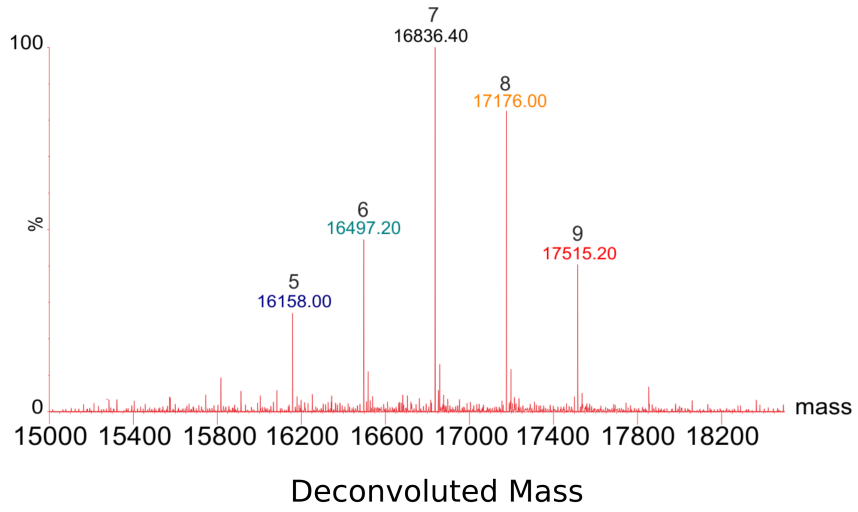


***Figure 3.7:*** *Monomeric α-synuclein labelled on lysine residues via NHS-biotin. Monomeric α-synuclein was labelled with biotin-NHS ester, desalted and lyophilized. The resultant protein was analysed by MS revealing 5 major peaks separated by the weight of an additional biotin. The the number above each peak denotes the calculated number of biotins conjugated to monomeric α-synuclein to arrive at the given molecular weight.*

.

### 3.3.4 Production of Elongated Biotinylated $\alpha$-Synuclein Fibrils

Having produced labelled $\alpha$-synuclein monomer it was then necessary to demonstrate that the synthesis of fibrils and their mature morphology was unaffected by the addition of labelled monomer. When labelled $\alpha$-synuclein was spiked into the fibril growth reaction at a ratio $>$ 1:20 (labelled : unlabelled monomer), biotin labelled fibrils appeared to retain the morphology of unlabelled fibrils (Fig. 3.9). Furthermore, the fibril growth kinetics of labelled fibrils remained similar to that of unlabelled fibrils. However, when spiked in at a concentration of 10% or greater, fibril growth kinetics showed notable changes including a reduction in the slope of the curve, and reduced maximum fluorescence (Fig. 3.8). Elongated fibrils (5% labelled monomer) appear in the insoluble fraction of a pelleting assay and appear fibrillar by EM (Fig. 3.9). These data suggest that biotin-labelled $\alpha$-synuclein monomer is incorporated into fibrils produced by elongation and that the morphology of these fibrils, characterised in detail elsewhere [227, 337, 342] are unaffected by the addition of the biotin label.

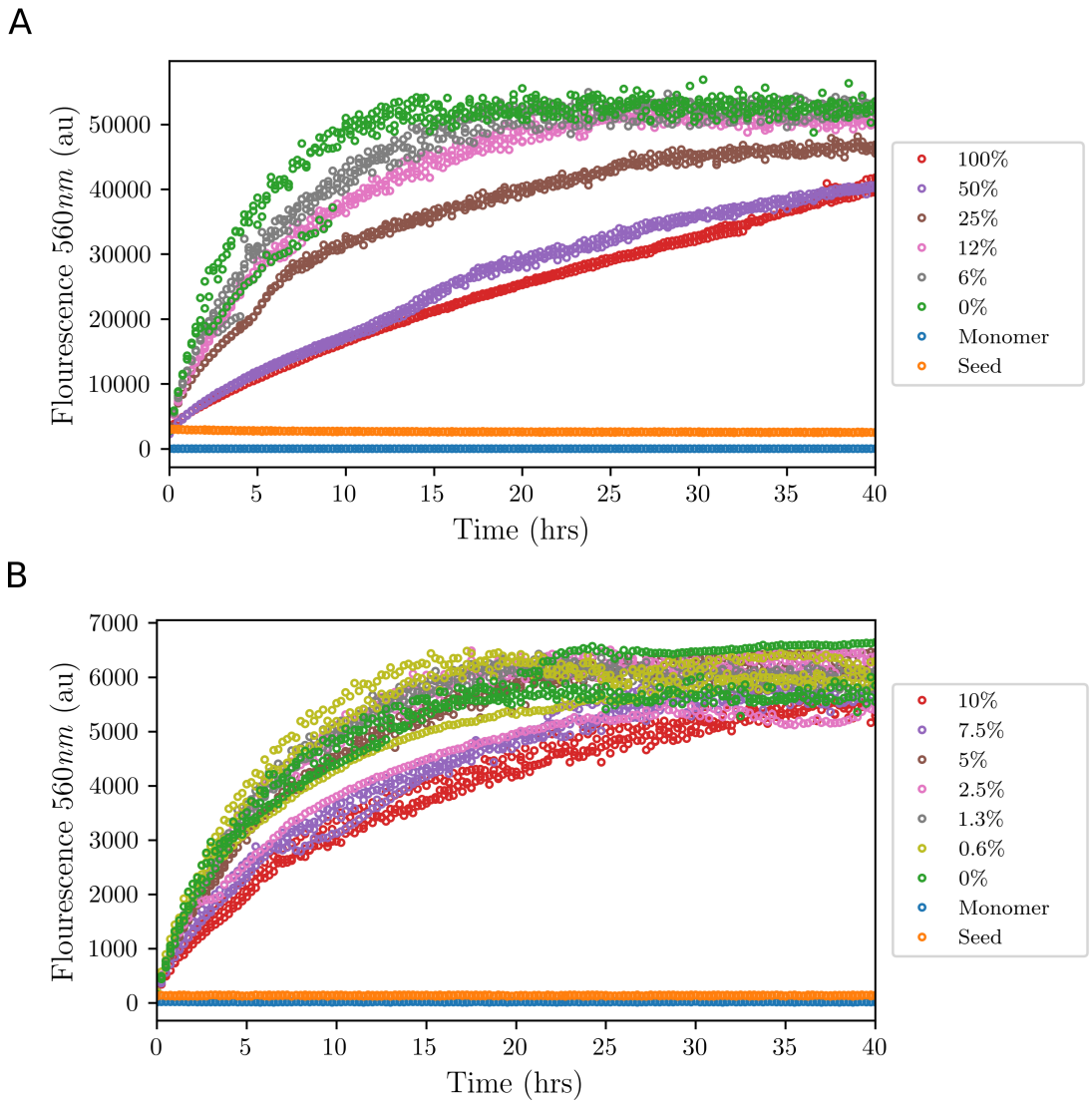


***Figure 3.8:*** *Elongating fibrils with low concentrations of biotinylated monomer does not affect rate of elongation. A and B) ThT fibril seed elongation curves. α-synuclein fibril seeds (10% w/w) were incubated with unlabelled α-synuclein monomer spiked with biotinylated monomer at the percentages of A) 6% to 100% and B) 0.6% to 10%. Under conditions where the percentage of spiked labelled monomer is less than 5% the growth curve overlays that of α-synuclein fibril seed + unlabelled α-synuclein monomer. Seed refers to α-synuclein seed alone. Monomer refers to unlabelled monomeric α-synuclein alone.*

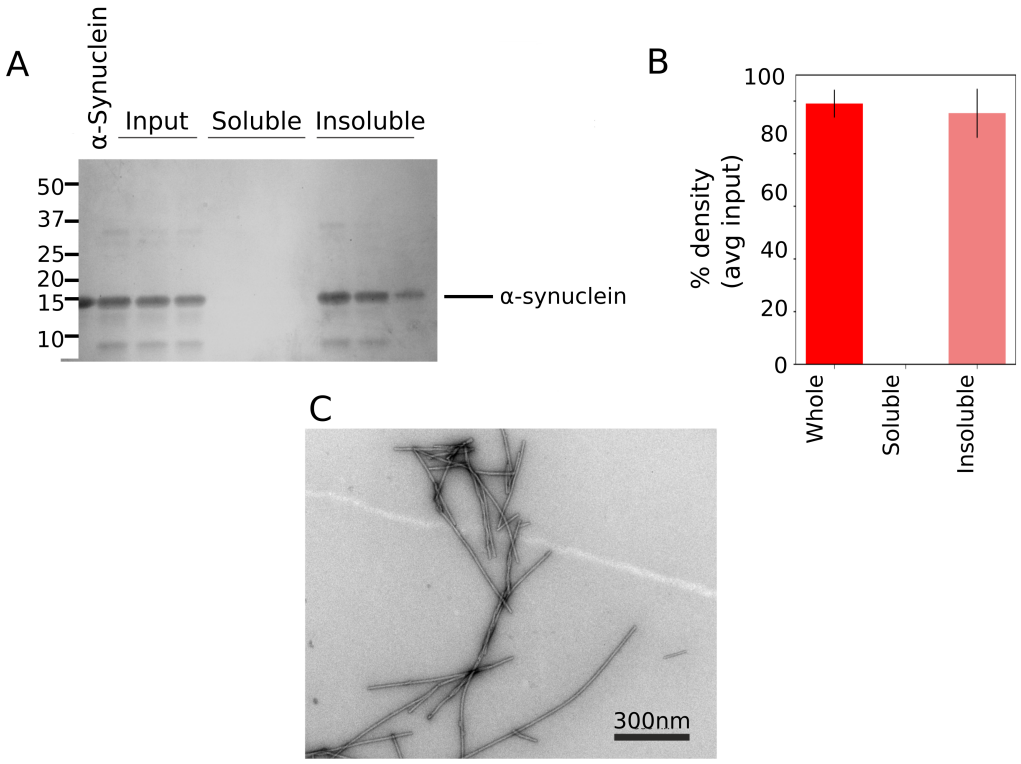


***Figure 3.9:*** *Characterising elongated biotinylated fibrils. Biotinylated fibrils were synthesised by elongation of fibril seeds with biotinylated α-synuclein monomers (10% Seed 5% Biotinylated Monomer w/w 85% Unlabelled Monomer). A) Pelleting assay (centrifugation at 16400×g for* 40 min*) of biotinylated α-synuclein fibril indicating presence of insoluble aggregates. Input denotes the lanes prior to centrifugation. α-synuclein denotes monomeric protein. Experiment was performed in triplicate to enable densitometry analysis. B) Bar chart showing the densitometry analysis of A. Error bars denote SEM C) EM negative stain micrograph of pelleted fibrils (A) showing fibrillar morphology of elongated labelled fibrils*

### 3.3.5 Elongated Biotinylated $\alpha$-Synuclein Fibrils can be Isolated by Streptavidin Coated Magnetic Beads

Prior to studying cellular uptake and capacity to seed intracellular inclusions it was important to demonstrate that the labelled fibrils could be pulled down from buffer. Several methods of isolation exist including centrifugal isolation using agarose beads, and magnetic isolation using ferrous beads. The decision was made to use magnetic isolation as it was thought that centrifugal isolation, in the context of an system capable of inducing aggregation within cells, may result in non-specific isolation. Therefore for this experiment streptavidin-coated Dynabeads were chosen to isolate biotinylated $\alpha$-synuclein fibrils. It was shown that such beads were able to isolate elongated biotinylated fibril (Fig. 3.10). Furthermore, there was no evidence that streptavidin beads isolated unlabelled fibrils.

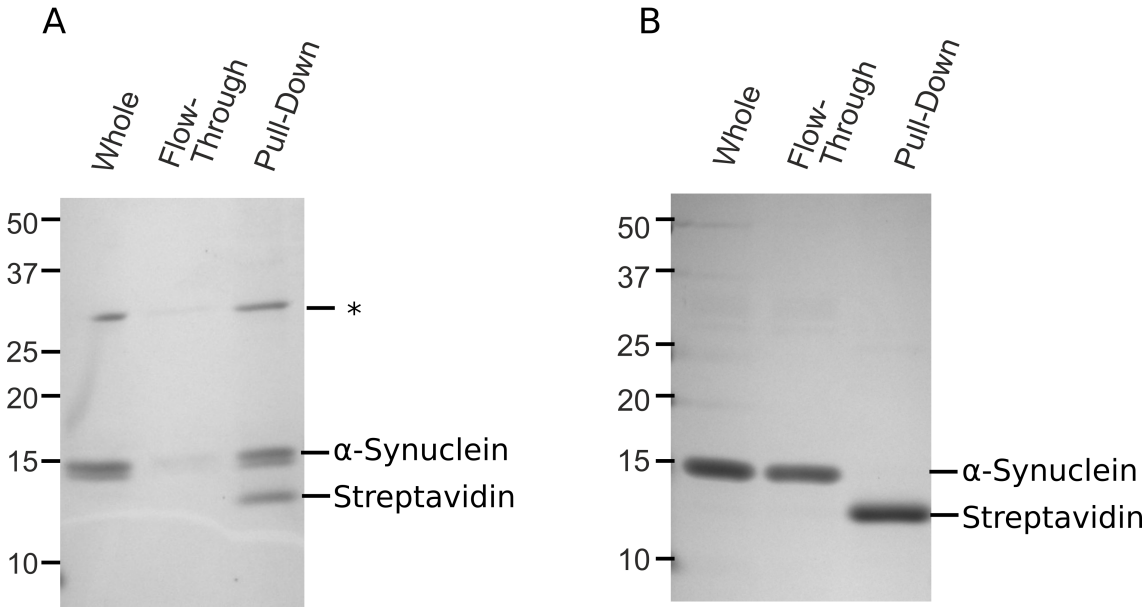


***Figure 3.10:*** *Biotinylated fibrils are pulled down from buffer using streptavidin magnetic beads. Elongated biotinylated fibrils were incubated with Streptavidin coated Dynabeads™ for 30min at 4°C in PBS. Magnetic beads were then isolated and the unbound fraction retained (Flow-Through). The beads were washed three times in PBS + 0.1% Tween 20, to give the binding fraction (Pull-Down). SDS-PAGE (Coomassie stain) of A) biotinylated fibril and B) WT unlabelled fibril pull-down. Location of streptavidin and α-synuclein indicated. * denotes a band 30kDa predicted to be an α-synuclein dimer.*

### 3.3.6 Elongated Fibrils are not Internalised by SH-SY5Y Cells

Having demonstrated that it was possible to produce biotinylated $\alpha$-synuclein fibrils and that those fibrils could be extracted from the buffer using a magnetic isolation system, it was then necessary to demonstrate the functionality of the other major component of the system: cellular internalisation of fibrils. Numerous studies have demonstrated that fibrils incubated in the cell culture medium are internalised by cells through endocytosis [253, 259, 262, 337]. Therefore biotinylated fibrils were incubated with cells and their uptake analysed.

Previous studies have used fibrils labelled with fluorescent tags to track their internalisation by SH-SY5Y cells [253, 259, 262, 337]. Therefore, to demonstrate internalisation, fibrils labelled with one or more of the fluorescent marker TAMRA, were produced in a similar manner to the method for producing biotinylated fibrils. Namely monomeric $\alpha$-synuclein was labelled with NHS-conjugated TAMRA and spiked into a fibril growth reaction. The labelling of monomeric $\alpha$-synuclein was shown to have a lower efficiency to biotin labelling when analysed by MS (Fig. 3.11) but nonetheless, the majority of $\alpha$-synuclein monomer was labelled with TAMRA.

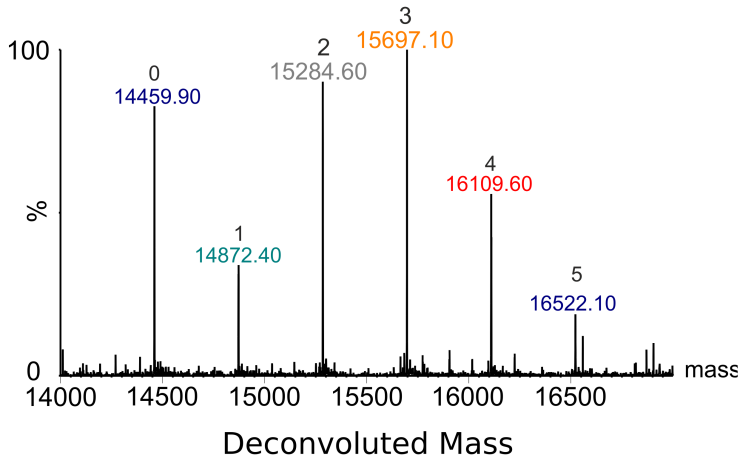


***Figure 3.11:*** *Monomeric $\alpha$-synuclein labelled on lysine residues with NHS-TAMRA. A) Deconvoluted MS spectra of monomeric $\alpha$-synuclein labelled with TAMRA-NHS conjugate. Major mass peaks are separated by the mass of a conjugated TAMRA label. Numbers above the peaks indicate the calculated number of TAMRA labels conjugated to $\alpha$-synuclein necessary to appear at that molecular weight.*

When spiked into the elongation reaction at 1% of the total monomer concentration, the fibril growth curve appeared to overlap that of the unlabelled monomer (Fig. 3.12). At monomer concentrations higher than 1% however the fibril elongation reaction quickly deviated from that of the unlabelled monomer (Fig. 3.12). When the

endpoint of the fibril elongation reaction was analysed be EM for fibrils elongated in monomer containing 1% TAMRA labelled monomer, the fibril morphology appeared unaffected (Fig. 3.13). These data demonstrate TAMRA labelled, elongated $\alpha$-synuclein fibrils can be generated and these fibrils closely resemble unlabelled fibrils.

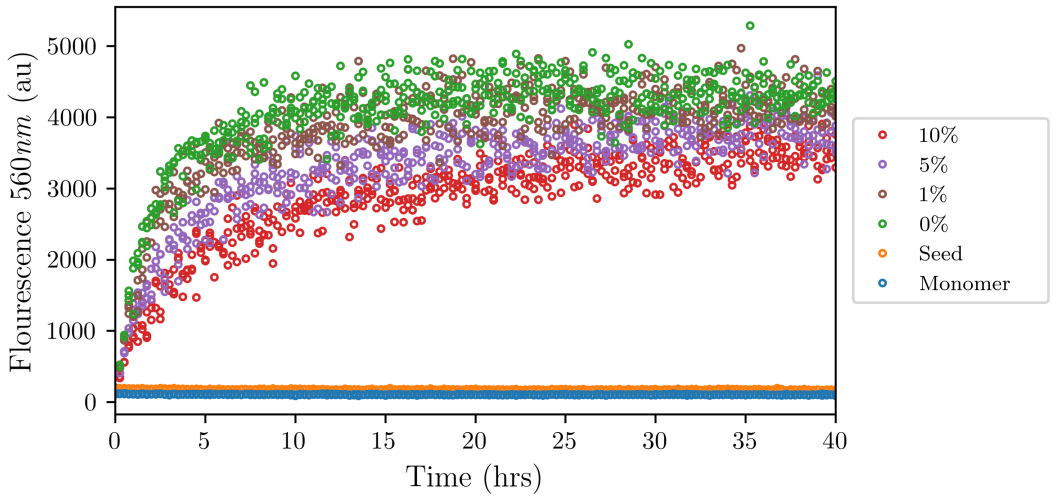


***Figure 3.12:*** *Characterising elongated TAMRA labelled fibrils. $\alpha$-synuclein fibril seeds elongated with monomeric $\alpha$-synuclein containing 1% TAMRA labelled monomer. No biotinylated $\alpha$-synuclein monomer was added to this fibril assembly reaction. ThT elongation curve of $\alpha$-synuclein fibril seed elongation (10% fibril seed) in monomeric $\alpha$-synuclein containing a increasing proportions (given as % values in the legend) of TAMRA labelled monomer. Seed refers to $\alpha$-synuclein seed alone. Monomer refers to unlabelled monomeric $\alpha$-synuclein alone.*

Having successfully synthesised fluorescent fibrils it was then possible to demonstrate internalisation by SH-SY5Y cells. SH-SY5Y cells were chosen as they are a neuronal like cell type commonly used as a model in the study of neurodegenerative amyloid diseases, including the study of $\alpha$-synuclein related cellular dysfunction [347]. Fibrils were added to the culture media of these cells at a concentration of 1 µM (monomer equivalent) consistent with that used by other internalisation studies [253, 259, 262]. However, unlike previous studies [259, 262], there was little to no evidence of internalisation by cells when treated cells were observed by confocal-microscopy, as shown by a lack of co-localisation with Lysotracker™ staining (Fig. 3.14). Instead labelled $\alpha$-synuclein localised to the plasma membrane of treated cells suggesting that elongated $\alpha$-synuclein fibrils were not endocytosed by the cells.

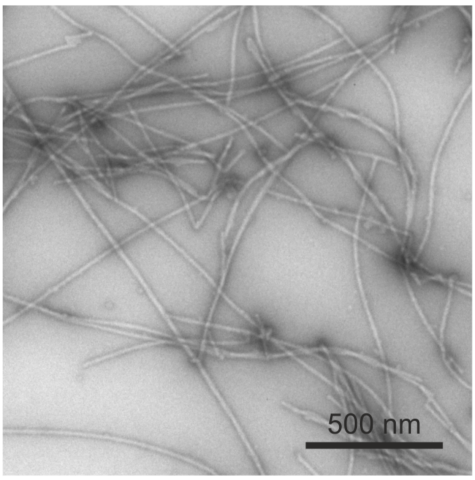


***Figure 3.13:*** *Characterising elongated TAMRA labelled fibrils. EM micrograph of α-synuclein fibril seeds (10% w/w) elongated with monomeric α-synuclein containing 1% TAMRA labelled monomer. No biotinylated α-synuclein monomer was added to this fibril assembly reaction.*

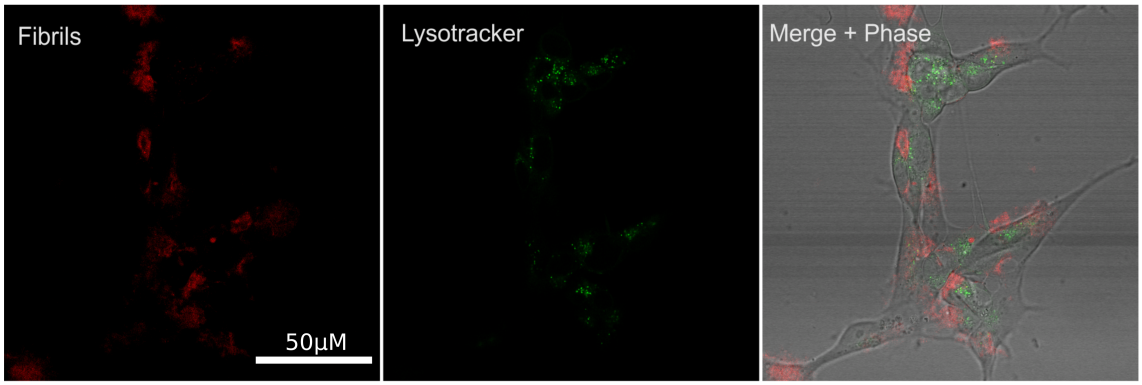


***Figure 3.14:*** *Elongated TAMRA labelled α-synuclein fibrils were not internalised by SH-SY5Y cells. SH-SY5Y cells were incubated with TAMRA-labelled fibrils for* 24 h*, and stained with Lysotracker™ to visualise the lysosomes. Shown is a representative image acquired by confocal microscopy of the internalisation by SH-SY5Y cells. Image taken on LSM770 confocal microscope at 40×magnification*

### 3.3.7 Biotin Labelled Monomeric $\alpha$-Synuclein Fails to Assemble Into $\alpha$-Synuclein Fibril Seeds

Due to the failure to demonstrate internalisation of labelled $\alpha$-synuclein fibrils generated by elongated seeds with TAMRA labelled monomers, another approach was necessary. It has been shown that in the case of $\beta_2$M fibrils fibril length is a key determinant for internalisation, with shorter fibrils being internalised while longer fibrils remain on the cell surface [340]. Therefore, it was hypothesised that the shorter fibril seeds may be internalised by the fibrils more readily than the elongated fibrils.

In order to test this hypothesis, an attempt was made to synthesise fibril seeds from monomeric $\alpha$-synuclein spiked with labelled $\alpha$-synuclein monomer. However, the addition of biotinylated monomer (even as low as 1:1000 biotinylated:unlabelled monomer) to the fibril synthesis reaction negatively affected the morphology of the fibrils, as observed by EM. The morphology appeared to more closely resemble amorphous aggregates the higher the concentration of labelled monomer (Fig. 3.15 B). Furthermore, given a calculated fibril length of 50 nm for fibril seeds and knowing the mass per unit length of a $\alpha$-synuclein fibril [355] to equate to 5 subunits/nm the average number of monomers within a fibril seed is 250. Therefore, at a ratio of 1:1000, on average only one in four fibrils would contain a labelled monomer. This is unsuitable for pull-downs as most fibrils generated by this method do not contain biotin.

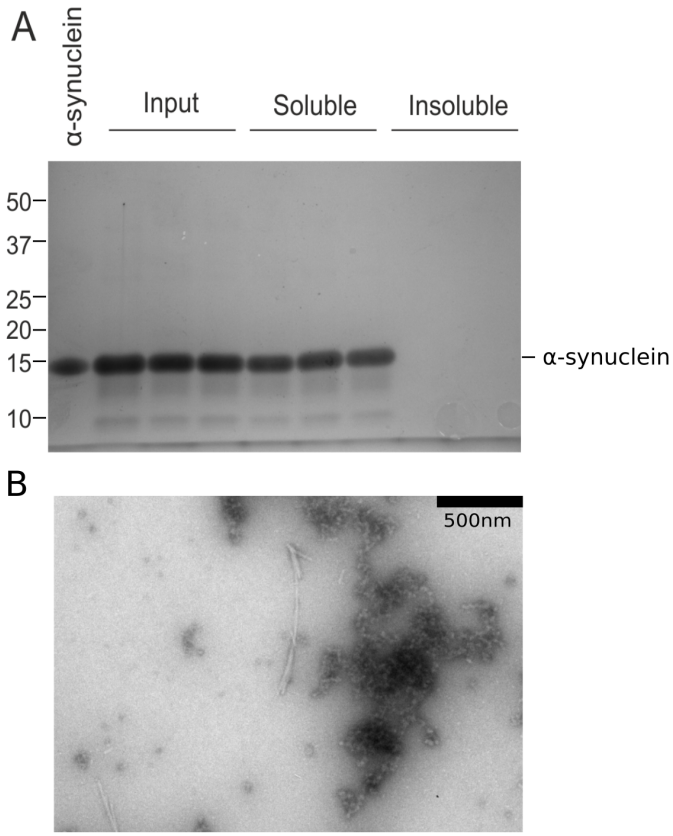


***Figure 3.15:*** *Biotinylated monomeric α-synuclein is unable to assemble into amyloid fibrils. α-synuclein monomer spiked with 1% biotinylated monomer was incubated for 3 days under conditions for the synthesis of α-synuclein fibril seeds. A) Pelleting assay showing resulting aggregate appearing largely in the soluble fraction. B) EM negative stain micrograph of reaction end product showing a number of amorphous aggregates.*

### 3.3.8 A18C $\alpha$-Synuclein Monomer Assembles Into Fibril Seeds

One possible explanation for the failure to synthesise morphologically fibrillar aggregates from lysine labelled $\alpha$-synuclein monomer, is that the presence of the label disrupts the ability of the protein to form a cross-β structure. This possibility is supported out by several high resolution structures of $\alpha$-synuclein fibrils that clearly identify several lysine residues within the region of the protein responsible for forming the β-sheet structure [232, 233, 356]. Indeed, a number of lysine residues were present in the β-sheet region of all identified structural variants. Furthermore, at least one lysine residue (K80) has been shown to play an important role in the protofilament interface, forming a salt bridge with E46 [233]. Therefore, selective labelling of a site distant from the fibril core and uninvolved with subunit stacking, β-sheet formation, or protofilament interactions, may enable synthesis of a labelled, morphologically

fibrillar, $\alpha$-synuclein aggregates.

To enable site specific labelling the decision was made to leverage cysteine reactive maleimide chemistry. Since $\alpha$-synuclein has no natural cysteines, introduction of a cysteine by site specific mutation enables precise control of the location of the biotin label. Several sites present themselves as viable targets: A90C has been used in several previous studies to label fibrils with a fluorescent tag [253, 259]. However this residue is within the fibril core in several structural studies [232], and there has been little research as to the structural effects of labelling in this location. Another possible location is A140C, as it is far removed from the fibril core and has no known involvement with $\alpha$-synuclein fibril formation. However, there is some evidence to suggest that the C-terminus of $\alpha$-synuclein is cleaved intracellularly in LBs [357]. Therefore, there is the possibility that a biotin label in this location may be lost following internalisation.

Rather, another location, $\alpha$-synuclein A18C presented as the most promising location for the site specific labelling of $\alpha$-synuclein. As with A140, this site is distant from the fibril core and does not appear to participate in protofilament interactions. $\alpha$-synuclein A18C mutant, $\alpha$-synuclein monomer was therefore recombinantly expressed and purified from *E.coli* in the same manner as WT monomeric $\alpha$-synuclein. MS analysis of the purified protein demonstrate the presence of a peak matching the predicted MW of a dimeric $\alpha$-synuclein cysteine mutant. The SEC trace of $\alpha$-synuclein A18C monomer purification demonstrates that the protein is monomeric in the presence of the redox reagent DTT (Fig. 3.16A). MS analysis of the purified protein identified a single, denoting a mass within 1kDa of the predicted mass of dimeric A18C $\alpha$-synuclein.

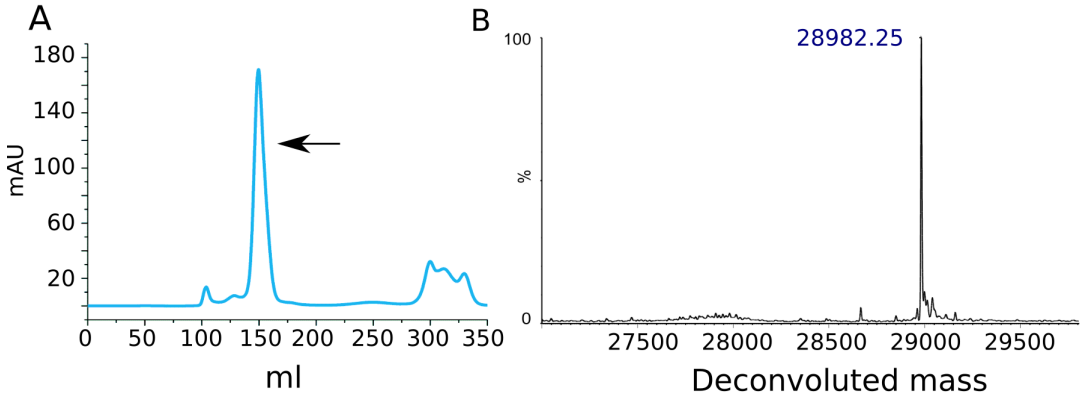


***Figure 3.16:*** *Recombinant A18C $\alpha$-synuclein purified as a monomer. A) SEC trace of A18C $\alpha$-synuclein purification showing largely monomeric conformation. Only the protein from the large peak at 150ml was collected and lyophilized. Arrow denotes collected peak. B) Deconvoluted MS spectra showing the molecular weight of the purified protein. This closely matches the theoretical weight of dimeric $\alpha$-synuclein of 28983.14 Da.*

Having expressed and purified monomeric α-synuclein A18C, fibril seeds of α-synuclein A18C were synthesised from 100% cysteine mutant α-synuclein, to ensure that the mutation had no detrimental effect on the morphology. Indeed, when examined by EM the fibrils appeared to have no visible difference to those formed from WT α-synuclein monomer (Fig. 3.17). This suggests that fibrillar morphology of α-synuclein is unaffected by the presence of the α-synuclein A18C mutation.

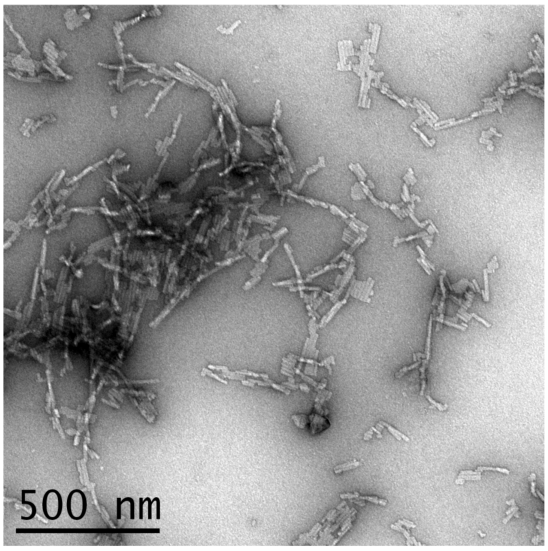


***Figure 3.17:*** *Characterisation of fibril seeds generated from α-synuclein A18C monomer. α-synuclein A18C fibril seeds were generated by incubation of α-synuclein A18C (500μM) at 42°C for three days under constant agitation by magnetic stir bar. EM micrograph of fibril seeds showing the morphologically fibrillar structure.*

### 3.3.9 α-Synuclein A18C Fibril Seeds are Effectively Labelled with Biotin-Maleimide

Using the the successfully synthesised α-synuclein A18C (100% α-synuclein A18C monomer) fibril seeds, it was then possible to label the fibrils in a site specific manner with biotin-maleimide. Fibril seeds were used in instead of elongated fibrils as they were predicted to be more likely internalised by SH-SY5Y cells. In contrast to the earlier methodology of labelling monomeric α-synuclein prior to fibrillation fibril seeds were instead labelled post fibrillation which has been shown to be successful in previous studies [253]. This method has several advantages: first there is a lower chance of the label affecting fibrillation as the cross-β core of the fibril has already formed, secondly it will be possible to compare morphology by EM both before and after biotin labelling to confirm there are no gross structural changes.

In order to demonstrate efficient labelling by biotin maleimide, fibrils were depolymerised by incubation with hexafluoro-2-propanol (HFIP) and the resultant

monomeric $\alpha$-synuclein analysed by MS. The MS spectra of the depolymerised, $\alpha$-synuclein A18C fibril, clearly indicates the presence of modification. The MW of this modification matches that calculated for a biotin conjugation. By this measure it is possible to estimate that 45% of the monomeric subunits are labelled (Fig. 3.18A). Moreover, the morphology of fibrils labelled with biotin maleimide were observed to be unchanged when compared to unlabelled fibrils when examined by EM (Fig. 3.18 B). These data indicate that fibril seeds produced from $\alpha$-synuclein A18C monomeric $\alpha$-synuclein can be labelled effectively with biotin-maleimide, and that this modification does not affect the resultant fibril morphology.

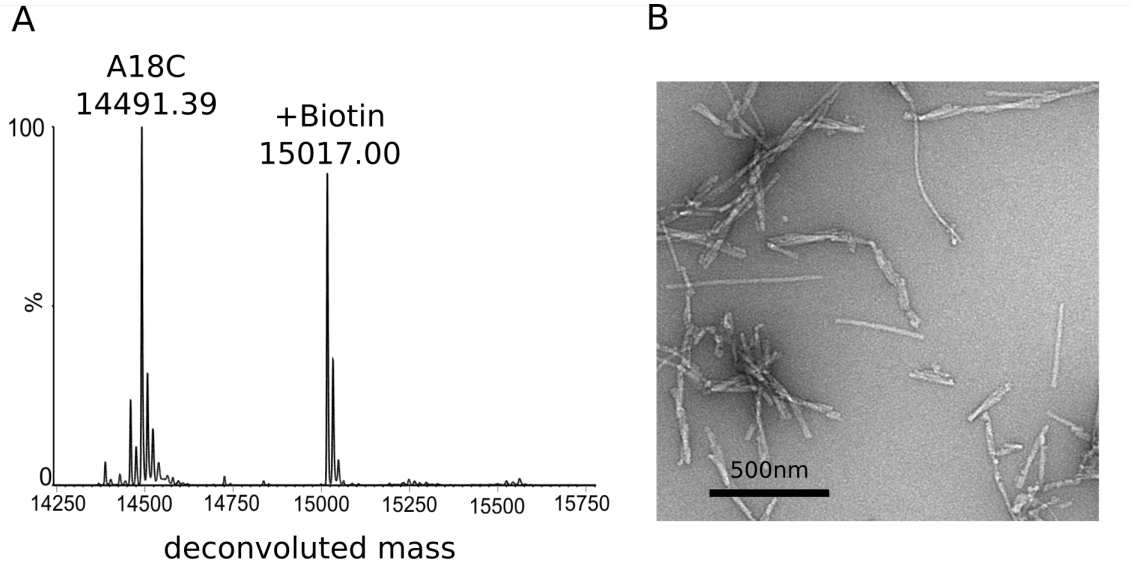


***Figure 3.18:*** *Characterisation of biotinylated $\alpha$-synuclein A18C fibril seeds. $\alpha$-synuclein A18C fibril seeds generated by fibrillation of $\alpha$-synuclein A18C monomer, were labelled with biotin maleimide and desalted by repeated pelleting of the fibrils. A) Deconvoluted MS spectrum of $\alpha$-synuclein A18C fibrils labelled with biotin-maleimide and depolymerised via HFIP incubation. The two major peaks can be identified. The first denotes monomeric A18C $\alpha$-synuclein at* 14 491 Da *and the second denotes monomeric protein with the additional conjugation of biotin (predicted* 15 016.40 Da*, acquired* 15 017.00 Da*). B) negative stained EM micrograph of $\alpha$-synuclein A18C fibril seeds labelled with biotin maleimide showing fibrillar morphology.*

### 3.3.10 Biotin Labelled $\alpha$-Synuclein A18C Fibrils can be Isolated From Buffer by Streptavidin Magnetic Bead Pull-Down

It was then confirmed that labelled $\alpha$-synuclein A18C fibrils could be isolated by streptavidin magnetic bead pull-down. Biotinylated $\alpha$-synuclein fibril seeds, generated from labelling of fibril seeds synthesised (Fig. 3.18) from recombinant $\alpha$-synuclein A18C monomer with biotin maleimide, were incubated with Streptavidin

coated Dynabeads. When the isolated fraction of the pull-down was compared to the unbound (flow-through) fraction it was evident that this method of isolation is capable of recovering all biotinylated fibril seed. To confirm this is not the result of non-specific binding of fibril seeds to the magnetic beads, pull-downs of unlabelled WT $\alpha$-synuclein fibril seeds were performed. In contrast to biotinylated $\alpha$-synuclein A18C fibril seed, no pull-down of unlabeled WT $\alpha$-synuclein fibril seed was observed.

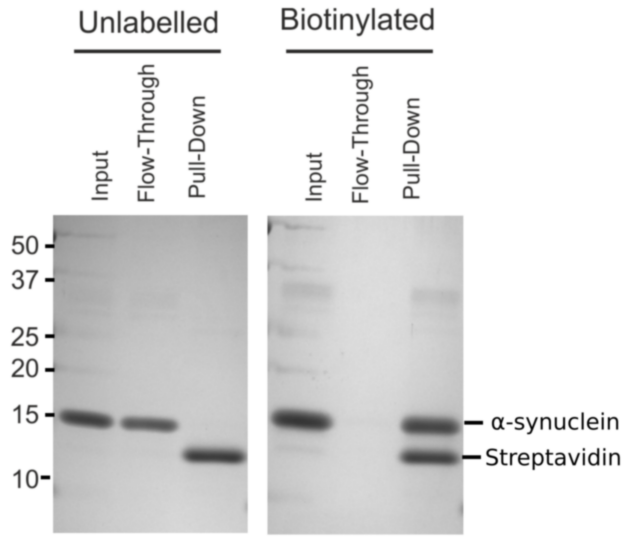


***Figure 3.19:*** *Biotinylated $\alpha$-synuclein A18C fibril seeds can be isolated from buffer using magnetic streptavidin beads. SDS-PAGE (Coomassie stain) of pull-down experiment. Unlabelled fibril seeds (Unlabelled) and biotinylated $\alpha$-synuclein A18C fibril seeds (Biotinylated) were incubated with streptavidin magnetic beads for 1hr. The unbound fraction was removed and termed Flow Through. The bound fraction was washed three times in PBS + 0.1% Tween 20. This washed pellet was termed Pull-Down. The lower band seen in the pull-down lanes with a MW* 12 kDa *corresponds to that of streptavidin, while the higher band* 15 kDa *corresponds to the MW of monomeric $\alpha$-synuclein*

### 3.3.11 Biotin Labelled $\alpha$-Synuclein A18C Fibrils are Internalised by SH-SY5Y Cells

As shown above, elongated WT $\alpha$-synuclein fibrils were not internalised by cells, possibly as a result of the fibril length. Previous studies have demonstrated that shortening fibrils via fragmentation can increase the degree of internalisation of amyloid aggregates [340]. With a system in place for generating $\alpha$-synuclein fibril seeds that can be conjugated to biotin, the next step was to ensure that the fibril seeds can be internalised by cells. $\alpha$-synuclein A18C fibril seeds were therefore labelled with an AlexaFlour-594 maleimide conjugate in the same manner as the labelling with biotin maleimide. For this purpose fibril seeds were dual labelled with

biotin and AlexaFlour-594. This was done by adding both biotin maleimide and AlexaFlour-594 maleimide to unlabelled $\alpha$-synuclein A18C fibril seeds. As was the case with $\alpha$-synuclein A18C fibril seeds labelled with biotin there appeared to be no observable change in morphology when examined by negative stain EM (Fig. 3.20).

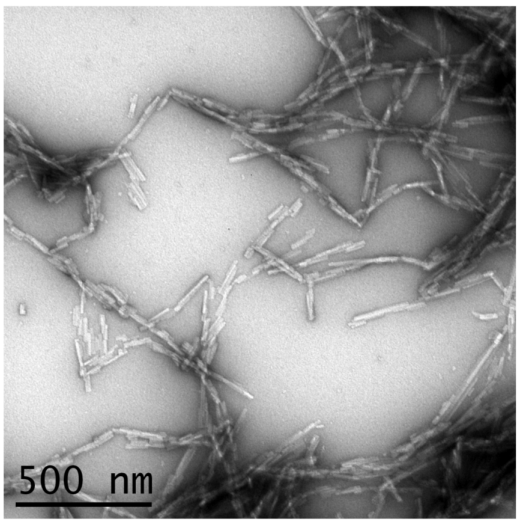


***Figure 3.20:*** *Characterisation of biotinylated and AlexaFlour-594 labelled $\alpha$-synuclein A18C fibril seeds. $\alpha$-synuclein A18C fibril seeds generated by fibrillation of $\alpha$-synuclein A18C monomer, were labelled with biotin maleimide and AlexaFlour-594 maleimide and desalted by repeated pelleting of the A18C $\alpha$-synuclein fibril seeds. Negative stain EM micrograph of $\alpha$-synuclein A18C fibril seeds labelled with biotin maleimide and AlexaFlour-594 showing fibrillar morphology.*

Having established that A18C $\alpha$-synuclein fibril seeds are morphologically unaffected by the addition of a fluorescent tag, dual labelled (biotin, AlexaFlour-594) $\alpha$-synuclein A18C fibrils were then applied to SH-SY5Y cells to observe internalisation by confocal microscopy. Previous studies have observed co-localisation of $\alpha$-synuclein fibrils with components of the endolysosomal pathway [256].

Following 24 h incubation with $\alpha$-synuclein fibril seeds it was shown that, in contrast to the longer elongated fibrils, dual labelled $\alpha$-synuclein A18C fibril seeds were more readily internalised by SH-SY5Y cells. Confocal images showed the presence of distinct puncta within the cell (Fig. 3.21A), not seen in the images of elongated fibrils (Fig. 3.14), some of which co-localised with puncta visualised with Lysotracker™. These data demonstrate that the A18C fibril seeds are internalised to some extent, thus are suitable or identifying intracellular interactions of $\alpha$-synuclein fibrils, a key tenet of this work.

Futhermore, in order to demonstrate that biotinylated fibril seeds are also internalised by SH-SY5Y cells, and do not behave differently due to the change in the label, an equivalent imaging experiment using biotinylated fibrils was conducted (Fig. 3.22). As before SH-SY5Y cells were incubated with fibril seeds for 24 h and then fixed

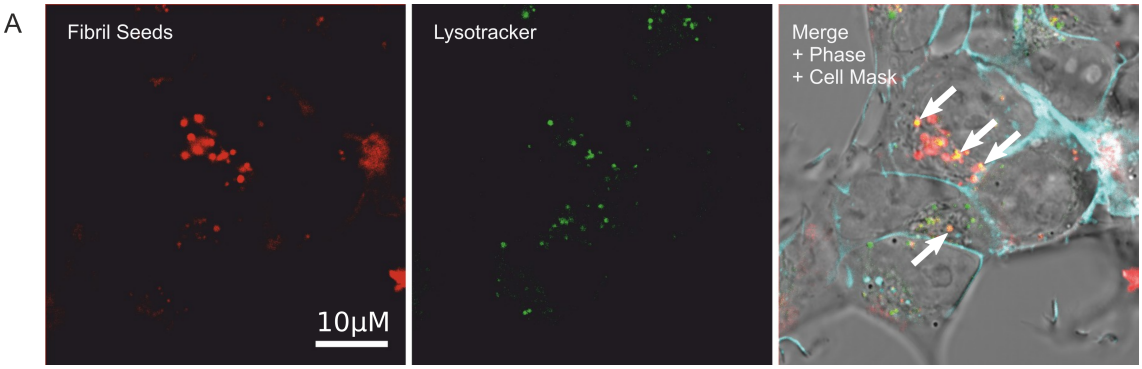


***Figure 3.21:*** *α-Synuclein A18C fibril seeds are internalised by SH-SY5Y cells. SH-SY5Y cells were incubated with dual labelled (biotin, AlexaFlour-594) α-synuclein A18C fibrils seeds for 24hrs. Cells were then stained with Lysotracker™ to visualise endolysosomal structures. Representative image acquired on an LSM700 confocal microscope at 40×magnification. Red denotes AlexaFlour-594 labelled α-synuclein A18C fibrils. Green denotes Lysotracker positive puncta. White arrows denotes example of co-localisation of fibrils and endolysosomal compartments.*

and permeabilised. The fixed cells were then probed with Streptavidin conjugated to Texas Red. Cells were probed with an anti-LAMP1 antibody for endolysosomal identification. These data revealed that there was evidence of internalisation of biotinylated α-synuclein fibril seeds as seen by the presence of red punctate staining within the cells (Fig. 3.22), which co-localised, in part, with LAMP1.

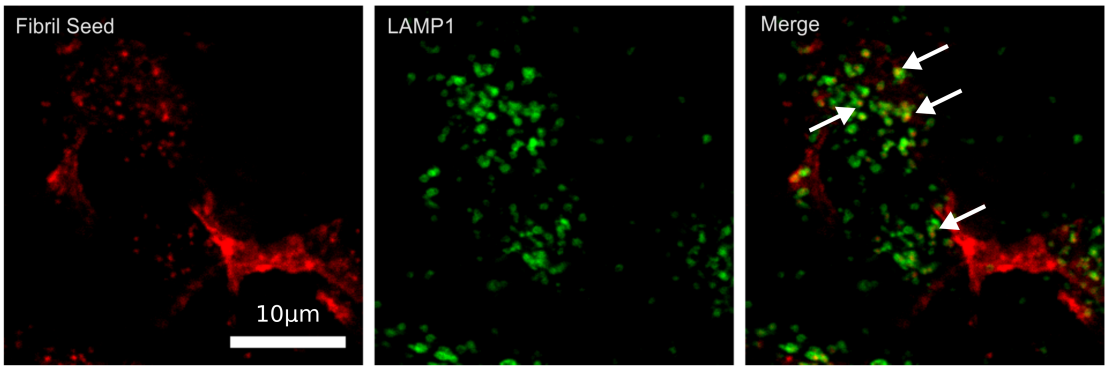


***Figure 3.22:*** *Biotinylated α-synuclein A18C fibril seeds are internalised by SH-SY5Y cells. SH-SY5Y cells were incubated with biotinylated α-synuclein A18C fibrils seeds for 24hrs. Cells were then formaldehyde fixed and probed for LAMP1 (anti-LAMP1 mouse monoclonal) to visualise lysosomal structures, and biotin (Streptavidin Texas Red) to visualise biotinylated α-synuclein A18C fibrils. Representative image acquired on an LSM700 confocal microscope at 40×magnification. Red denotes biotinylated α-synuclein A18C fibrils. Green denotes LAMP1 positive puncta. White arrows denotes example of co-localisation of fibrils and LAMP1 positive puncta.*

Finally, to ensure the biotinylated α-synuclein A18C fibrils produced here replicate the functionality of those demonstrated elsewhere [263], the ability of these fibrils to seed intracellular inclusions of α-synuclein was assessed. For this purpose SH-SY5Y

cells overexpressing a GFP-tagged variant of $\alpha$-synuclein were used. The presence of intracellular inclusions could then be determined through the identification of distinct intracellular puncta formation by GFP-$\alpha$-synuclein. Following a 5 day incubation with AlexaFlour-594 (Fig. 3.23) labelled and biotin labelled fibril seeds there was indeed evidence of intracellular puncta formation. Together, these data suggest that biotinylated $\alpha$-synuclein fibril seeds are internalised by cells and are capable of seeding intracellular inclusion formation as others have described [263]. Furthermore, the the seeding of GFP-$\alpha$-synuclein puncta is indicative of fibrils accessing the cytoplasm of the cell and seeding cytoplasmic $\alpha$-synuclein aggregation.

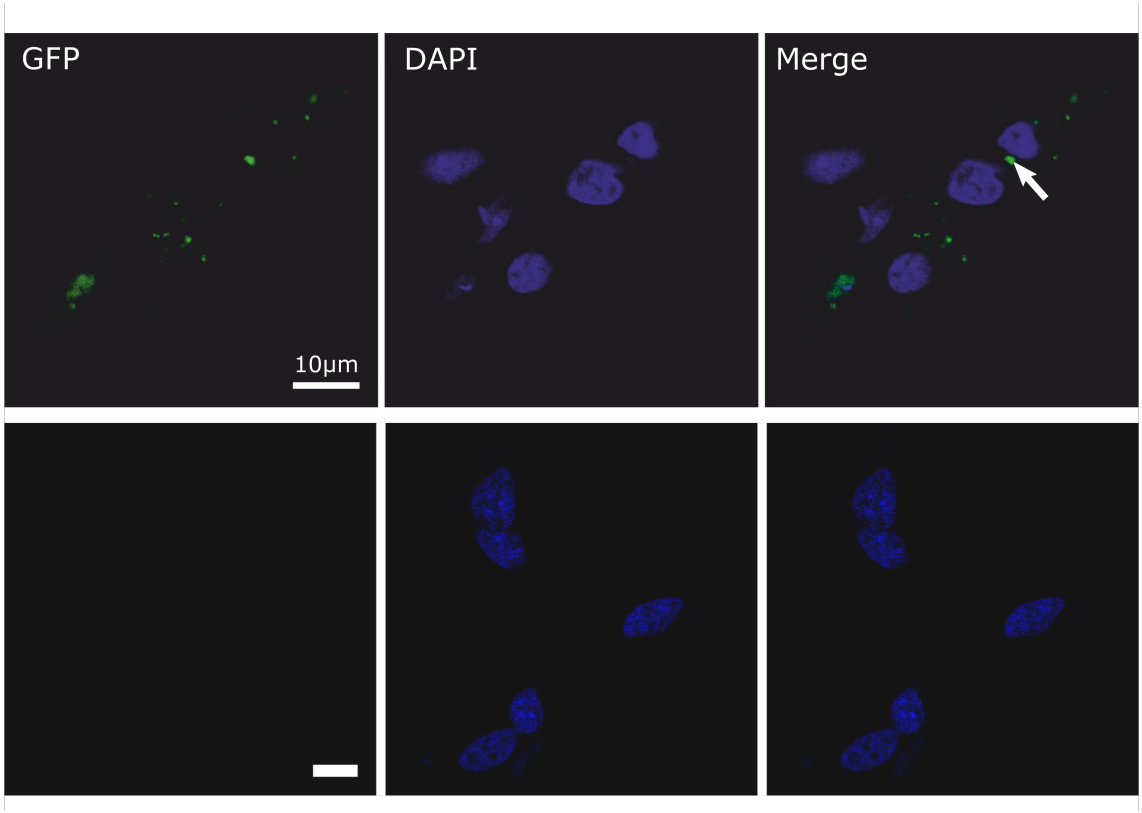


***Figure 3.23:*** *Biotinylated $\alpha$-synuclein A18C fibril seeds induce inclusion body formation in cells overexpressing GFP tagged $\alpha$-synuclein. Top: SH-SY5Y cells overexpressing GFP-$\alpha$-synuclein were incubated with biotinylated $\alpha$-synuclein A18C fibril seeds for 5 days. Cells were then fixed and washed to remove soluble GFP $\alpha$-synuclein and GFP-$\alpha$-synuclein puncta visualised by confocal microscopy. Bottom: Control GFP-$\alpha$-synuclein expressing SH-SY5Y cells not exposed to $\alpha$-synuclein A18C fibrils permeabilised and fixed in the same manner. Green denotes GFP, Blue denotes Hoechst nuclear stain. The white arrow denotes example of intracellular puncta.*

## 3.4 Discussion

The aim of this work is to identify the intracellular interactors of extracellularly added $\alpha$-synuclein fibrils, following their internalisation by SH-SY5Y cells. Herein a system was developed to allow the isolation of fibrils that were successfully internalised by SH-SY5Y cells. Firstly *in vitro* synthesis of performed fibrils from recombinant $\alpha$-synuclein monomer produced fibrils that were functionally and morphologically similar to those previously described [227, 259, 342]. Synthesised fibril seeds can subsequently be labelled with biotin and thereby isolated through the use of streptavidin-coated magnetic beads. Furthermore, it was shown that incubation of biotinylated fibril seeds, with SH-SY5Y cells, resulted in the formation of puncta indicative of the internalisation of $\alpha$-synuclein fibril seeds. Additionally, following internalisation, there was evidence of co-localisation with endolysosomal compartments and intracellular seeding of endogenous $\alpha$-synuclein aggregation, in line with the findings of previous studies [256, 259].

During the development of this system a number of issues were encountered that were overcome to develop this system. These problems included a failure of SH-SY5Y cells to internalise elongated fibrils and the inability to form morphologically fibrillar aggregates when synthesising fibril seeds from lysine biotinylated monomeric protein.

### 3.4.1 Internalisation of fibrils by neuronal-like SH-SY5Y cells

There is an abundance of evidence from previous study to indicate that neuronal-like cells, such as SH-SY5Y cells, can internalise preformed $\alpha$-synuclein fibrils from cell culture media [253, 259, 262]. Herein it was found that while $\alpha$-synuclein fibril seeds are internalised by SH-SY5Y cells elongated $\alpha$-synuclein fibrils were not. This finding is perhaps accounted for by the length of the fibrils. It has previously been demonstrated that in the case of $\beta_2$M amyloid fibrils, short fragmented fibrils are readily internalised while longer fibrils are not [340]. Indeed, the data presented here likewise suggests much greater internalisation of short fragmented $\alpha$-synuclein fibril seeds ( 75nm in length) than elongated $\alpha$-synuclein fibrils (>500nm in length). Furthermore, this finding is in line with other studies of $\alpha$-synuclein fibril internalisation, in which $\alpha$-synuclein fibrils with a length of 50-100nm were used to demonstrate internalisation [260].

Internalisation of $\alpha$-synuclein fibrils could also be affected by the lack of cell surface receptors on SH-SY5Y cells that are present on the surface of primary neuronal cells. This hypothesis may be supported by a previous failure to replicate internalisation seen in other studies in HEK-293 cells [263]. This cell line is an

embryonic kidney cell line and as such lacks a neuronal phenotype including several receptors found to be important in α-synuclein fibril uptake [260, 358, 359]. Indeed the SH-SY5Y cell used herein lacks the receptor leukocyte activation gene 3 (LAG3), shown elsewhere to be highly important for internalisation of α-synuclein fibrils [260]. Another study, investigating the mechanism by which α-synuclein fibrils are endocytosed, found evidence that SH-SY5Y cell surface receptors were capable of binding only 8% the number of α-synuclein fibrils bound by primary neuronal cells [260]. Together with evidence of greater α-synuclein fibril internalisation by primary neuronal cells than by SH-SY5Y cells in many studies [259, 262], this may suggest that SH-SY5Y cells lack one or more receptors to enable efficient internalisation of α-synuclein fibrils.

Short fibril seeds were shown to be internalised by SH-SY5Y cells where they co-localised, at least in part, with lysosomal puncta. This is in line with previous findings that have demonstrated the presence of α-synuclein fibrils in lysosomal compartments following internalisation by neuronal like cells [256, 360]. Futhermore, it was shown here that exogenous α-synuclein fibril seeds were capable of inducing the aggregation of endogenous α-synuclein protein, and the formation of intracellular inclusion bodies, in a manner similar to that shown elsewhere [253]

### 3.4.2 Difficulties Generating Lysine Labelled Fibril Seeds

Due to the failure of SH-SY5Y cells to internalise elongated α-synuclein fibrils, an effort was made to produce the shorter fibril seeds from biotinylated monomer. However, the addition of monomeric α-synuclein, lysine labelled with biotin, to the fibril synthesis reaction aggregates that appeared amorphous by EM. One possible explanation for this finding is the position of the lysine residues in the fibril structure of α-synuclein. A number of studies have been conducted to elucidate the structure of α-synuclein fibrils. Though the structure of the fibril varies between these studies, a common kernel, responsible for the inter-subunit and inter-sheet interactions of the fibril, has been identified [18, 233, 234] which encompasses residues 35-95.

This stretch (residues 35-95) includes 5 of the 15 lysine residues present in α-synuclein. Combined with the number of biotin labels present on the monomeric α-synuclein (an average of 7), there is a high probability that at least one of the lysines within this core region of the fibril are labelled. The presence of such a label within this region may disrupt the β-sheet stacking of the α-synuclein monomeric subunits via steric hindrance of interaction, thereby preventing the formation of protofibrils. Indeed, steric hindrance has previously been shown impair the formation of α-synuclein fibrils [361]. Furthermore, study of the structure of α-synuclein fibrils identified the presence of a salt bridge between E46 and K80 [233], an interaction

that would be perturbed by the presence of a biotin molecule conjugated to this residue.

Another possibility is that the biotinylation of one or more key lysine residues interferes with the inter-protofibril interface, preventing the formation of the mature fibril. Cryo-EM studies that have successfully elucidated the structure of this interface, have shown a number of lysines facing into this interface. One such study identified K43, K45 and K58 as forming a cluster withing the interface via binding of an ion [233]. The presence of a biotin molecule on any one of these side chains may therefore disrupt the formation of a inter-protofilament interface.

However, this does not explain the finding that the same biotinylated monomer was capable of elongating fibril seeds. It was shown that when lysine biotinylated $\alpha$-synuclein monomer was present at less than 5% of the monomeric protein, $\alpha$-synuclein fibril seeds elongated at the same rate as those added to unlabelled monomer. Furthermore the elongated fibrils contained biotinylated subunits and these biotinylated elongated fibrils appeared morphologically similar to that of unlabeled elongated fibrils. Were biotinylated monomers of $\alpha$-synuclein interfering with the *de novo* synthesis of $\alpha$-synuclein fibrils, it may be expected that they would likewise disrupt the elongation of $\alpha$-synuclein fibrils. Therefore, it may be the case that one or more lysines play a role in the formation of the protofibrillar oligomer, required for *de novo* synthesis but not for elongation. Were this the case, biotinylation of a key lysine may prevent nucleation, thereby preventing the formation of a mature $\alpha$-synuclein fibril.

### 3.4.3 Conclusions and Future Directions

In this chapter a system by which $\alpha$-synuclein fibril seeds, henceforth simply termed $\alpha$-synuclein fibrils, can be synthesised, labelled and internalised by SH-SY5Y cells and isolated by means of streptavidin coated magnetic beads, has been demonstrated. The following chapters will explore the use of this system in identifying cellular proteins that interact with biotinylated $\alpha$-synuclein fibrils both in the context of interaction occurring in cell lysate and interaction following cellular internalisation.

One goal of this study is to investigate the intracellular interactions of a defined fibrillar species of $\alpha$-synuclein. It has been demonstrated that a large number of fibrillar conformations of $\alpha$-synuclein exist, some of which have been characterised at near atomic resolution. By synthesising fibrils *in vitro* under defined conditions, it enables future study to potentially identify differences in the interactomes of $\alpha$-synuclein fibrils displaying divergent morphologies, thereby elucidating the mechanisms by which fibril strains can differ in their cellular toxicity [247, 362].

The $\alpha$-synuclein fibril strain generated here has been characterised previously

[227, 337, 342]. At the time of developing this system, few high resolution structures of $\alpha$-synuclein fibrils existed. Since then a number of structures of $\alpha$-synuclein fibrils produced under a variety of conditions, have been elucidated [232–234]. Had these structures been available at the time when this system was under development one may have been chosen so as to enable further investigation of conformation specific interactions. Nonetheless, many of the methods used here may be applied in the future to various fibril polymorphs with existing high resolution structures, thereby permitting identification of structurally dependant interactions.

# 4

# Identification of Protein Interactors of $\alpha$-synuclein Fibrils in Cell Lysate

## 4.1 Aims

The aim of this chapter was to identify proteins from cell lysate that interact with $\alpha$-synuclein amyloid fibrils and monomeric $\alpha$-synuclein, and to identify biological processes and cellular components that were overrepresented within these interactomes. A further aim of this chapter was to compare these interactomes to identify those $\alpha$-synuclein interacting proteins, along with overrepresented biological functions or cellular components, that were specific to either fibrillar or monomeric $\alpha$-synuclein, as well as those shared by both monomeric and fibrillar $\alpha$-synuclein interactomes.

## 4.2 Introduction

This study aims to identify proteins that interact with $\alpha$-synuclein fibrils, in order to better understand the mechanisms of pathogenesis in the synucleinopathies. Traditionally studies investigating the pathogenesis of amyloid diseases have used targeted, hypothesis-driven approaches that focus on pre-selected proteins of interest. Indeed, it was by this method that A$\beta$, the major protein present in the amyloid plaques found in patients with Alzheimer's disease [363], was identified. Furthermore, this technique was used to further strengthen the link between $\alpha$-synuclein and LBs in Parkinson's disease [191]. However, the use of this approach may limit the discovery of novel proteins involved in the $\alpha$-synuclein amyloid driven pathogenesis, since only proteins already suspected of having a role in Parkinson's disease will be studied.

One alternative to this hypothesis-driven method is hypothesis-free, omics based methodologies. These methodologies include genomic, transcriptomic, epigenetic and proteomic techniques, all of which offer a high-throughput, unbiased approach for the discovery of novel pathways for human pathogenesis. Indeed, genomic studies enabled the identification of $\alpha$-synuclein as a key protein involved in the pathogenesis of Parkinson's disease, demonstrating a link between a mutations in the SNCA gene and familial Parkinson's disease cases [364–366]. Likewise, these techniques have been used to identify novel risk factors in other amyloid diseases such as Alzheimer's disease, where they provide the basis for new hypothesis-driven studies [367, 368].

### 4.2.1 Proteomics

The term proteomics refers to the study of the proteins and the proteome. Tandem MS is a commonly used technique in the field to identify proteins within a sample [369]. This technique can be further enhanced via several methodologies that permit relative quantification of the identified proteins between samples. Several of these quantitative techniques rely on the use of isobaric tags, covalently attached to digested peptides prior to analysis by tandem-MS. By analysing the tandem-MS spectra of these peptides it is then possible to quantify their presence, and therefore that of their associated protein, between samples. The quantitative approach taken herein utilised an isobaric tagging approach known as TMT. The use of an isobaric tagging based approach to quantitative proteomics provides several benefits over other quantitative methods such as SILAC: it enables a large number of samples to be compared simultaneously (up to 11) and does not require cells to be grown in labelled media as SILAC does. The use of this techniques enables the quantification of proteins interacting with isolated $\alpha$-synuclein relative to the interactors of the

beads alone. Using this method protein interactors of $\alpha$-synuclein can be defined.

Proteomics based study is especially helpful in the study of amyloid-related diseases, due to complexity and multifaceted nature of these disorders. Furthermore, there is evidence to suggest that there is limited correlation between RNA expression and protein levels, particularly in amyloid affected tissues [370]. Therefore, the findings of genomic studies can serve to highlight the genes involved, while proteomics and related methods can validated and dissect these findings with regards to proteome. There are two primary areas of research into amyloid related disease that have been investigated by previous proteomics-based studies. These are: research into the metabolic events leading to the disease, and the identification of biomarkers for the diagnosis and monitoring of the disease. Investigations into the metabolic events can be further subdivided into those that examine the global proteomic changes of the cells or tissues and those that examine interactomes through the use of pull-downs or other isolation techniques.

Several previous studies have leveraged quantitative proteomics to investigate the wide ranging interactions of amyloidogenic proteins including poly-Q expanded Huntingtin protein [267], synthetic amyloidogenic peptides [312], and $\alpha$-synuclein. Using a pull-down methodology poly-Q expanded huntingtin aggregates were isolated from cells overexpressing the protein [267]. It was found that many of the proteins shown to be interacting with the amyloid protein were found to be ribonucleic acid (RNA) binding proteins as well as proteins involved in ribosome biogenesis, translation, transcription and vesicle transport [267]. A similar methodology of protein overexpression within the cell, followed by isolation of amyloid aggregates was conducted on artificial amyloid proteins [312]. This study identified a number of the amyloid interactors played a role in the nuclear import export machinery [312]. The interactome of $\alpha$-synuclein has also been investigated through the identification of proteins found in LB-like inclusions that form following incubation of neuronal cells with pre-formed amyloid fibrils [371]. Of note was the discovery of a number of mitochondrial proteins within the interactome, combined with a finding that mitochondrial function was disrupted in inclusion forming cells [371].

### 4.2.2 Bioinformatic Tools

The use of proteomics in identifying changing or interacting proteomes of amyloidogenic proteins would be of limited usefulness however, were it necessary for each identified protein to be individually investigated. The study of poly-Q huntingtin interactions, for example, identified nearly one thousand individual proteins [267], while studies of whole cells or tissue samples can easily identify ten times that number [372, 373]. Many bioinformatic tools have been developed [326, 327, 374–380]

to enable meaningful conclusions to be drawn from large proteomic data sets. A key family of bioinformatic tools, used widely to analyse proteomic data tools is term enrichment analysis software, that aims to identify commonalities between the function and or location of identified proteins that is overrepresented compared to the whole population.

The implementation of such tools requires that there is information on the function and cellular location of every protein under investigation. Equally important is that this data be in a standardised and easily searchable format. The Gene Ontology is a major bioinformatic initiative that began over a decade ago to develop a central repository for structured annotations of genes and gene products [381]. The Gene Ontology provides an ontology of annotation terms, representing gene properties. These annotations are organised as a directional acyclic graph, with each child annotation being more specific than its parent.

The primary relation of a child annotation to a parent is a straightforward increase in specificity of the term (ie. mitochondria and membrane bounded organelle) and is referred to as an 'is a' relation (eg. ribosome is a cytoplasmic part). Every annotation in the graph can be traced via 'is a' relations to one and only one, of three primary domains: cellular component, the parts of a cell or its extracellular environment; molecular function, the activity of a gene product at the molecular level such as binding or catalysis; and biological process, operations or sets of molecular events that form a definable process in living tissue. In addition to 'is a' relationships between annotations in the Gene Ontology there exist other optional relationships such as 'part of', denoting that the child is physically 'part of' the parent (eg mitochondrial membrane 'part of' mitochondrial envelope). These additional relationships enable a complex hierarchy of annotation terms to be traversed in a logical, and biologically meaningful manner.

Bioinformatic tools make use of this ontological system of annotation alongside the central repository managed by EMBL-EBI, in order to identify common annotations. Common enrichment analysis tools such as Panther [377], DAVID [378, 379], ClueGO [327], and BiNGO [326] to name but a few, calculate the enrichment of every GO term associated with the sample under analysis against a given background. GO term enrichment is calculated as follows. First the number of proteins in the sample, annotated with the GO term are computed. Next is calculated the probability of finding that number of proteins, annotated with the GO term, in a random sample of the same size, drawn from the background. This probability (p-value) is often then adjusted to account for the multiple tests (i.e. the number of GO terms being evaluated) increasing the false positive (or false discovery) rate. This adjusted p-value is known as the FDR. If this FDR falls below a certain threshold (generally 0.05) the GO term is considered significantly enriched in the sample. Using this method it

is possible to identify biological pathways, and subcellular structures most affected in the proteomic study. This method is especially useful in studies in which a subset of proteins is isolated from a background of cellular proteins, as is the case with pull-down studies.

When such analysis was conducted on the proteomic data of artificial poly-Q expanded huntingtin proteins, over expressed within cells it was shown that proteins involved in binding RNA were highly enriched, as were proteins involved in ribosome biogenesis [267]. By making use of this method the focus of the study could be directed onto specific questions; further study demonstrated that the expression of the poly-Q expanded huntingtin protein caused significant mislocalisation of the ribosomal biogenesis factor fibrillarin highly suggestive of disruption to ribosome biogenesis [267]. Each GO term enrichment tool-set offers its own advantages for simplifying the process of identifying meaningful terms that have been enriched. For example tools like DAVID [379] enable clustering of GO terms by semantic similarity, collecting related terms into groups. The tool used herein, BiNGO, enables visualisation of enriched GO terms in the context of the GO term network. This permits the researcher to quickly identify likely terms of interest without being overwhelmed by terms that are either too narrow or too broad to be of biological value [326].

The kyoto encyclopedia of genes and genomes (KEGG) pathway database is another method by which key functions of an interactome can be identified. It is a collection of pathway maps linking many entities including genes, proteins, RNAs and chemical reactions, as well as disease genes and drug targets [382–385]. By assessing the cellular pathways linked to the proteins within the interactome and comparing the rate of pathway occurrence with its occurrence in the background proteome it is possible to identify those pathways that are overrepresented within the interactome.

Other bioinformatic tools include the protein protein interaction tool STRING [376]. This tool was developed with the intention of identifying and cataloging the multitude of known interactions between gene products. Using multiple methods including curated interaction annotations, including both functional and physical interactions, the tool provides a vast web of protein-protein interactions. Protein-protein interactions are identified by a number of methods including derived from experimental results, to automated annotation based on the known interaction of gene orthologs, to automated text-mining of research articles containing reference to both proteins in the abstract By providing a set of proteins the service will provide a visual representation, in the form of a vertex-edge graph, of the interactions between the provided set [386].

By examining clusters of proteins that are closely interacting with one another,

it is possible to extrapolate potential cellular aspects that may be affected by the experimental condition under investigation. This has been used alongside other bioinformatic techniques to acquire a clear picture of the changes that occur in the hippocampal proteome of Alzheimer's disease mouse models with neurofibrillary tangles [320]. Analysis revealed age dependent changes in inflammatory and synaptic signalling proteins, and represents a significant utility as a novel resource for the research into the Aβ tau protein crossover, and the pathophysiological changes that occur in vivo.

### 4.2.3 Overview

To identify cell lysate protiens interacting with $\alpha$-synuclein fibrils and monomer, biotinylated A18C fibrillar and monomeric $\alpha$-synuclein was incubated with lysate from SH-SY5Y cells. $\alpha$-synuclein fibrils/monomer were then isolated using the streptavidin coated magnetic bead isolation strategy developed in the Chapter 3. Interacting proteins from the lysate were then identified by TMT-based quantitative proteomics, using quantification to eliminate proteins only interacting with the streptavidin coated magnetic beads. Following identification of the proteins associating with $\alpha$-synuclein fibrils, bioinformatic analysis was performed to identify enriched annotation terms, and protein-protein interaction clusters in order to identify pathways and subcellular locations which may be affected by the presence of $\alpha$-synuclein fibrils.

## 4.3 Results

### 4.3.1 Isolation of $\alpha$-Synuclein Fibrils From SH-SY5Y Cell Lysate

To identify the fibrillar interactome of $\alpha$-synuclein cells, the methodology of fibril isolation developed in the previous chapter was applied to lysate derived from the SH-SY5Y neuroblastoma cell line. The experiment was conducted in triplicate with two experimental conditions. In the first condition (termed Control) streptavidin coated magnetic beads were added directly to the lysate and the pull-down was performed as previously described in Section 3.3.10. This would allow the proteins that interact with the magnetic beads, in the absence of fibrils to be identified. In the second condition (termed Fibril), biotinylated A18C $\alpha$-synuclein amyloid fibril seeds (Hereafter termed $\alpha$-synuclein fibrils (described previously in Section 3.3.9) were incubated with the lysate for 30 min prior to the addition of the streptavidin coated magnetic beads. The results of the fibril pull-down were analysed by SDS-PAGE stained with Silver-Stain (Fig. 4.1). These data showed that $\alpha$-synuclein fibrils were isolated from cell lysates and that proteins derived from the cell lysate were pulled down with the $\alpha$-synuclein fibrils to a greater extent than in the control in absence of $\alpha$-synuclein fibrils. These samples were then analysed by TMT proteomics. By quantifying the peptides in the fibril sample relative to its matched control sample it would then be possible to identify proteins that specifically interacted with $\alpha$-synuclein fibrils.

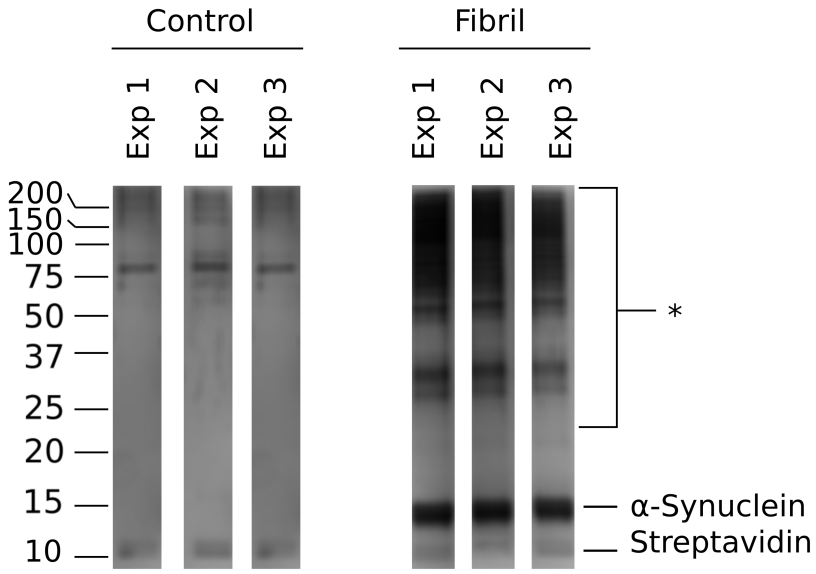


***Figure 4.1:*** *Fibrillar α-synuclein was isolated from cell lysate along with a number of cellular proteins. Cell lysate derived from SH-SY5Y cells was incubated in the presence (Fibril) or in the absence of fibrils (Control) for* 30 min. *Magnetic streptavidin beads were then added and the pull-down performed. The experiment was performed in triplicate to enable statistical analysis of the quantitative proteomics results, and samples of each pull-down fraction analysed by SDS-PAGE and stained with silver stain. The bands representing α-synuclein fibrils and streptavidin are marked. * denotes potential cellular interactors.*

### 4.3.2 Strategy for Defining Proteins That Interact With α-Synuclein Amyloid Fibrils

Proteomics analysis identified a total of 2249 proteins between all pull-down experiments. A number of these proteins were known contaminants, or were identified by only 1 peptide, thereby lowering the confidence of the identification. As a consequence such proteins were excluded, leaving a pool of 1382 proteins. In order to define a protein as an interactor of fibrillar α-synuclein a strategy was required to differentiate them from the non-specific interactions, ie. interactions that occurred due to an interaction between the protein and the streptavidin coated magnetic beads used for isolation. A distinction was made between these two types of interactions by examining two properties of the protein in question: the mean fold change in protein abundance between the α-synuclein fibril negative sample and the α-synuclein fibril positive sample, and the p-value of this change.

For a protein to be considered a specific interactor of α-synuclein fibrils, opposed to an interactor of streptavidin coated magnetic beads, it must meet the following thresholds: a mean fold change in abundance of $> 1.5$, and a p-value of $<0.05$. This

method of analysis was chosen as it accounts for not only the absolute fold change but also the variation between samples, weighting those with tighter spread above those with wide variation. A graphical representation of this gating strategy is shown in Figure 4.2. Using this strategy proteins in the top right sextant were defined as interactors of $\alpha$-synuclein fibrils. This comprised a total of 991 proteins identified as $\alpha$-synuclein fibril interactors.

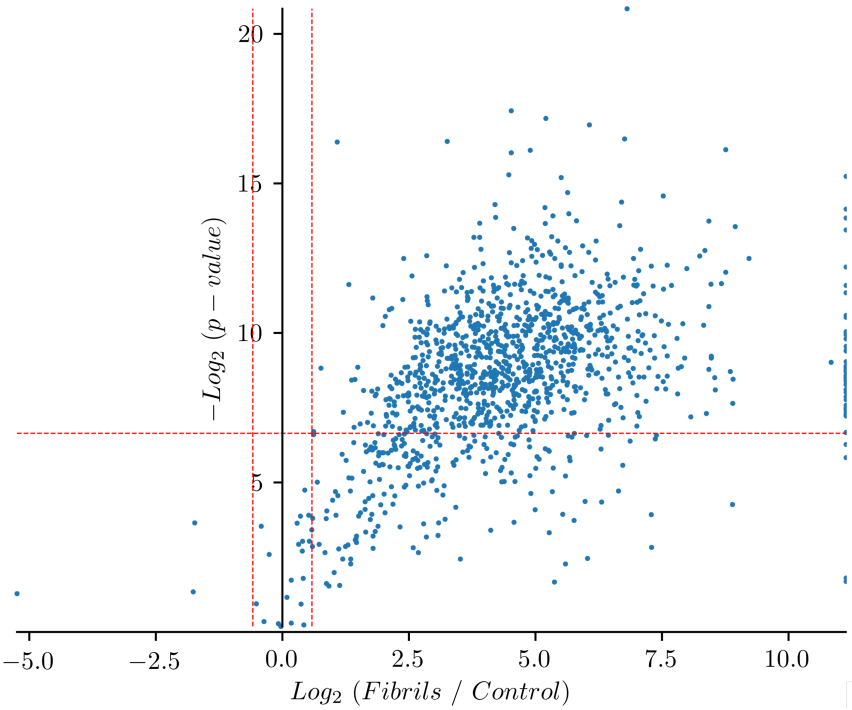


***Figure 4.2:*** *Proteins identified as specifically interacting with $\alpha$-synuclein fibrils. Volcano plot showing the ratio of abundance of each protein pulled down with $\alpha$-synuclein fibrils from cell lysate, compared to the control sample pulldown to which no fibril was added. The ratio is plotted against the p-value of this ratio (n=3). The red lines denote the cutoff for a protein to be considered an fibril interactor (ratio $> 1.5$, p-value $< 0.01$). Each point on this scatter plot represents a single protein identified by TMT proteomics.*

### 4.3.3 Interactome of $\alpha$-Synuclein Fibrils Contains Many Nuclear and RNA Binding Proteins

Having identified the proteins that were interacting with $\alpha$-synuclein fibrils it was of interest to identify cellular locations and biological functions that were overrepresented in the interacting protein set when compared to their representation in the human proteome. This was performed by utilising GO term annotations collated and managed by the Gene Ontology project [374, 375]. By comparing the number of proteins annotated with a given term in a sample set against the number of proteins

annotated with the same term in a background set it is possible to identify terms that are over-represented or enriched in the sample set.

GO term enrichment analysis was conducted on the full $\alpha$-synuclein fibril interactome (Fig. 4.2) using the proteome of the SH-SY5Y cell as a background [387]. For this purpose the identified interactome was further filtered by the presence of the protein in the SH-SY5Y cell proteome (812 proteins in total). All following bioinformatic analysis was conducted on this filtered dataset. From the results of this GO term enrichment analysis it is clear that many of the proteins identified as $\alpha$-synuclein fibril interactors were present in the cell nucleus as well as components of the cellular cytoskeleton (Fig. 4.3). The ribosome was also identified as a major location of $\alpha$-synuclein fibril interactors. Furthermore the biological function of the interacting proteins was heavily focused around RNA interactions and RNA proteins (Fig. 4.4). Other notable biological functions identified by this enrichment analysis were proteins involved in gene translation and chromosomal organisation.

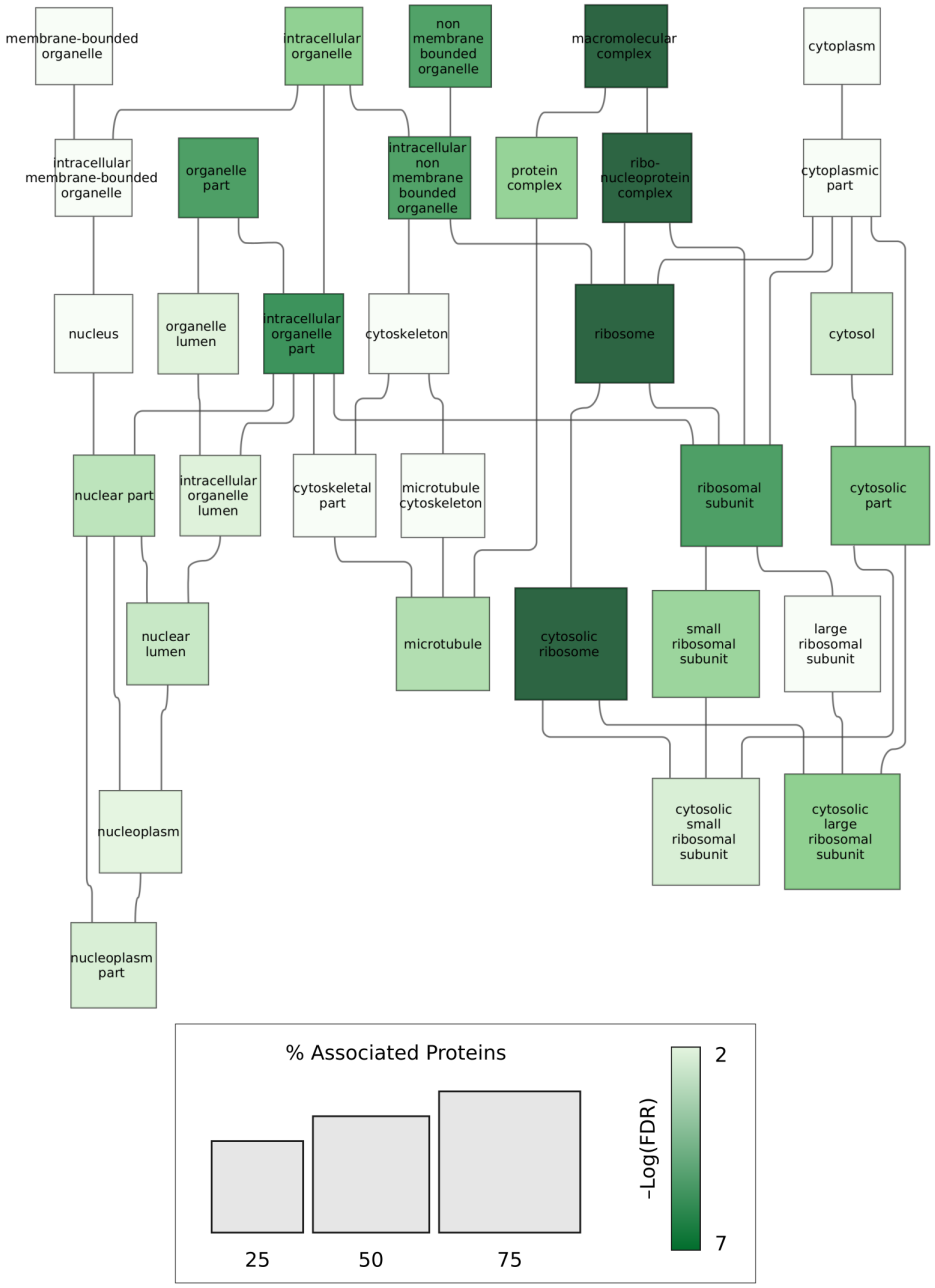


***Figure 4.3:*** *Proteins interacting with fibrils are enriched in proteins located in the nucleus, cytoskeleton and ribosomes. GO term (Cellular Component) enrichment analysis performed on fibril interactors of α-synuclein. Hierarchical graph showing the GO terms enriched in α-synuclein fibril interactors and their relationships to one and other. Node colour saturation denotes significance with, white nodes not significantly enriched (FDR > 0.05). Node size denotes the number of α-synuclein fibril interacting proteins possessing this annotation.*

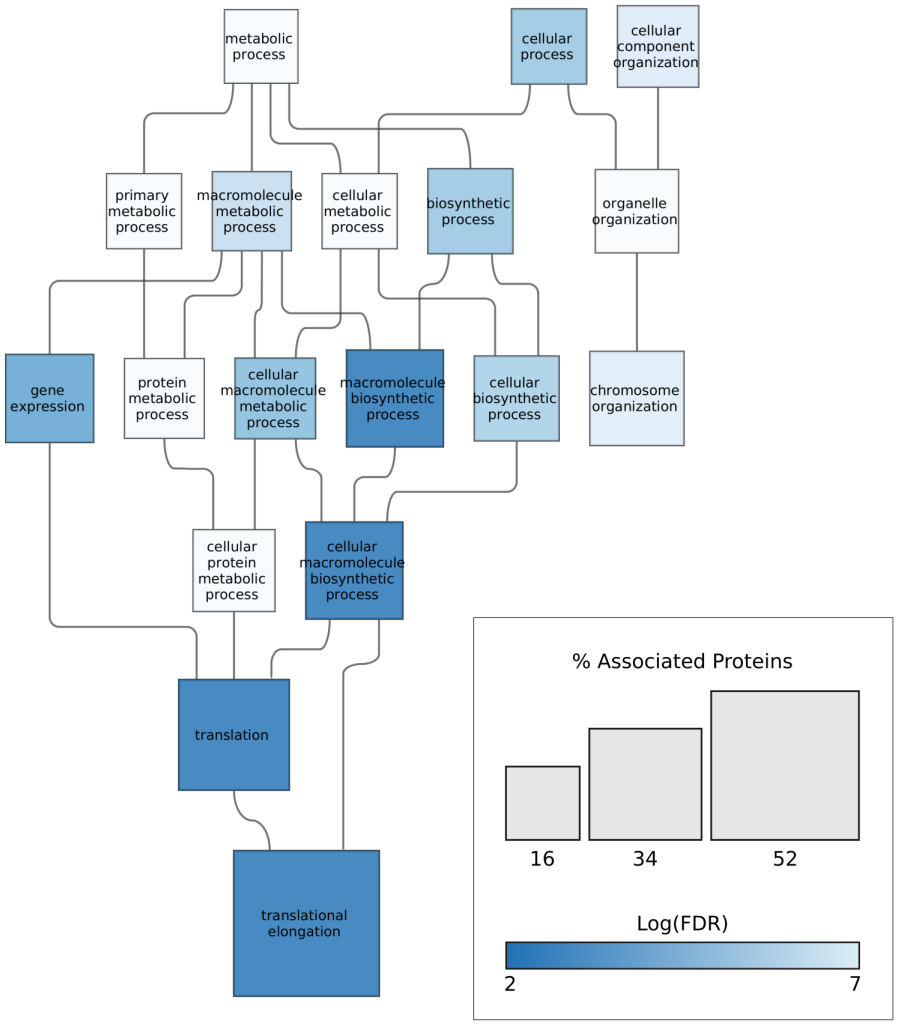


***Figure 4.4:*** *proteins interacting with fibrils are enriched in proteins involved in translation. GO term (Biological Process) enrichment analysis performed on fibril interactors of α-synuclein. Hierarchical graph showing the GO terms enriched in α-synuclein fibril interactors and their relationships to one and other. Node colour saturation denotes significance with, white nodes not significantly enriched (FDR > 0.05). Node size denotes the number of α-synuclein fibril interacting proteins possessing this annotation.*

### 4.3.4 Protein Interaction Network of $\alpha$-Synuclein Interactors Identified Several Clusters of RNA Interacting Proteins

In order to further investigate the role of proteins found to interact with $\alpha$-synuclein fibrils, with the aim of identifying potential pathogenic or protective pathways, a protein-protein interaction network of proteins that interact with fibrillar $\alpha$-synuclein was constructed using protein interaction data from StringDB [376]. StringDB is a useful tool for assessing protein-protein interactions and visualising clusters of closely interacting proteins within larger sets, providing data on many protein-protein interactions derived from several sources including: experimental evidence, gene expression analysis and text mining [376]. $\alpha$-synuclein fibril interacting proteins were analysed by this tool to identify highly interacting protein clusters. The identification of such clusters may suggest the isolation of protein complexes, which would both strengthen the case for individual proteins being true interactors of $\alpha$-synuclein fibrils and potentially point to new avenues for future research.

The full network of $\alpha$-synuclein fibril interacting proteins was too large to meaningfully visualise. Therefore the network was clustered using the MCL algorithm for clustering [388]. Unlike some other clustering algorithms that require the user to input the number of clusters as a parameter, this algorithm automatically identifies the number of clusters by looking at the interconnection between the proteins. In this way highly interconnected groups of proteins will be assigned to independent clusters. The largest five clusters identified by MCL clustering analysis were visualised (Fig. 4.5). Furthermore, interaction clusters that contain several proteins each highly enriched (i.e. the protein has a low p-value and fibril:ratio Fig. 4.2), may be of significant interest. Therefore, in order to visualise the enrichment the size of each protein node in the interaction network was set as proportional to the fold change of the protein abundance (ie. the protein position in the X axis of Fig. 4.2), while the transparency of the protein node was set proportional to the p-value of this change (i.e. the protein position in the Y axis of Fig. 4.2). The result is that the closer the protein is to the top right of the volcano plot (Fig. 4.2) the larger and more opaque it appears in the network (Fig. 4.5).

Two major clusters readily identified in this network can been seen coloured in red and blue. Both contain a number of closely interacting proteins, that are highly enriched in the $\alpha$-synuclein fibril interactome (Fig. 4.5). In order to gain a better understanding for the proteins that these clusters represent, GO terms associated with each cluster were identified and visualised (Fig. 4.6). From this it can be seen that the largest cluster (Fig. 4.6 Blue) represents ribosomal associated proteins, including a large number of structural ribosomal components. The second major

cluster (Fig. 4.5 Red), is dominated by spliceosomal protein components.

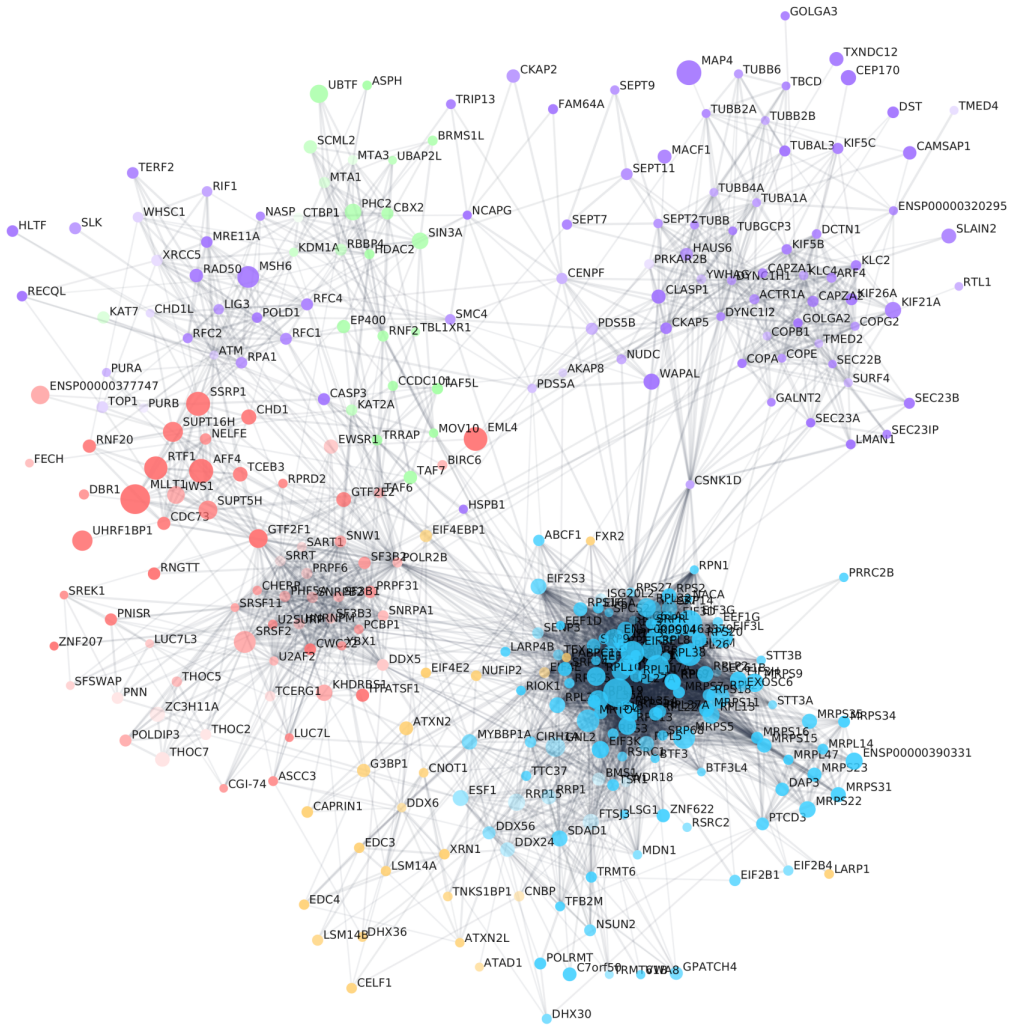


***Figure 4.5:*** *Protein-protein interaction network of α-synuclein fibril interactors. Network of protein-protein interactors compiled by the StringDB service. The network was clustered using the MCL algorithm, and nodes coloured based on the cluster in which they appear. Node size denotes the ratio of the protein abundance vs control (Fig. 4.2 X axis). Node transparency denotes the p-value of the abundance ratio (Fig. 4.2 Y axis)*

Another major protein interaction cluster that can be identified in the interactome of α-synuclein fibrils, can be seen (Fig. 4.5 purple). The proteins contained by this cluster appear to represent proteins of the Golgi, endoplasmic reticulum and microtubular proteins. Due to the diverse nature of these proteins and the apparent presence of two identifiable clusters within this cluster, MCL clustering was performed on this cluster to generate a number of sub-clusters that could be investigated with greater accuracy. From this analysis it was possible to identify two major clusters

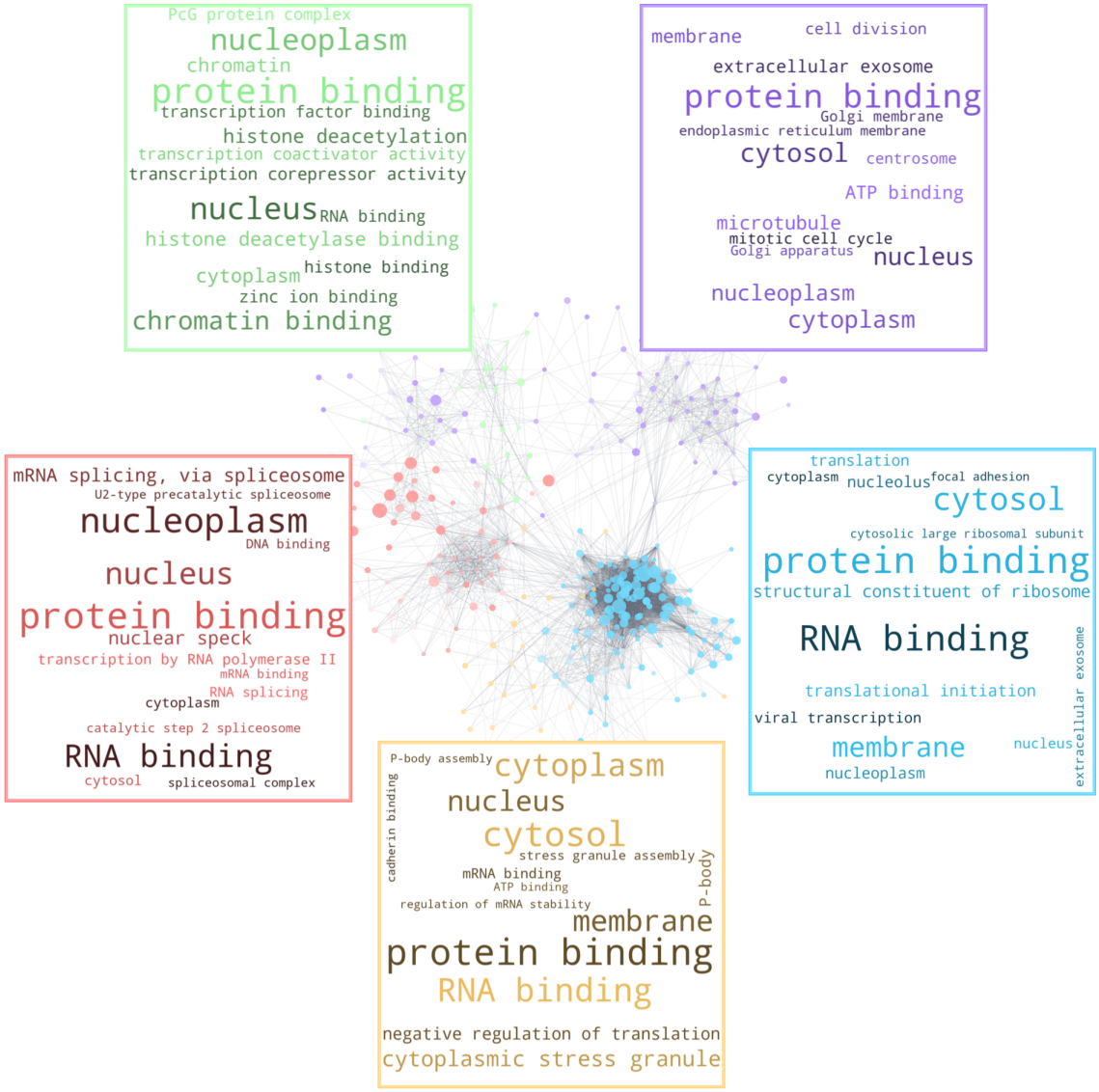


***Figure 4.6:*** *GO terms associated with the protein-protein interaction clusters (Fig. 4.5). GO term clouds generated from GO terms associated with proteins in each StringDB network cluster.*

(Fig. 4.7).

The largest of these sub-clusters contained several proteins found in the Golgi and ER and as well as exosomes (Fig. 4.7 B Right panel). Further investigation of the KEGG pathways [382–384] associated with this sub-cluster identified several pathways including endocytosis and phagocytosis. Furthermore, several synaptic pathways were also found to be associated with the cluster. Interestingly, in addition to other pathways, several amyloid disease pathways were found to be strongly associated with this cluster including Huntington's disease, Alzheimer's disease and Parkinson's disease among others (Fig. 4.7 C Right Panel).

The second major sub-cluster (Fig. 4.7 Purple), identified in interactors of $\alpha$-synuclein fibrils, contained a number of proteins involved in DNA repair, replication and maintenance (Fig. 4.7 B Left Panel) including the DNA mismatch repair protein Msh6 that was highly enriched in the interactome of $\alpha$-synuclein fibrils (Fig. 4.7 A). Further KEGG pathway analysis of this sub-cluster revealed similar pathways were associated. These pathways included DNA mismatch repair DNA replication and non-homologous end-joining (Fig. 4.7 C Left Panel). These data clearly indicate that the interactome of $\alpha$-synuclein fibrils is heavily populated by proteins involved in DNA and RNA functions as well as a number of proteins involved in the endosomal pathway.

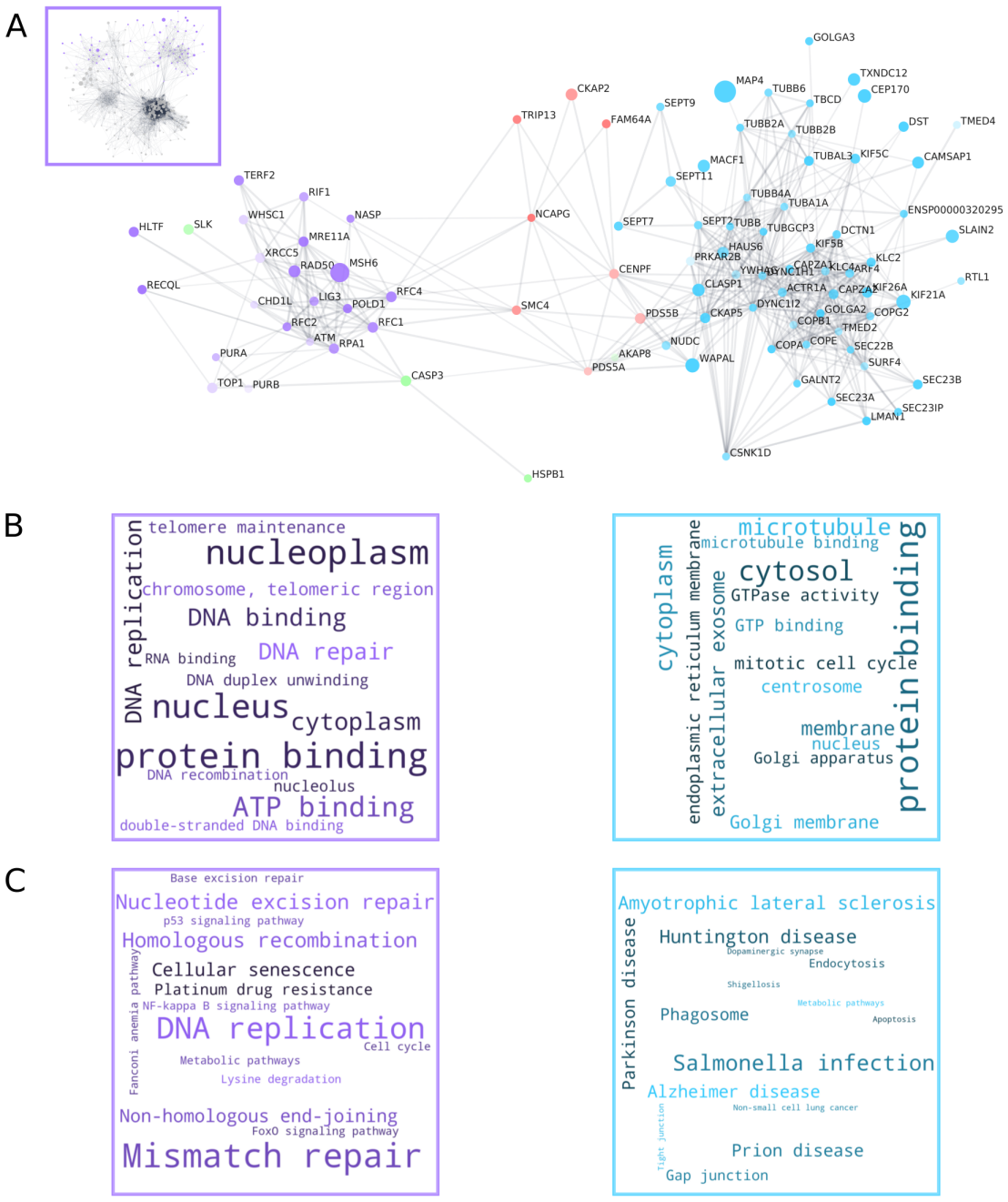


***Figure 4.7:*** *Sub-cluster of protein-protein interaction network of α-synuclein fibril interactors. A) Network of protein-protein interactors in the purple cluster identified in Fig. 4.5. The network was sub-clustered using the MCL algorithm, and nodes coloured based on the cluster in which they appear. Node size denotes the ratio of the protein abundance vs control (Fig. 4.2 X axis). Node transparency denotes the p-value of the abundance ratio (Fig. 4.2 Y axis). B) GO terms associated with the individual sub-clusters identified by colour. C) KEGG pathways associated with the individual sub-clusters identified by colour*

### 4.3.5 Proteins Interacting with $\alpha$-Synuclein Fibrils Have Limited Representation in the Interactomes of Other Amyloid Aggregates

In order to further investigate the identified interactome of $\alpha$-synuclein fibrils, the proteins shown to interact with $\alpha$-synuclein fibrils were compared with studies that have previously leveraged proteomics to identify protein interactomes of other amyloidogenic proteins and to study the proteome of cortical LBs. One such study investigated the proteins present in cortical LBs (Fig. 4.8 LB Genes [389]). Another study identified the interactome of various poly-Q expansions of the amyloid protein Huntingin (Fig. 4.8 Q64 and Q150 Interactors [320]). Q150 expansion huntingtin was shown to be primarily fibrillar while the Q64 expansion was largely oligomeric [320]. Further, a study investigating the interactome of an 'artificial' amyloid, a protein designed to form the cross-β structure typical of amyloid fibres (Fig. 4.8 Artificial Amyloid Interactors [312]).

The current interactome was compared to proteins that were enriched in LB like inclusions after 14 or 21 days in murine neuronal cells following treatment with $\alpha$-synuclein pre-formed fibrils generated from murine $\alpha$-synuclein (Fig. 4.8 Upregulated Pff 14 Day and Upregulated Pff 21 Day [371]). Due to the murine origin of these proteins, comparison to the current data set involved first identifying the human orthologs of the protein. For this purpose the latest version (2021) of PylomeDB was leveraged, to map each murine protein to its highest ranked human ortholog [390].

For each external dataset the proteins were compared to the current dataset and the intersection of proteins identified. The similarity of the two datasets was then computed by means of the Jaccard similarity coefficient in which the size of the intersection of the two datasets is divided by the size of the union of the datasets. The resultant value is a number between 0 and 1 where 1 indicates that all proteins found in one data set are found in the other and vice versa (i.e. the datasets are identical) and 0 indicates that there is not intersection between the data sets. The resultant plots for each external data set indicates that there is only limited similarity between the current data set and that of the Q64 and Q150 huntingtin interactors ( 0.1) and less similarity with the other datasets(Fig. 4.8 A).

Furthermore, mapping the proteins of the other datasets onto the volcano plot (Fig. 4.2) demonstrates that the proteins identified in other studies are not only found in the specific interactors of $\alpha$-synuclein fibrils but rather distributed throughout the proteins identified by this study, including both bead background binding proteins and fibril specific interactors (Fig. 4.8 B). Together these data suggest that there are some similarities between this and other amyloid protein interactomes as well as proteins of the LB. However, the limited number of similarities as well as their

distribution throughout the interactome suggests this similarity is minimal.

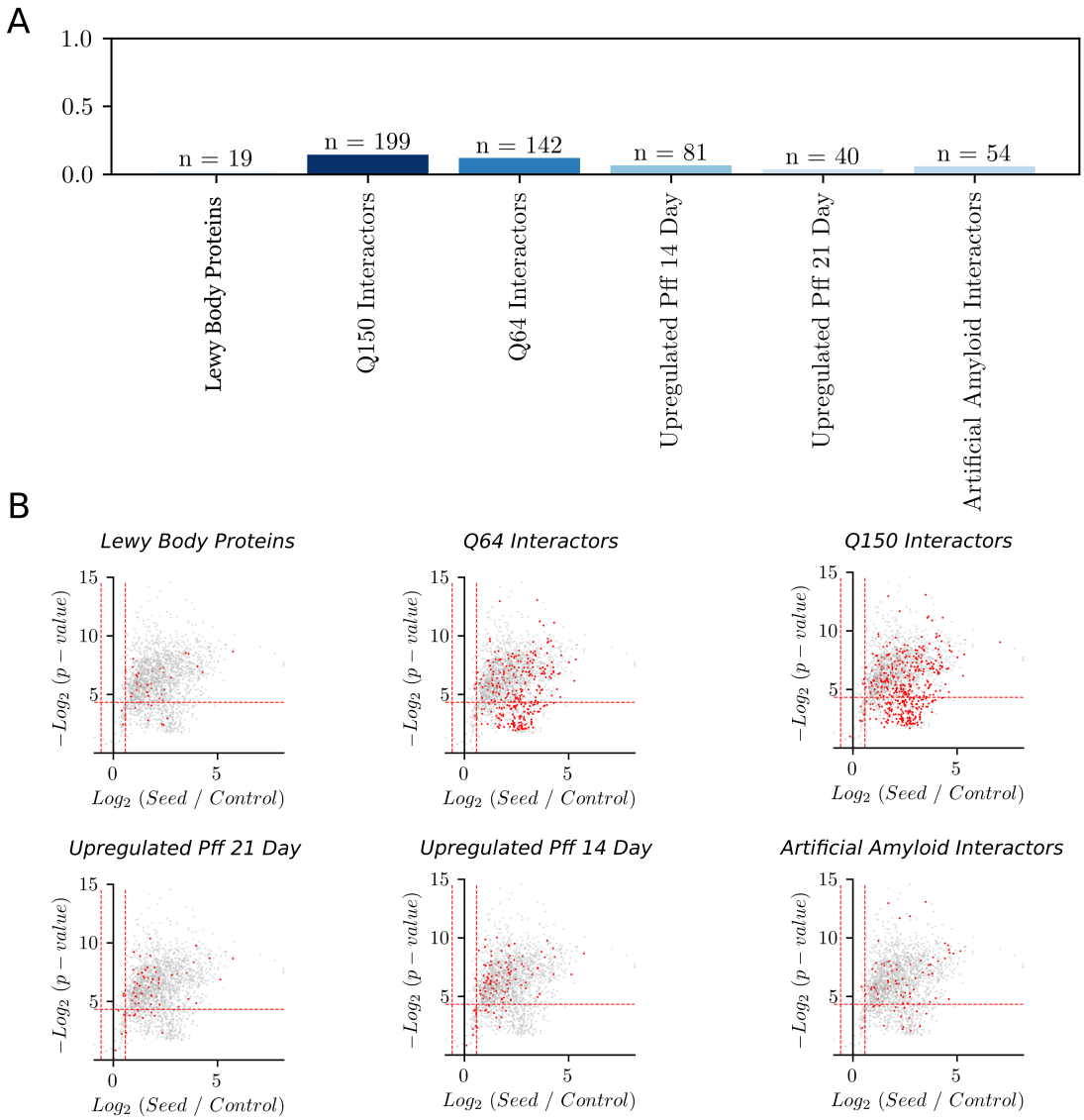


***Figure 4.8:*** *Similarity between α-synuclein fibril interactors and interactors and proteins identified in other proteomic studies of amyloid proteins. For each external dataset the proteins were compared to the current dataset and the intersection of proteins identified. The similarity of the two datasets was then computed by means of the Jaccard similarity coefficient. A) Bar chart of the calculated Jaccard Similarity Index between the proteins identified in this study as α-synuclein fibril interactors and the proteins identified as interactors of other fibrils or α-synuclein proteoforms. (Lewy Body Genes: [389], Q150 Interactors [320], Q64 Interactors [320],Upregulated Pff 14 Day [371], Upregulated Pff 21 Day [371], Artificial Amyloid Interactors [312]). For interactomes derived from mouse proteomes [371] were mapped to human orthologs using the PylomeDB mapping [390]. B) Volcano plot shown in Fig. 4.2 with the matching interactors of from the indicated study shown in red.*

### 4.3.6 Identification of Proteins Interacting with Monomeric $\alpha$-Synuclein

The investigation of the interactions of fibrillar $\alpha$-synuclein raised the question of whether these interactions were specific for $\alpha$-synuclein fibrils or whether the interacting proteins also bound to the monomeric form of $\alpha$-synuclein. Therefore another experiment was undertaken in which monomeric $\alpha$-synuclein was added to SH-SY5Y cell lysate in place of fibrillar $\alpha$-synuclein and isolated under the same conditions. This was done in parallel to the isolation of fibrillar $\alpha$-synuclein to enable direct comparison of protein abundances between fibrillar $\alpha$-synuclein and monomeric $\alpha$-synuclein. As previously samples were analysed by SDS-PAGE (Fig. 4.9). These data show the presence of isolated monomeric $\alpha$-synuclein in addition to a number of cellular proteins.

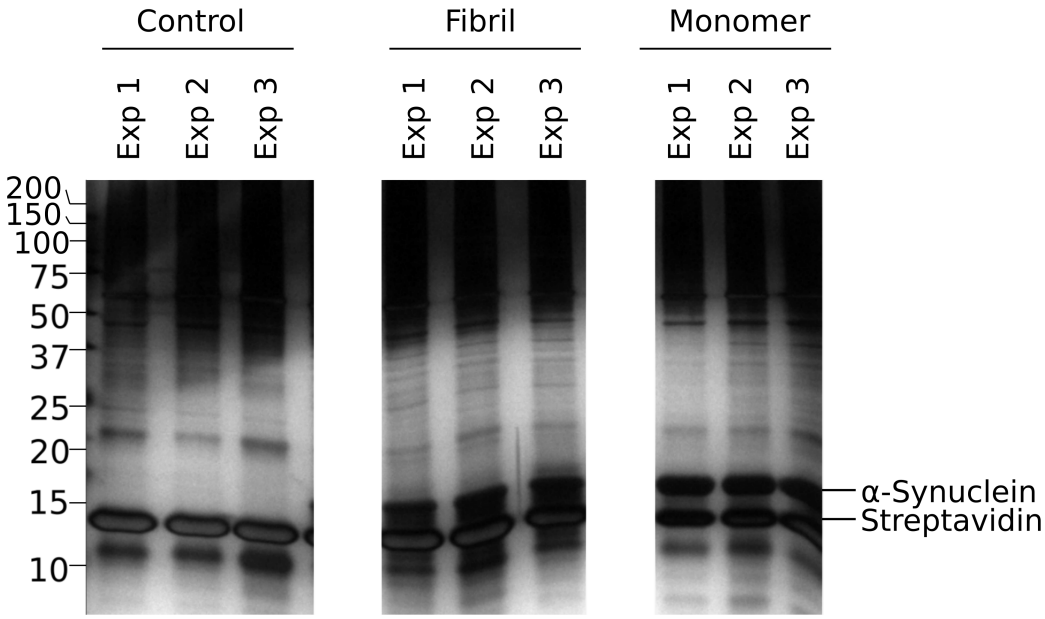


***Figure 4.9:*** *Monomeric $\alpha$-synuclein was isolated from cell lysate along with a number of cellular proteins. Cell lysate derived from SH-SY5Y cells was incubated in the presence monomeric $\alpha$-synuclein (Monomer) fibrillar $\alpha$-synuclein (Fibrils) or in their absence (Control) for* 30 min*. Magnetic streptavidin beads were then added and the pull-down performed. The experiment was performed in triplicate to enable statistical analysis of the quantitative proteomics results, and samples of each pull-down fraction analysed by SDS-PAGE and stained with silver stain. The bands representing $\alpha$-synuclein and streptavidin are marked.*

This experiment was modified in one important aspect: in order to isolate the same monomer equivalent concentration of monomeric $\alpha$-synuclein as fibrillar $\alpha$-synuclein a significantly larger quantity of beads was required. A consequence of this

was higher concentration of SH-SY5Y cellular proteins binding to the beads that can be seen in the control lanes shown in Fig. 4.9.

Proteomic analysis of these samples by TMT proteomics identified 3421 total proteins of which 1355 were excluded for being a contaminant or for being identified by only 1 peptide, leaving 2066 proteins. The discrepancy seen between the number of proteins identified by the previous experiment (Section 4.3.1) and the number of proteins identified here, especially under control conditions, is likely due to the higher concentration of beads required to pull-down monomeric $\alpha$-synuclein.

In order to define proteins as interactors of monomeric $\alpha$-synuclein an identical strategy to that used to identify fibrillar $\alpha$-synuclein interactors (4.3.2) was employed to differentiate them from the non-specific interactions, ie. interactions that occurred due to an interaction between the protein and the streptavidin coated magnetic beads used for isolation. As previously this distinction was made by quantifying the mean fold change in protein abundance between the $\alpha$-synuclein negative sample and the $\alpha$-synuclein positive sample, and the p-value of this change. For a protein to be considered a specific interactor of monomeric $\alpha$-synuclein, opposed to an interactor of it must have a mean fold change in abundance of $> 1.5$, and a p-value of $<0.05$ (Fig. 4.10).

By this method 1408 proteins were identified as interactors of monomeric $\alpha$-synuclein and 1573 proteins were identified as fibrillar $\alpha$-synuclein interactors. Of those fibrillar interacting proteins, 565 were found in the fibrillar $\alpha$-synuclein interactome described above, an overlap of 57% and a probability of independence (i.e. probability that the overlap occurred by chance) of $1.93 \times 10^{-63}$.

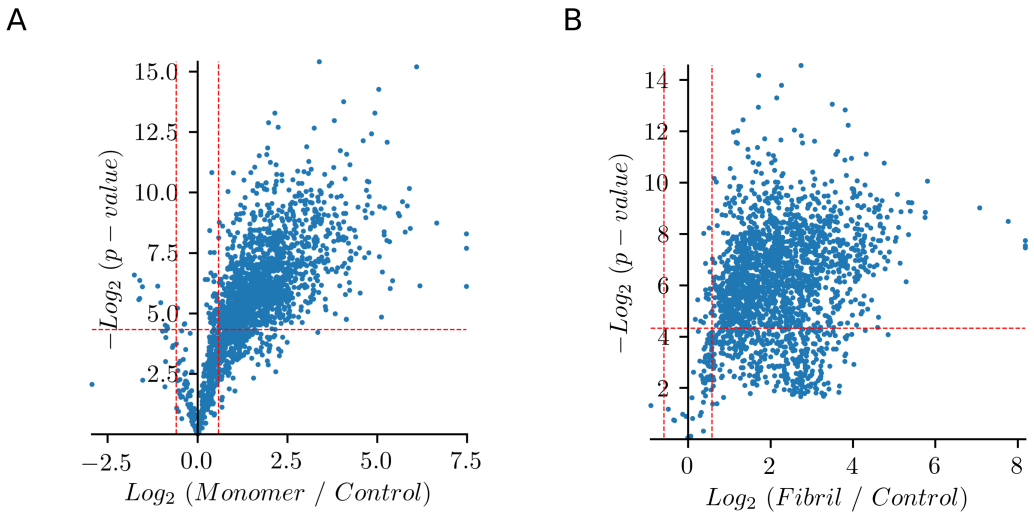


***Figure 4.10:*** *Proteins identified as interacting with monomeric and fibrillar α-synuclein. Volcano plot showing the ratio of the abundance of each protein identified by TMT proteomics, in α-synuclein monomeric samples (A) or fibrillar samples (B), to the abundance of the protein in the control sample, to which no α-synuclein monomer had been added. The ratio is plotted against the p-value of this ratio (n=3). The red lines denote the cutoff for a protein to be considered an monomer interactor (ratio > 1.5, p-value < 0.01)*

### 4.3.7 The Monomeric α-Synuclein Interactome is Enriched in RNA Interacting Proteins

Having identified the proteins that specifically interact with monomeric α-synuclein, a similar bioinformatic pipeline was followed to that described above for the interactome of fibrillar α-synuclein (4.3.3). GO terms, enriched in the monomeric α-synuclein interactome, were first identified. By this method it was shown that monomeric proteins were enriched in proteins involved in RNA transcription (Fig. 4.11) including ribosomal subunit components (Fig. 4.12). Futhermore the interactome was enriched in nuclear located proteins (Fig. 4.12), specifically including those involved in chromosomal remodeling (Fig. 4.11). These findings are closely related to those of fibrillar α-synuclein (4.3.3), suggesting a degree of similarity between monomeric and fibrillar α-synuclein interactors.

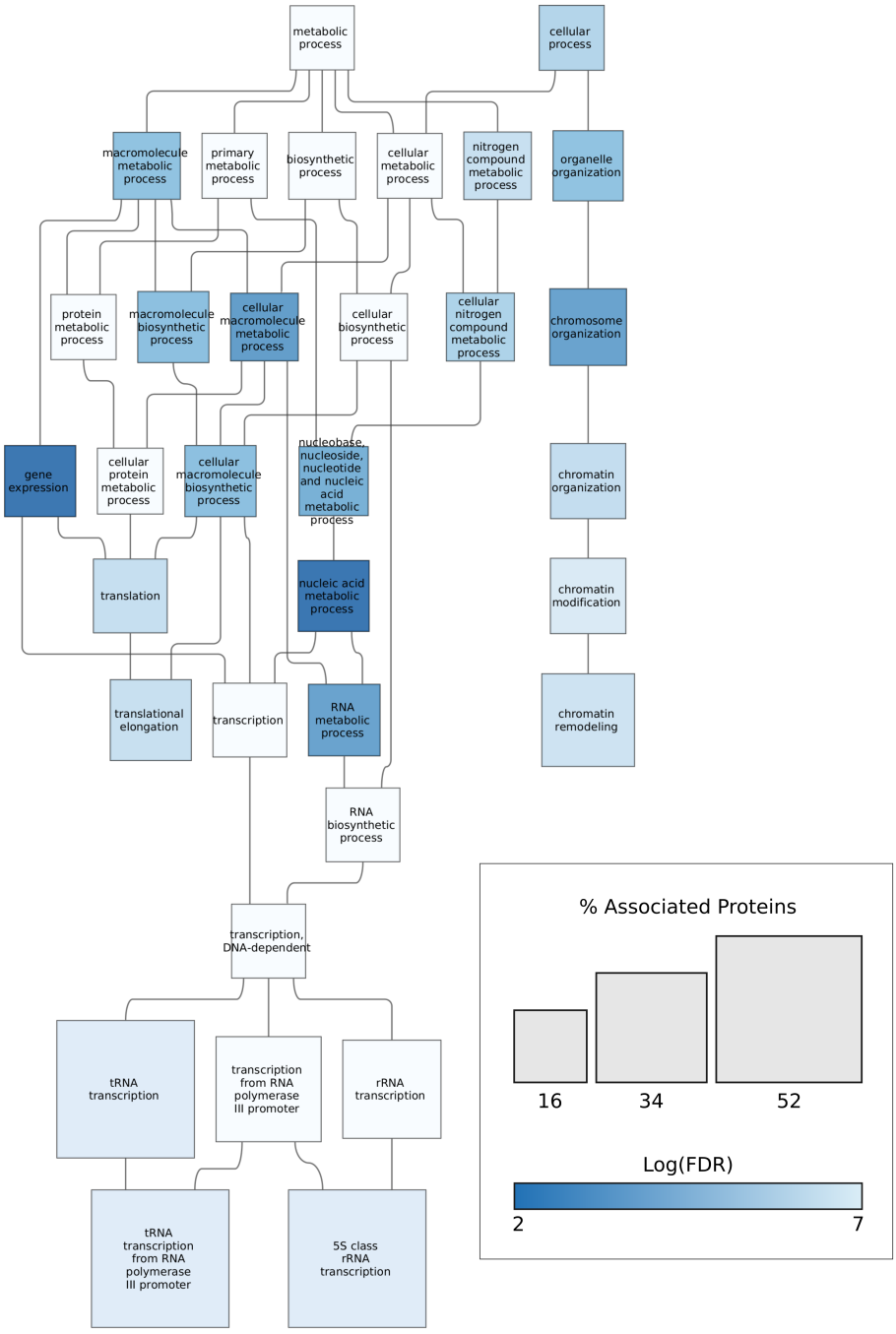


***Figure 4.11:*** *Proteins interacting with monomeric α-synuclein are enriched in proteins involved in chromatin remodeling and transcription. GO term (Biological Process) enrichment analysis performed on monomer interactors of α-synuclein. Hierarchical graph showing the GO terms enriched in α-synuclein monomer interactors and their relationships to one and other. Node colour saturation denotes significance with, white nodes not significantly enriched (FDR < 0.1). Node size denotes the number of α-synuclein monomer interacting proteins possessing this annotation.*

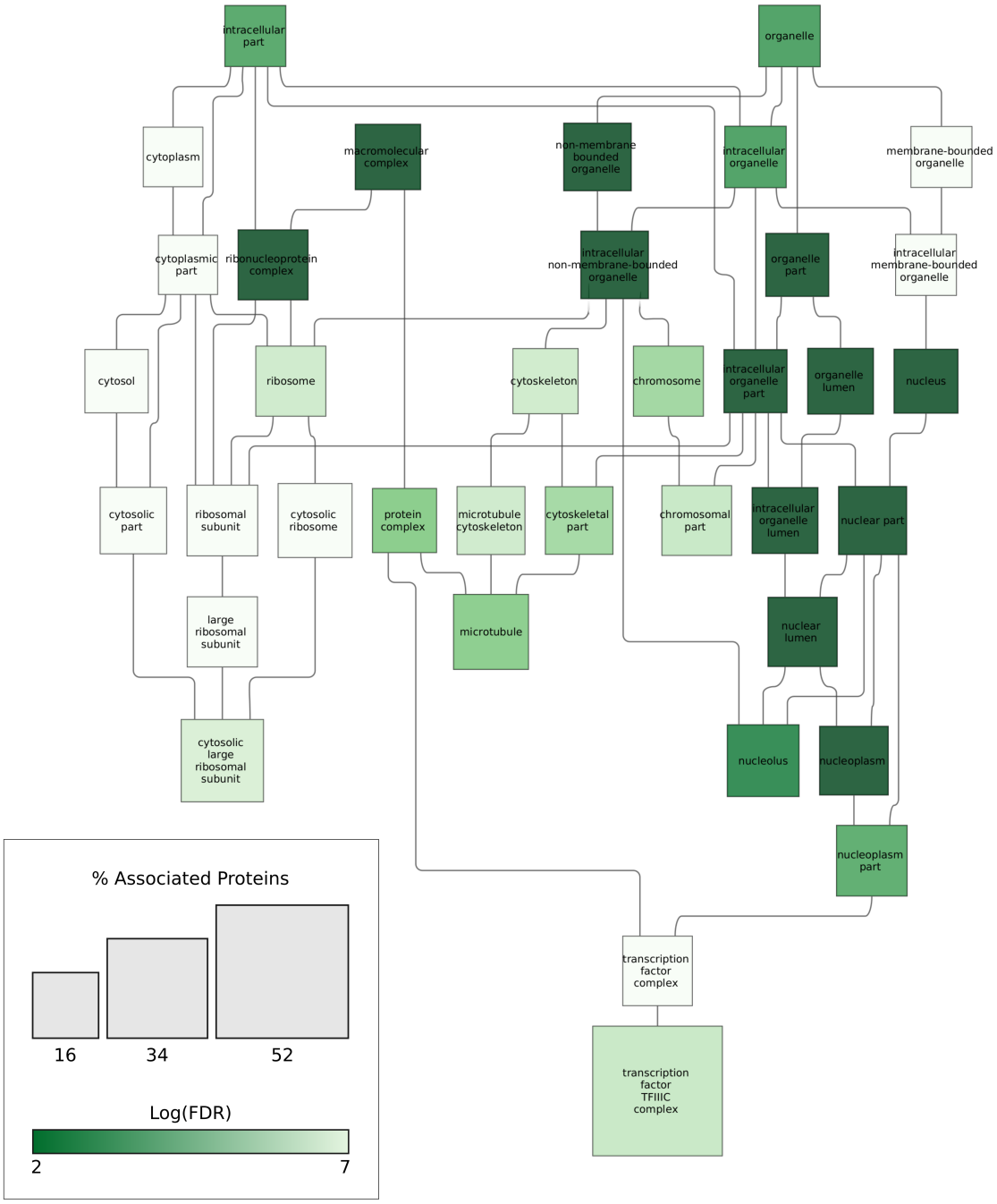


***Figure 4.12:*** *Proteins interacting with monomeric α-synuclein are enriched in proteins located in the nucleus, cytoskeleton and ribosomes. GO term (Cellular Component) enrichment analysis performed on fibril interactors of α-synuclein. Hierarchical graph showing the GO terms enriched in α-synuclein monomer interactors and their relationships to one and other. Node colour saturation denotes significance with, white nodes not significantly enriched (FDR < 0.1). Node size denotes the number of α-synuclein monomer interacting proteins possessing this annotation.*

### 4.3.8 RNA Binding Proteins are a Common Feature of the Monomeric $\alpha$-Synuclein Interactome

In order to further investigate the interactome of monomeric $\alpha$-synuclein the StringDB service was used to construct a protein-protein interaction network of the monomeric $\alpha$-synuclein interactome. This was done as above (4.3.4) and the network likewise clustered by the MCL clustering algorithm. The largest five clusters were then inspected to identify GO terms that describe each cluster. It was shown that monomeric $\alpha$-synuclein interacts with several large clusters, including those containing proteins involved in ribosomal translation, and RNA splicing as well as proteins involved in import and export of proteins from the nucleus (Fig. 4.13 and Fig. 4.14).

As was the case with the interactome of fibrillar $\alpha$-synuclein, the largest cluster of protein interactions identified represented ribosomal subunit proteins as, ribosomal associated proteins (Fig. 4.13 and Fig. 4.14 Blue). The second largest cluster (Fig. 4.13 and Fig. 4.14 Purple) was similarly closely related to a cluster identified in that of fibrillar $\alpha$-synuclein. The other major clusters identified involved proteins involved in RNA protein import and export from the nucleus (Fig. 4.13 and Fig. 4.14 Yellow), proteins found in cell microtubules and extracellular exosomes and involved in mitotic cell division (Fig. 4.13 and Fig. 4.14). From this initial investigation into the interactome of monomeric $\alpha$-synuclein it can be seen that many of the same protein functions and cellular locations can be found in both the fibrillar and monomeric $\alpha$-synuclein interactomes.

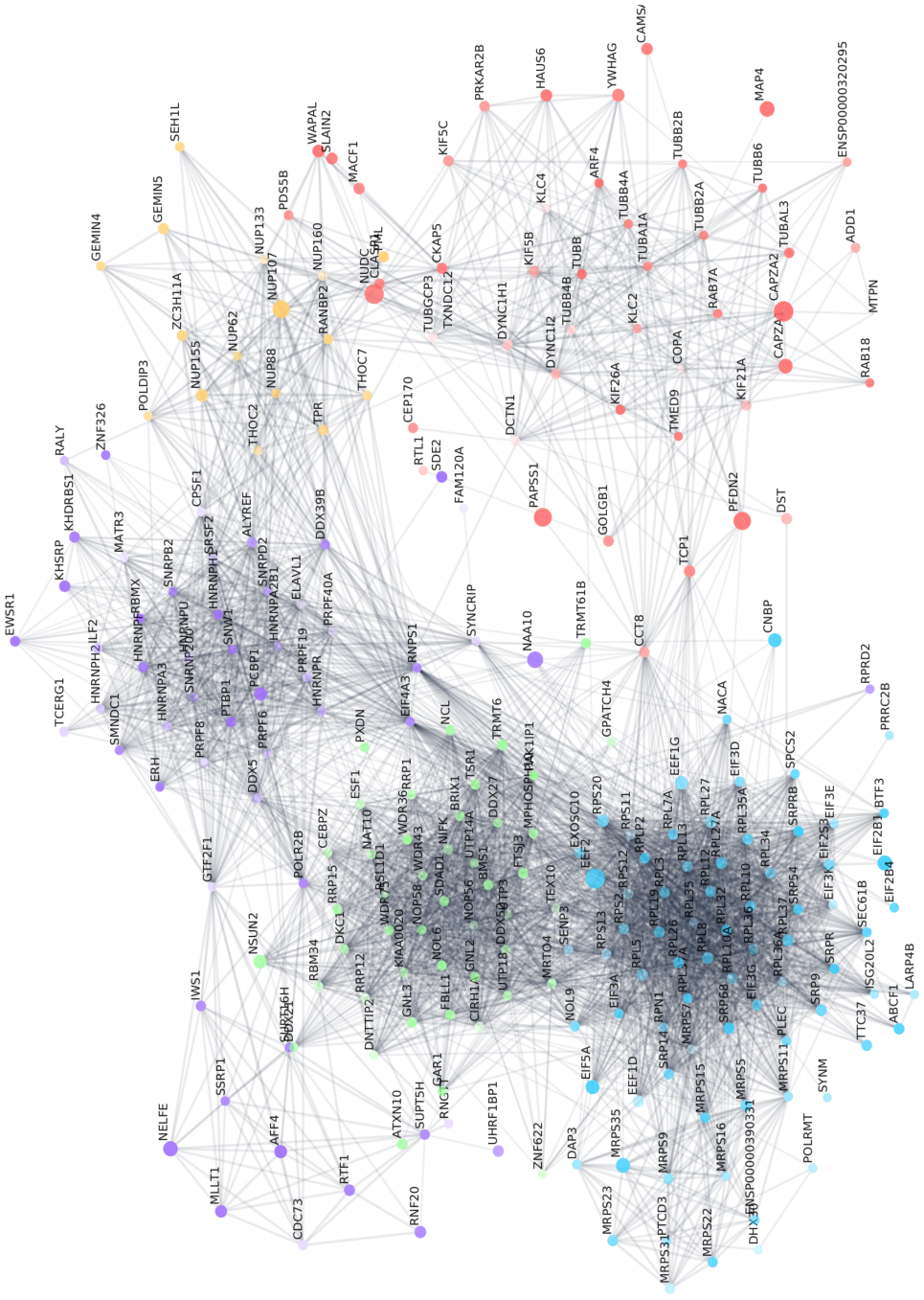


***Figure 4.13:*** *Protein-protein interaction network of α-synuclein monomer interactors. Network of protein-protein interactors compiled by the StringDB service. The network was clustered using the MCL algorithm, and nodes coloured based on the cluster in which they appear. Node size denotes the ratio of the protein abundance vs control (Fig. 4.10 X axis). Node transparency denotes the p-value of the abundance ratio (Fig. 4.10 Y axis)*

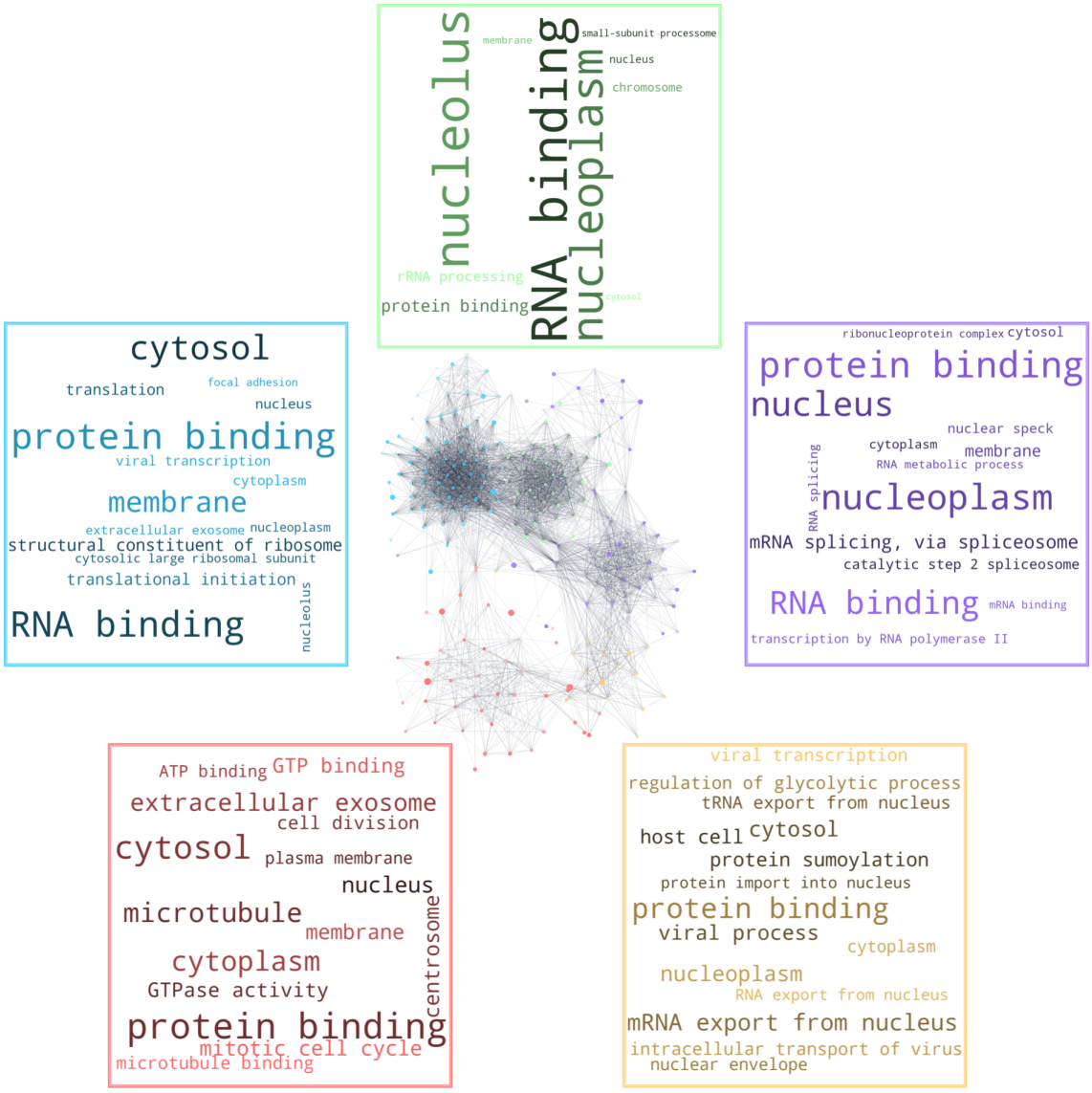


***Figure 4.14:*** *GO terms associated with the protein-protein interaction clusters (Fig. 4.13). GO term clouds generated from GO terms associated with proteins in each StringDB network cluster.*

### 4.3.9 There is Limited Similarity Between The Monomeric $\alpha$-Synuclein Interactome and Proteins Identified as Amyloid Interactors by Other Studies

Finally, as with the processing pipeline of the fibrillar $\alpha$-synuclein interactome, the similarity of the monomeric $\alpha$-synuclein interactome to multiple other proteomic studies investigating amyloid interactors [312, 320, 389, 391], or proteins upregulated following treatment with amyloid proteins [371], was computed by means of the Jaccard similarity coefficient. The resultant similarity coefficients closely resembled that of fibrillar $\alpha$-synuclein with the highest similarity being linked to Q150 and Q64 interactors (Fig. 4.15). Similarly, as was seen in the fibrillar interactome of fibrillar $\alpha$-synuclein the proteins identified by other studies were evenly distributed among the specific and non-specific interactors of monomeric $\alpha$-synuclein, when amyloid interactors are plotted onto the all proteins identified by this experiment (Fig. 4.10).

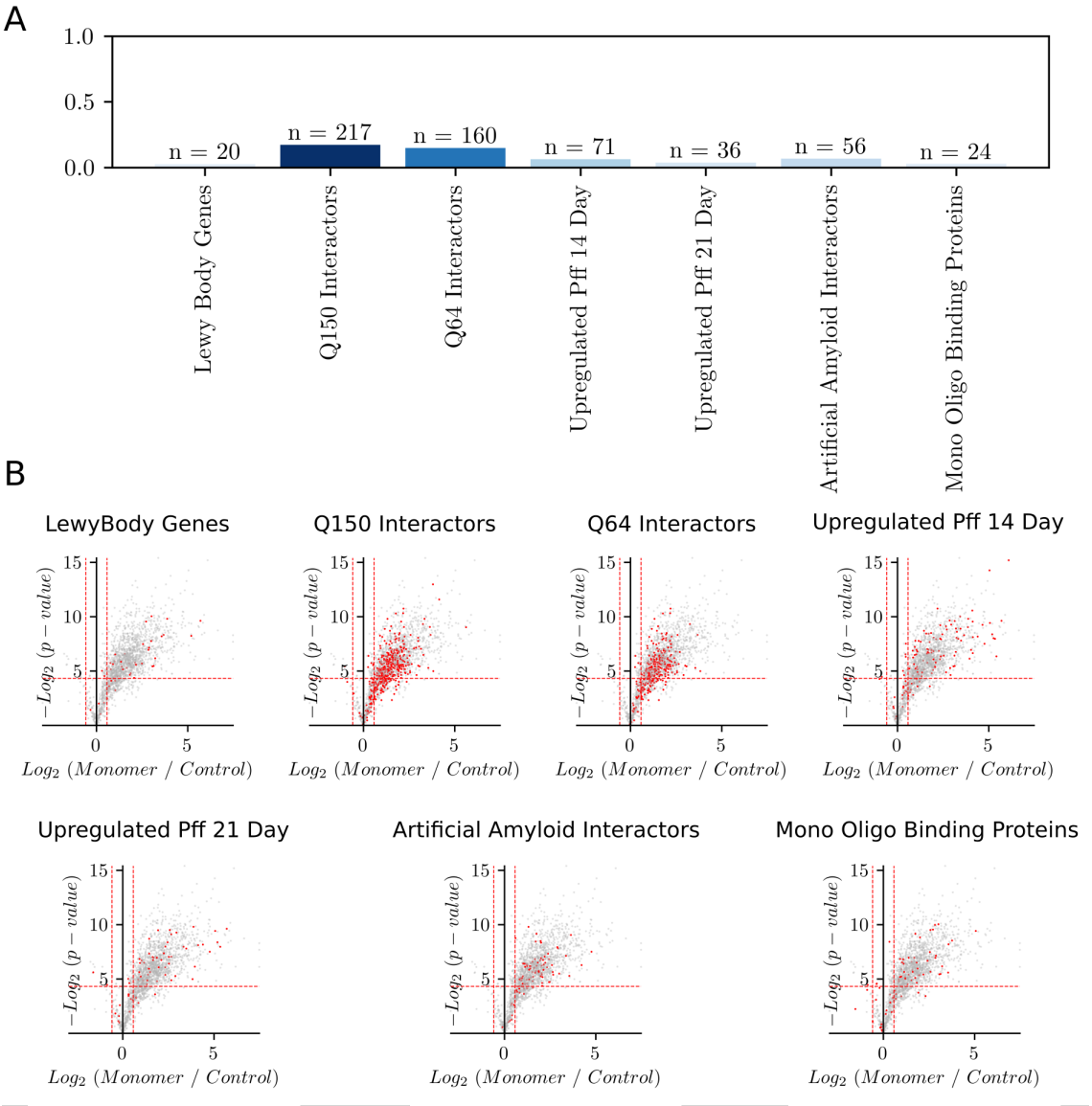


***Figure 4.15:*** *Similarity between monomer interactors and interactors identified in other proteomic studies. A) Bar chart of the calculated Jaccard Similarity Index between the proteins identified in this study as α-synuclein Monomer interactors and the proteins identified as interactors of other fibrils or α-synuclein proteoforms. (Lewy Body Genes: [389], Q150 Interactors [320], Q64 Interactors [320],Upregulated Pff 14 Day [371], Upregulated Pff 21 Day [371], Artificial Amyloid Interactors [312], Monomer Oligomer Interactors [391]). For interactomes derived from mouse proteomes [371] were mapped to human orthologs using the PylomeDB mapping [390]. B) Volcano plot shown in Fig. 4.10 with the matching interactors of from the indicated study shown in red.*

### 4.3.10 The Interactome Shared by Monomeric and Fibrillar $\alpha$-Synuclein is Enriched in Ribosomal Proteins

In order to better define the interactions of $\alpha$-synuclein in its fibrillar and monomeric forms, the $\alpha$-synuclein interactome was next divided into three sets: proteins only interacting with fibrillar and not monomeric $\alpha$-synuclein (411 proteins); proteins only interacting with monomeric and not fibrillar $\alpha$-synuclein (246 proteins); and protein interacting with both monomeric and fibrillar $\alpha$-synuclein (ie. the intersection of the two sets) (1165 proteins). For this purpose the interactome defined in the second experiment (Section 4.3.6) was used as the interactome for fibrillar $\alpha$-synuclein. It was of interest to identify the GO terms and protein clusters that were common between the fibrillar $\alpha$-synuclein interactome and the monomeric $\alpha$-synuclein interactome. To this end GO term enrichment analysis was performed on the common interactome.

The results of this analysis demonstrated that the intersection of the monomeric and fibrillar $\alpha$-synuclein interactomes was enriched in proteins involved primarily in translation, being located in the nucleus, and the ribosome, specifically large ribosomal subunit members. Further, proteins involved in chromatin modification were also enriched in this data set as were proteins located in the cellular cytoskeleton including microtubular proteins.

When the interaction network of this intersection of monomeric and fibrillar $\alpha$-synuclein is visualised and clustered as previously (4.3.4) it was possible to identify a number of clusters that were common to both monomeric and fibrillar $\alpha$-synuclein interactomes. One of which is a major cluster, identified in blue, containing several proteins that are highly enriched in the fibrillar sample (Fig. 4.18). By examining the GO terms associated with proteins of this cluster it is evident that it represents proteins associated with the ribosome (Fig. 4.19). Due to the size of this cluster, it was isolated and further clustering performed to generate a number of subclusters. By this method it was possible to tease apart a number of other sub-groups of protein interactors (Fig. 4.20). The largest and most intra-connected of these subgroups represents structural components of the ribosome as well as a number of ribosomal associated proteins, as predicted by the parent group (Fig. 4.20 Blue). The second largest sub-cluster represents a number of microtubular proteins (Fig. 4.20 Purple), while the third group represents a number of nuclear proteins involved in chromatin modification (Fig. 4.20 Red). This major group, therefore, accounts for most of the GO terms shown to be enriched in this dataset (Fig. 4.16 and Fig. 4.17).

The other major protein interaction clusters identified for the interactome of both fibrillar and monomeric $\alpha$-synuclein, include proteins involved in mRNA splicing and RNA transport including several members of the THO complex and a number of

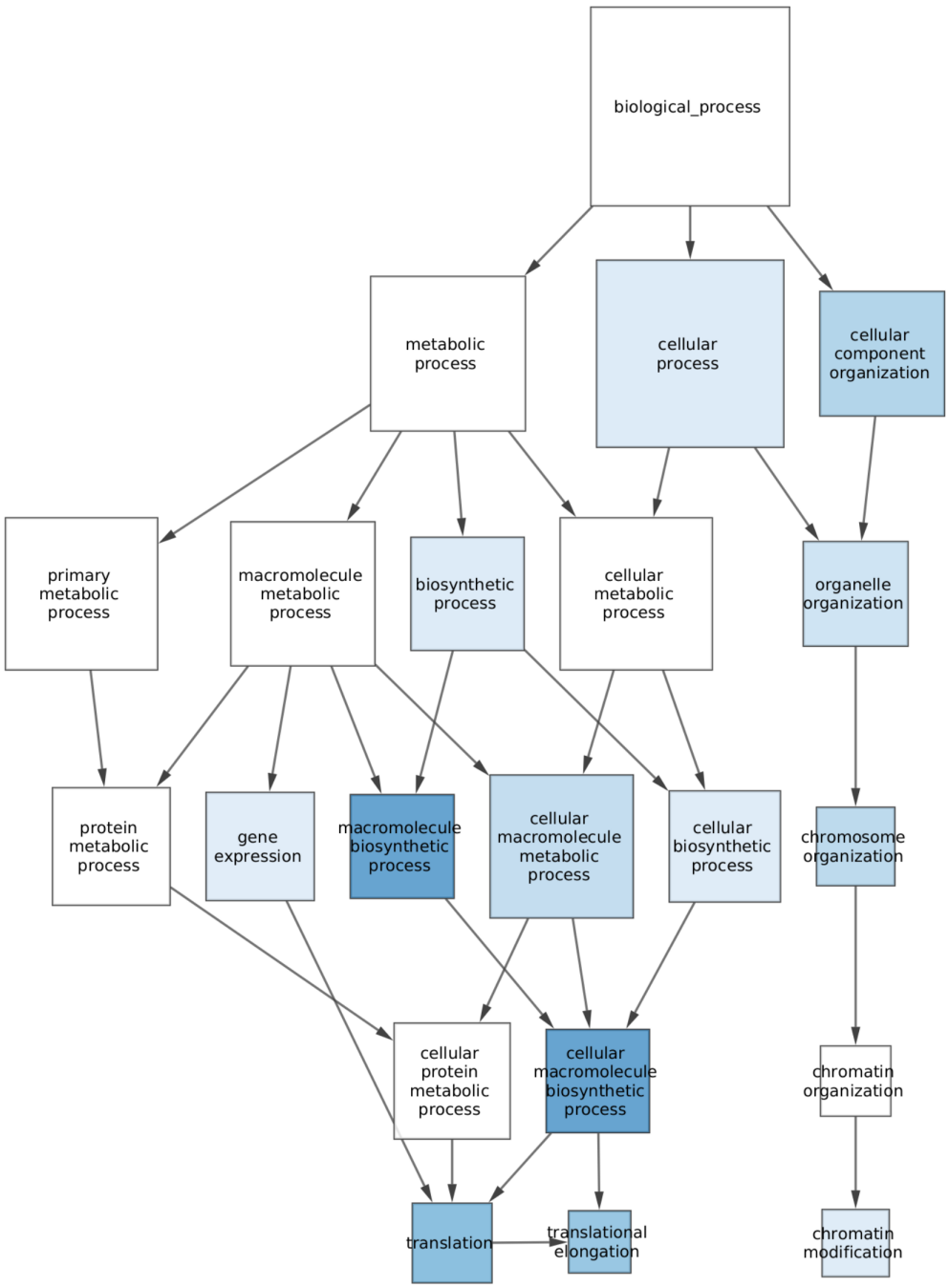


***Figure 4.16:*** *Proteins interacting with monomeric and fibrillar α-synuclein are enriched in proteins involved in chromatin remodeling and transcription. GO term (Biological Process) enrichment analysis performed on the interactome representing the intersection of monomeric α-synuclein interactors and fibrillar α-synuclein interactors. Hierarchical graph showing the GO terms enriched in α-synuclein interactors and their relationships to one and other. Node colour saturation denotes significance with, white nodes not significantly enriched (FDR < 0.1). Node size denotes the number of α-synuclein interacting proteins possessing this annotation.*

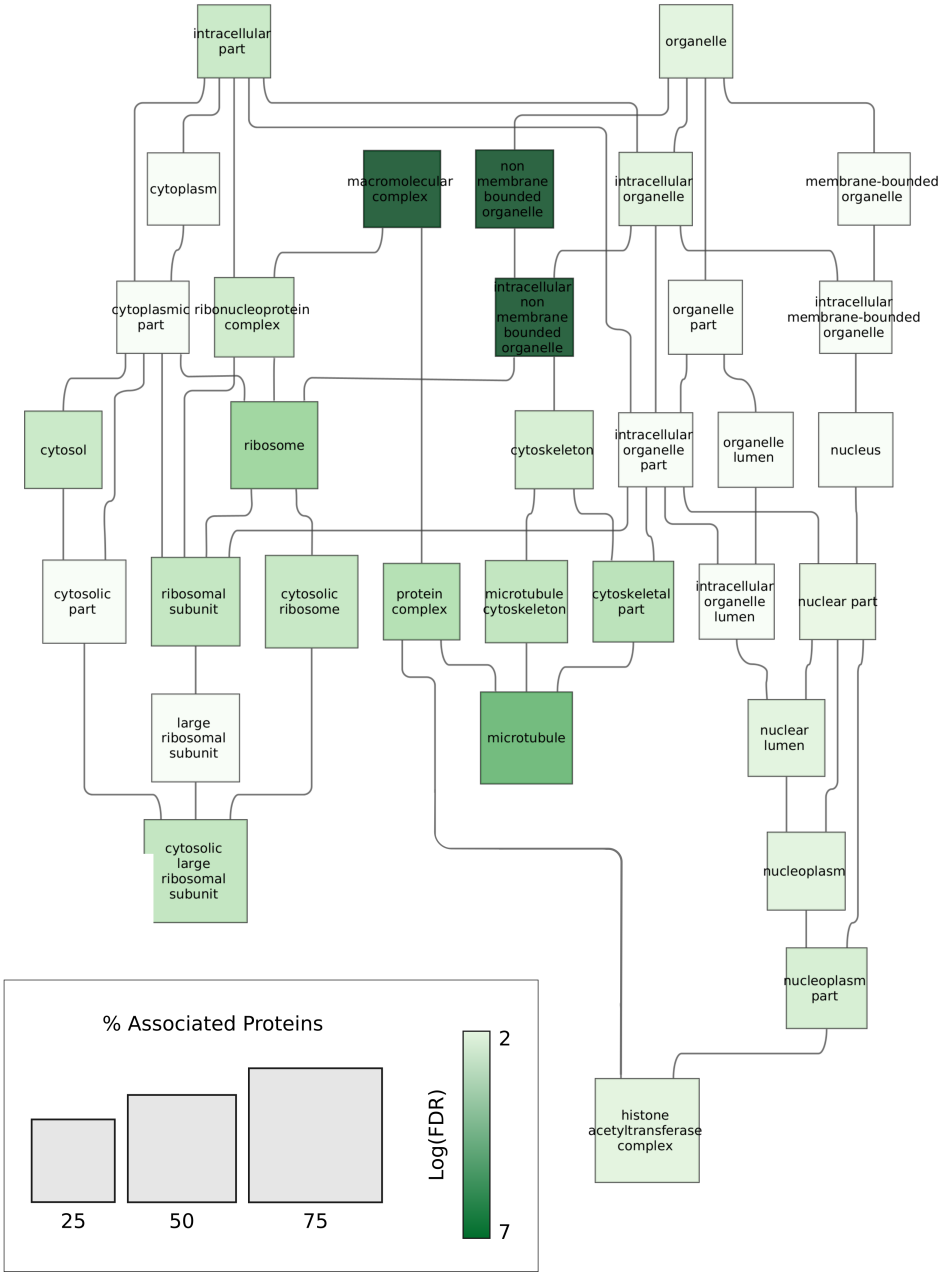


***Figure 4.17:*** *Proteins interacting with both monomeric and fibrillar α-synuclein are enriched in proteins located in the nucleus, cytoskeleton and ribosome. GO term (Cellular Component) enrichment analysis performed on the interactome representing the intersection of monomeric α-synuclein interactors and fibrillar α-synuclein interactors. Hierarchical graph showing the GO terms enriched in α-synuclein interactors and their relationships to one and other. Node colour saturation denotes significance with, white nodes not significantly enriched (FDR < 0.1). Node size denotes the number of α-synuclein interacting proteins possessing this annotation.*

nuclear pore proteins, such as NUP88. Furthermore, a number of apoptotic proteins were also identified including caspase-3 (CASP3) and Anamorisin (CIAPIN1), as were several other mitochondrial proteins involved in RNA modification (Fig. 4.18 and Fig. 4.19 Yellow). Additionally a cluster of proteins heavily involved in protein ubiquitination was also identified (Fig. 4.18 and Fig. 4.19 Green), along with a cluster of proteins involved in DNA maintenance and repair (Fig. 4.18 and Fig. 4.19 Red).

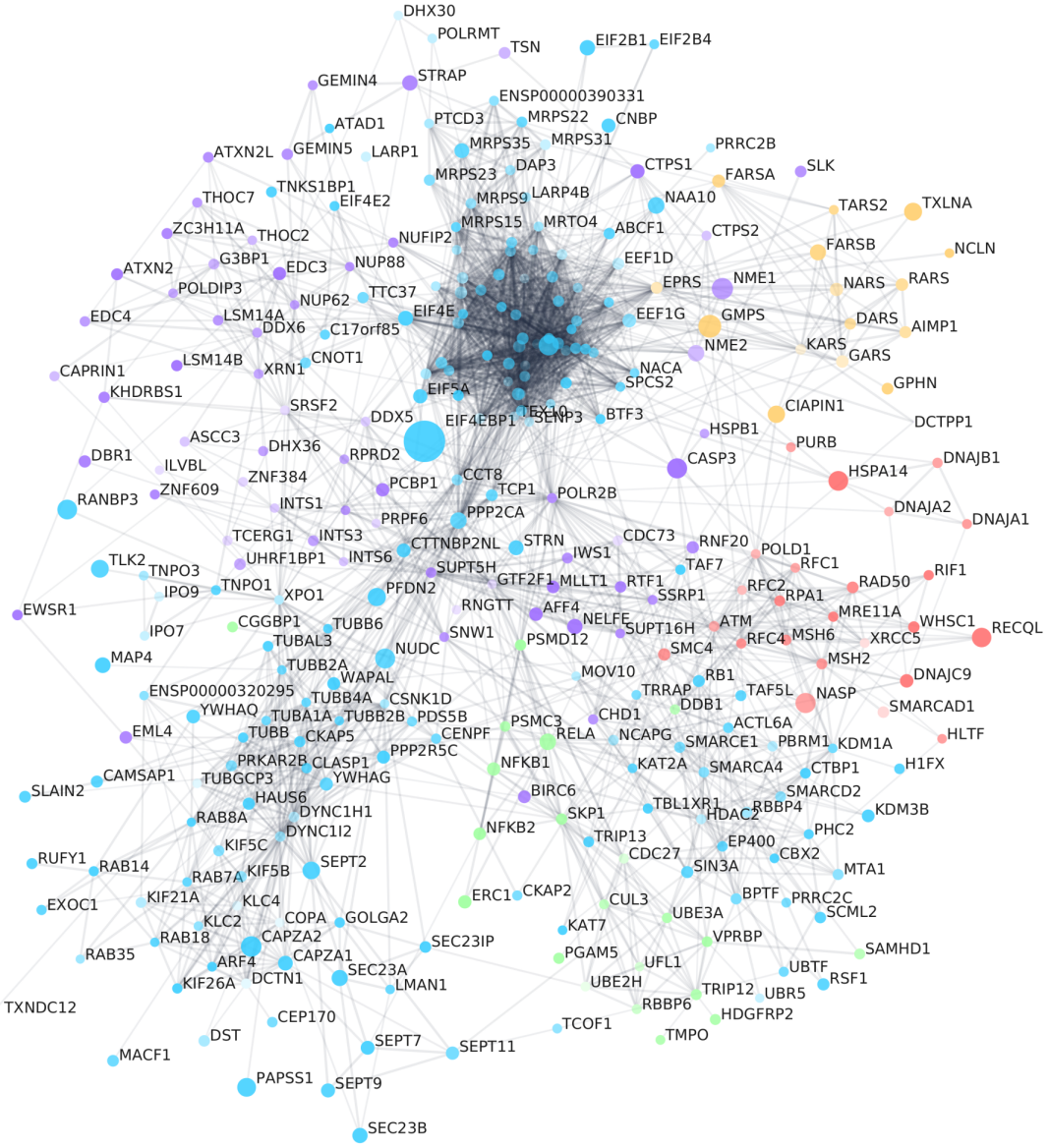


***Figure 4.18:*** *Protein-protein interaction network of α-synuclein interactors of both monomeric and fibrillar α-synuclein. Network of protein-protein interactors compiled by the StringDB service of proteins present in both the monomeric and fibrillar interactor sets, excluding those only present in one. The network was clustered using the MCL algorithm, and nodes coloured based on the cluster in which they appear. Node size denotes the ratio of the protein abundance vs control (Fig. 4.2 X axis). Node transparency denotes the p-value of the abundance ratio (Fig. 4.2 Y axis)*

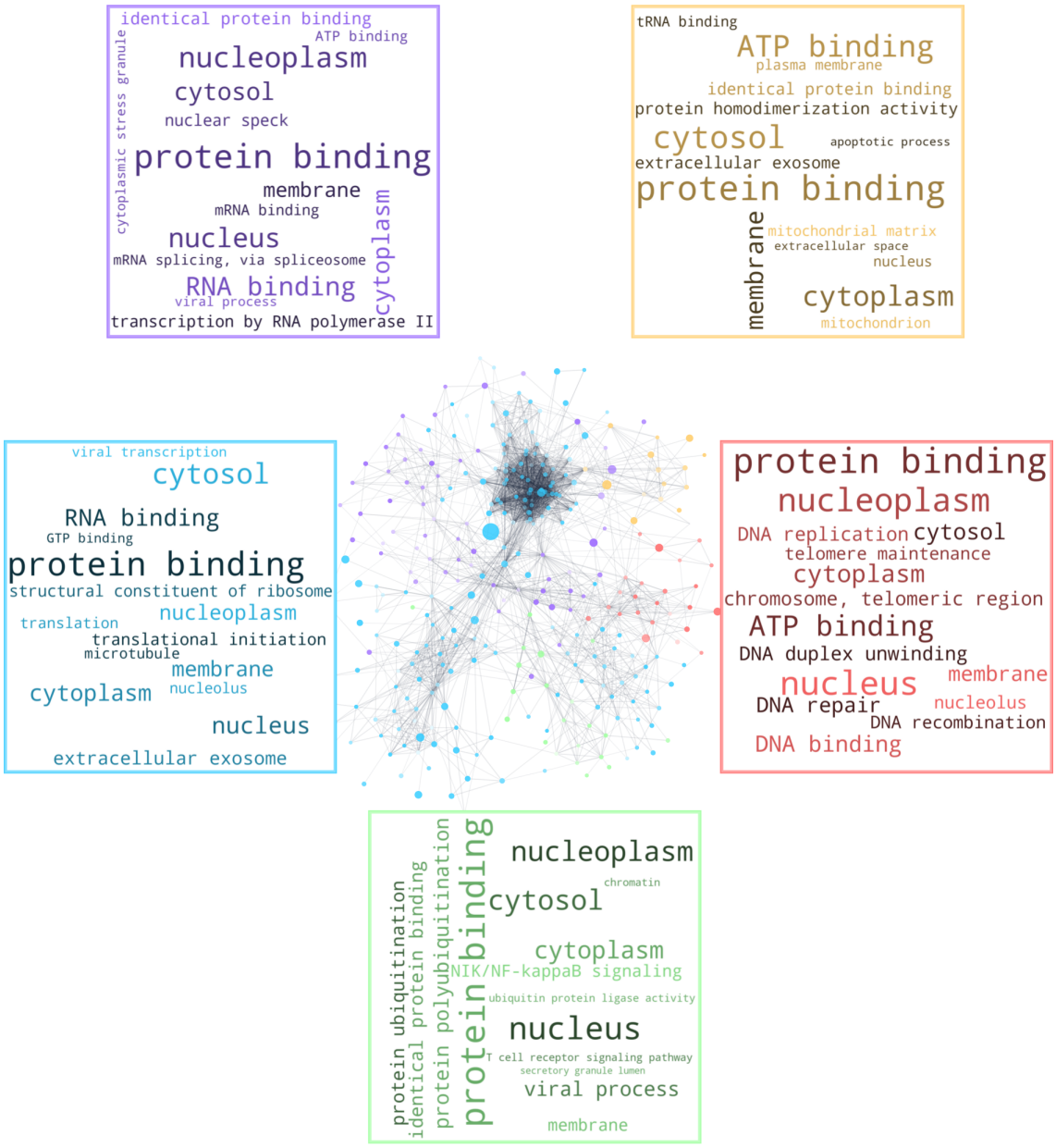


***Figure 4.19:*** *GO terms associated with the protein-protein interaction clusters of both monomeric and fibrillar α-synuclein (Fig. 4.18). GO term clouds generated from GO terms associated with proteins in each StringDB network cluster.*

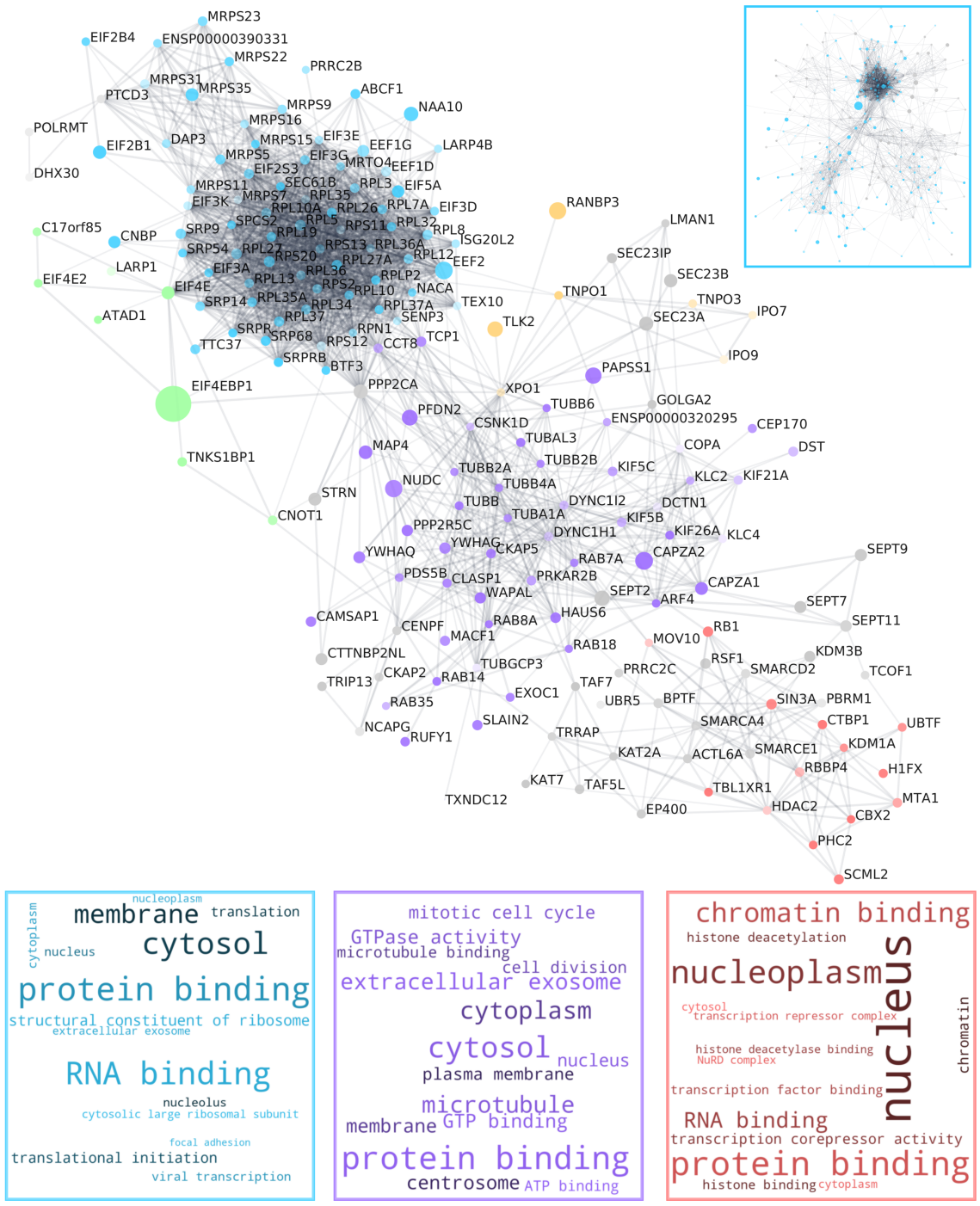


***Figure 4.20:*** *Sub-cluster of protein-protein interaction network of α-synuclein monomer and fibrillar interactors. Network of protein-protein interactors in the blue cluster identified in Fig. 4.18. The network was sub-clustered using the MCL algorithm, and nodes coloured based on the cluster in which they appear. Node size denotes the ratio of the protein abundance vs control (Fig. 4.10 X axis). Node transparency denotes the p-value of the abundance ratio (Fig. 4.10 Y axis)*

### 4.3.11 Proteins interacting specifically with monomeric $\alpha$-Synuclein are enriched in RNA transport and processing proteins

Having identified the proteins that interact with both fibrillar and monomeric $\alpha$-synuclein, proteins that specifically interacted with either monomer or fibrillar $\alpha$-synuclein were then investigated. The interactome of monomeric $\alpha$-synuclein, having excluded proteins that also interact with fibrillar $\alpha$-synuclein was enriched in proteins involved in the processing of RNA in addition to the transport of RNA from the nucleus to the cytoplasm (Fig. 4.21) including an overrepresentation of proteins present in the in the nuclear pore complex (Fig. 4.22). Furthermore, there was enrichment in proteins involved in chromatin assembly alongside an enrichment in proteins interacting with the condensed chromosome (Fig. 4.21 and Fig. 4.22). Additionally a significant number of proteins were found to be involved in RNA stabilisation and ribosome biogenesis (Fig. 4.21). Overall these data suggest that many of the proteins interacting specifically with monomeric $\alpha$-synuclein are involved in the processing or transport of RNA and DNA.

When the interactome of monomeric $\alpha$-synuclein was visualised as a protein interaction network, having excluded proteins that also interact with fibrillar $\alpha$-synuclein it was possible to identify two highly intra-connected clusters related to the the functions and locations identified above (Fig. 4.23 Purple). The first cluster (Fig. 4.23 Purple) contains proteins involved in RNA processing, including a number of transferases (e.g. FBLL1 and NAT10) along with a number of proteins invloved in ribosome biogenesis (e.g. CEBPZ and BRIX1). The second major cluster includes proteins invloved in RNA export and splicing including a number highly enriched nuclear pore proteins (e.g. NUP155, NUP107 and NUP160) in addition to RNA splicing proteins such as Polypyrimidine tract-binding protein-1 (PTBP1) and a number of heterogenous nuclear ribonucleoproteins (Fig. 4.23 Blue).

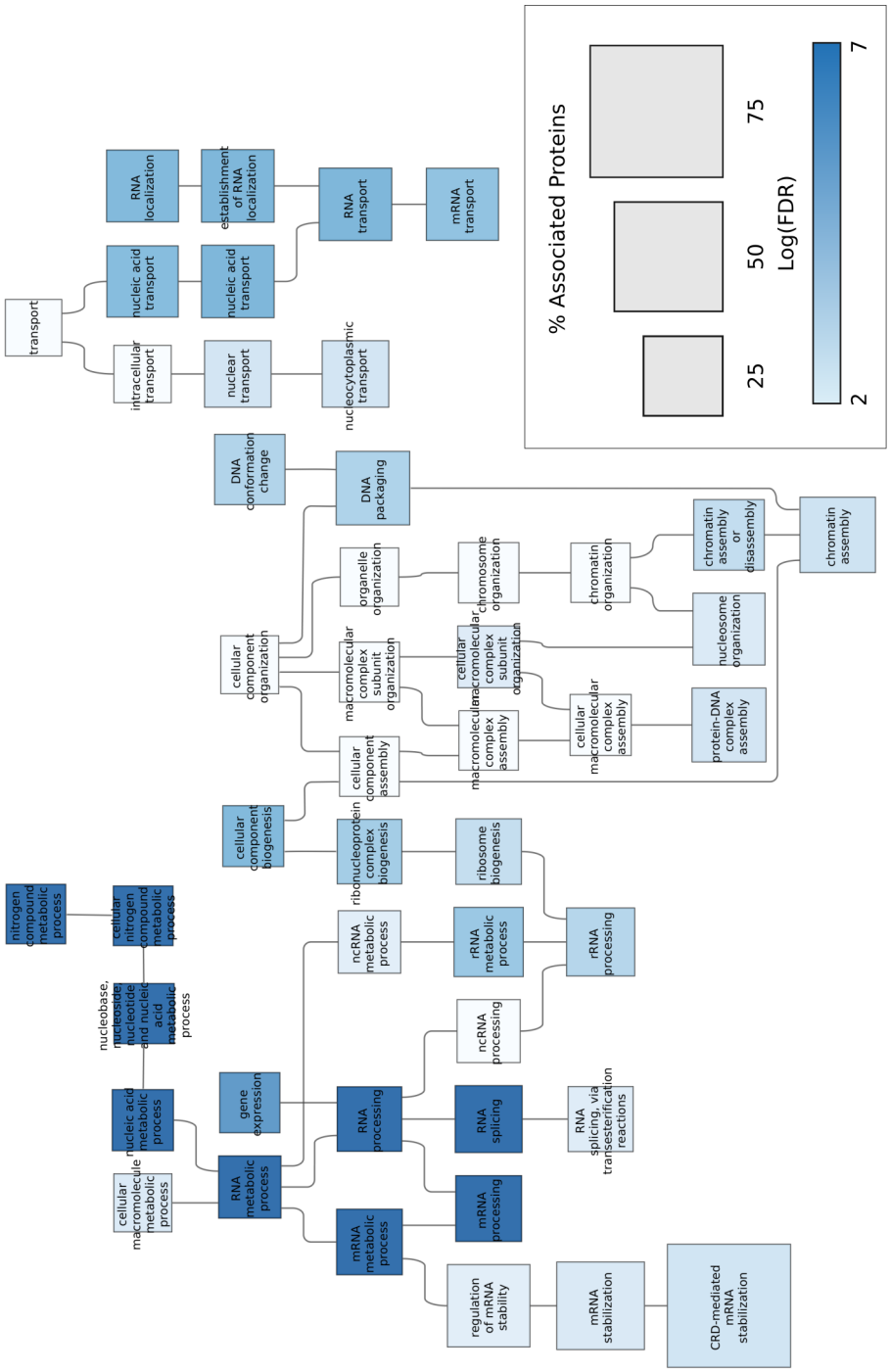


***Figure 4.21:*** *Proteins interacting with monomer, when fibril interactors are excluded, are enriched in proteins involved in translation. GO term (Biological Process) enrichment analysis performed on monomer interactors after excluding α-synuclein fibril interactors. Hierarchical graph showing the GO terms enriched in monomeric α-synuclein interactors and their relationships. Node color denotes significance; white nodes not significantly enriched (FDR < 0.1). Node size denotes the number of monomeric α-synuclein interacting proteins possessing this annotation.*

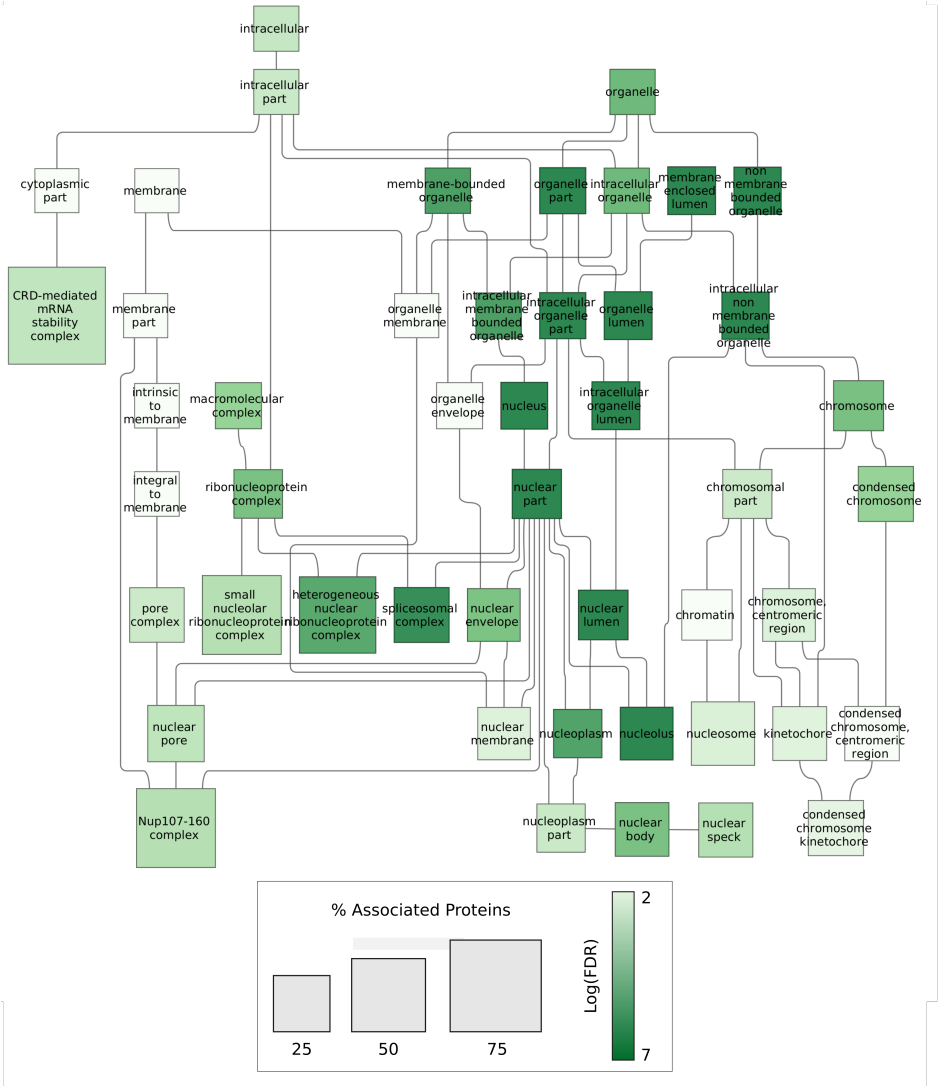


***Figure 4.22:*** *Proteins interacting with monomer, when fibril interactors are excluded, are enriched in proteins located in the nuclear pore complex. GO term (Cellular Component) enrichment analysis performed on monomer interactors of α-synuclein, after excluding fibril interactors of α-synuclein. Hierarchical graph showing the GO terms enriched in monomeric α-synuclein interactors and their relationships to one and other. Node colour saturation denotes significance with, white nodes not significantly enriched (FDR < 0.1). Node size denotes the number of monomeric α-synuclein interacting proteins possessing this annotation.*

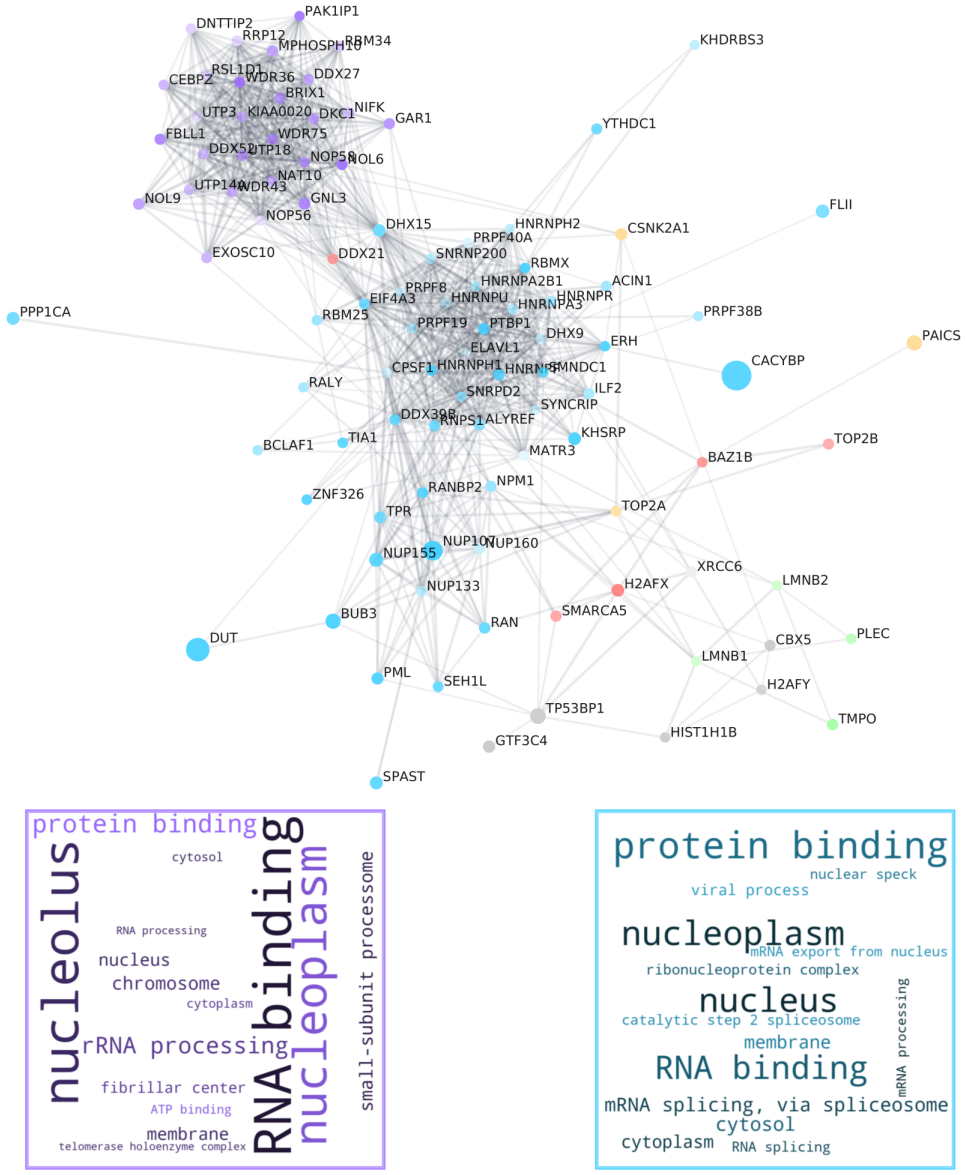


***Figure 4.23:*** *Protein-protein interaction network of α-synuclein monomer interactors, having excluded α-synuclein fibril interactors. Top: Network of protein-protein interactors compiled by the StringDB service. The network was clustered using the MCL algorithm, and nodes coloured based on the cluster in which they appear. Node size denotes the ratio of the protein abundance vs control (Fig. 4.10 X axis). Node transparency denotes the p-value of the abundance ratio (Fig. 4.10 Y axis). Bottom: GO term clouds generated from GO terms associated with proteins the two largest StringDB network clusters.*

### 4.3.12 Proteins Interacting Specifically with $\alpha$-Synuclein Fibrils Contain a Large Number of Mitochondrial Proteins

As with the interactome of monomeric proteins, it was of significant interest to identify proteins proteins present only in the interactome of fibrillar $\alpha$-synuclein, having excluded the monomeric $\alpha$-synuclein interactors. These analysis identified mitochondrial proteins to be overrepresented in this interactome (Fig. 4.25). Specifically proteins involved in oxidative phosphorylation and mitochondrial transport were overrepresented in this dataset (Fig. 4.24). Of note was the observation that proteins of the mitochondrial outer membrane were overrepresented (Fig. 4.25) increasing the likelihood of this finding being physiologically relevant as it is the outer mitochondrial membrane that is most likely to be accessible to $\alpha$-synuclein fibrils. Furthermore, based on the overrepresented terms, these mitochondrial proteins appear to be focused around the respiratory chain (Fig. 4.25).

Other overrepresented protein catagories include ribosomal subunit proteins, proteins of the endoplasmic reticulum and spliceosomal complex proteins. Interestingly here there is some overlap in the cellular component GO terms overrepresented in this data set (i.e. only fibril interactors) and the intersection dataset (i.e. fibril interactors and monomeric interactors). Both datasets were enriched in GO terms relating to small ribosomal subunit proteins (Fig. 4.17) suggesting $\alpha$-synuclein fibrils may have a higher affinity for proteins of the small ribosomal subunit. Another finding of note is the overrepresentation of proteins of the sub-synaptic reticulum, a potential route by which fibrillar $\alpha$-synuclein may disrupt synaptic function, an early pathogenic step in the development of Parkinson's disease [187].

The protein interaction network of the fibrillar $\alpha$-synuclein interactome, having excluded proteins interacting with monomeric $\alpha$-synuclein, resulted in a visualisation of several protein clusters representing the overrepresented terms identified above. The largest cluster, as with the full interaction network of fibrillar $\alpha$-synuclein (Fig. 4.5), represents ribosomal subunit proteins (Fig. 4.27 and Fig. 4.26 Blue). Likewise the interactome of both monomeric and fibrillar $\alpha$-synuclein contained a number of ribosomal subunit proteins (Fig. 4.18. However, whereas the common interactome contained largely proteins of the large ribosomal subunit (Fig. 4.18), the fibril specific interactome contained primarily proteins of the small ribosomal subunit (Fig. 4.26 and Fig. 4.18).

The second major intra-connected cluster of proteins identified in the interactome of fibrils alone, are comprised of nuclear proteins involved in the RNA splicing. This includes a pre-mRNA processing factors (PRPF31) essential for the formation of the spliceosome, several splicing factors of the SF3B complex (SF3B1, 2 and 3)

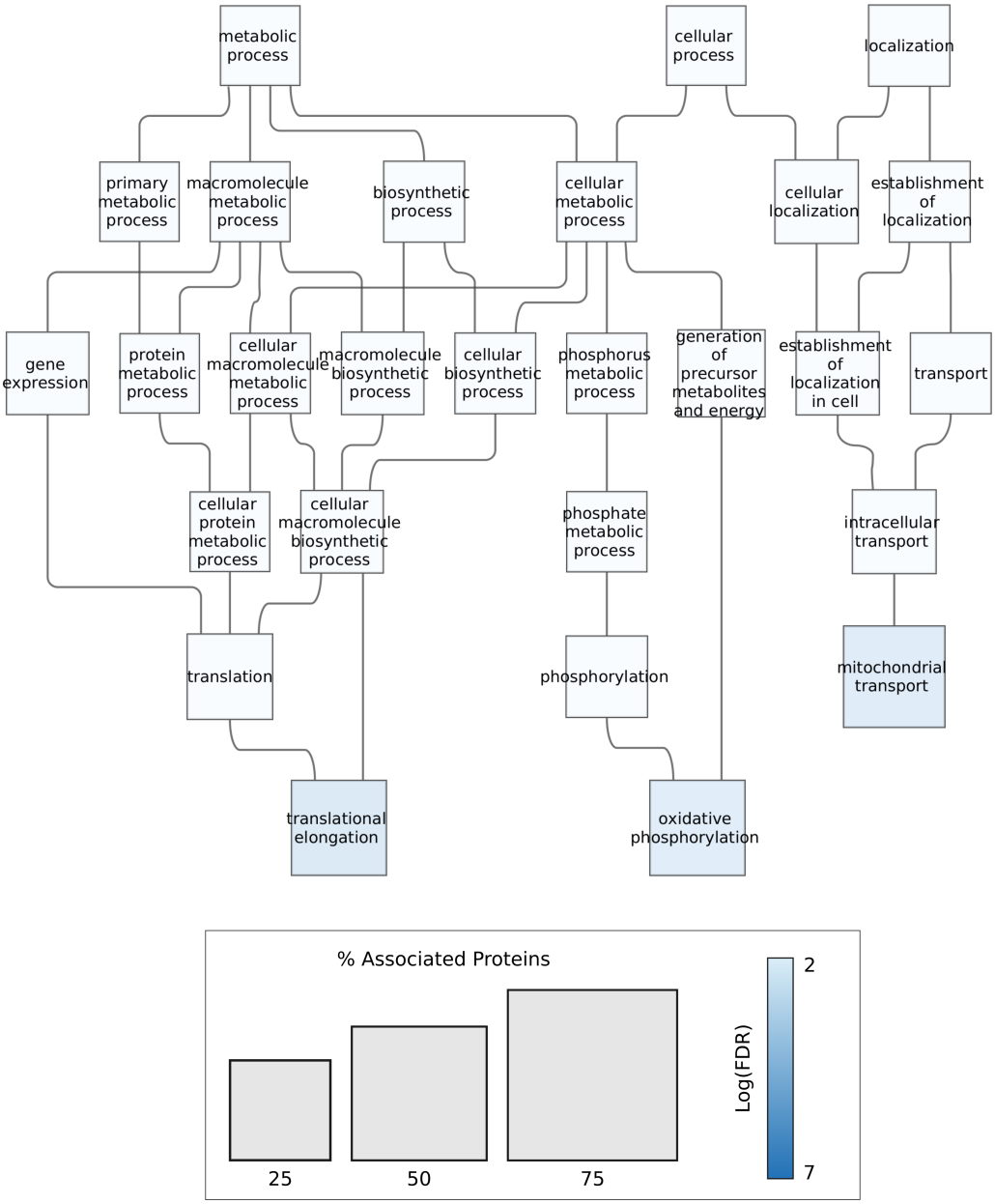


***Figure 4.24:*** *Proteins interacting with α-synuclein fibril, when monomer interactors are excluded, are enriched in proteins involved in gene expression and mitochondrial transport. GO term (Biological Process) enrichment analysis performed on fibril interactors after excluding α-synuclein monomer interactors. Hierarchical graph showing the GO terms enriched in fibrillar α-synuclein interactors and their relationships to one and other. Node colour saturation denotes significance with, white nodes not significantly enriched (FDR < 0.1). Node size denotes the number of fibrillar α-synuclein interacting proteins possessing this annotation.*

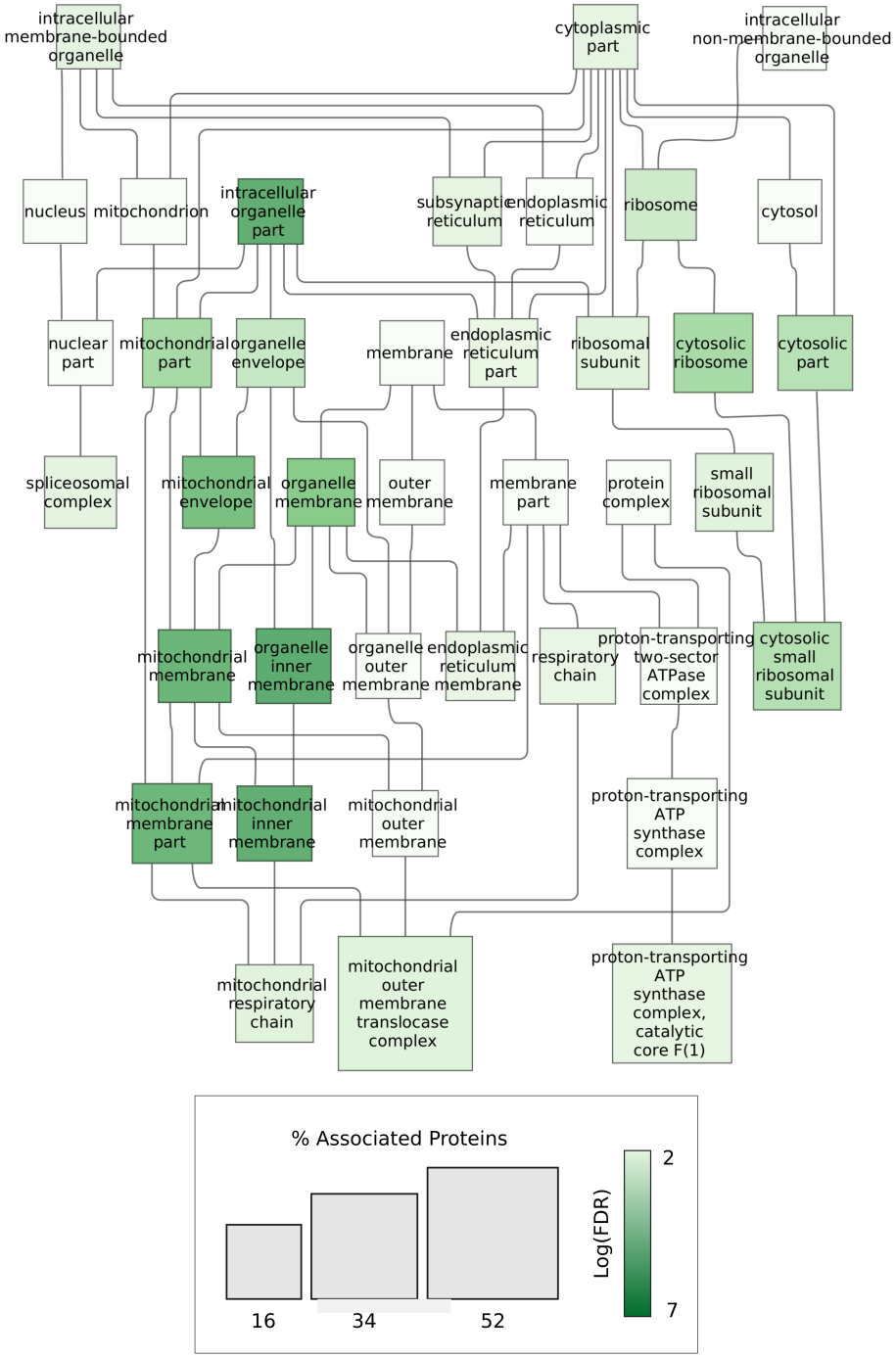


***Figure 4.25:*** *Proteins interacting with α-synuclein fibril, when monomer interactors are excluded, are enriched in proteins found in the mitochondria and ribosomes. GO term (Cellular Component) enrichment analysis performed on monomer interactors of α-synuclein, after excluding fibril interactors of α-synuclein. Hierarchical graph showing the GO terms enriched in fibrillar α-synuclein interactors and their relationship. Node colour denotes significance; white nodes not significantly enriched (FDR < 0.1). Node size denotes the number of fibrillar α-synuclein interacting proteins possessing this annotation.*

important in the recognition of branch point sequences and facilitating spliceosomal assembly and activation. Together these data indicate a high abundance of RNA binding proteins present in the fibril interactome. This is similar to the data on both monomeric and combined monomeric and fibrillar $\alpha$-synuclein interactomes.

Another significant cluster of proteins identified in the interaction network of fibrillar $\alpha$-synuclein, having excluded monomeric $\alpha$-synuclein interactors, contains a number of mitochondrial proteins involved specifically the ATP biosythsis and proton transmembrane transport (Fig. 4.26 and Fig. 4.27). In order to better investigate these mitochondrial interactors of fibrillar $\alpha$-synuclein, all proteins interacting specifically with $\alpha$-synuclein fibrils, excluding monomeric interactors, were filtered by proteins annotated with terms related to mitochondria. A protein interaction network of these filtered proteins was then generated (Fig. 4.28 A). This network included a number of key mitochondrial transport proteins including translocase of outer membrane proteins (TOMM40, 70A and 22), essential for protein transport into the mitochondria [392].

Futhermore, this mitochondrial related subset of the fibril specific interactome, contained several reduced nicotinamide adenine dinucleotide (NAD) (NADH) dehydrogenase enzymes (NDUFA9, S3, A4, B10, V1, B4 and S2) (Fig. 4.28 A). These proteins form subunits of NADH ubiquinone oxioreductase (Complex I of the electron transport chain) responsible for transferring electrons from NADH to ubiquinone. Further mitochondrial proteins identified as fibril specific interactors include a member of mitochondrial Complex IV (COX4I1) and several subunits of mitochondrial ATP synthase (ATP5L, ATP5C1 and ATP5A1). Interestingly, many of the KEGG pathways associated with these mitochondrial proteins, relate to neurodegenerative, amyloid related diseases (Fig. 4.28 B).

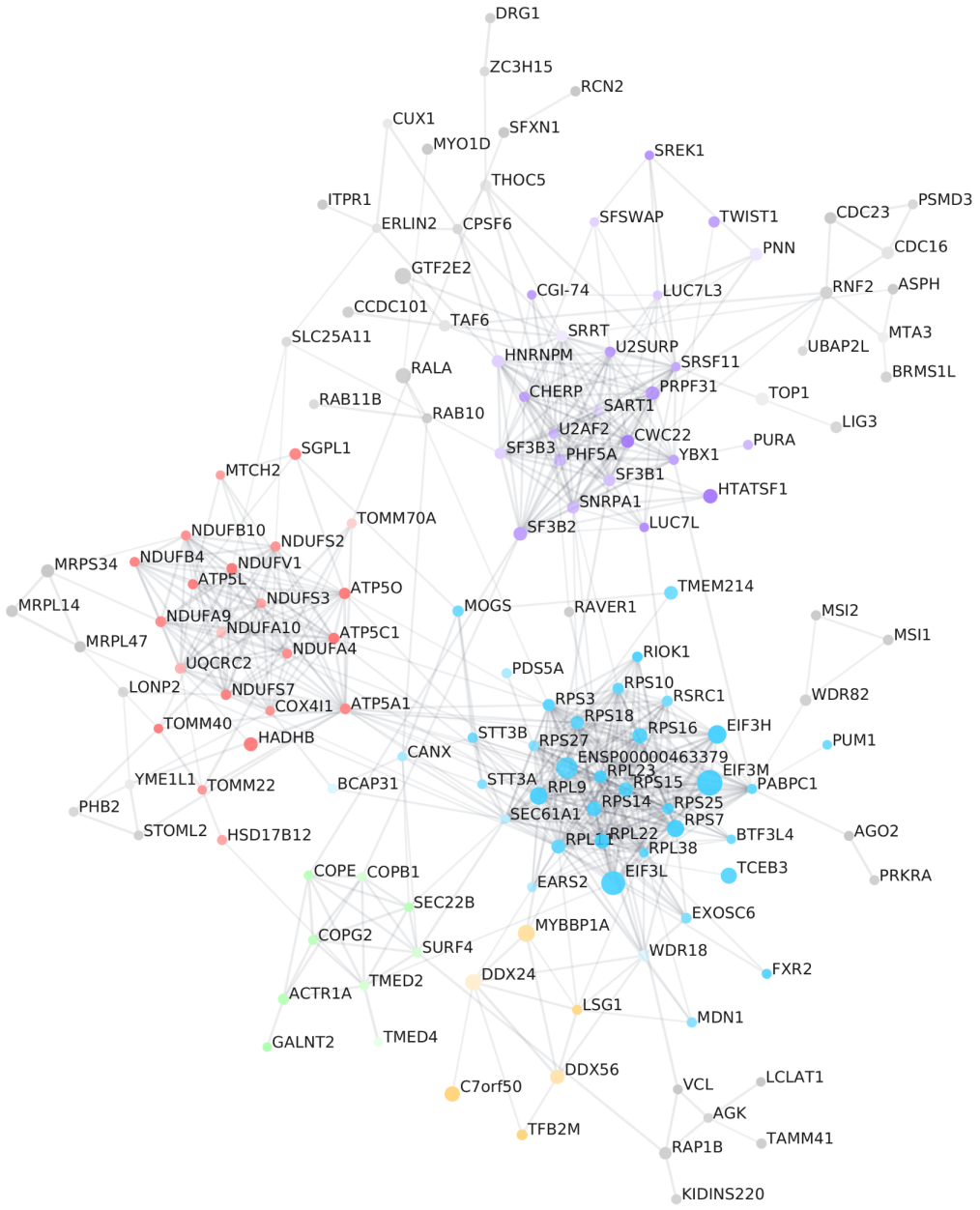


***Figure 4.26:*** *Protein-protein interaction network of α-synuclein fibrillar α-synuclein, when monomeric α-synuclein interactors are excluded. Network of protein-protein interactors compiled by the StringDB service of proteins present in the fibrillar interactor set, excluding those present in the monomeric interactor set. The network was clustered using the MCL algorithm, and nodes coloured based on the cluster in which they appear. Node size denotes the ratio of the protein abundance vs control (Fig. 4.2 X axis). Node transparency denotes the p-value of the abundance ratio (Fig. 4.2 Y axis)*


***Figure 4.27:*** *GO terms associated with the protein-protein interaction clusters of fibrillar α-synuclein when monomeric α-synuclein interactors are excluded(Fig. 4.26). GO term clouds generated from GO terms associated with proteins in each StringDB network cluster.*

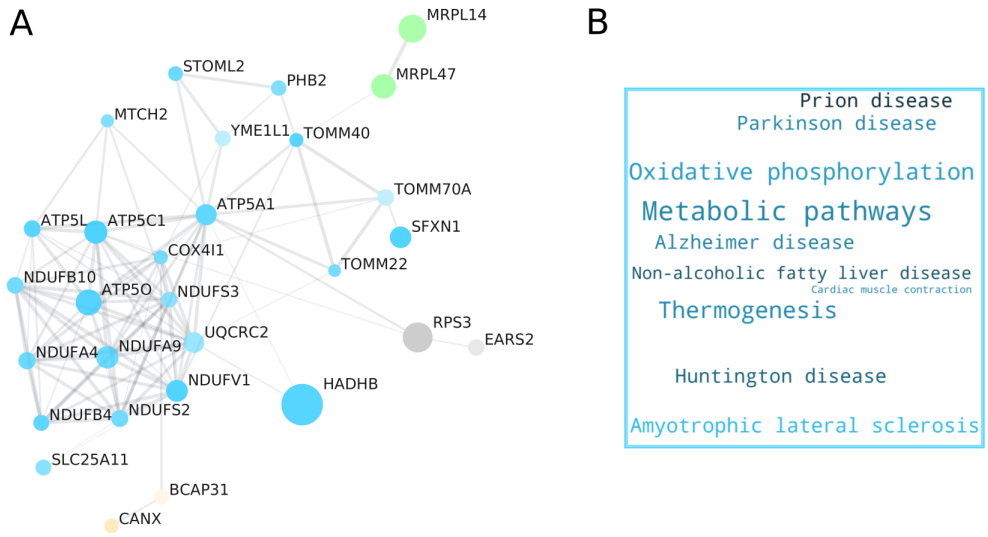


***Figure 4.28:*** *Mitochondrial protein-protein interaction network of α-synuclein fibrillar α-synuclein, when monomeric α-synuclein interactors are excluded. Left: Network of protein-protein interactors, filtered by presence in Mitochondria, of proteins present in the fibrillar interactor set, excluding those present in the monomeric interactor set. The network was clustered using the MCL algorithm, and nodes coloured based on the cluster in which they appear. Node size denotes the ratio of the protein abundance vs control (Fig. 4.2 X axis). Node transparency denotes the p-value of the abundance ratio (Fig. 4.2 Y axis). Right: KEGG network terms associated with the largest cluster in the network*

### 4.3.13 Proteins Found in Greater Abundance in the $\alpha$-Synuclein Fibril Interactome are Involved in Mitochondrial and Ribosomal Functions

The data presented above has characterised the interactome of fibrillar $\alpha$-synuclein, looking at proteins that bound only fibrillar $\alpha$-synuclein while excluding the monomeric $\alpha$-synuclein interactors. This fibril specific interactome can be expanded by examining the proteins that bind to fibrillar $\alpha$-synuclein in greater abundance than to monomeric $\alpha$-synuclein. By this method it is possible to identify proteins that though interacting with monomeric $\alpha$-synuclein, have a far greater propensity for interaction with the fibrillar form of the protein. To this end, for each protein a ratio of its mean abundance in the fibrillar samples and its mean abundance in the monomeric samples was calculated, and this ratio plotted against its p-value, as was previously done to identify fibrillar $\alpha$-synuclein specific interactions over binding to the streptavidin dynabeads (Fig. 4.2). Likewise the same cut offs were used (p-value $< 0.05$, fold change $> 1.5$) were used to identify proteins that preferentially interacted with fibrillar $\alpha$-synuclein.

The cellular locations of the proteins that by this method were identified as being enriched in the interactome of $\alpha$-synuclein fibrils were then elucidated by GO term enrichment analysis. For this purpose the ClueGo enrichment analysis software was leveraged [327]. By comparing the number of background proteins that are common between GO terms, so called semantic similarity, ClueGO can generate a network of terms and from this cluster semantically similar GO terms into groups. This method is advantageous when the graph generated by BiNGO is too large to practically display. By using this analysis it was possible to identify a number of locations upregulated in the proteins enriched in the fibrillar interactome (Fig. 4.29 B). These results indicated that proteins related to mitochondrial, ribosomal and ribosomal initiation function were upregulated in this dataset (Fig. 4.29 B).

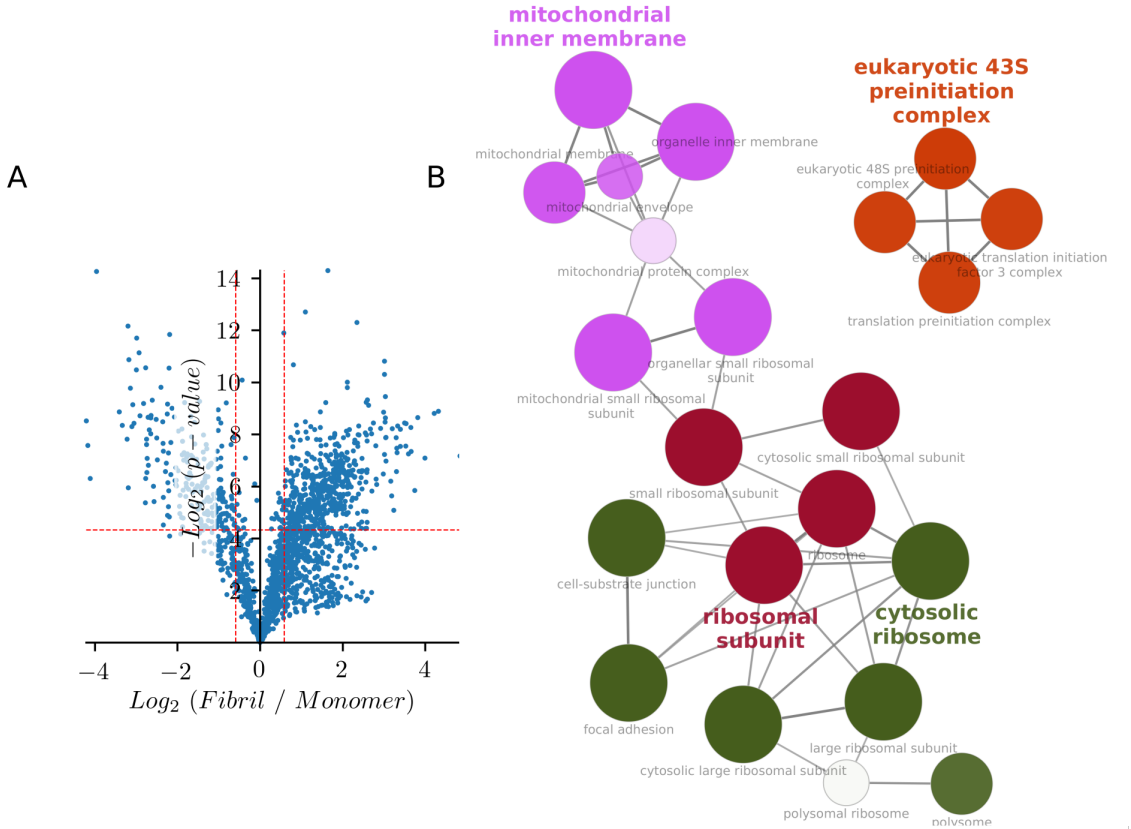


***Figure 4.29:*** *Proteins enriched in the fibril interactome are associated with translation and mitochondrial function. A) Volcano plot showing the ratio of abundance of each protein interacting with α-synuclein fibril samples in cell lysate, to their abundance in the monomeric α-synuclein interaction samples. The ratio is plotted against the p-value of this ratio (n=3). The red lines denote the cutoff for a protein to be considered an fibril interactor (ratio > 1.5, p-value < 0.01). Red arrow denotes sextant representing proteins enriched in the fibril interactome. B) ClueGO enrichment analysis of the terms associated with proteins enriched in the fibrillar interactome. The node size denotes the number of proteins associated with the term, the node color denotes the canonical group to which the term belongs, the term representing the group in labelled in bold.*

### 4.3.14 Monomeric but not Fibrillar $\alpha$-Synuclein Preferentially Interacts with Soluble, Low Complexity Proteins.

Finally, it was of interest whether unstructured proteins were enriched in the interactome of $\alpha$-synuclein fibrils as has been demonstrated with other similar amyloid aggregates [320]. Given the large number of proteins shown to interact with RNA in each interactome examined here and the tendency for RNA binding proteins to contain LCRs (i.e. compositionally biased regions, on average 18 residues in length, containing one to four amino-acids), it was hypothesised that the interactomes identified herein may be enriched in proteins containing long LCRs. The program fLPS has been developed to identify LCRs of proteins [329]. Using this method it was shown that there was a slight though statistically significant increase in the average length of LCRs in $\alpha$-synuclein interacting proteins when compared to the SH-SY5Y cell proteome for both monomeric and fibrillar $\alpha$-synuclein (Fig. 4.30 B). When the proteins were further analysed by their presence exclusively in the fibrillar interactome, the monomeric interactome, or the intersection of the two interactomes, it was noted that the monomeric interactors and the interactors of both monomeric and fibrillar $\alpha$-synuclein, but not the interactors of exclusively fibrillar $\alpha$-synuclein, showed a small but statistically significant increase in the longest LCR (Fig. 4.31 B).

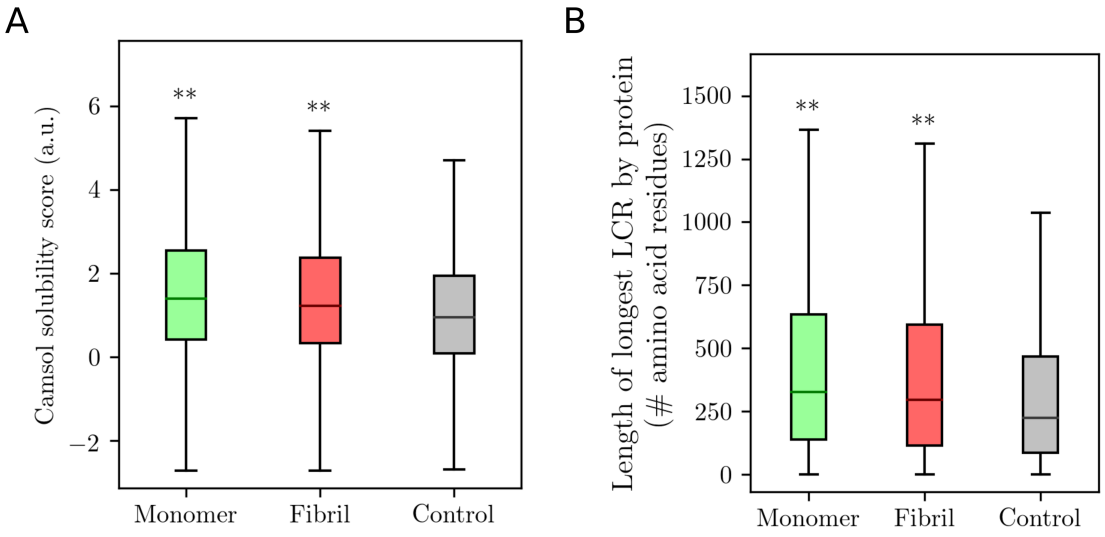


***Figure 4.30:*** *Solubility and complexity of proteins interacting with $\alpha$-synuclein. Box and whisker diagrams of solubility scores. A) Solubility scores of all proteins interacting with Monomeric $\alpha$-synuclein (Monomer), fibrillar $\alpha$-synuclein (Fibril), and the solubility scores of all proteins present in the SH-SY5Y cell proteome (Control). Protein solubility was estimated by Camsol. B) Length of LCR for the same conditions. ** denotes p-value of condition compared to control of $< 0.01$*

Additionally, due to the amyloid nature of $\alpha$-synuclein, it was hypothesised that $\alpha$-synuclein may preferentially bind to aggregation prone proteins. To assess this possibility, the Camsol protein solubility predictor was used [328]. It was shown that, as was the case with low complexity regions both monomeric and fibrillar $\alpha$-synuclein interactors were enriched in proteins of a higher solubility (lower aggregation propensity) than the background (Fig. 4.30). Interestingly, this is the inverse of what the hypothesis predicted. When this was separated into the component interactomes as before, it could be seen that only the intersection of the interactomes was enriched in Low complexity proteins (Fig. 4.31 B). Moreover both the combined interactome and the interactome of monomeric $\alpha$-synuclein when the fibril interactome was excluded, but not the interactome of fibrillar $\alpha$-synuclein when the monomeric interactome was excluded, showed an increase in average protein solubility (Fig. 4.31 A). These data suggest that a region of monomeric $\alpha$-synuclein, that remains at least partially accessible within the fibrillar conformation, is responsible for binding highly soluble proteins.

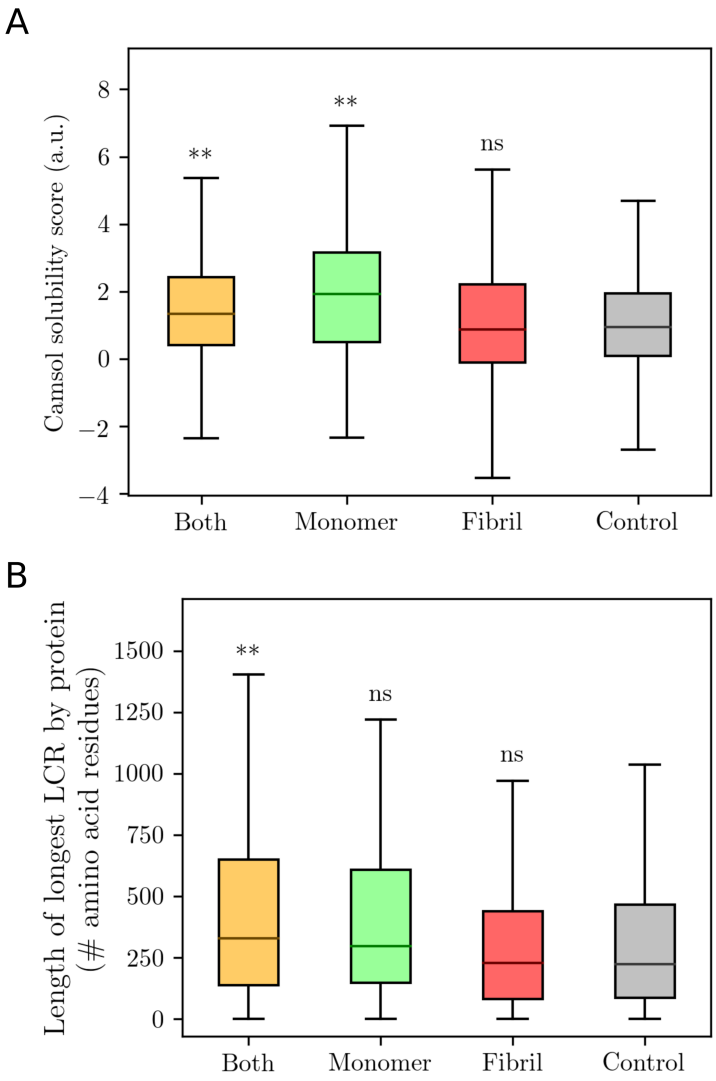


***Figure 4.31:*** *Solubility and complexity of proteins interacting with α-synuclein. Box and whisker diagrams of solubility scores A) Solubility scores of all proteins interacting with Monomeric α-synuclein (Monomer) excluding fibrillar interactors, fibrillar α-synuclein (Fibril), excluding monomeric interactors, the intersection of the monomeric and fibrillar α-synuclein interactomes (Both) and the solubility scores of all proteins present in the SH-SY5Y cell proteome (Control). Protein solubility was estimated by Camsol. B) Length of LCR for the same conditions. ** denotes p-value of condition compared to control of* $< 0.01$

## 4.4 Discussion

Herein, quantitative proteomics was performed to study the interaction of $\alpha$-synuclein fibrils with cellular proteins from a cell lysate of SH-SY5Y cells. Furthermore, it was effectively used to distinguish between proteins interacting with monomeric $\alpha$-synuclein and those interacting with fibrillar $\alpha$-synuclein, by excluding fibrillar $\alpha$-synuclein interactors from the monomeric $\alpha$-synuclein interactome and vice versa. Moreover, the interactomes of fibrillar and monomeric $\alpha$-synuclein were further distinguished through quantitative proteomics, by comparing the abundance of each protein within the fibrillar and monomeric $\alpha$-synuclein interactomes. It was found that a number of key cellular locations were associated with fibrillar $\alpha$-synuclein interaction and not monomeric $\alpha$-synuclein, suggesting potential pathogenic pathways for fibrillar $\alpha$-synuclein. Furthermore, it was shown that a number of proteins found to interact with both fibrillar and monomeric $\alpha$-synuclein were involved in RNA binding.

### 4.4.1 A large number of RNA interacting proteins were found in the $\alpha$-Synuclein interactome

It was shown that 36% of proteins (293 proteins of 812) identified as interactors of fibrillar $\alpha$-synuclein possessed the GO term RNA binding. Indeed, the GO term "RNA binding" was significantly enriched (FDR $4.12 \times 10^{-12}$) in the $\alpha$-synuclein fibril binding proteins when compared to the SH-SY5Y cell proteome [387]. This is in line with the findings of other studies that have showed RNA binding by a number of different amyloidogenic fibrils [267, 312]. Investigation into the interactions of artificial amyloid proteins (those designed *in silico* to form cross-β fibrils) showed that proteins involved in the RNA metabolic process accounted for over 35% (54 of 153) of all proteins interacting specifically with the the fibril prone protein. Indeed this term, RNA metabolic process, was enriched 4.5 fold over the background with an FDR of 2.89E-18.

Furthermore, this finding was consistent with a later study investigating the amyloidogenic protein, poly-Q expanded huntingtin [267]. Proteomic analysis of aggregates isolated from overexpressing poly-Q expanded huntingtin showed strong enrichment (p-value $<$ 1E-30) of many terms associated with RNA including mRNA metabolic processing, RNA splicing and RNA processing [267]. Also consistent with the previous work [312] was the finding that this enrichment was specific to the oligomeric and fibrillar states of the protein; the proteome of monomeric amyloid proteins were not enriched in RNA binding proteins. Taken together with the data presented here, it suggests that RNA binding proteins have an affinity to amyloid

fibrils regardless of the sequence of the monomeric subunit.

One suggested explanation for this finding, and one supported by others [267], is that amyloid fibrils preferentially interact with proteins containing long LCRs, compositionally biased regions containing repetitive sequences of one to four amino acids. A feature of many RNA binding proteins is the presence of such LCRs [314], and can mediate the formation of reversible, higher order aggregates that under disease conditions transition from liquid to solid phase [393, 394]. Indeed, the data presented here supports this hypothesis, as there was a significant increase in proteins with long LCRs over the background of the SH-SY5Y cell proteome, in the interactome shared by both $\alpha$-synuclein monomer and $\alpha$-synuclein fibrils. These data further suggest that binding to LCRs is dependent on a feature of monomeric $\alpha$-synuclein that is shared by $\alpha$-synuclein fibrils.

However, an alternative explanation for these data is the direct binding of amyloid fibrils to RNA. This is supported by the observation that strongly negatively charged molecules including RNA and glycosaminoglycan (GAG)s such as heparin are commonly associated with amyloid deposits [395–399]. Furthermore, GAGs bind directly to Aβ with a much higher affinity for the fibrillar form of the protein than for the monomeric conformation [400] and data presented here shows an enrichment in GAGs isolated alongside $\alpha$-synuclein fibrils. Both GAGs and RNA have also been implicated in accelerating fibril formation in amylin [401], transthyretin [402], $\beta_2$M [403], tau [404] and Aβ40/42 [405]. Moreover, in vitro studies have demonstrated that the removal of these co-factors can lead to the spontaneous shedding of monomeric protein from amyloid fibrils [406].

Therefore, it is possible to hypothesise that RNA may interact with $\alpha$-synuclein fibrils in the context of a cell lysate, and indeed in the context of the RNA-fibril interactions observed by others [267, 312]. RNA binding proteins may therefore be isolated alongside $\alpha$-synuclein fibrils due to interactions with RNA. Moreover, were this the case, and were it true for multiple amyloid fibrils it may explain other observations, such as the sequestration of ribosomes within poly-Q expanded huntingtin inclusions, observed by EM [407], a finding that agrees with the large number of ribosomal proteins identified in this study and the previous studies into amyloid protein interactomes [267, 312]. Under this hypothesis ribosomes may not interact directly with amyloid fibrils but be sequestered as a result of mRNA interactions. Since RNA binding proteins make up a significant proportion of many amyloid fibril interactomes, this may represent a significant finding.

### 4.4.2 Ribosomal protein preferentially interact with fibrillar $\alpha$-Synuclein

Herein, it was found that a number of ribosomal and ribosomal associated proteins were found to interact $\alpha$-synuclein fibrils, including members of both the small (40S) and the large (60S) ribosomal subunits along with a number of key translation initiation factors. It is also worth noting that although translational proteins were found in the interactome of monomeric $\alpha$-synuclein, very few such proteins were found to be unique to the monomeric $\alpha$-synuclein interactome. Conversely a number of ribosomal proteins, specifically of the small ribosomal subunit were found to exclusively interact with fibrillar $\alpha$-synuclein.

An explanation for this finding requires further investigation but may reflect a higher capacity for ribosomal binding by the fibrillar conformation of $\alpha$-synuclein, thereby increasing the probability of detecting low abundance, or weakly interacting, proteins associated with ribosomes. Indeed this hypothesis is supported by the finding that when proteins were filtered based on their increased abundance in the fibrillar interactome when compared to the monomeric interactome, ribosomal proteins (from both the small and large ribosomal subunits) were heavily enriched. It is likely however, given the presence of ribosomal proteins in the interactome of monomeric $\alpha$-synuclein, that the interaction depends a region of the protein not occluded by the fibrillar fold, rather enhanced by its presence.

The observed interaction of $\alpha$-synuclein (especially in its fibrillar form) with ribosomal, and ribosome associated proteins, is of some interest as it may point to a pathophysiological process leading to cellular disruption, caused by $\alpha$-synuclein aggregation. The possibility that disruption to ribosomal function and deregulation of translation may play a role in the development of neurodegenerative diseases has gained traction in recent years. There are a number of studies that have shown that a disruption to proper ribosomal function can lead to cognitive deficiencies, cellular stress and neuronal dysfunction [144, 267, 407–416]. Furthermore, it has been demonstrated that ribosomal components can directly interact with cellular amyloid aggregates.

Translation in eukaryotic cells proceeds via three distinct stages; translation initiation, elongation and termination [417], in which initiation, the rate determining step, is controlled by a number of eukaryotic initiation factor (eIF)s [418]. EIF proteins play a number of important roles in the initiation of translation including the activation of mRNA and the assembly of ribosomal subunits. The most common form of translation initiation is termed cap-dependant initiation, and involves the formation of a pre-initiation complex consisting of the 40s ribosomal subunit and a number of eIFs [419]. This complex subsequently recruits the 60s large ribosomal

subunit leading to the formation of the 80s, translation competent, ribosomal complex. The formation of the 80s ribosome is accompanied by the concomitant release of the eIF protein complex [420]. Initiation of translation is followed by elongation, facilitated by eukaryotic elongation factor (eEF)2 [421], that functions to mediate the positioning of the correct tRNA to the acceptor site of the ribosome, and promote the translocation of the ribosome to the next codon [422]

Herein it is shown that several translation factors, including a number of initiation and elongation factors, are present in the interactome of $\alpha$-synuclein fibrils, and that abundance of eIF proteins interacting with fibrillar $\alpha$-synuclein is greater than their abundance in the monomeric $\alpha$-synuclein interactome. One implication of these data is the sequestration of eIF proteins, by $\alpha$-synuclein fibrils into LBs. Previous work has demonstrated that cases of Parkinson's disease are associated with a significant reduction in the activity of eIF2a [144, 408], while repression of eIF2a activity and concomitant translational repression, has been implicated in the mediation of prion disease development [409]. Furthermore, an increase in the activity of eEF2 inhibitor eEF2 kinase (eEF2K) [410]. Furthermore, an increase in eEF2K activity was observed in a mouse model of Parkinson's disease, while inhibition of eEF2K reduced cytotoxicity [410]. Though there is no evidence that eEF2K interacts with $\alpha$-synuclein, sequestration of eEF2, a protein found in the interactome of $\alpha$-synuclein fibrils, may lead to similar neuronal defects.

Interestingly, one protein that stood out among the interactors of fibrillar $\alpha$-synuclein for the magnitude of its enrichment was the the translational inhibitor eIF4E binding protein (4E-BP1). Though it may appear that this is in contradiction to a proposed hypothesis that reduction of translation by translation factor sequestration, may play a role in $\alpha$-synuclein induced neurodegeneration (sequestration of 4E-BP1 would likely increase translation), other studies have clearly demonstrated a link between inhibition of 4E-BP1 activity and neurodegeneration. It has been shown in Huntington's disease, for example, that a reduction in 4E-BP1 is linked to a depletion of proteins with functions relating to neuronal structure [411]. Furthermore an increase in eIF4E activity, through upregulation of the gene, or depletion of 4E-BP1, leads to the development of an autism spectrum disorder in mice and an increased ratio of excitatory to inhibitory synaptic signals [412].

Moreover, in relation to Parkinson's disease, 4E-BP1 has been shown to play an important role in protecting neurons in cases of pd-like cellular stress, including cellular insult with $\alpha$-synuclein fibrils. In this case it was observed that overexpression of 4E-BP1 led to a marked reduction in $\alpha$-synuclein aggregation and neurotoxicity [413]. It is hypothesised that this neuroprotective effect is the result of reducing the burden on the cells proteostasis machinery, associated with newly synthesised proteins, at a time when the cell is under considerable stress from misfolded amyloid

proteins [413].

In addition to translation initiation and elongation factors many ribosomal subunit proteins were found to be part of the interactome of $\alpha$-synuclein fibrils. Studies have previously shown that sequestration or disruption of ribosomal proteins occurs in a number of neurodegenerative diseases. LRRK2, a common site for familial and sporadic Parkinson's disease linked mutations, is dependent on the ribosomal protein s15 for its cytotoxic and neurodegenerative effects [414]. Indeed, increased expression of the gain of function G2019S LRRK2 mutation significantly suppresses translation [415]. The mechanism by which s15 mediates LRRK2 dependent cytotoxicity is not yet fully elucidated but it is of note that the ribosomal protein was among the interactors of fibrillar $\alpha$-synuclein. Moreover, there is evidence to suggest that a reduction in ribosomal function, via suppression of ribosomal biogenesis, represents a key pathway for cellular damage by poly-Q expanded huntingtin [267].

It is not unfounded to hypothesise that ribosomal proteins may be adversely sequestered by an amyloid fibrils. Indeed, a number of amyloid proteins have been shown to sequester ribosomal subunits into intracellular inclusions [407, 416]. It was shown, for example, through the use of in-cell cryo-electron tomography, that structures resembling that of intact ribosomes are sequestered within the boundary of fibrillar inclusion bodies formed in cells overexpressing poly-Q expanded huntingtin [407]. Furthermore, the amyloid protein tau has been shown to sequester ribosomes *in vitro* [416], while *in vivo* incubation of tau protein with a cell line leads to the significant reduction of translational capacity of the cell [416].

Taken together, these findings suggest that fibrillar $\alpha$-synuclein has the potential to induce translational disfunction via the sequestration of ribosomes, or by sequestration of translation initiation or elongation factors. The resultant disruption to protein synthesis may contribute to the loss of neuronal function seen in Parkinson's disease and the development of a neurodegenerative phenotype.

### 4.4.3 Fibrillar $\alpha$-Synuclein may cause mitochondrial disruption

Another major protein group identified as interactors of $\alpha$-synuclein, were a number proteins located in the mitochondria. Specifically, a number of protein subunits of Complex I and IV, components of the mitochondrial respiratory chain, as well as a number of mitochondrial import proteins, were identified as specific interactors of fibrillar $\alpha$-synuclein, being absent from the interactome of monomeric $\alpha$-synuclein. This finding may suggest a gain of function pathway to neurodegeneration by fibrillar $\alpha$-synuclein, through the disruption of mitochondrial function. Indeed, there is a growing body of evidence to suggest that mitochondrial disfunction

occurs in Parkinson's disease [423]. For example, the postmortem brain tissue of Parkinson's disease patients shows deficits in mitochondrial activity [424, 425], while mitochondrial toxins targeting the electron transport chain can cause Parkinson's disease-like symptoms in human and animal models [426, 427].

Furthermore, the aggregation of $\alpha$-synuclein, and associated development of neuronal abnormalities, appears to be linked with mitochondrial dysfunction. $\alpha$-synuclein has been shown to accumulate in the mitochondria where it interacts with the inner mitochondrial membrane where it impairs mitochondrial function and increases the formation of reactive oxygen species (ROS) [428, 429]. Given the lack of mitochondrial proteins in the interactome of monomeric $\alpha$-synuclein observed herein, it is likely that this interaction is dependent on the aggregated conformation of the protein, though mitochondrial import appears dependant on the unstructured N-terminal region [429].

Moreover, it has been demonstrated that the treatment of neuronal cells with fibrillar $\alpha$-synuclein leads to the the sequestration of mitochondrial structures within LB-like intracellular inclusions when examined by correlative light EM [371]. This is further supported by evidence that a number of mitochondrial proteins including members of the translocase of outer mitochondrial membrane (TOMM) complex were identified within these inclusions [371]. This is accompanied by an accumulation of $\alpha$-synuclein phosphorylated as serine 129, a hallmark of pathogenic aggregation, at the mitochondrial membrane [371]. The possibility that externally applied $\alpha$-synuclein possesses mitotoxic properties is further supported by evidence that a highly toxic species of $\alpha$-synuclein, generated following internalisation, localises to the mitochondrial membrane where it is associated with membrane depolarisation, mitochondrial fragmentation, and a release of the apoptotic marker, cytochrome c [430].

A number of pathways to mitochondrial dysfunction by $\alpha$-synuclein have been proposed. These include interference with the mitochondrial import machinery, such as the TOMM complex, and disruption of the respiratory chain through inhibition of Complex I activity. Both Complex I components and proteins of the TOMM complex were found to be present in the interactome of fibrillar $\alpha$-synuclein. There is growing evidence to suggest that the the inhibition of complex I plays a role in the development of Parkinson's disease [423]. Specifically, it has been proposed that $\alpha$-synuclein may directly impair complex I function following mitochondrial import [429]. Furthermore, transgenic mice that overexpress the A53T mutant in dopaminergic neurons show a severe reduction in complex I function in addition to an increase in mitophagy *in vivo* [428].

It is of note however that evidence from experiments using isolated mitochondria suggests that the reduction of complex I function is the result of prefibrillar $\alpha$-

synuclein oligomers and not mature $\alpha$-synuclein fibrils [431]. Furthermore, *in vivo* studies demonstrated that it was oligomeric $\alpha$-synuclein that accumulated on the inner mitochondrial membrane prior to complex I dysfunction [428]. Therefore, though the loss of complex I function is likely dependent on an aggregated form of $\alpha$-synuclein, there being little evidence of complex I proteins in the interactome of monomeric $\alpha$-synuclein, fibrillar $\alpha$-synuclein may not play a direct role in complex I inhibition.

Another major mitochondrial pathway that has been shown by a number of studies to be associated with the development of Parkinson's disease is the mitochondrial import pathway via the TOMM complex. It has been demonstrated that there is a significant reduction in the abundance of the the mitochondrial import protein TOMM40 (identified herein as an interactor of fibrillar $\alpha$-synuclein) in the brains of Parkinson's disease patients [432]. Furthermore, overexpression of TOMM40 recovered the mitochondrial deficits and oxidative burden seen in Parkinson's disease mouse models [432]. $\alpha$-synuclein has been reported to have a mitochondrial targeting sequence at it s N-terminus, enabling mitochondrial import via this complex [429].

Likewise, $\alpha$-synuclein phosphorylated at serine 129 have been shown to bind TOMM complex protein TOMM20, but not TOMM22 or TOMM40, preventing interaction with its co-receptor TOMM22, thereby inhibiting mitochondrial protein import [433]. The reduction of mitochondrial import was associated with an increase in ROS production and impairment of mitochondrial function [433]. Interestingly, no interaction between $\alpha$-synuclein fibrils and TOMM20 was observed herein, though TOMM22 and TOMM40 were present in the fibril interactome. An explanation for this discrepancy requires further investigation, and may lie with interaction seen here being the result of indirect association potentially though binding of the other TOMM complex protein TOMM70.

Further evidence to support the role of impairment of mitochondrial import in the development of neurodegenerative diseases comes from the investigation into Huntington's disease. It was shown that recombinant poly-Q expanded huntingtin, a protein strongly associated with the development of the disease, directly inhibited mitochondrial protein import in a cellular context [434]. Furthermore, mitochondria extracted from the brain synaptosomes of a mouse model of Huntington's disease, exhibited a protein import deficits [434].

In summary, the evidence presented herein suggests that $\alpha$-synuclein fibrils have the capacity to interact with mitochondria, potentially disrupting mitochondrial protein import leading to mitochondrial dysfunction and neuronal damage. Furthermore, this study provides evidence that aggregated, not monomeric $\alpha$-synuclein is responsible for interaction with Complex I proteins resulting in impairment of mitochondrial respiration and cellular dysfunction.

### 4.4.4 Conclusions

Herein a number of proteins from the SH-SY5Y cell proteome were found to interact with $\alpha$-synuclein fibrils. Furthermore, the specificity of these interactions to the fibrillar conformation of $\alpha$-synuclein were determined by comparison to the interactome of monomeric $\alpha$-synuclein. Of these proteins, RNA binding proteins as well as mitochondrial and ribosomal proteins were significantly enriched in this $\alpha$-synuclein, fibril specific, interactome. These results point to a number of potential mechanisms by which $\alpha$-synuclein can impair cellular function. These include the disruption of ribosomal function through sequestration of the ribosome itself, or indirectly through the disruption of translation initiation, and impairment of mitochondrial function through disruption of mitochondrial protein import. Further investigation is required to determine the relevance of these findings in the context of the cellular environment as well as to untangle the effects of these interactions on the proper functioning of the cell.

Finally the findings presented here represent the interactions of fibrillar $\alpha$-synuclein outside of the context of a physiological cellular environment and may therefore not represent the true interactions of fibrillar $\alpha$-synuclein following internalisation by cells. Therefore, in order for this study to have greater relevance, the next chapter examines interactions of $\alpha$-synuclein fibrils with cellular proteins following the internalisation of $\alpha$-synuclein fibrils by SH-SY5Y cells. Comparing the results of that experiment with the data presented here will permit the identification of pathologically relevant $\alpha$-synuclein fibril interactions.

# 5

# Identification of the Interactome of Cell Internalised $\alpha$-Synuclein Fibrils

## 5.1 Aims

The aim of this chapter is to identify the interactome of $\alpha$-synuclein fibrils following internalisation by SH-SY5Y cells. A further aim was to identify and characterise those interacting proteins that were specific to internalised $\alpha$-synuclein fibrils and those that were only seen in the interactome of lysate exposed $\alpha$-synuclein fibrils.

## 5.2 Introduction

### 5.2.1 $\alpha$-Synuclein Internalisation by Neuronal and Neuronal-Like Cells

There is a growing body of evidence to suggest that the progression of synucleinopathies such as Parkinson's disease rely on the cell to cell transmission of pathogenic $\alpha$-synuclein aggregates. Braak et al. [187] was the first study to describe the progressive degeneration occurring in the brains of Parkinson's disease patients (A phenomenon that has become known as Braak staging, and is used to classify the extent of Parkinson's disease in the brain), that appears to spread outwards from a single origin rather than develop simultaneously in multiple locations. Moreover, it has been demonstrated that in individuals with confirmed cases of Parkinson's disease and LB pathology, healthy neuronal grafts within the substantia nigra will begin to develop LB pathology in the years following the graft [251].

Indeed, as detailed in the introduction of Chapter 3, $\alpha$-synuclein fibrils have been shown to travel both between cells in culture, and from the culture media into healthy cells, leading to the development of LB-like pathology in the recipient cell [253, 259, 262, 263]. A number of mechanisms by which $\alpha$-synuclein fibrils can enter cells have been proposed, and the path $\alpha$-synuclein fibrils take following endocytosis partially studied.

### 5.2.2 Endocytic Internalisation of $\alpha$-Synuclein

A number of mechanisms by which $\alpha$-synuclein fibrils can enter cells have been described including receptor mediated endocytosis, macropinocytosis and inter-neuronal transit via nanotubes [260, 358, 359, 435]. Of most relevance to the present study, is the pathway of endocytosis. A role for endocytosis in the internalisation of $\alpha$-synuclein fibrils has been demonstrated by both low temperature incubation, known to inhibit endocytosis, and thorough dynamin inhibition, likewise preventing endocytic function [259]. Moreover, $\alpha$-synuclein fibril internalisation may depend on the clathrin-mediated endocytic pathway with co-localisation at the cell membrane occurring between exogenous $\alpha$-synuclein fibrils and transferrin [360], a protein known to be endocytosed via this pathway [436].

A number of plasma membrane receptors mediating the endocytosis of $\alpha$-synuclein fibrils have been identified. Mao et al. [260] identified the plasma membrane receptor LAG3 as a potential target. It was demonstrated that $\alpha$-synuclein fibrils bind to this receptor *in vitro* and that deletion of this receptor severely reduces $\alpha$-synuclein fibril internalisation by primary neurons [260]. Another potential receptor $\alpha$-synuclein

fibril endocytosis is the prion protein $PrP^C$ [359]. The lack of this cell surface receptor, both *in vitro* and in PrP knockout mice, markedly reduced the internalisation of $\alpha$-synuclein fibrils either applied to the media of cell culture or injected into the brains of mice, respectively [359].

Finally there is evidence to suggest a role of heparan sulfate proteoglycan in the internalisation of $\alpha$-synuclein fibrils, via macropinocytosis [437]. In non-neuronal cells $\alpha$-synuclein fibrils have been shown to bind to heparan sulfate chains prior to internalisation [437]. Moreover, it was shown that soluble heparin in the culture media can inhibit this interaction, reducing the internalisation of $\alpha$-synuclein fibrils [438].

### 5.2.3 Post Internalisation Trafficking of $\alpha$-Synuclein

Following the uptake of extracellular $\alpha$-synuclein fibrils, the aggregates can be found in endosomal compartments [360]. These compartments act as sorting stations that can recycle internalised material to the extracellular environment or mature into late endosomes which fuse with lysosomes, delivering their contents for degradation [439]. Following internalisation exogenous $\alpha$-synuclein fibrils effectively co-localised with markers of early and recycling endosomes as well as those of late endosomal and lysosomal membranes, including LAMP1 [360]. However only a small proportion of exogenous $\alpha$-synuclein co-localises with lysosomal compartment markers after several days of incubation [360], suggesting that exogenous $\alpha$-synuclein fibrils escape trafficking to lysosomes or are rapidly broken down once delivered to this organelle.

Seeding of intracellular inclusions by exogenous $\alpha$-synuclein fibrils is thought to require the escape of fibrils from the endolysosomal pathway into the cytosol [440]. This can occur via endolysosomal rupture, induced by the $\alpha$-synuclein aggregates either added extracellularly or through cell to cell transfer [440, 441]. It has been observed that the inclusion bodies formed after the internalisation of exogenous $\alpha$-synuclein fibrils co-localise with components of the endolysosomal pathway [440]. Moreover, the addition of exogenous $\alpha$-synuclein fibrils results in the redistribution of Galectin-3, indicative of endolysosomal-rupture [441]. Indeed impairment of the endolysosomal membrane by the addition of a lysomotropic detergent, rendered cells more susceptible to the formation of intracellular inclusion bodies, showing a significant increase in both number and size of intracellular inclusions [440].

In line with the pathogenic significance of the inclusion bodies, the formation of such intracellular LB-like inclusions has been linked with an increase in synaptic and neuronal loss [253, 262]. Following the addition of exogenous $\alpha$-synuclein fibrils, there is a significant reduction in a subpopulation of synaptic proteins following the addition of exogenous $\alpha$-synuclein fibrils including proteins of the synaptic vesicle associated

SNARE complex, as well proteins associated with SNARE complex assembly [262]. This is followed, after 14 days by significant decrease in the number of neurons in culture [262]. Moreover, it has been shown that the exposure of primary neurons to exogenous $\alpha$-synuclein induces the release of activated caspase 3 and concomitant neuronal fragmentation, both signs of apoptosis [262].

Indeed, the capacity for a $\alpha$-synuclein fibrils to seed inclusion formation appears to be closely related to the toxic effects of fibril exposure [442]. Inhibiting the ability of fibrils to effectively elongate through the use of a small molecule inhibitor, significantly reduces the capacity of fibrils to induce a loss of membrane integrity in primary neuronal [442]. Furthermore, a loss of aggregation competent monomeric $\alpha$-synuclein prevented the appearance of fibril induced toxicity, indicating intracellular inclusion formation is the driving force behind fibril induced toxicity [442].

The formation of $\alpha$-synuclein inclusions in cells is increased through than enhancement of endocytosis, suggesting a direct correlation between internalisation of the exogenous $\alpha$-synuclein fibril and the formation of endogenous aggregates [262]. Furthermore, in cell-to-cell transmission studies it has been shown that $\alpha$-synuclein aggregates originating in one cell can be found within the intracellular inclusions of other cells [253, 262]. As such, intracellular inclusions can act as a marker for both effective internalisation, with the suppression of endocytosis significantly abating their formation [253, 262, 263], and effective induction of $\alpha$-synuclein pathology in a cellular model.

### 5.2.4 Overview

Herein the interactome of $\alpha$-synuclein fibrils following their internalisation by SH-SY5Y cells was determined. To this end biotin labelled A18C $\alpha$-synuclein fibril seeds (the development of which was discussed in (Chapter 3 hereafter referred to as $\alpha$-synuclein fibrils) were incubated with SH-SY5Y cells for 24hrs, at which point fibril internalisation was evident. $\alpha$-synuclein fibrils were then isolated by means of streptavidin magnetic beads following cell lysis and the interactome identified by means of TMT proteomics. From this data, a number of key targets of internalised $\alpha$-synuclein fibrils were identified, including a number of mitochondrial proteins, nuclear pore proteins and proteins involved in the trafficking of endolysosomal compartments.

## 5.3 Results

### 5.3.1 $\alpha$-Synuclein Fibrils Were Internalised by Cells and Isolated by Streptavidin Magnetic Bead Pull-Down

Identification of proteins that interact with $\alpha$-synuclein fibril following cellular internalisation was achieved by streptavidin magnetic bead pull-down of the biotinylated $\alpha$-synuclein fibrils. In Chapter 3 it was demonstrated that SH-SY5Y cells internalised biotinylated fibrils following 24hr incubation. Therefore, for the purpose of identifying intracellular $\alpha$-synuclein fibril interactions post-internalisation SH-SY5Y cells were incubated with 1µM biotinylated $\alpha$-synuclein fibrils for 24hrs. Following this period of incubation, cells were lysed and a pull-down performed as previously described in Section 3.3.10 and Chapter 4.

Proteins interacting with $\alpha$-synuclein fibrils following cellular internalisation, were identified by TMT proteomics. In order to exclude from this interactome proteins that interact to the same degree with the streptavidin coated magnetic beads used to isolate the $\alpha$-synuclein fibrils, a pull-down was also performed on cells that had not been exposed to $\alpha$-synuclein fibrils. To enable quantitative proteomics data to be analysed with a sufficient degree of statistical power, triplicate experimental repeats were performed.

In order to draw reliable and meaningful conclusions from the proteomics data generated from this experiment it was important to ensure that the fibril pull-downs were conducted on cells in which there was evidence of fibril internalisation. To this end, a subset of cells in each experimental repeat, following 24hr incubation with $\alpha$-synuclein fibrils, were fixed and probed with fluorescently labelled streptavidin to detect biotinylated $\alpha$-synuclein fibrils and with antibodies specific for the endolysosomal protein LAMP1, to visualise endolysosomal structures. Internalisation was then confirmed by confocal microscopy. It was demonstrated that for each of the three experimental repeats there was evidence of co-localisation of biotinylated $\alpha$-synuclein fibrils with SH-SY5Y LAMP1 positive puncta, following 24hr incubation (Fig. 5.1).

Having determined internalisation of biotinylated $\alpha$-synuclein fibrils in each of three experimental repeats, streptavidin magnetic bead pull-downs were performed on the remainder of the cells as well as on SH-SY5Y cells not exposed to biotinylated $\alpha$-synuclein fibrils. Following magnetic bead pull-down a fraction of the sample was analysed by Coomassie stained SDS-PAGE and streptavidin probed western blot to demonstrate isolation of cellular proteins and biotinylated $\alpha$-synuclein fibrils respectively (Fig. 5.2). SH-SY5Y cellular proteins were isolated both in the presence and absence of biotinylated $\alpha$-synuclein fibrils (Fig. 5.1A). Furthermore, it can be seen

that in the three repeats of streptavidin magnetic bead pull-down from cells exposed to biotinylated $\alpha$-synuclein fibrils, there is evidence of biotinylated $\alpha$-synuclein fibril (Fig. 5.1B). These data suggest that biotinylated $\alpha$-synuclein fibrils were pulled down following internalisation by SH-SY5Y cells, and that cellular proteins were co-isolated. The pull-down samples were then analysed by TMT proteomics.

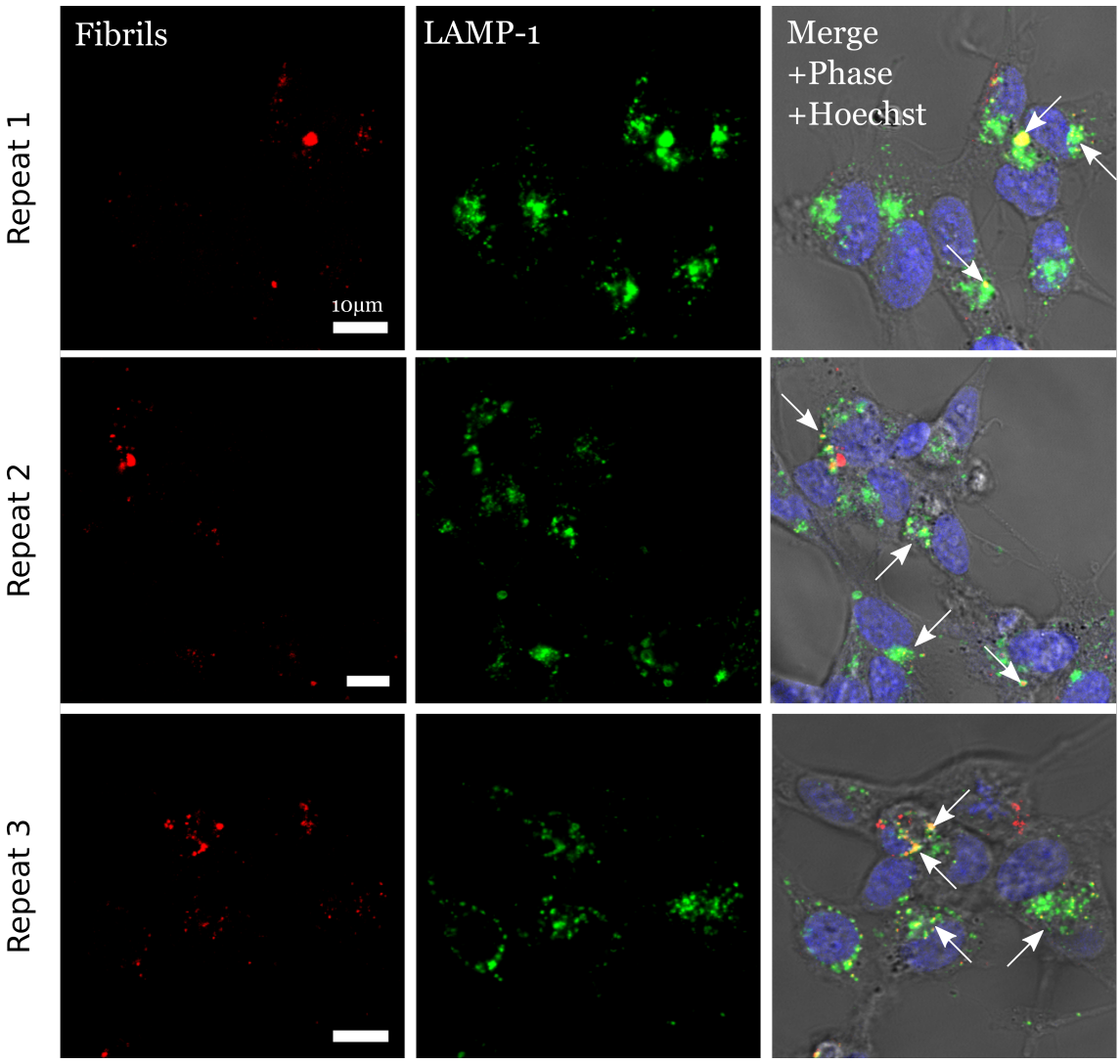


***Figure 5.1:*** *Evidence of SH-SY5Y cell internalisation of biotinylated α-synuclein fibrils in the three pull-down experiments. Three pull-down experiments were performed for proteomics. SH-SY5Y cells were incubated with biotinylated α-synuclein fibrils for 24hrs. A subset of cells were examined for evidence of internalisation. Cells were probed with LAMP1 to visualise endolysosomal structures and fluorophore conjugated streptavidin to visualise biotinylated α-synuclein fibrils. Representative images of the three experiments (Top: 1, Center: 2, Bottom: 3) acquired on an LSM700 confocal microscope at 40× magnification. Red denotes biotinylated α-synuclein fibrils. Green denotes LAMP1 positive puncta. White arrows denote examples of co-localisation of fibrils and endolysosomal compartments.*

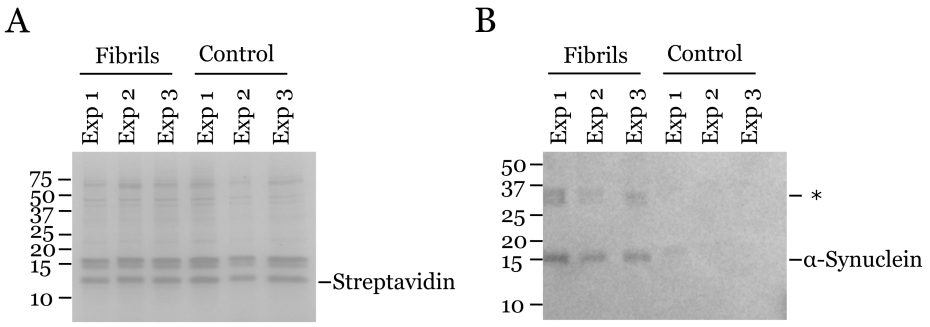


***Figure 5.2:*** *Biotinylated α-synuclein fibrils are isolated from from SH-SY5Y cells following cellular internalisation. Triplicate experiments of cells incubated with (Fibrils) or without (Control) biotinylated α-synuclein fibrils for 24hrs were lysed and biotinylated α-synuclein fibrils isolated by streptavidin magnetic bead pull-down. A) SDS-PAGE (Coomassie stain) of the pull-down experiment. The lower band seen in the pull-down lanes with a MW* 12 kDa *corresponds to that of streptavidin, while the higher bands correspond to SH-SY5Y cellular proteins. B) western blot of pull-down samples probed for biotin. The single band corresponds to the MW of α-synuclein. * denotes a band appearing at a MW of dimeric α-synuclein.*

### 5.3.2 Strategy for Defining Proteins That Interact With $\alpha$-Synuclein Fibrils Following Cellular Internalisation

Proteomics analysis identified a total of 2556 proteins, when combining experimental and control samples. A number of these proteins were known contaminants, or were identified by less than 2 peptides, thereby lowering the confidence of the identification. As a consequence such proteins were excluded, leaving a pool of 1382 proteins. In order to define a protein as an interactor of fibrillar $\alpha$-synuclein a strategy was required to differentiate them from the background interactions, ie. interactions that occurred due to an interaction between the protein and the streptavidin magnetic beads used for isolation. The same strategy as was employed for identification of cell lysate interactors of $\alpha$-synuclein fibrils (Chapter 4) was employed here (Fig. 5.3). Two properties of the protein in question: the mean fold change in protein abundance between the pull-down samples derived from SH-SY5Y cells incubated with (Fibril) and without (Control) $\alpha$-synuclein fibrils, and the p-value of this change.

Proteins were considered to be interactors of $\alpha$-synuclein fibrils, as opposed to an interactor of streptavidin magnetic beads, if the mean fold change in protein abundance and the p-values of this change, met the following thresholds: a mean fold change of $> 1.5$, and a p-value of $<0.05$. A graphical representation of this gating strategy is shown in Fig. 5.3. Using this strategy proteins in the top right sextant were defined as interactors of the $\alpha$-synuclein fibrils. This comprised a total of 969 proteins identified as interacting with $\alpha$-synuclein fibrils, following incubation of $\alpha$-synuclein fibrils with SH-SY5Y cells. Hereafter this interactome is termed the internalised $\alpha$-synuclein fibril interactome.

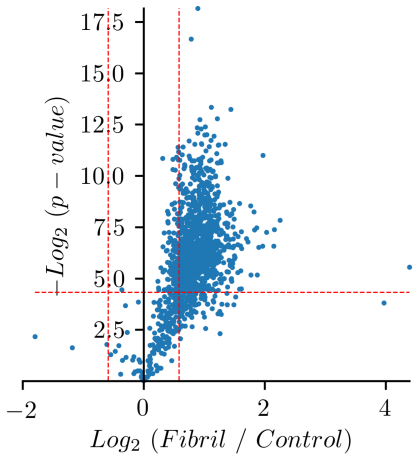


***Figure 5.3:*** *Gating strategy for identifying proteins as interactors of α-synuclein fibrils following internalisation by SH-SY5Y cells. Volcano plot showing the ratio of abundance of each protein in pull-down samples derived from cells incubated with (Fibril) or without (Control) α-synuclein fibrils. The abundance ratio is plotted against the p-value of this ratio (n=3). The red lines denote the cutoff for a protein to be considered an fibril interactor (ratio > 1.5, p-value < 0.01). Each point on this scatter plot represents a single protein identified by TMT proteomics.*

### 5.3.3 Interactors of Internalised α-Synuclein Fibrils are Enriched in Nuclear Import and Export Proteins

Having identified the proteins that were specifically interacting with α-synuclein fibrils following internalisation by SH-SY5Y cells, it was of interest to identify cellular locations and biological functions that were overrepresented in the interacting protein set when compared to their representation in the human proteome. As previously (Section 4.3.3), this was performed by utilising GO term annotations collated and managed by the Gene Ontology project [374, 375]using BiNGO [326] or ClueGO [327] cytoscape plugins. These tools enable visualisation of GO terms overrepresented in the sample (i.e. α-synuclein fibril interactors), when compared with the GO term's representation in a background protein list. In this instance the background used was that of the SH-SY5Y cell proteome [387].

To enable the SH-SY5Y cell proteome [387] to be utilised as the background for the GO term overrepresentation analysis, the proteins identified as intracellular α-synuclein fibril interactors must first be filtered by their presence in the proteome of the SH-SY5Y cell. Having applied this filter the number of proteins identified as intracellular α-synuclein fibril interactors was 478. All of the following bioinformatic analysis was conducted on this this filtered dataset.

GO term enrichment analysis of this dataset using the SH-SY5Y cell proteome

[387] as the background, revealed that $\alpha$-synuclein fibrils preferentially interact with proteins of the nuclear pore complex as well as ribosomal and spliceosomal proteins (Fig. 5.4). Furthermore, proteins involved in localisation to the endoplasmic reticulum and ribosome biogenesis were also overrepresented in the post-internalisation interactome of $\alpha$-synuclein fibrils (Fig. 5.5). As was shown in the case of lysate interactors of $\alpha$-synuclein fibrils, RNA binding proteins were also highly enriched (FDR $< 1 \times 10^{-18}$). Interestingly, an overrepresentation proteins involved in of viral gene expression were also identified. These proteins were primarily ribosomal proteins as well as a number of nuclear pore proteins.

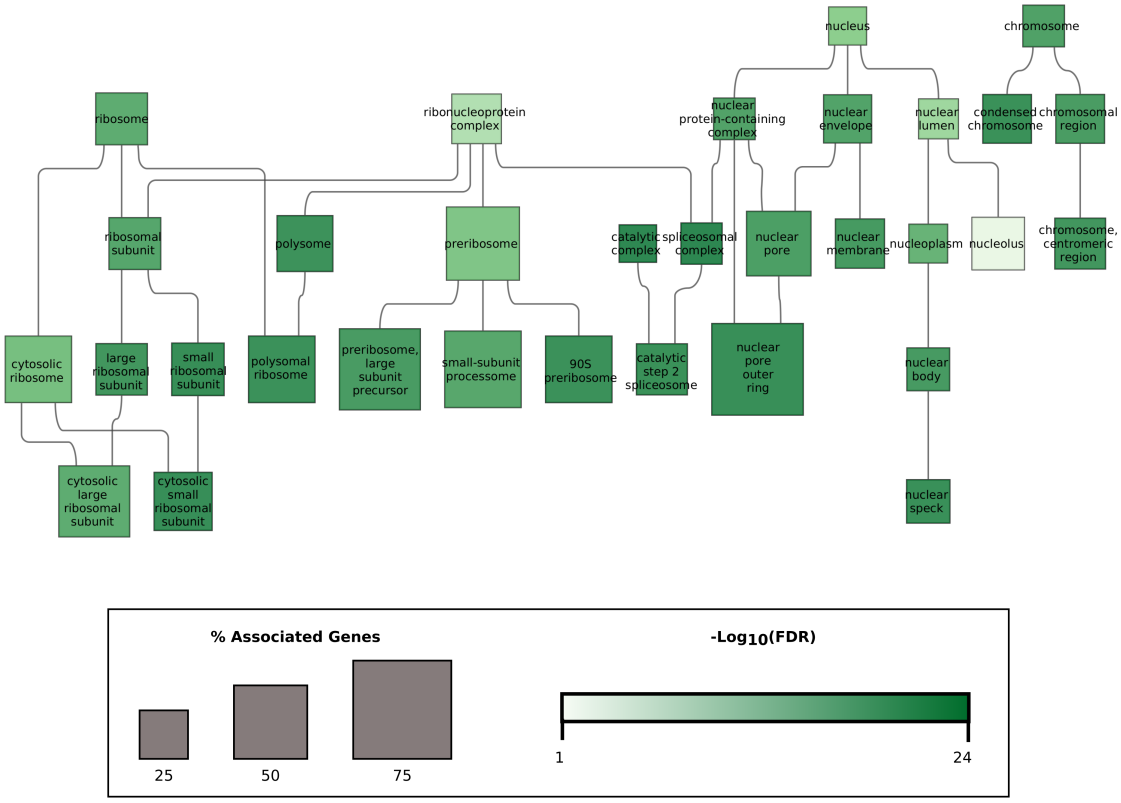


***Figure 5.4:*** *Proteins interacting with $\alpha$-synuclein fibrils, following internalisation, are enriched in nuclear pore and ribosomal proteins. GO term enrichment analysis (limited to the cellular component namespace), performed on post-internalisation interactors of $\alpha$-synuclein fibrils. Hierarchical graph showing the GO terms enriched in $\alpha$-synuclein interactors and their relationships to other terms. Node colour saturation denotes significance of the enrichment (FDR). White nodes are not significantly enriched (FDR $> 0.05$). Node size denotes the percentage proteins annotated with this term in the background proteome, that were present in $\alpha$-synuclein fibril interactome.*

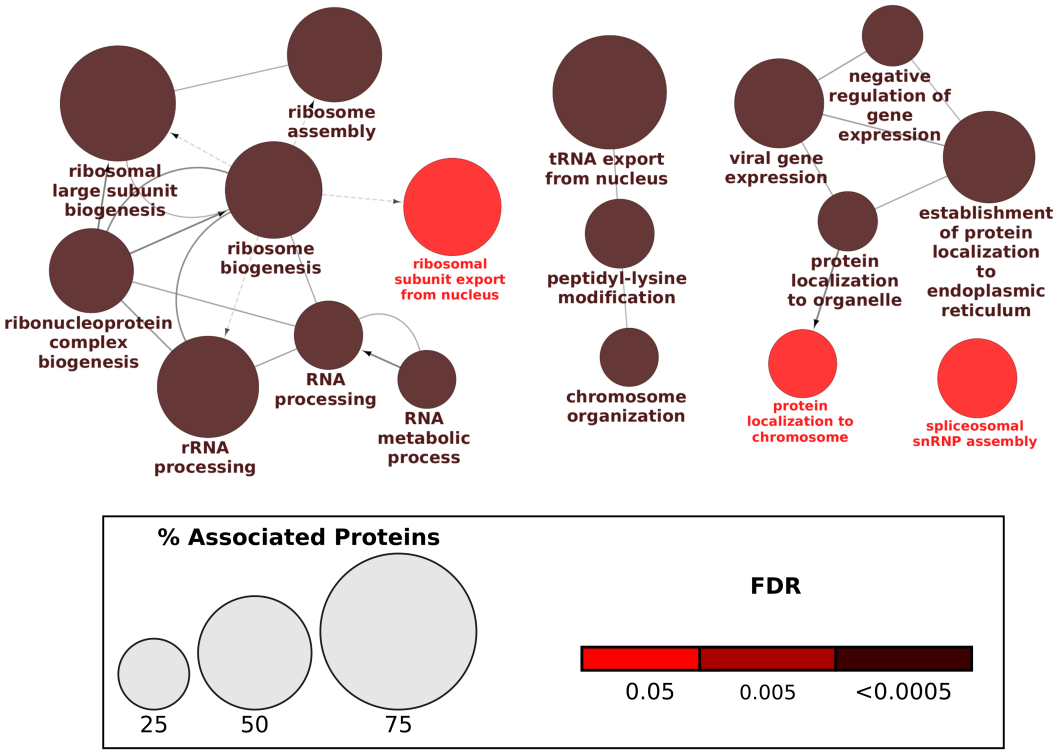


***Figure 5.5:*** *Proteins interacting with α-synuclein fibrils, following internalisation, are enriched in proteins involved in ribosome biogenesis and translation. GO term enrichment analysis (limited to the biological process namespace), performed on post-internalisation interactors of α-synuclein fibrils. ClueGO [327] GO enrichment analysis of internalised α-synuclein fibril interactors. Highly similar terms (by shared proteins) were grouped together and the most highly enriched term (by FDR) within the group is depicted. Node colour denotes the significance of enrichment (FDR). Node size denotes the percentage proteins annotated with this term in the background proteome, that were present in α-synuclein fibril interactome. Undirected edges denote kappa similarity of terms > 0.4. directed edges denote an "is a" relationship between terms.*

### 5.3.4 Post-Internalisation Protein Interaction Network of $\alpha$-Synuclein Fibrils Contain Transport and RNA Processing Clusters

The post-internalisation, protein interactome of $\alpha$-synuclein fibrils was further investigated through the visualisation of the inter-protein interactions occurring within the interactome. By utilising the protein-protein interaction data, collated by the StringDB [376] database, the interactome of $\alpha$-synuclein fibrils following internalisation by SH-SY5Y cells could be visualised. Furthermore, the use of the MCL [388] clustering algorithm, groups of closely interacting proteins, likely to be involved in related functional pathways, could be easily identified. This algorithm identifies clusters based on the interconnectedness of the graph, without the need for a predefined number of clusters. The use of the MCL clustering algorithm additionally enabled proteins with few partners to be discarded allowing for clearer visualisation an otherwise crowded network.

The post-internalisation interactome of $\alpha$-synuclein fibrils was graphed by these means and the five largest clusters identified by the MCL clustering algorithm visualised. Highly enriched proteins (i.e those proteins with a large and statistically significant positive fold change between Control and Fibril samples) are of interest especially if several such proteins appear in a cluster. The presence of such a cluster may indicate high affinity of $\alpha$-synuclein fibrils for a particular complex. Therefore, in order to visualise the enrichment the size of each protein node in the interaction network was set as proportional to the fold change of the protein abundance (ie. the protein position in the X axis of Fig. 5.3), while the transparency of the protein node was set proportional to the p-value of this change (i.e. the protein position in the Y axis of Fig. 5.3). The result is that the closer the protein is to the top right of the volcano plot (Fig. 5.3) the larger and more opaque it appears in the network (Fig. 5.6).

In order to identify what each cluster represents, GO terms associated with each protein in the cluster was identified. The frequency of each term associated with the cluster was then computed and a term cloud generated in order to visualise the functions associated with the cluster. Each term in the term cloud is roughly proportional to the frequency of the term in the cluster, though some adjustments are made to enable the printing of terms with greater lengths (Fig. 5.7).

The two highly identifiable clusters were readily identified by this analysis and can be seen in Fig. 5.6 coloured blue and purple. Both contain a number of closely interacting proteins, that are highly enriched in the $\alpha$-synuclein fibril interactome (Fig. 5.6). Analysis of the terms associated with these clusters (Fig. 5.7) revealed proteins involved in RNA processing and translation (Fig. 5.6 and Fig. 5.7 Blue) in

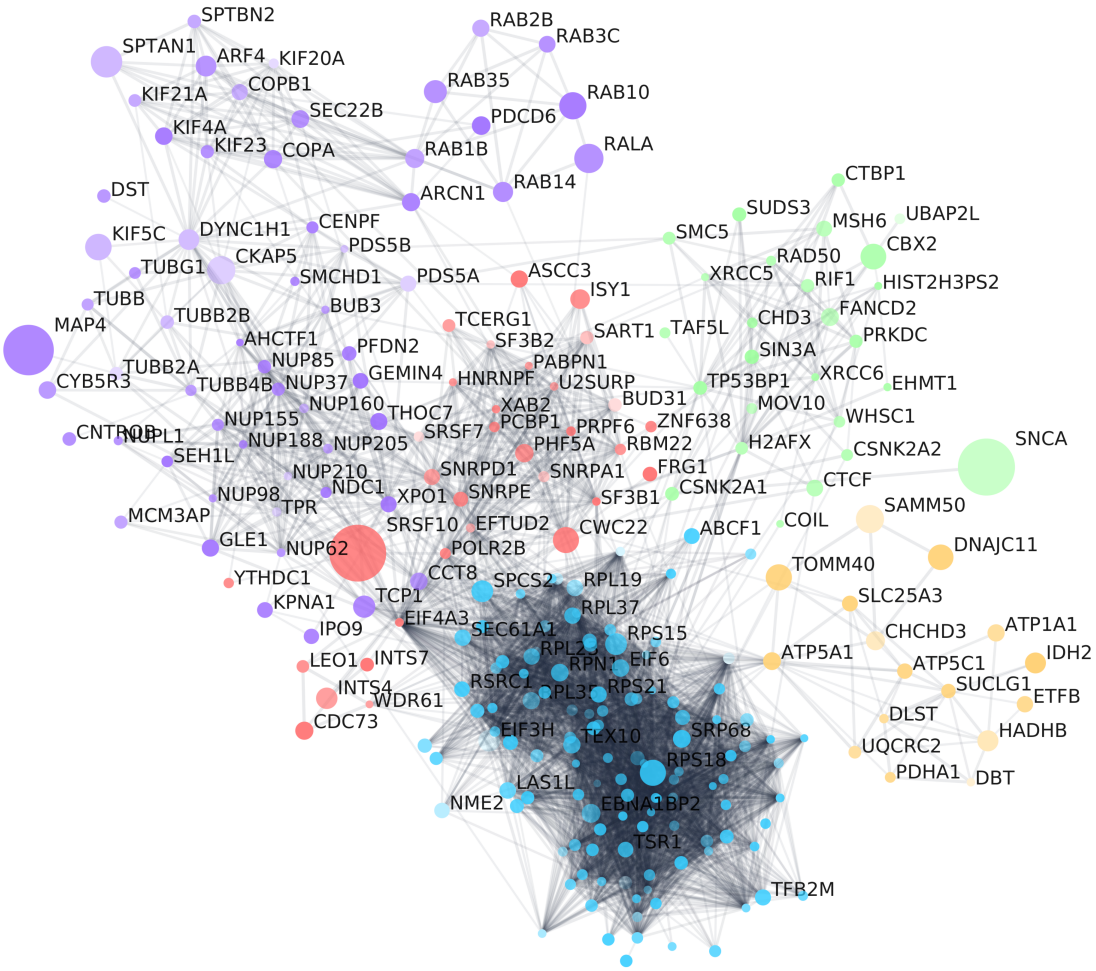


***Figure 5.6:*** *Protein-protein interaction network of α-synuclein fibril interactors following internalisation by SH-SY5Y cells. Network of protein-protein interactors compiled by the StringDB service. The network was clustered using the MCL algorithm and the five largest clusters visualised, and nodes coloured based on the cluster in which they appear. Node size denotes the ratio of the protein abundance vs pull-down of cells not exposed to α-synuclein fibrils (Fig. 5.3 X axis). Node transparency denotes the p-value of the abundance change (Fig. 5.3 Y axis)*

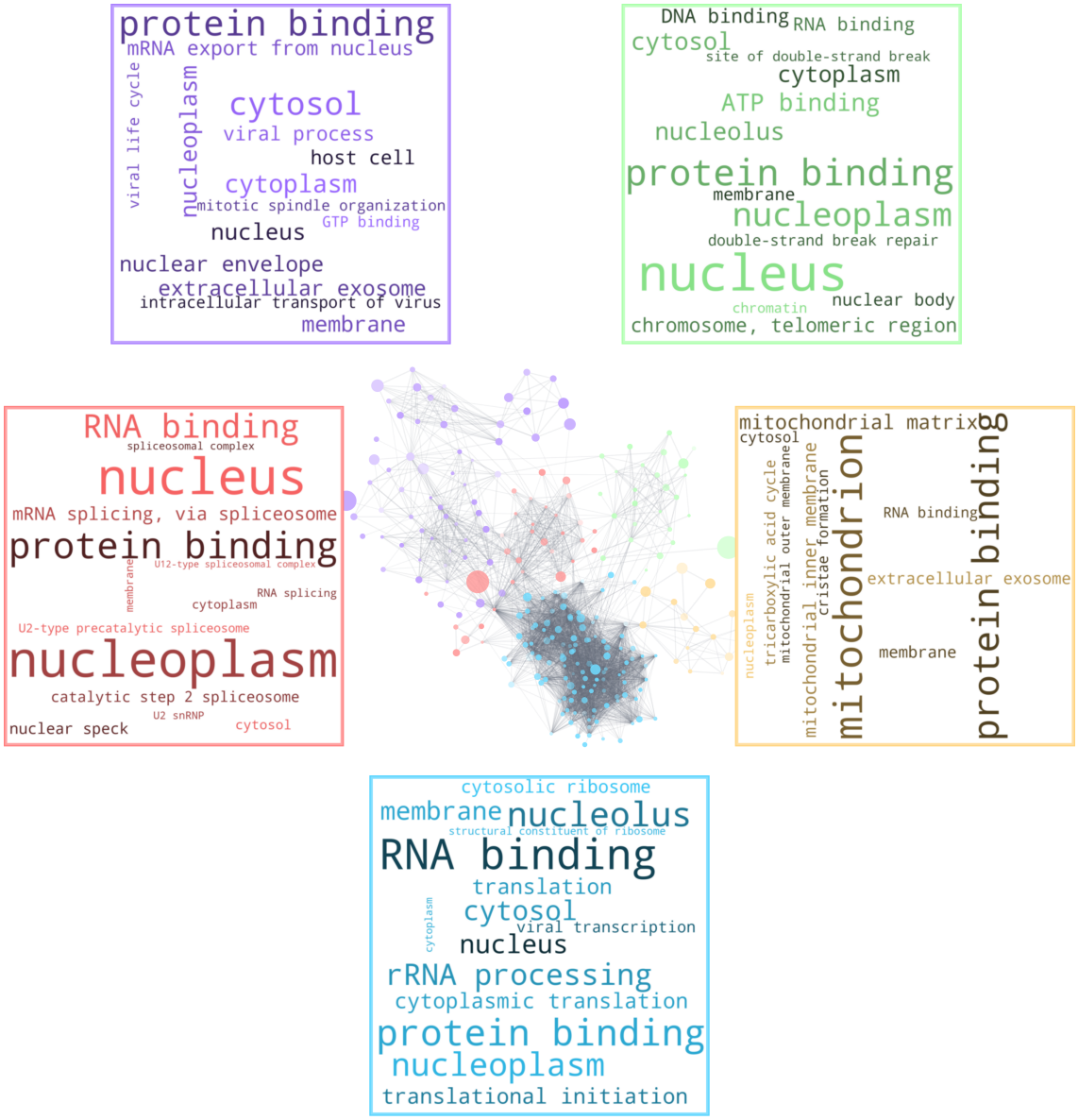


***Figure 5.7:*** *GO Terms Associated with the Protein-Protein Interaction Clusters (Fig. 5.6). GO term clouds generated from GO terms associated with proteins in each StringDB network cluster. The size of each term is generally proportional to the frequency of the term within the cluster though the size of some terms are reduced to enable printing within the figure boundary.*

addition to transport and endosomal proteins (Fig. 5.6 and Fig. 5.7 Purple).

Other notable findings of this analysis included the identification of a number of mitochondrial proteins (Figs. 5.6 and 5.7 Yellow). Additionally many of these proteins had large and significant fold changes, indicating a high degree of interaction with internalised $\alpha$-synuclein fibrils. These proteins included the mitochondrial import protein TOMM40. However, it is worth noting that no mitochondrial GO term was significantly enriched in the interactome, indicating that though individual proteins may have a high degree of interaction with internalised $\alpha$-synuclein fibrils, mitochondrial proteins as a group were not unduly represented by the interactome.

Finally, another notable finding of this high level analysis was a large cluster of spliceosomal proteins that were also identified among the interactors of $\alpha$-synuclein following cellular internalisation (Figs. 5.6 and 5.7 Red). One such spliceosomal protein, SRSF10 was particularly notable for its enrichment within the interactome of internalised $\alpha$-synuclein fibrils (Fig. 5.6).

Closer visual inspection of several of the protein-protein interaction clusters shown in Fig. 5.6 reveals that they are likely composed of two or more subgroups. This is especially evident for the clusters identified in blue and purple (Fig. 5.6). For this reason these clusters (Fig. 5.6 Blue and Purple) were isolated and regrouped by the MCL algorithm with an inflation parameter of 4 resulting in a more fine grained clustering. Re-clustering the first protein-protein network cluster (Figs. 5.6 and 5.7 Blue) representing a number of RNA processing and translation proteins revealed two distinct subclusters (Fig. 5.8). The GO terms associated with these clusters were also mapped to enable determination of the major roles and locations attributable to each cluster (Fig. 5.9).

The first of these subclusters (Figs. 5.8 and 5.9 Blue) represented a densely clustered network of RNA processing proteins while the second of these clusters (Figs. 5.8 and 5.9 Purple) largely represented cytosolic ribosomal subunit proteins. Relying on GO terms alone it was difficult to decipher the true nature of the sub cluster shown in blue (Figs. 5.8 and 5.9 Blue). Therefore KEGG pathways associated with the cluster were also identified. Only one such pathway was linked to the cluster shown in Blue (Figs. 5.8 and 5.9) which identified the cluster as representing the ribosomal biogenesis pathway.

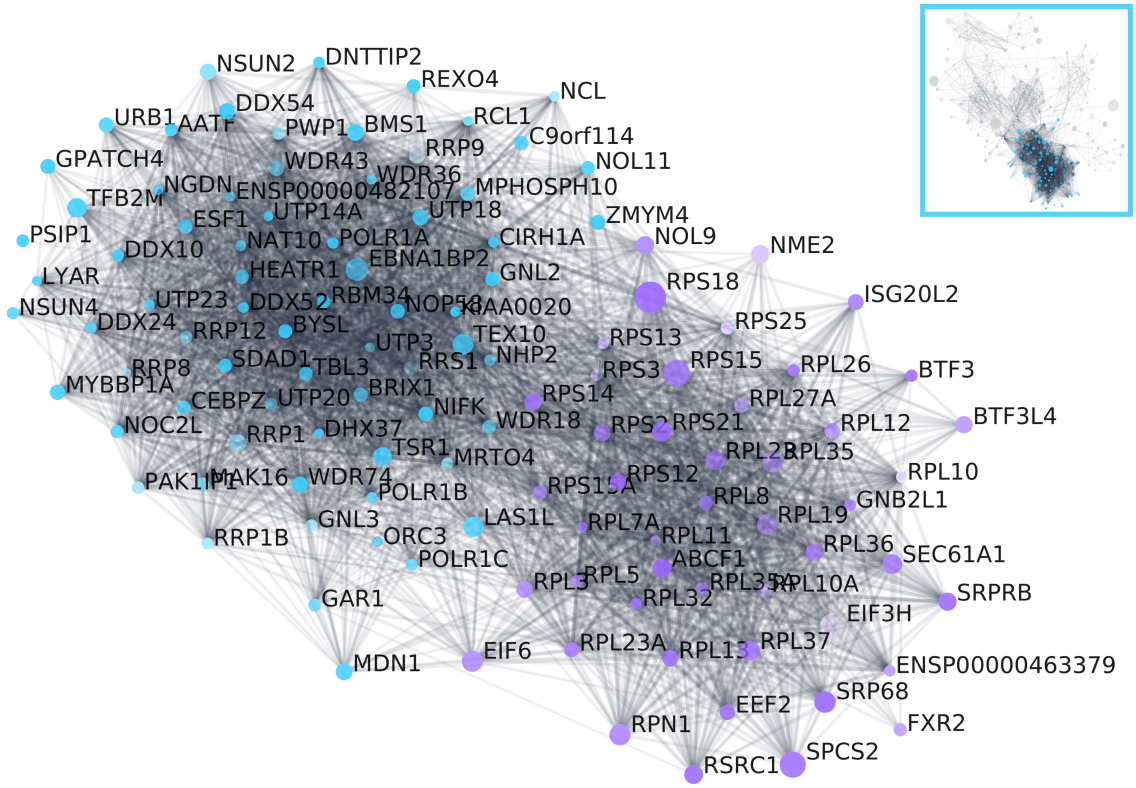


***Figure 5.8:*** *Sub clusters of protein-protein interaction network of α-synuclein fibril interactors following internalisation by SH-SY5Y cells. Network of protein-protein interactors compiled by the StringDB service taken from the Blue cluster identified in Fig. 5.6. The network was clustered using the MCL algorithm (inflation factor 4) and the two largest clusters visualised, and nodes coloured based on the cluster in which they appear. Node size denotes the ratio of the protein abundance vs pull-down of cells not exposed to α-synuclein fibrils (Fig. 5.3 X axis). Node transparency denotes the p-value of the abundance change (Fig. 5.3 Y axis)*

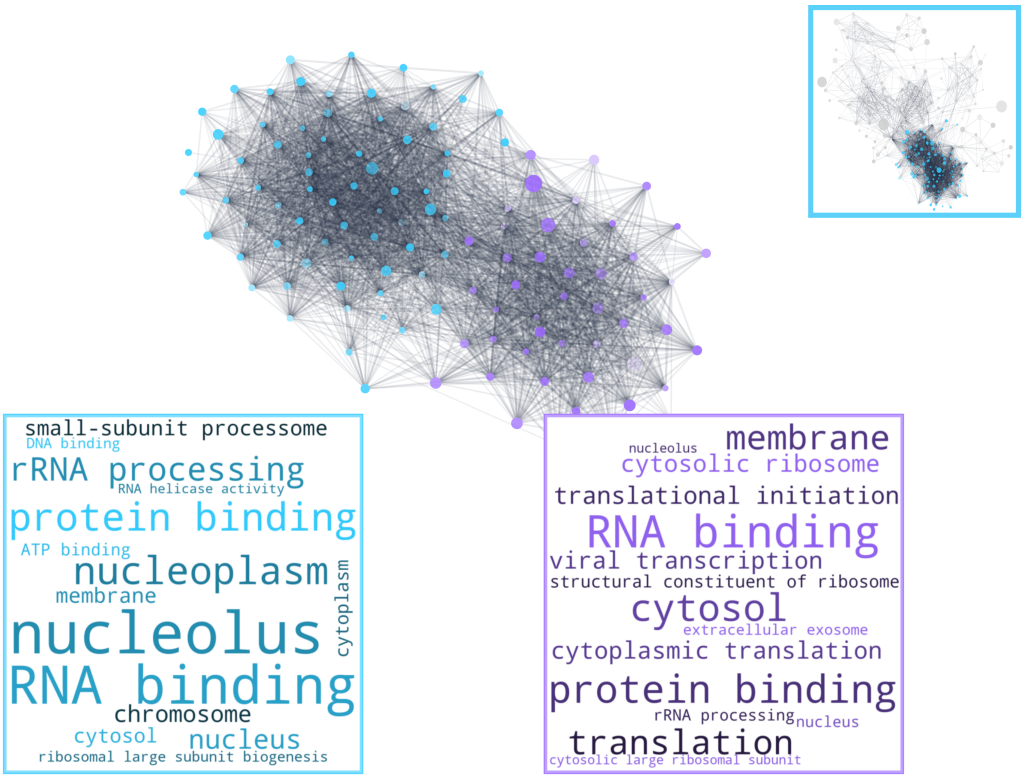


***Figure 5.9:*** *GO terms associated with the reclustered protein-protein interaction network (Fig. 5.8). GO term clouds generated from GO terms associated with proteins in each StringDB network cluster. The size of each term is generally proportional to the frequency of the term within the cluster though the size of some terms are reduced to enable printing within the figure boundary.*

Reclustering the other primary cluster identified in Fig. 5.6 (Purple) using the aforementioned clustering parameters (MCL algorithm, inflation parameter of 4) revealed five sub clusters. The largest of these subclusters represent proteins involved in nuclear import and export (Figs. 5.10 and 5.11 Blue). This sub-cluster includes a number of nuclear pore proteins as well as Tho complex subunit (THOC)7, a protein that is somewhat significantly enriched within the interactome of internalised $\alpha$-synuclein fibrils.

The other major cluster (Figs. 5.10 and 5.11 Purple) represents proteins involved in vesicle mediated protein transport, and includes a number proteins present in the endoplasmic reticulum, the Golgi apparatus and the extracellular exosome. Interestingly many of these proteins were highly enriched in the interactome of internalised $\alpha$-synuclein fibrils including a number of Rab family proteins, GTPases key regulators of intracellular transport. Finally, a number of regulators of mitotic cell division and microtubule organisation (Figs. 5.10 and 5.11 Green and Red). These proteins included MAP4, a protein involved in microtubule assembly, that was found to be highly enriched within the interactome of internalised $\alpha$-synuclein fibrils.

Together, data from these analyses, identify proteins involved in protein transport as well as a number of proteins involved in nuclear import/ export were highly enriched in the interactome of internalised $\alpha$-synuclein fibrils. Furthermore, a number of mitochondrial and spliceosomal proteins including TOMM40 and SRSF10 were notable for their abundance within the interactome.

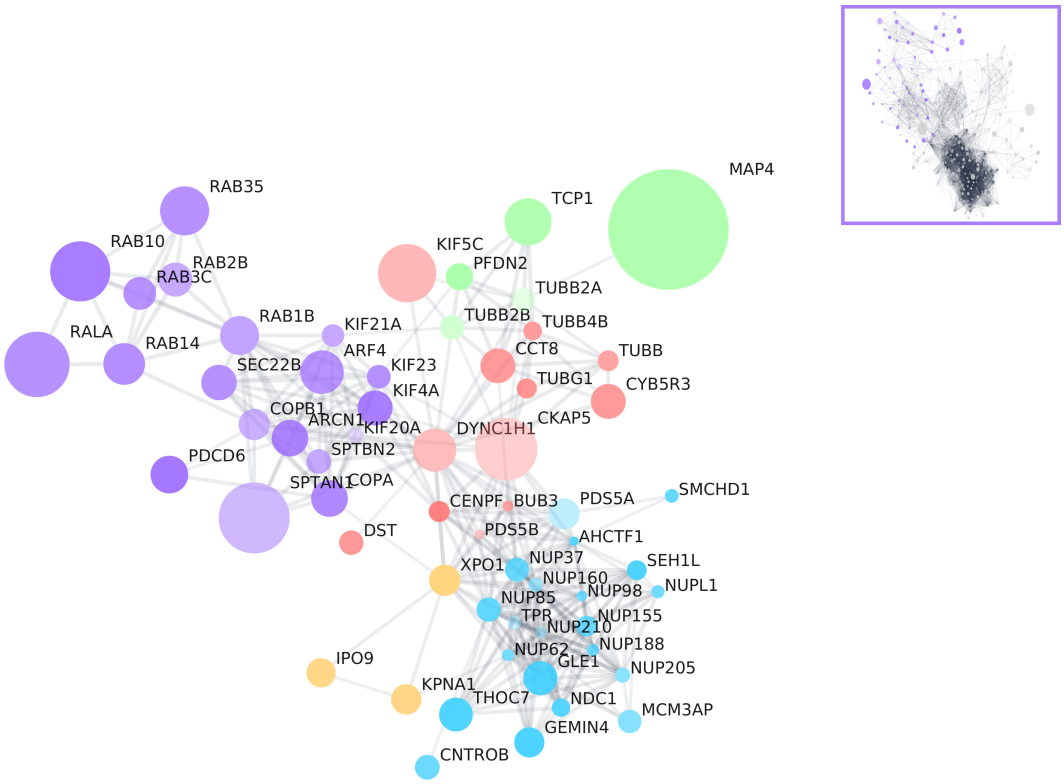


***Figure 5.10:*** *Sub clusters of protein-protein interaction network of α-synuclein fibril interactors following internalisation by SH-SY5Y cells. Network of protein-protein interactors compiled by the StringDB service taken from the Purple cluster identified in Fig. 5.6. The network was clustered using the MCL algorithm (inflation factor 4) and the five largest clusters visualised. Nodes were coloured based on the cluster in which they appear. Node size denotes the ratio of the protein abundance vs pull-down of cells not exposed to α-synuclein fibrils (Fig. 5.3 X axis). Node transparency denotes the p-value of the abundance change (Fig. 5.3 Y axis)*

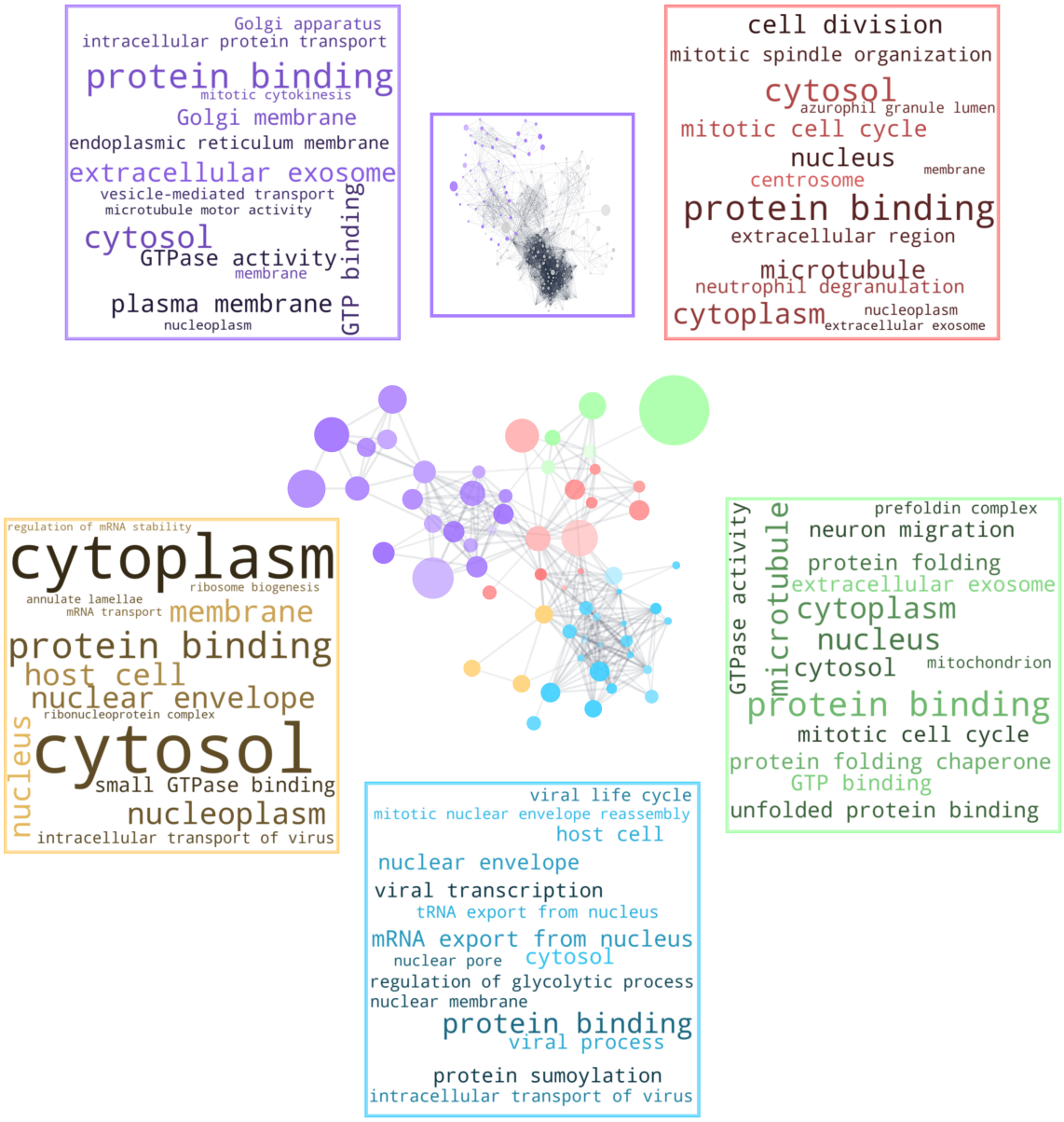


***Figure 5.11:*** *GO terms associated with the reclustered protein-protein interaction network shown in Fig. 5.10. GO term clouds generated from GO terms associated with proteins in each StringDB network cluster. The size of each term is generally proportional to the frequency of the term within the cluster though the size of some terms are reduced to enable printing within the figure boundary.*

### 5.3.5 Proteins Interacting With Internalised $\alpha$-Synuclein Fibrils are Represented in the Interactomes of Huntingtin Amyloid Aggregates

Further investigation into the interactome of internalised $\alpha$-synuclein fibrils was conducted by comparing the proteins identified herein with those identified by other studies investigating the interactions of $\alpha$-synuclein fibrils or other amyloid proteins. The studies compared in this manner likewise leveraged proteomics to identify protein interactomes. One such study investigated the proteins present in cortical LBs (Fig. 5.12 LB Genes [389]). Another study identified the interactome of various poly-Q expansions of the amyloid protein Huntingtin (Fig. 5.12 Q64 and Q150 Interactors [320]). Q150 expansion huntingtin was shown to be primarily fibrillar while the Q64 expansion was largely oligomeric [320]. Further, a study investigating the interactome of an 'artificial' amyloid, a protein designed to form the cross-β structure typical of amyloid fibres (Fig. 5.12 Artificial Amyloid Interactors [312]).

The interactome of internalised fibrillar $\alpha$-synuclein identified herein was compared to proteins that were enriched in LB like inclusions after 14 or 21 days in murine neuronal cells following treatment with $\alpha$-synuclein pre-formed fibrils (Fig. 5.12). Due to the murine origin of these proteins, comparison to the current data set involved first identifying the human orthologs of the protein. For this purpose the latest version (2021) of PylomeDB was leveraged, to map each murine protein to its highest ranked human ortholog [390].

In the case of each external dataset, proteins were compared to the interactome of internalised $\alpha$-synuclein fibrils. The proteins present in both datasets were then identified. The similarity of the two interactomes was inferred by means of the Jaccard similarity coefficient, a value between 0 and 1 where 1 indicates that the datasets are identical and 0 indicates that there is no overlap between the interactomes. The resultant plots for each external data set indicates that there is a degree of similarity between the interactome of internalised $\alpha$-synuclein fibrils and that of the Q64 and Q150 huntingtin interactors ( 0.25). However, there is a degree of similarity between the interactome of internalised $\alpha$-synuclein fibrils and the other datasets was low (>0.05 similarity) (Fig. 5.12).

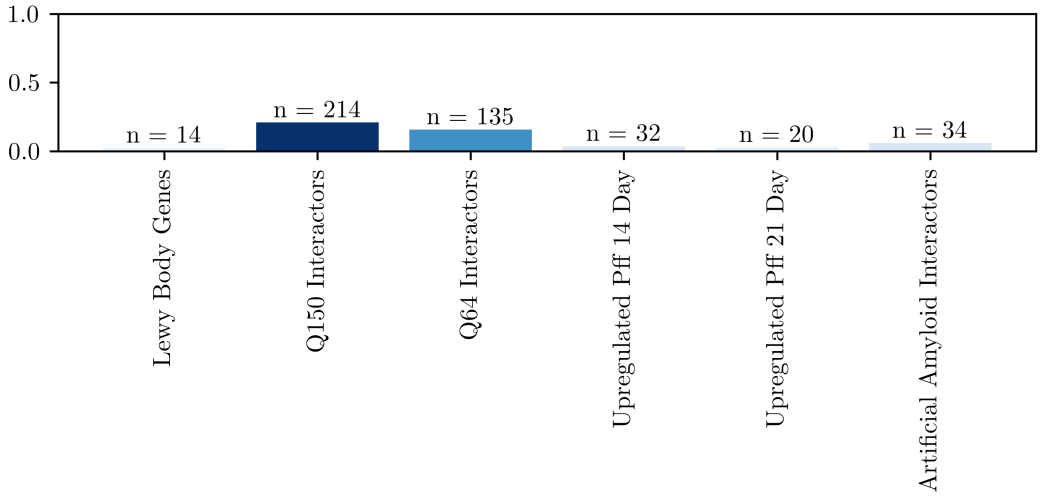


***Figure 5.12:*** *Similarity between internalised α-synuclein fibril interactors and proteins identified in other proteomic studies of amyloid proteins. For each external dataset the proteins were compared to the current dataset and the intersection of proteins identified. The similarity of the two datasets was then computed by means of the Jaccard similarity coefficient. Bar chart of the calculated Jaccard Similarity Index between the proteins identified in this study as α-synuclein fibril interactors and the proteins identified as interactors of other fibrils, α-synuclein proteoforms, or proteins present in LBs or LB-like structures. (Lewy Body Genes: [389], Q150 Interactors [320], Q64 Interactors [320],Upregulated Pff 14 Day [371], Upregulated Pff 21 Day [371], Artificial Amyloid Interactors [312]). For interactomes derived from mouse proteomes [371] were mapped to human orthologs using the PylomeDB mapping [390].*

### 5.3.6 Characterising Internalised α-Synuclein Fibril Interactors Present in the α-Synuclein Fibril Lysate Interactome.

In the previous chapter the interactome of α-synuclein fibrils exposed to SH-SY5Y cell lysate was determined. It is of interest which proteins identified in the interactome of α-synuclein fibrils exposed to lysate were also identified as interactors of internalised α-synuclein, as such proteins may represent proteins that readily associate with α-synuclein fibrils intracellularly following internalisation. However, this does not exclude the possibility that these interactions occured following cell lysis, prior to magnetic bead pull-down.

For this purpose the intersection of the lysate interactome of α-synuclein fibrils and the interactome of internalised α-synuclein fibrils was identified. The lysate interactome used was that characterised in the experiment alongside the interactors of monomeric interactors defined in Section 4.3.6. This interactome was chosen so as to allow later comparison with the monomeric α-synuclein interactome. This

interactome is hereafter termed the lysate interactome. The intersection of lysate interactome and the interactome of internalised $\alpha$-synuclein fibrils represented 246 proteins and is hereafter termed the cell and lysate interactome. A further 232 proteins were identified as interacting only with $\alpha$-synuclein fibrils, following internalisation by SH-SY5Y cells (hereafter termed the cell not lysate interactome) while 567 proteins were identified as only interacting with $\alpha$-synuclein fibrils in the context of exposure of $\alpha$-synuclein fibrils to cell lysate (hereafter termed the lysate not cell interactome). The lysate not cell interactome may represent proteins that only bind in lysates and thus may not bind fibrils taken up into the cell by endocytosis.

The cell and lysate interactome, representing the overlap of lysate and intracellular interactors of $\alpha$-synuclein fibrils, was then analysed in a similar manner to the complete interactome of internalised $\alpha$-synuclein fibrils. GO term overrepresentation analysis was conducted with the proteome of the SH-SY5Y cell as the background and by these means it was shown that the cell and lysate interactome was enriched in proteins involved in protein transport and ribosome biogenesis (Fig. 5.13).

Further analysis of the the common interactome was conducted by mapping the protein-protein interactions using protein interaction data provided by StringDB. The interaction network was then clustered by the MCL algorithm, to identify groups of highly interacting proteins, and the identity of the clusters determined by assigning cluster GO terms. Furthermore, in order to visualise proteins that that were present in high abundance in the internalised $\alpha$-synuclein fibril interactome, the enrichment of the in the protein in the interactome was mapped to the node size as was done for the complete interactome (Section 5.3.4).

By this method a number of protein clusters were identified in the interactome, common to both internalised and lysate exposed $\alpha$-synuclein fibrils. The largest and most densely interconnected of these clusters was that representing ribosomal subunit and translation initiation proteins (Figs. 5.14 and 5.15 Blue). Additionally, several mitochondrial proteins were also found to be present in this interactome (Figs. 5.14 and 5.15 Green) though it is worth noting that once again no specific mitochondrial term was overrepresented in this interactome. A further cluster of proteins identified within this interactome was that representing proteins involved in cellular trafficking and protein targeting (Figs. 5.14 and 5.15 Purple), a term that was enriched in both this filtered interactome and the full interactome of internalised $\alpha$-synuclein fibrils.

These data suggest that proteins involved in cellular trafficking as well as those involved in translation initiation and ribosomal function, readily associate with $\alpha$-synuclein fibrils irrespective of whether the fibrils are incubated with cells or with cell lysate. Furthermore, this extends to a number of specific mitochondrial proteins though mitochondria as a cellular structure are not unduly targeted. Though of interest, it is worth noting that such interactions occurring when $\alpha$-synuclein fibrils

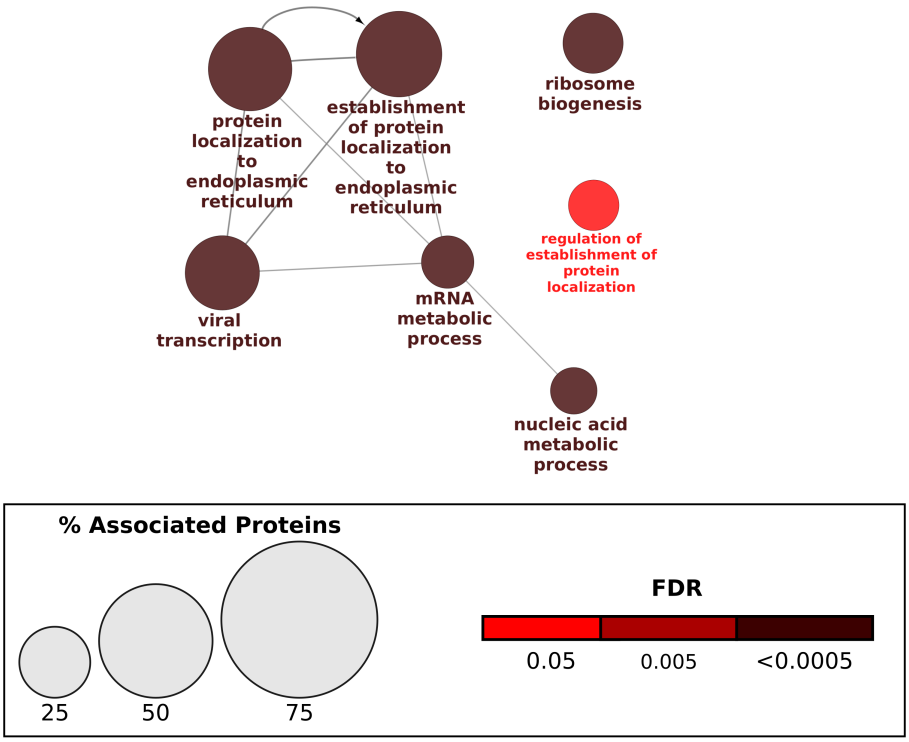


***Figure 5.13:*** *Proteins interacting with α-synuclein fibrils, both following internalisation and in cell lysate, are enriched in proteins involved in ribosome biogenesis and protein transport. GO term enrichment analysis (limited to the biological process namespace), performed on the intersection of intracellular α-synuclein fibril interactors and α-synuclein fibril lysate interactors. Cluster graph, generated by ClueGO [327] depicting GO terms enriched in α-synuclein fibril interactors and their similarity to one and other, as calculated by the proteins shared between the terms. Highly similar terms are clustered into groups denoted by shape. Node colour saturation denotes the significance of enrichment (FDR). Node size denotes the percentage proteins annotated with this term in the background proteome, that were present in α-synuclein fibril interactome.*

are incubated with cells, may occur following cell lysis.

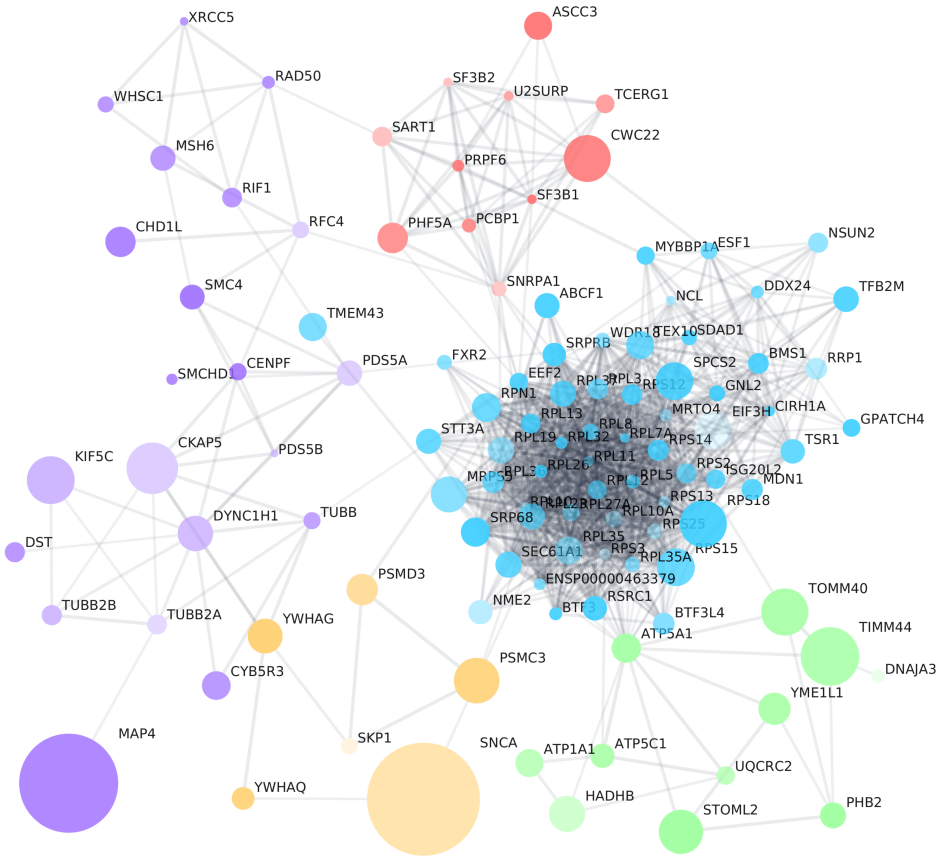


***Figure 5.14:*** *Protein-protein interaction network of the common interactome of α-synuclein fibril interactors following internalisation by SH-SY5Y cells and lysate interactors of α-synuclein fibrils. Network of protein-protein interactors compiled by the StringDB database. The network was clustered using the MCL algorithm and the five largest clusters visualised. Nodes were coloured based on the cluster in which they appear. Node size denotes the ratio of the protein abundance vs pull-down of cells not exposed to α-synuclein fibrils (Fig. 5.3 X axis). Node transparency denotes the p-value of the abundance change (Fig. 5.3 Y axis)*

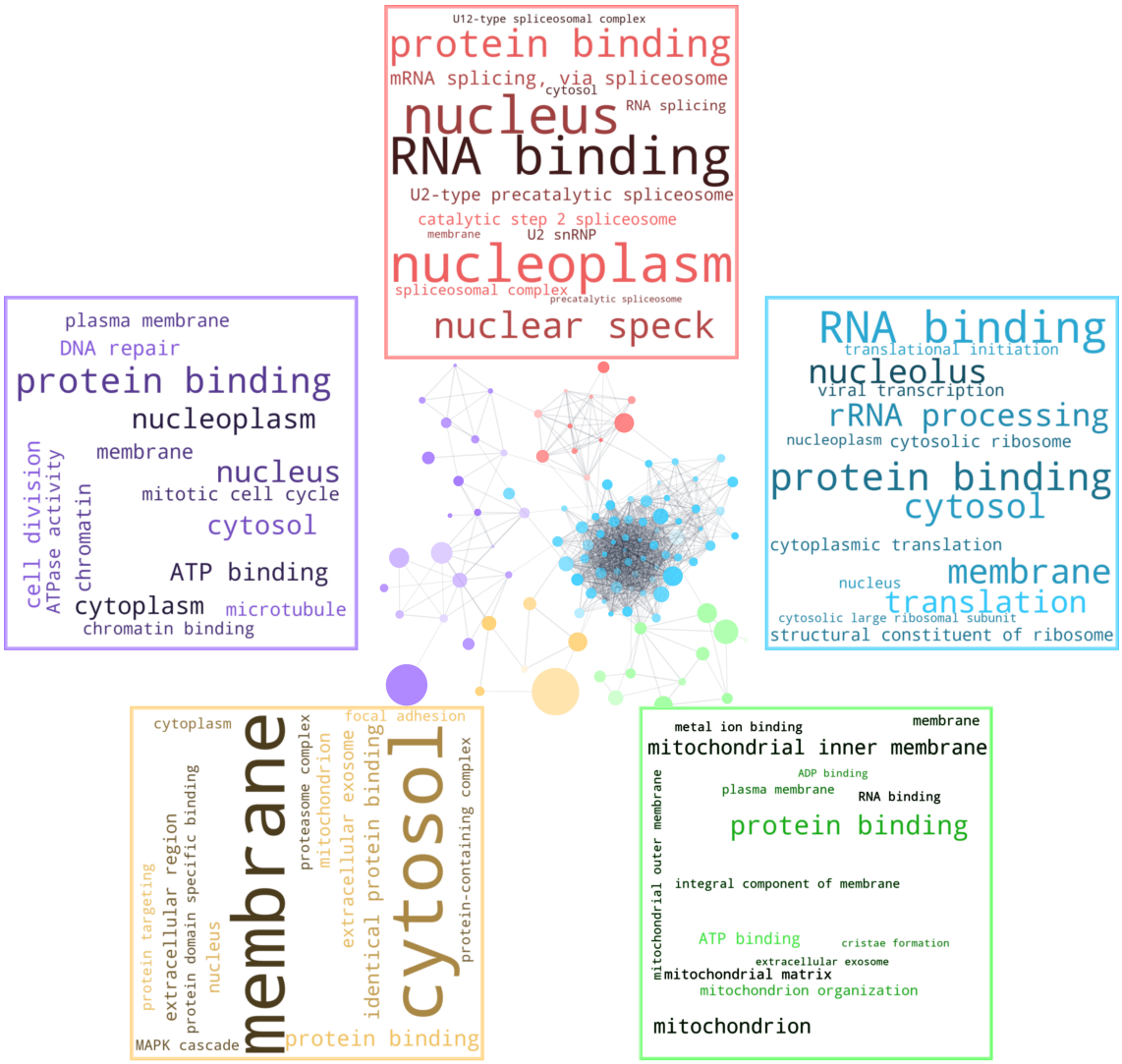


***Figure 5.15:*** *GO terms associated with the protein-protein interaction network shown in Fig. 5.14. GO term clouds generated from GO terms associated with proteins in each StringDB network cluster. The size of each term is generally proportional to the frequency of the term within the cluster though the size of some terms are reduced to enable printing within the figure boundary.*

### 5.3.7 Proteins Present Only in the Interactome of Internalised $\alpha$-Synuclein Fibrils are Enriched in Proteins Involved in Nuclear Transport and Ribosome Biogenesis

Having characterised the cell and lysate interactome, representing proteins shared by the interactomes of both internalised $\alpha$-synuclein fibrils and $\alpha$-synuclein fibrils exposed to lysate, it was then of interest to characterise the interactomes of proteins unique to the interactome of internalised $\alpha$-synuclein fibrils, termed the cell not lysate interactome. This interactome may represent those proteins with a lower affinity for $\alpha$-synuclein fibrils, thereby out competed by other proteins in the context of the cell lysate, but are nonetheless physiologically relevant interactors. Moreover, this interactome may represent interactions that occur only in the context of an intact cell, an environment not reproduced within the cell lysate.

To this end the the cell not lysate interactome was analysed for GO terms enriched over the background of the SH-SY5Y cell proteome. Due to the large number of enriched results ClueGO, grouping by term similarity was employed in which two or more terms associated with many common genes are considered similar and thus grouped together. The leading term, by significance level, can then be identified and visualised. Furthermore this analysis permits straightforward visualisation of both cellular compartment terms alongside biological process terms (Fig. 5.16). The results of this analysis identified several terms overrepresented in this interactome. These include proteins involved in nuclear transport, specifically proteins of the nuclear pore complex, ribosome biogenesis and chromosomal organisation.

Further investigation of the cell not lysate interactome by analysis of the protein-protein interaction network was conducted to identify any protein-protein clusters that are highly abundant in the interactome. As previously, this was conducted using protein interaction data from the StringDB database and clustered by MCL clustering algorithm. This analysis revealed five distinct, though highly intra-connected protein-protein interaction clusters. The largest of these clusters represents proteins involved in ribosomal biogenesis and RNA pre-processing. (Figs. 5.17 and 5.18 Blue).

Another cluster of note, identified by this analysis, is that representing a number of nuclear pore proteins (Figs. 5.17 and 5.18 including a number of nuclearporins). Finally, a smaller protein cluster was identified containing proteins present in the endoplasmic reticulum, Golgi apparatus and exosomes. It is noteworthy as many of these proteins were highly abundant in the interactome of internalised $\alpha$-synuclein fibrils (Figs. 5.17 and 5.18 Yellow), visualised by the size and opacity of the nodes.

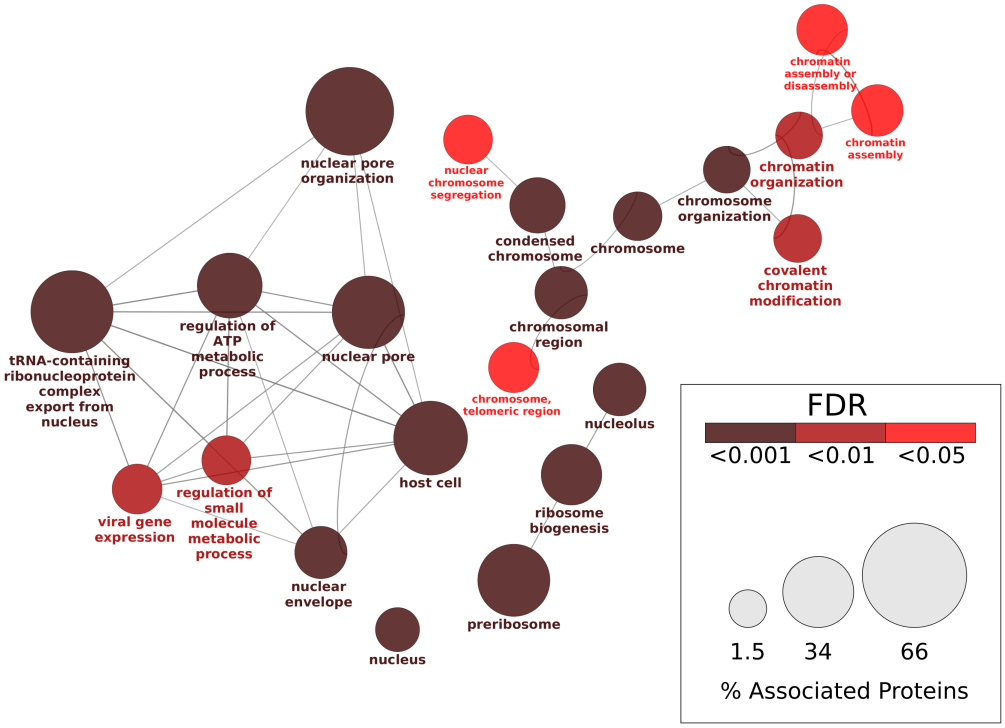


***Figure 5.16:*** *Proteins interacting with α-synuclein fibrils, following internalisation but not in cell lysate, are enriched in proteins involved in nuclear export, ribosome biogenesis and chromosome organisation. GO term enrichment analysis (limited to the biological process and cellular component namespaces), performed on the interactome intracellular α-synuclein fibrils when proteins in the lysate interactors of α-synuclein fibrils are excluded. Cluster graph, generated by ClueGO [327] depicting GO terms enriched in this interactome, grouped by semantic similarity, with the most significant term of each group displayed. Connections between terms denote a degree of semantic similarity. The significance of GO term enrichment (FDR) is denoted by node color. Node size denotes the percentage proteins, annotated with this term in the background proteome, that were present in the interactome.*

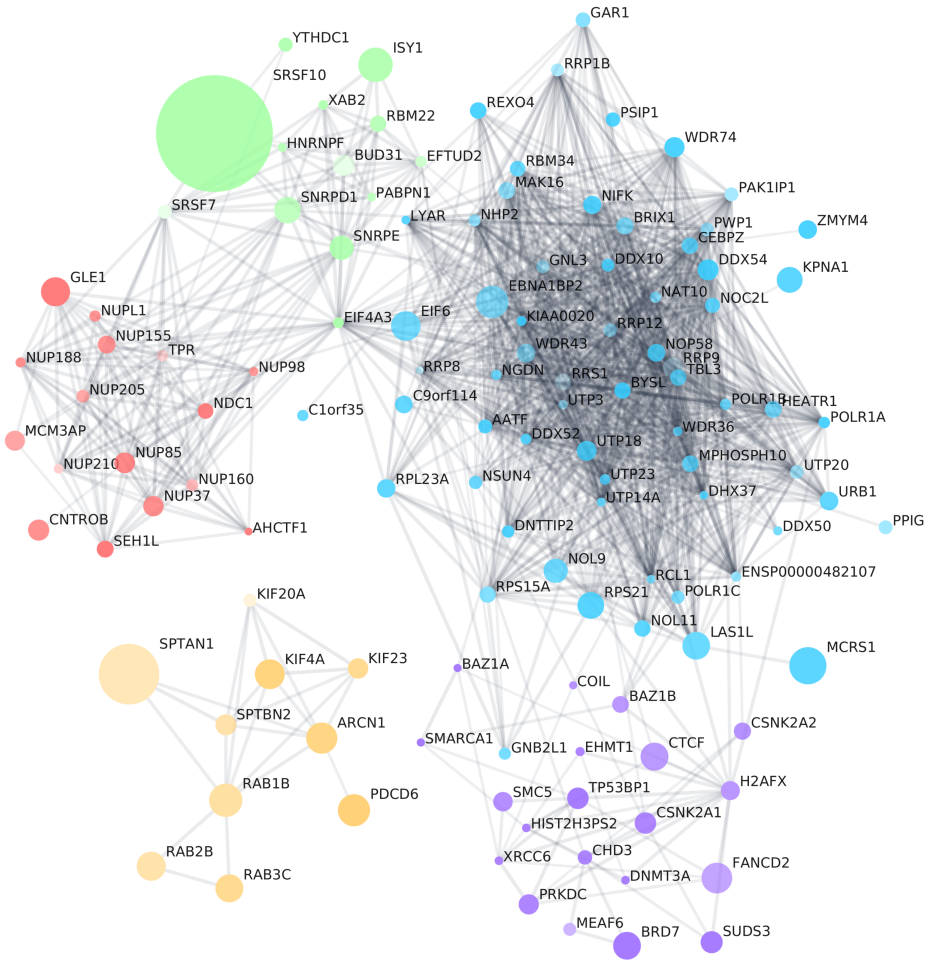


***Figure 5.17:*** *Protein-protein interaction network of the intracellular α-synuclein fibril interactome when lysate interactors are excluded. Network of protein-protein interactors compiled by the StringDB database. The network was clustered using the MCL algorithm and the five largest clusters visualised. Nodes were coloured based on the cluster in which they appear. Node size denotes the ratio of the protein abundance vs pull-down of cells not exposed to α-synuclein fibrils (Fig. 5.3 X axis). Node transparency denotes the p-value of the abundance change (Fig. 5.3 Y axis)*

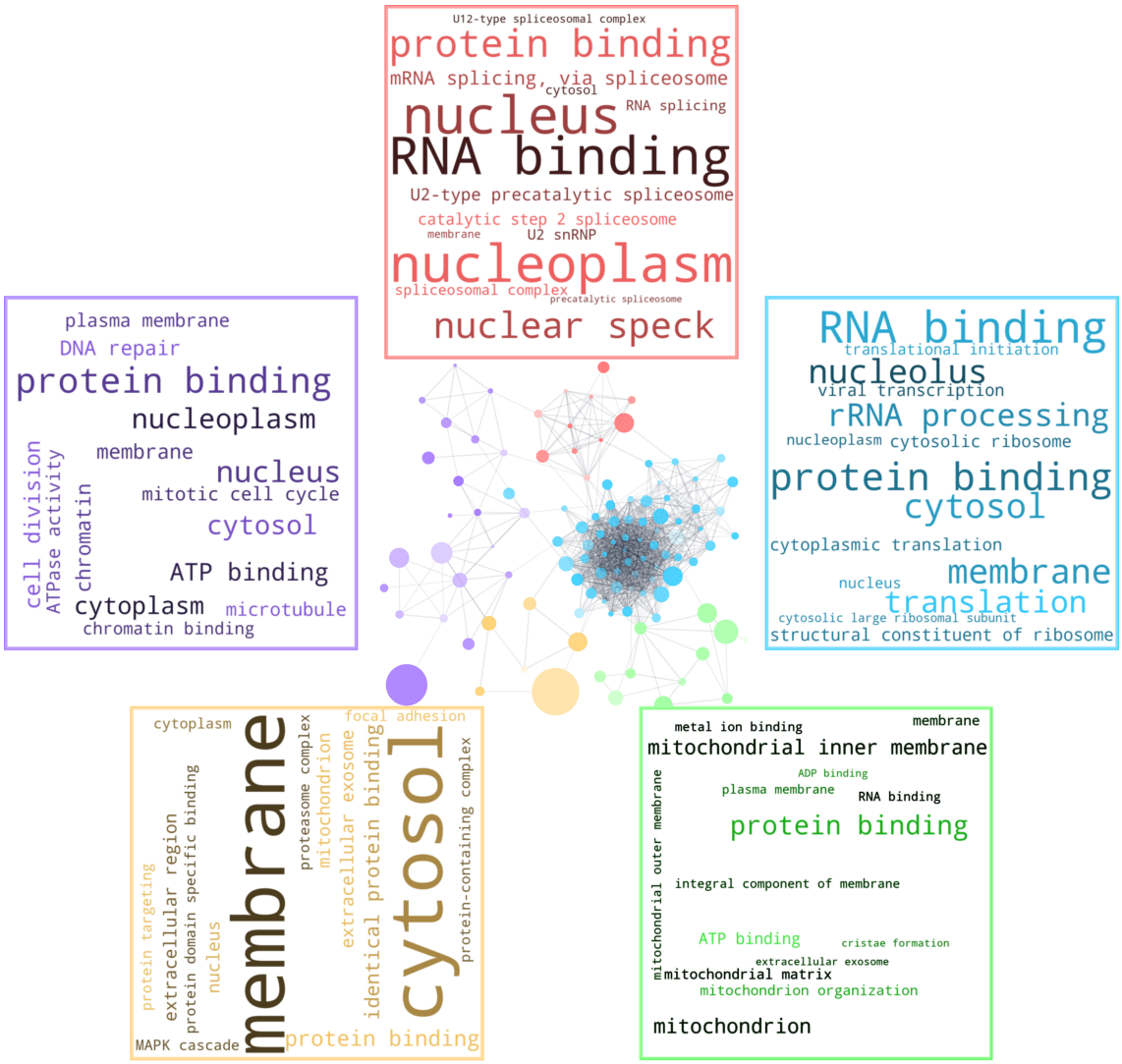


***Figure 5.18:*** *GO terms associated with the protein-protein interaction network shown in Fig. 5.17. GO term clouds generated from GO terms associated with proteins in each StringDB network cluster. The size of each term is generally proportional to the frequency of the term within the cluster though the size of some terms are reduced to enable printing within the figure boundary.*

### 5.3.8 Proteins Identified as Interactors of Internalised $\alpha$-Synuclein That are Not Interactors of Monomeric $\alpha$-Synuclein, are Enriched in Nuclear Pore Proteins

As with the lysate interacting proteins of $\alpha$-synuclein fibrils (Section 4.3.6), it was of interest to further characterise the protein interactors of internalised $\alpha$-synuclein fibrils by identifying those that specifically interact with the fibrillar form of $\alpha$-synuclein compared to those interacting with the monomeric form of $\alpha$-synuclein. To this end the interactome of internalised $\alpha$-synuclein fibrils was filtered of proteins present in the lysate derived interactome of $\alpha$-synuclein monomer. The resulting interactome represents proteins only interacting with internalised $\alpha$-synuclein fibrils and not interacting with monomeric $\alpha$-synuclein in lysate. GO term analysis of this interactome identified two primary areas that were enriched in this interactome. These were, ribosome biogenesis and nuclear pore proteins. These findings closely resemble that of the cell not lysate interactome (i.e. the interactome in which lysate interactions of $\alpha$-synuclein fibrils were excluded) (Fig. 5.19).

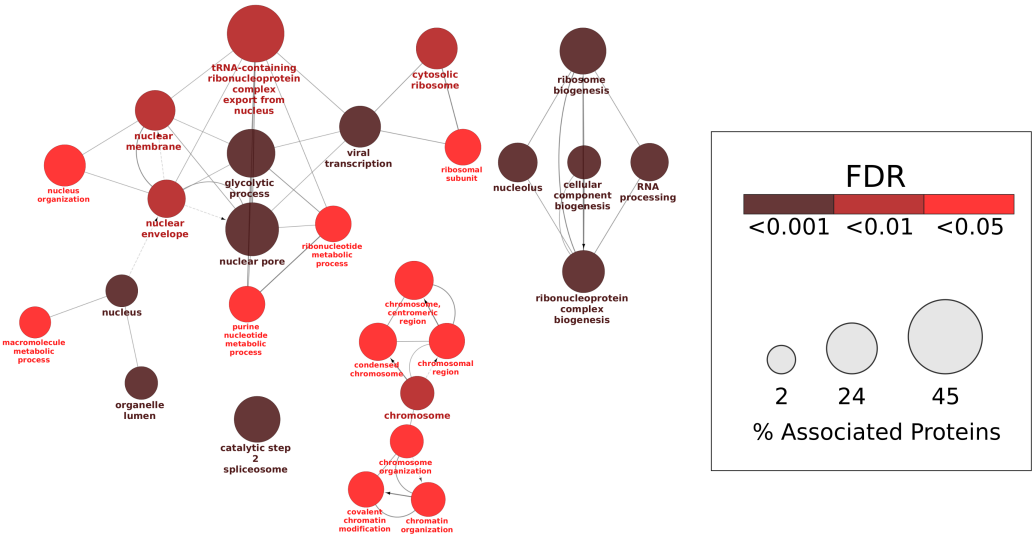


***Figure 5.19:*** *Proteins interacting with internalised $\alpha$-synuclein fibrils, but not monomeric $\alpha$-synuclein in cell lysate, are enriched in nuclear pore proteins and proteins involved in ribosome biogenesis. GO term enrichment analysis (limited to the biological process and cellular component namespaces), performed on the interactome intracellular $\alpha$-synuclein fibrils when proteins in the lysate interactors of $\alpha$-synuclein fibrils are excluded. Cluster graph, generated by ClueGO [327] depicting GO terms enriched in this interactome, grouped by semantic similarity, with the most significant term of each group displayed. Connections between terms denote a degree of semantic similarity. The significance of GO term enrichment (FDR) is denoted by node color. Node size denotes the percentage proteins, annotated with this term in the background proteome, that were present in the interactome.*

### 5.3.9 Plasma Membrane and Endolysosomal Interactors of Internalised $\alpha$-Synuclein Fibrils Interactors

It has been shown that $\alpha$-synuclein interacts with plasma membrane components, leading to internalisation by endocytosis [260]. $\alpha$-synuclein is then trafficked via the endolysosomal pathway where $\alpha$-synuclein fibrils have been shown to cause a degree of lysosomal impairment [360]. Therefore, to investigate the proteins that may interact with $\alpha$-synuclein fibrils during internalisation, the complete interactome of internalised $\alpha$-synuclein fibrils was filtered for the presence of the protein in the plasma membrane, in addition to endosomal and lysosomal compartments. This was done based on the presence of related GO annotations on the protein.

By visualising these selected proteins as a protein-protein interaction network it was possible to identify a number of clusters potentially relevant to the internalisation of $\alpha$-synuclein fibrils (Fig. 5.20). These included a number of Rab family proteins, guanosine triphosphate (GTP)ases involved in the coordination of endocytosis [443]. Furthermore, a number of proteins involved in the G-protein receptor signalling pathways were identified, including GNAS a key subunit of the G-protein complex, and GNAI2 a protein that has been implicated in regulating the surface density of dopamine receptors [444]. Finally a small number of lysosomal proteins were found to associate with internalised $\alpha$-synuclein. However, when further investigated, these proteins appeared to be only transiently lysosomal. Indeed, the primary roles of these proteins appears to as heparan sulfate proteoglycan (Curated Uniprot Entries [445]).

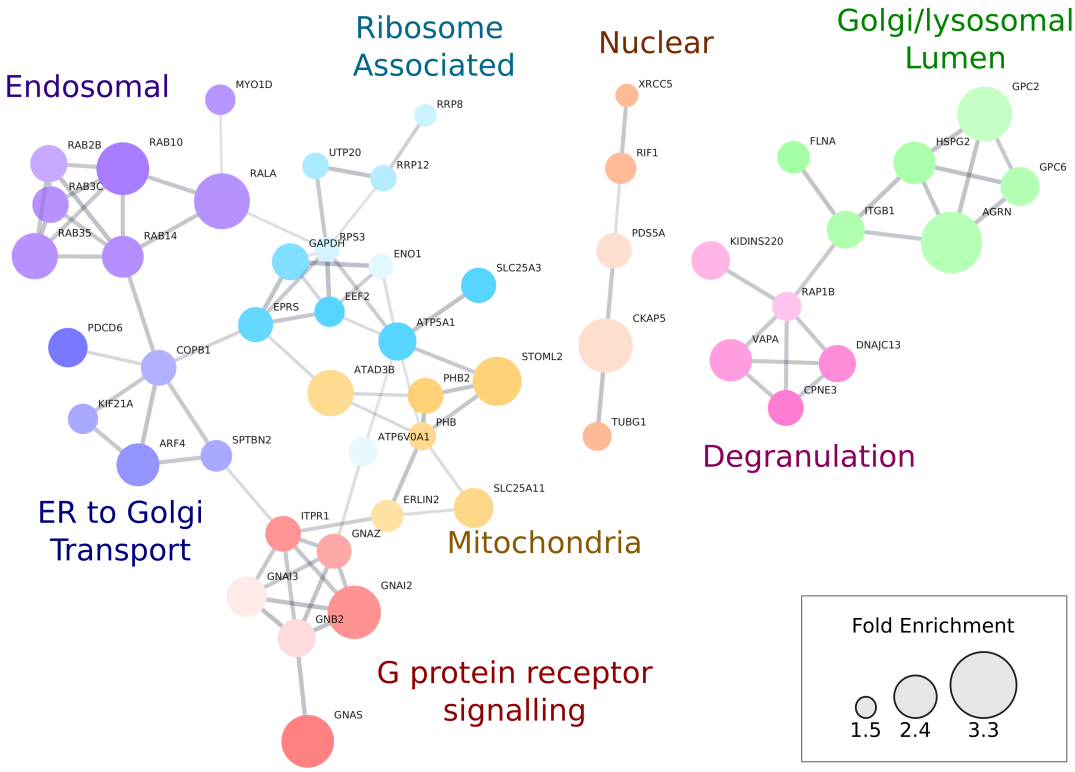


***Figure 5.20:*** *Protein-protein interaction network of the intracellular α-synuclein fibril interactome filtered for plasma membrane and endolysosomal proteins. Network of protein-protein interactors of α-synuclein, that were annotated with GO terms relating to the plasma membrane, the endosome or lysosome. Protein-protein interactions compiled by the StringDB database. The network was clustered using the MCL algorithm (inflation parameter 1.8) and the five largest clusters visualised. Nodes were coloured based on the cluster in which they appear. Node size denotes the ratio of the protein abundance vs pull-down of cells not exposed to α-synuclein fibrils (Fig. 5.3 X axis). Node transparency denotes the p-value of the abundance change (Fig. 5.3 Y axis). Terms beside each cluster refer to GO terms with a high annotation frequency within the cluster.*

### 5.3.10 Internalised $\alpha$-Synuclein Preferentially Interacts With Low-Complexity Proteins

Finally, given the propensity of $\alpha$-synuclein fibrils to interact preferentially with low complexity, soluble proteins in the cell lysate Section 4.3.14, it was of interest to discover whether this remained true for proteins internalised by SH-SY5Y cells. This is especially pertinent as amyloid propensity for binding low complexity proteins has been demonstrated with intracellular aggregates of the amyloid protein huntingtin [320]. Further, as with the lysate interactome of $\alpha$-synuclein fibrils, a large number of RNA binding proteins were identified as interacting with internalised $\alpha$-synuclein fibrils; RNA binding proteins typically contain longer LCRs (i.e. compositionally biased regions, on average 18 residues in length, containing one to four amino-acids), than are present in the cell proteome. Therefore, it was hypothesised that the interactomes identified herein may be enriched in proteins containing long LCRs. LCR identification was made via the fLPS software using [329].

Using this method it was shown that there was a statistically significant increase in the average length of the longest LCR in the interactome of internalised $\alpha$-synuclein fibrils over that of all proteins in the SH-SY5Y cell proteome (Fig. 5.21 A). Furthermore, this enrichment remained even when proteins interacting with lysate exposed $\alpha$-synuclein fibrils were excluded (Fig. 5.21 B, Cell Only), previously termed the cell not lysate, interactome. There were no significant differences between the cell not lysate interactome and either the cell and lysate interactome (Fig. 5.21 B Both) or the lysate not cell interactome (Fig. 5.21 B Lysate Only).

Additionally, in the previous chapter it was shown that lysate exposed $\alpha$-synuclein fibrils preferentially bound soluble proteins (Section 4.3.14). Notably this finding does not support the proposed hypothesis that $\alpha$-synuclein fibrils, due to their amyloid nature, may preferentially interact with other, amyloid prone, low solubility proteins. It was therefore of interest to ascertain whether this finding remained true for internalised $\alpha$-synuclein fibrils. To assess this possibility, the Camsol protein solubility predictor [328] was used to categorise proteins as soluble or insoluble. It was shown that, as was the case for lysate exposed $\alpha$-synuclein fibrils, the interactome of internalised $\alpha$-synuclein fibrils was enriched in soluble proteins when compared to the solubility of proteins in the SH-SY5Y cell proteome (Fig. 5.22 A). It is worth noting however that this enrichment, though statistically significant, only represents a small increase in average solubility. However, when the analysis was conducted on the cell and lysate interactome of $\alpha$-synuclein fibrils (i.e. that representing interactors of internalised $\alpha$-synuclein fibrils after excluding interactors of lysate exposed $\alpha$-synuclein fibrils), no significance could be found.

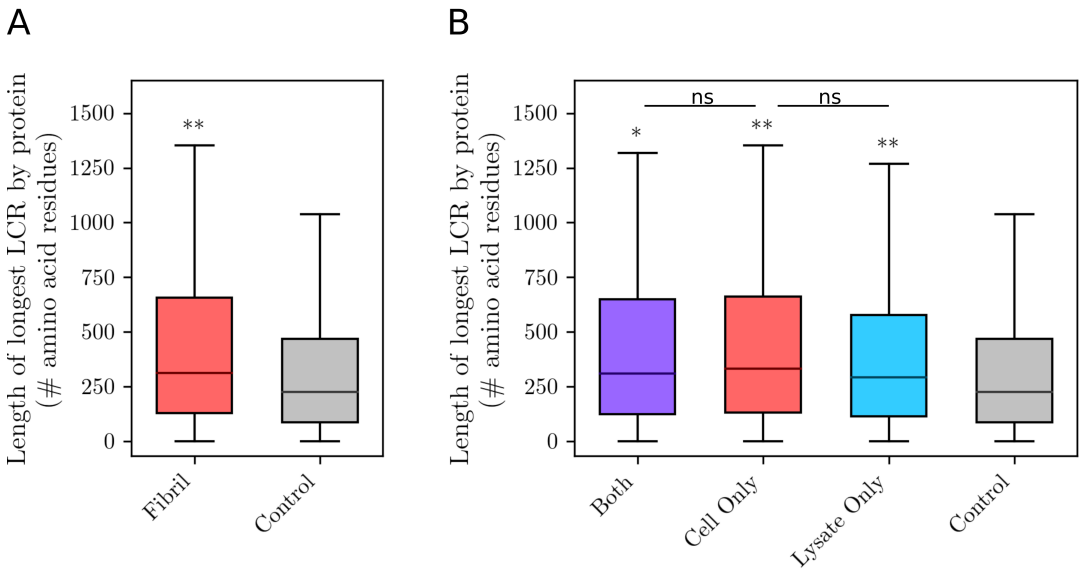


***Figure 5.21:*** *Complexity of proteins interacting with internalised and lysate exposed α-synuclein fibrils. Box and whisker diagrams depicting the length of the longest LCR by protein (a measure of protein complexity).A) Complexity of proteins interacting with internalised fibrils (Fibril) and the complexity of proteins in the SH-SY5Y cell proteome (Control). B) Complexity of proteins that interact with: both internalised α-synuclein fibrils and lysate exposed α-synuclein fibrils (Both), internalised α-synuclein fibrils when lysate exposed α-synuclein fibril interactors are excluded (Cell Only), and lysate exposed α-synuclein fibril interactors when internalised α-synuclein fibril interactors are excluded (Lysate Only). The symbol above each boxplot denotes p-value of comparing medians of the interactome with that of the SH-SY5Y cell proteome (Control). Lines between boxplots indicate p-value of comparing the medians of the indicated interactomes. ** < 0.01, * < 0.05, ns = not significant*

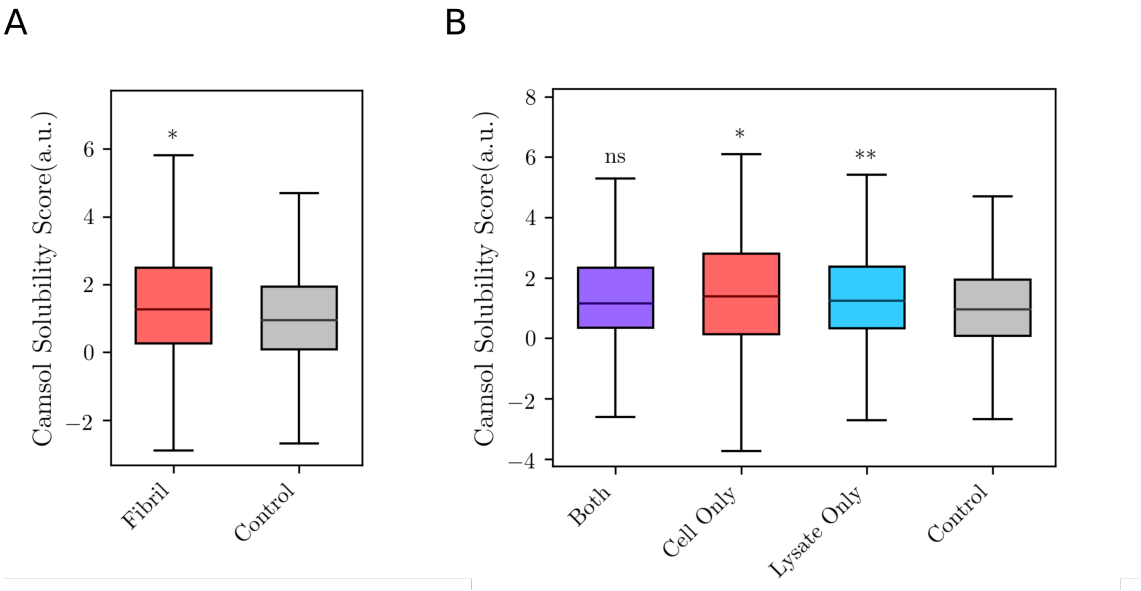


***Figure 5.22:*** *Solubility proteins interacting with internalised α-synuclein. Box and whisker diagrams depicting the solubility, as measured by Camsol [328], of all proteins within a dataset. A) Solubility of proteins interacting with internalised fibrils (Fibril) and the solubility of proteins in the SH-SY5Y cell proteome (Control). B) Solubility of proteins that interact with: both internalised α-synuclein fibrils and lysate exposed α-synuclein fibrils (Both), internalised α-synuclein fibrils when lysate exposed α-synuclein fibril interactors are excluded (Cell Only), and lysate exposed α-synuclein fibril interactors when internalised α-synuclein fibril interactors are excluded (Lysate Only). The symbol above each boxplot denotes p-value of comparing medians of a given interactome with that of the SH-SY5Y cell proteome (Control). Lines between boxplots indicate p-value of comparing the medians of the indicated interactomes. ** < 0.01, * < 0.05, ns = not significant*

## 5.4 Discussion

Herein, the interactome of $\alpha$-synuclein fibrils, following internalisation by SH-SY5Y cells was characterised through the use of quantitative proteomics. Through comparison of the interactome of internalised $\alpha$-synuclein fibrils with that of lysate exposed $\alpha$-synuclein fibrils it was further possible to identify proteins that are likely to interact in cells after internalisation. Moreover, it was possible, through comparison of the interactome of internalised $\alpha$-synuclein fibrils with that of lysate exposed $\alpha$-synuclein monomer, to identify a number of intracellularly interacting proteins whose interaction with $\alpha$-synuclein may depend on the fibrillar conformation of the amyloid protein. It was found that a number of key cellular locations were associated with internalised $\alpha$-synuclein fibrils, suggesting potential pathogenic pathways following internalisation.

### 5.4.1 Rab Proteins Interact With $\alpha$-Synuclein During Internalisation

$\alpha$-synuclein fibrils have been shown to be internalised by cells through endocytic pathways [260, 358, 359, 435]. Following internalisation $\alpha$-synuclein is thought to transit through the endolysosomal pathway before escaping into the cytoplasm [360, 440, 441]. Indeed, herein it was demonstrated that internalised $\alpha$-synuclein fibrils localised with both LAMP1, and endolysosomal marker, and Lysotracker™-positive acidic vesicles, indicative, of lysosomal compartments. Therefore, it was of interest to identify proteins that interact with $\alpha$-synuclein during internalisation, as such proteins may provide insight into the mechanisms by which $\alpha$-synuclein fibrils are internalised, and by which they escape the endolysosomal compartments.

Herein, a number of Rab family proteins were identified as interacting with internalised $\alpha$-synuclein fibrils. Moreover, these proteins were highly abundant in the interactome suggesting strong interactions. Rab family GTPases are key regulators of intracellular membrane trafficking, located on the cytosolic face of the membranes. Rab proteins are involved in the formation of transport vesicles and their fusion with membranes [446–448]. These proteins cycle between an inactive guanosine diphosphate (GDP)-bound form and an active GTP-bound form, capable of recruiting downstream effectors, directly responsible for vesicle formation, movement, tethering and fusion [446–448]. Rab proteins are closely involved in the process of endocytosis, acting as a rate-limiting regulator of recycling internalised vesicles back to the plasma membrane [449] as well as regulating the biogenesis of lysosomal compartments [450].

There are at least 60 genes encoding Rab proteins in the human genome, with

each protein responsible for one or more functions within the endolysosomal and excretory pathways. Rab5, for example, is primarily associated with endocytosis and the formation of the early endosome [451, 452]. Rab35 promotes endosomal recycling [453] while Rab7 has been shown to drive early to late endosomal transition and fusion of late endocytic structures and lysosomes [450]. Rabs 1, 2 on the other hand are thought to participate in ER to Golgi, intra-Golgi and protein export traffic [454, 455], though both have additionally been implicated in retrograde traffic and the formation of autophagosomes [455, 456]. Rab3 however, is primarily associated with synaptic vesicles where it primes the neurotransmitter filled vesicles for release [457].

Defects in membrane trafficking are found in a number of neurodegenerative diseases and as important regulators of membrane trafficking, Rab proteins may play a role in the development of these conditions [458]. Indeed, herein, a number of Rab proteins were found to interact with $\alpha$-synuclein following incubation of $\alpha$-synuclein fibrils with SH-SY5Y cells. These interactors included Rab1, Rab3 and Rab35. Furthermore, both Rab1 and Rab35 have previously been implicated in the development of Parkinson's disease and other synucleinopathies [459]. Rab35 has been proposed as an effective biomarker of Parkinson's disease development and progression, showing increased levels in the serum of Parkinson's disease patients and the substantia nigra but not the striatum of mouse models of the disease [460]. Rab1, on the other hand has been directly implicated in $\alpha$-synuclein related cellular toxicity [238]. It was shown that $\alpha$-synuclein overexpression is liable to cause accumulation within the ER, eventually to the collapse of ER to Golgi traffic and eventual neuronal loss. This disruption of ER to Golgi traffic and subsequent neuronal death can be recovered by overexpression of Rab1 [238].

Interestingly, Rab proteins Rab5 and Rab7 were found to interact with lysate exposed $\alpha$-synuclein fibrils but were not found in the interactome of internalised $\alpha$-synuclein fibrils. This finding may suggest that though $\alpha$-synuclein fibrils co-localise with Rab5 and Rab7 positive vesicles [461] they do not come into direct contact with these GTPases due to the localisation of the Rab proteins to the cytosolic face of the membrane. Futhermore, this finding may indicate that internalised $\alpha$-synuclein fibrils interact with Rab1, Rab2, Rab3 and Rab35 following escape into the cytosol, where it may have direct access to these proteins. Alternatively, there is evidence that endogenous $\alpha$-synuclein binds membrane associated Rab3 — this interaction being important for the physiological localisation of $\alpha$-synuclein to the membrane [462]. This raises the possibility that the $\alpha$-synuclein fibril interaction with Rab proteins, seen following internalisation by SH-SY5Y cells, is the result of sequestration of endogenous $\alpha$-synuclein that is in complex with Rab proteins. In either case sequestration of Rab proteins by internalised $\alpha$-synuclein fibrils may result in further cellular stress via the perturbation of ER to Golgi traffic [238].

### 5.4.2 Internalisation of $\alpha$-Synuclein Fibrils by SH-SY5Y Cells May be Mediated by Heparan Sulfate Glycoproteins

A number of proteins have been proposed as responsible for $\alpha$-synuclein fibril internalisation by neuronal and neuronal-like cells. These include LAG3 [260], $PrP^c$ [358], and heparan sulfate proteoglycans [437, 438]. To investigate the pathway by which $\alpha$-synuclein fibrils are internalised by SH-SY5Y cells, internalised $\alpha$-synuclein fibril interacting proteins, with links to the plasma membrane or endolysosomal compartments, were identified.

Among the limited number of endolysosomal proteins that were found within the interactome of internalised $\alpha$-synuclein fibrils, a number of heparan sulfate proteoglycans formed a distinct cluster. Combined with the lack of LAG3 or $PrP^c$ in the interactome, this points to the possibility that heparan sulphate proteoglycans may be responsible for $\alpha$-synuclein fibril internalisation in SH-SY5Y cells, as has been shown in other cell types, especially in the case of non-neuronal cells [437, 438]. Given the limited expression of other known endocytic receptors of $\alpha$-synuclein on the surface of SH-SY5Y cells, such as LAG3[260], this potentially represents the means of entry for $\alpha$-synuclein fibrils in this instance. Further investigation may include the use of heparin to competitively inhibit binding of $\alpha$-synuclein to the heparan sulfate proteoglycan, thereby confirming this as the means of entry.

### 5.4.3 Internalised $\alpha$-Synuclein Fibrils May Disrupt the Nuclear Pore Complex

A notable finding made herein was the identification of a number of proteins belonging to the nuclear pore complex (responsible for the transport of proteins and RNA to and from the nucleus), within the interactome of internalised $\alpha$-synuclein fibrils. Interestingly, these proteins were specific to the interactome of internalised $\alpha$-synuclein fibrils, being absent from that of lysate exposed $\alpha$-synuclein fibrils. Moreover, the GO terms, nuclear pore outer ring and nuclear pore, were overrepresented in the interactome of internalised $\alpha$-synuclein fibrils, suggesting selectivity of internalised $\alpha$-synuclein fibrils for proteins involved in this complex.

Nucleo-cytoplasmic transport is a highly conserved cellular mechanism that ensures the transport of nucleic acids and proteins across the nuclear membrane [463]. Proper functioning of this mechanism is especially important in non-dividing, post-mitotic cells such as neurons, where proteins involved in DNA maintenance and repair make use it to reach the nucleus [464, 465]. The cell relies on a conserved and dynamic structure, the nuclear pore complex, to facilitate nucleo-cytoplasmic

transport [463]. These complexes span the nuclear membrane and are constituted by proteins referred to as nuclearporins [466]. Though some small proteins can freely diffuse through this channel [463] the transit of most proteins through the pore is a highly coordinated and selective process mediated by importins and exportins such as karyopherin and THOC family proteins [467, 468].

Neurons appear particularly susceptible to disruption to the function of the nuclear pore complex as evidenced by the exclusively neurodegenerative consequences functional impairment of this complex [466]. This is thought to be due neurons relying on protein transport via these complexes to repair DNA damage that otherwise accumulates in these non-dividing cells [466]. A number of amyloidogenic proteins have previously been shown to disrupt the function of the nuclear pore complex including TDP-43 [469], huntingtin [470, 471] and even artificial amyloid proteins [315]. Indeed, there is evidence to suggest that amyloid aggregates are capable of causing mislocalisation of nuclearporins [469, 470] or exportin proteins [315].

It has been demonstrated, for example, that the interactome of intracellular TDP-43 aggregates, a pathogenic hallmark of amyotrophic lateral sclerosis (ALS) and frontotemporal dementia disease spectrum (FTD), is enriched in components of the nuclear pore complex and nucleo-cytoplasmic transport machinery [469]. This disruption lead to impairment of nuclear protein import and RNA export in neuronal cells [469]. Moreover, aggregation of artificial β-sheet proteins likewise interfered with nucleo-cytoplasmic transport and resulted in the sequestration of transport proteins including members of the THOC mRNA exportin family [315]. It was hypothesised that by sequestering THOC proteins, mRNA export from the nucleus was compromised thereby limiting protein synthesis and impairing cellular function [315].

The role of the nucleo-cytoplasmic machinery in the development of synucleinopathies such as Parkinson's disease is not yet clear. A number of studies have identified a link between transcription factor mislocalisation to the cytoplasm and the development of Parkinson's disease [472, 473], potentially implicating deregulation of the nucleo-cytoplasmic machinery in the development of the disease. Moreover, $\alpha$-synuclein has previously been shown to be capable of translocation to the nucleus [474]. $\alpha$-synuclein translocation into the nucleus is thought to occur via the nuclear-pore machinery in complex with a protein of the karyopherin family of importins [475]. Taken together, these data suggest that some amyloids can cause neuronal disruption through blockage or sequestration of the nucleo-cytoplasmic machinery. Moreover, $\alpha$-synuclein has been shown interact with a number of components of the nucleo-cytoplasmic machinery, raising the possibility that it too is capable of interfering with the proper functioning of this complex [475].

The data presented herein may support the possibility that $\alpha$-synuclein aggregates

disrupt the function of nucleo-cytoplasmic transport; a cluster of nucleoporins, as well as the exportin THOC7 and the importin karyopherin subunit α-5 were identified among interactors of internalised α-synuclein fibrils. This finding raises the possibility of sequestration of these proteins by internalised α-synuclein fibrils. Interestingly, nuclearporins were also identified in the interactome of monomeric α-synuclein when exposed to cell lysate, but not α-synuclein fibrils exposed to cell lysate. This finding may indicate that nuclearporins have lower affinity for α-synuclein fibrils than for α-synuclein monomer and will only bind in the absence of other competition, indicating that α-synuclein fibrils come into close proximity to the proteins following internalisation. Alternatively, it may be the result of endogenous monomeric α-synuclein bridging the interaction. This may indicate sequestration of nuclearporins during elongation of internalised α-synuclein fibrils by endogenous α-synuclein monomer. Further study is required to elucidate the potential for internalised α-synuclein fibrils to disrupt nucleo-cytoplasmic transport, but given the presence of nucleo-cytoplasmic deficiencies in other amyloid-related neurodegenerative diseases [315, 469], the finding is of significant interest.

### 5.4.4 Mitochondrial Interactions of Internalised α-Synuclein Fibrils

As was shown in the case of lysate exposed α-synuclein fibrils, a number of mitochondrial proteins were shown to interact with α-synuclein fibrils following internalisation by SH-SY5Y cells. Furthermore many of the mitochondrial proteins identified as interactors of internalised α-synuclein fibrils, were highly abundant within the interactome (enriched 2.5 fold over the background binding to the streptavidin magnetic beads). These enriched proteins included the mitochondrial import protein TOMM40 in addition to a number of ATP synthase proteins.

There is a weight of evidence to suggest that α-synuclein pathology may result from disruption to mitochondrial function [423–427]. Moreover, the aggregation of α-synuclein is thought to interfere with mitochondrial function through accumulation within the mitochondria [428, 429], and through sequestration of mitochondrion within intracellular inclusion bodies [371]. Indeed, impairment of the mitochondrial import protein TOMM40 resulting from α-synuclein aggregation is thought to play a role in neuronal dysfunction, with overexpression of TOMM40 recovering mitochondrial deficits seen in Parkinson's disease mouse models [432]. Herein it has been shown that α-synuclein fibrils interact with TOMM40 both in cell lysate and following cellular internalisation, marking interaction with this protein as a potential pathway for α-synuclein aggregation induced, cellular dysfunction. Likewise, this finding is in agreement with that of Yano et al. [434], wherein it was shown that the

amyloid poly-Q expanded huntingtin inhibits mitochondrial import within cells.

Another mitochondrial protein found to interact with $\alpha$-synuclein fibrils both in the context of a cell lysate and following internalisation of the fibril by SH-SY5Y cell is the ion channel protein voltage-dependent anion-selective channel (VDAC1)3. It has recently been shown that monomeric $\alpha$-synuclein can effectively regulate VDAC1 function, the binding of $\alpha$-synuclein to the VDAC1 channel leading to an increase in $Ca^{2+}$ flux [476]. Herein, there was also evidence of VDAC13 binding to monomeric $\alpha$-synuclein. $\alpha$-synuclein binding to VDAC1 induces shift to a conformationally closed state of the channel [476], making it virtually impermeable to ATP [477]. Indeed, in support of the hypothesis that $\alpha$-synuclein toxicity may be mediated via VDAC1, a yeast model of Parkinson's disease depends upon VDAC1 for the development of a pathological phenotype [478]. The data presented here suggests that interaction with VDAC1 proteins may not be exclusive to monomeric $\alpha$-synuclein. Furthermore, aberrant interaction by pathogenic forms of $\alpha$-synuclein may significantly impair VDAC1 function leading to mitochondrial stress, and ultimately cellular dysfunction.

However, it is of note that no mitochondrial related GO terms were over represented in the interactome of internalised $\alpha$-synuclein fibrils. This finding remained true even when proteins that had been identified as interactors of monomeric $\alpha$-synuclein in cell lysate were excluded from the interactome. This finding was in contrast to the interactome of lysate exposed $\alpha$-synuclein fibrils that was highly enriched in mitochondrial GO terms when the interactome of monomeric $\alpha$-synuclein was excluded. These findings suggest that a number of individual mitochondrial proteins may have a high affinity for $\alpha$-synuclein fibrils. However, unlike when $\alpha$-synuclein fibrils are exposed to cell lysate, only a small fraction of mitochondrial proteins interact with internalised $\alpha$-synuclein fibrils.

One explanation for this finding is the possibility that these proteins, with a high affinity for $\alpha$-synuclein fibrils, interact with $\alpha$-synuclein fibrils in the post-lysis environment and therefore do not represent true interactors of internalised $\alpha$-synuclein fibrils. This hypothesis is supported by evidence of a number of ATP synthases in the interactome of internalised $\alpha$-synuclein fibrils. These proteins, part of the mitochondrial respiratory chain, are not thought to be accessible to fibrillar $\alpha$-synuclein due to the inability of fibrils to cross the mitochondrial outer membrane [428, 431]. These interactions may therefore represent interactions occurring with $\alpha$-synuclein fibrils following cell lysis when the barrier of the mitochondrial membrane is removed. Indeed this represents one of the primary caveats of this study, that is the possibility of post-lysis interactions, and is discussed in more detail later.

### 5.4.5 Conclusions

Herein a number of SH-SY5Y cell proteins were found to interact with $\alpha$-synuclein fibrils following 24hr incubation of $\alpha$-synuclein fibrils with SH-SY5Y cells. This included a large number of RNA binding proteins, as well as several mitochondrial channel proteins such as TOMM40 and and VDAC12. Moreover, by comparing this interactome to that of lysate exposed $\alpha$-synuclein fibrils a number of protein interactors were identified that only interact within the context of the lice cell. These internalisation specific interactors of $\alpha$-synuclein included proteins of the nuclear pore complex and a number of Rab proteins including Rab1. These results point to a number of potential cellular effects of internalised $\alpha$-synuclein fibrils, including mitochondrial disruption, nuclear disruption (via sequestration of nuclear transport proteins) and ER stress resulting from impaired ER-to-Golgi transport. In conclusion, these findings provides important and unbiased identification of a number of potential pathways by which $\alpha$-synuclein fibrils may drive the neurodegeneration seen in a number of synucleinopathies such as Parkinson's disease. Future study may investigate the physiological and pathological relevance of these findings.

# 6

# Conclusions and Future Directions

Herein a system was developed to enable exogenous biotinylated $\alpha$-synuclein fibrils to be isolated following incubation with SH-SY5Y cell lysate or following incubation with SH-SY5Y cells. Following isolation, the use of TMT quantitative proteomics enabled the identification of proteins that preferentially bound the $\alpha$-synuclein fibrils over binding the streptavidin magnetic beads. By this method it was possible to characterise the interactomes of both monomeric and fibrillar $\alpha$-synuclein exposed to SH-SY5Y cell lysate as well as that of $\alpha$-synuclein fibrils following internalisation by SH-SY5Y cells.

Bioinformatic analysis of these interactomes enabled the unbiased identification of a number of pathways that may be affected by $\alpha$-synuclein fibrils. From these pathways a several key proteins and protein complexes were identified that warrant further investigation. Firstly, both lysate exposed and cell exposed $\alpha$-synuclein fibril interactomes were found to be enriched in RNA binding proteins. This finding may be linked to a propensity for $\alpha$-synuclein fibrils to bind proteins with long LCR regions, as many RNA binding proteins have been shown to possess long LCR regions [314].

A second major finding was that of internalised $\alpha$-synuclein fibrils interacting with components of the nucleo-cytoplasmic transport machinery. A number of nuclearporins, components of the nuclear pore complex, as well as several importin and exportin proteins, involved in enabling RNA and protein traffic via the the nuclear

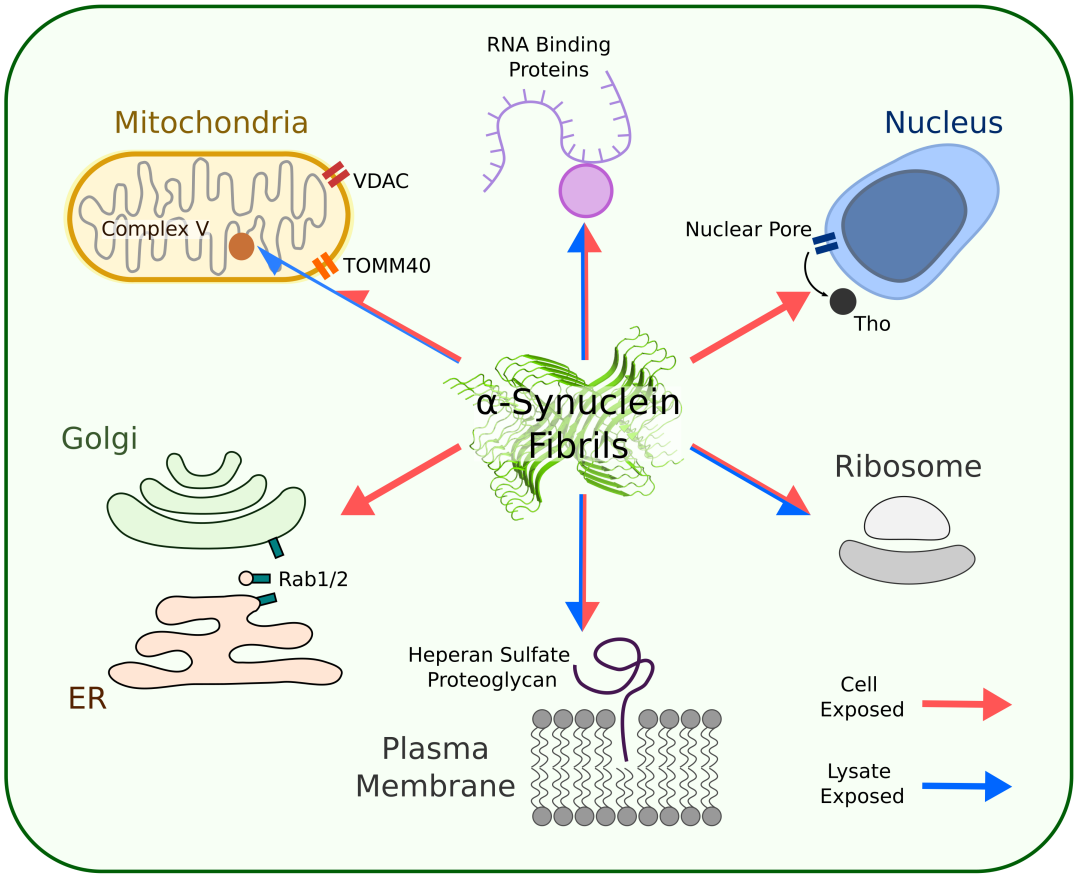


***Figure 6.1:*** *Summary of proteins found to interact with α-synuclein fibrils following exposure to lysate (Blue Arrows) or exposure to and internalisation by live cells cells (Red Arrows).*

pore, were found amongst the interactome of internalised $\alpha$-synuclein fibrils, but not lysate exposed $\alpha$-synuclein fibrils. Interestingly, these proteins were also found among the interactome of lysate exposed $\alpha$-synuclein monomer, raising the possibility that the interaction seen by internalised $\alpha$-synuclein fibrils is the result of sequestration of endogenous $\alpha$-synuclein, in complex with the nucleo-cytoplasmic transport protein. The resultant sequestration of nucleo-cytoplasmic transport proteins may lead to cellular damage by reducing the transport capacity of vital DNA repair proteins into the nucleus [466], or by reducing the translational capacity of the cell by sequestering key RNA transport proteins such as THOC [315].

Limiting the translational capacity of the cell may be further exacerbated by internalised $\alpha$-synuclein fibrils sequestering ribosomes and ribosomal subunit proteins. Indeed, this is in line with other studies of amyloid proteins, that have found ribosomal structures within intracellular inclusion bodies [407, 416]. Moreover, translational deficiencies have been linked to the development of synucleinopathies including Parkinson's disease [144, 408], marking this as a key pathway for further

investigation.

Interestingly, $\alpha$-synuclein fibrils were also found to interact with a number of Rab family proteins, involved in membrane trafficking, following internalisation by cells. Of particular interest are the Rab proteins Rab1 and Rab2 involved in ER to Golgi transport [479]. Defects in ER to Golgi trafficking have been found in a number of neurodegenerative diseases [458] and the observed interaction of internalised $\alpha$-synuclein fibrils with these proteins may point to this as a mechanism by which $\alpha$-synuclein fibrils effect cellular disruption.

Finally a number of mitochondrial proteins were identified in the interactomes of both internalised $\alpha$-synuclein fibrils and lysate exposed $\alpha$-synuclein fibrils. These include the outer membrane pores TOMM40 and VDAC1, and may further implicate mitochondrial dysfunction in the progression of cellular disruption resulting from $\alpha$-synuclein aggregation. Moreover, the lysate exposed interactome was shown to contain proteins of the mitochondrial complex V, a key component of the respiratory chain and previously implicated in Parkinson's disease. Further work, is required to identify whether the interaction of $\alpha$-synuclein fibrils with complex V proteins is of pathophysiological relevance. Together these findings point to a number of potential mechanisms by which $\alpha$-synuclein fibrils may cause cellular disruption and provide evidence for the effectiveness of the system developed herein.

It was noteworthy that this investigation into the cellular protein interactome of $\alpha$-synuclein fibrils failed to detect a number of proteins commonly associated with Parkinson's disease, including LRKK2 PINK1, as well as components of the proteostasis network such as Hsp70. The reason for this finding requires further investigation, however one possibility is that this study represents an early timepoint in the progression of the $\alpha$-synuclein pathology in a model system. Proteostastatic proteins such as Hsp70 are primarily focussed on preventing $\alpha$-synuclein monomer misfolding and may therefore only appear as an interactor of internalised fibrillar $\alpha$-synuclein when endogenous $\alpha$-synuclein monomer begins to aggregate. Data shown herein suggest the presence of intracellular inclusions of endogenous $\alpha$-synuclein appearing at around 5 days, following incubation with $\alpha$-synuclein fibrils.

The use of quantitative proteomics has enabled the characterisation of internalised and lysate exposed $\alpha$-synuclein fibril interactomes as well as the interactome of lysate exposed $\alpha$-synuclein monomer. Moreover, it has been demonstrated that it is possible to compare the protein abundances in two or more interactomes (in this instance monomeric and fibrillar $\alpha$-synuclein when exposed to cell lysate) to acquire an accurate picture of the conformational preferences of $\alpha$-synuclein binding proteins. An expansion to this work of potential interest would be the use of familial mutant $\alpha$-synuclein fibrils, such as E46K or A30P, to identify potential differences between the interactomes of these fibrils and that of WT $\alpha$-synuclein. These mutations

are linked with early onset of Parkinson's disease in patients and with a variety of cellular effects *in vitro*. By utilising the system developed herein, it may be possible to identify those pathways that are differentially affected by fibrils formed of these $\alpha$-synuclein mutants when compared to WT $\alpha$-synuclein fibrils. This could potentially uncover pathways responsible for the rapid progression and early onset of disease that occurs in patients possessing these mutations.

Furthermore, recent advances in cryo-EM techniques has lead to a number of polymorphic fibril structures being determined for $\alpha$-synuclein [232, 234]. At least one study has uncovered differences in the toxicity of $\alpha$-synuclein fibrils, dependant on the specific morphology of the fibril in question [247]. Therefore, future work using the protocols for fibril synthesis, set out by these structural studies, could identify differences in the proteins bound by the different morphologies, potentially elucidating the mechanism by which they cause divergent cellular effects.

As mentioned previously, proteins identified as interactors as interactors of internalised $\alpha$-synuclein fibrils are not guaranteed to originate from interactions occurring in a physiological context. Due to the need to lyse the cells prior to isolation of the $\alpha$-synuclein fibrils, there is the possibility that many of the interactions identified in the interactome of internalised $\alpha$-synuclein fibrils, occur post-lysis. Excluding cell lysate interactors of $\alpha$-synuclein fibrils from the interactome of fibrils isolated from cells may, at least in part, help to exclude interactions that occur post-lysis. However, the possibility remains that proteins pulled down with the fibrils may have bound after cell lysis.

One solution to this problem that is attractive for a number of reasons is the use of a photoactivatable crosslinker to covalently bond interactors of $\alpha$-synuclein occurring in a cellular environment. A photoactivatable crosslinker is a chemical reagent that, upon application of a ultra violet (UV) light, becomes highly reactive. This reactivity results in the formation of a covalent bond between the crosslinking reagent and proteins in close proximity to the reactive moiety. Many such chemical crosslinking reagents exist [480] including azide, benzophenone and diazirine crosslinkers. The use of photoactivatable crosslinkers to study intracellular protein protein interaction is an emerging field enabling the identification of weak interactions while excluding those occurring in a post-lysis environment [480]. Moreover, the use of this technique is unlikely to introduce artifacts of crosslinking due to the activatable nature of the crosslinking reagent.

In particular, a crosslinking reagent currently undergoing development in the University of Leeds Department of Chemistry by Dr. Martin Walko, combines a diazirine photoactivatable crosslinker onto which a small molecule such as biotin can be conjugated by click chemistry (personal communication and [481]). Moreover, the presence of a maleimide moiety enables this crosslinker to easily replace biotin

in the current experimental setup. Preliminary investigation of this crosslinking reagent has demonstrated that, when configured with biotin and conjugated by maleimide chemistry to the $\alpha$-synuclein fibril characterised herein, it is possible to isolate $\alpha$-synuclein fibrils by streptavidin magnetic bead isolation. However, time constraints prevented further work from being undertaken.

The use of this crosslinking reagent would enable the identification only of proteins that came into close proximity of the $\alpha$-synuclein fibrils within the intracellular environment. Moreover, low affinity and transient interactions that may be lost under wash conditions used herein for the pulldown of biotinylated $\alpha$-synuclein, would be maintained due to the covalent nature of the crosslinking interaction. Interactions that occur with $\alpha$-synuclein fibrils in a post lysis environment could then be removed under harsh wash conditions, such as those containing sodium dodecyl sulfate (SDS), that will remove all but the covalently bound interactors.

In summary this work demonstrates the application of proteomics and bioinformatics methods to understanding the role of $\alpha$-synuclein fibrils in the pathological processes that underpin the synucleopathies. The findings from this work will inform future research by highlighting new potential mechanisms by which $\alpha$-synuclein fibrils can disrupt cellular functions.

# REFERENCES


[1] JD Sipe and AS Cohen. “Review: history of the amyloid fibril.” In: *J Struct Biol* 130.2-3 (2000), pp. 88–98.

[2] N Friedreich and A Kekulé. “Zur Amyloidfrage”. In: *Archiv für pathologische Anatomie und Physiologie und für klinische Medicin* 16.1 (1859), pp. 50–65. DOI: 10.1007/BF01945246.

[3] P Divry. “Sur les proprietes optiques de 1’amyloide”. In: *cr soc. Bilge Biol.* 97 (1927), pp. 1808–1810.

[4] Holde Puchtler, Faye Sweat and M Levine. “On the binding of Congo red by amyloid”. In: *Journal of Histochemistry & Cytochemistry* 10.3 (1962), pp. 355–364.

[5] MG Iadanza et al. “A new era for understanding amyloid structures and disease.” In: *Nat Rev Mol Cell Biol* 19.12 (2018), pp. 755–773. DOI: 10.1038/s41580-018-0060-8.

[6] AS Cohen and E Calkins. “Electron microscopic observations on a fibrous component in amyloid of diverse origins.” In: *Nature* 183.4669 (1959), pp. 1202–3.

[7] AJ Geddes et al. “"Cross-beta" conformation in proteins.” In: *J Mol Biol* 32.2 (1968), pp. 343–58.

[8] William T Astbury and Ashton Street. “X-ray studies of the structure of hair, wool, and related fibres.-i. general”. In: *Philosophical Transactions of the Royal Society of London. Series A, Containing Papers of a Mathematical or Physical Character* 230.681-693 (1931), pp. 75–101.

[9] EP Benditt et al. “The major proteins of human and monkey amyloid substance: Common properties including unusual N-terminal amino acid sequences.” In: *FEBS Lett* 19.2 (1971), pp. 169–173.

[10] GG Glenner et al. “Creation of "amyloid" fibrils from Bence Jones proteins in vitro.” In: *Science* 174.4010 (1971), pp. 712–4.

[11] PP Costa, AS Figueira and FR Bravo. "Amyloid fibril protein related to prealbumin in familial amyloidotic polyneuropathy." In: *Proc Natl Acad Sci U S A* 75.9 (1978), pp. 4499–503.

[12] JH Choi et al. "Molecular modeling of the misfolded insulin subunit and amyloid fibril." In: *Biophys J* 97.12 (2009), pp. 3187–95. DOI: 10.1016/j.bpj.2009.09.042.

[13] MR Sawaya et al. "Atomic structures of amyloid cross-beta spines reveal varied steric zippers." In: *Nature* 447.7143 (2007), pp. 453–7.

[14] P Krotee et al. "Atomic structures of fibrillar segments of hIAPP suggest tightly mated β-sheets are important for cytotoxicity." In: *Elife* 6 (2017).

[15] JA Rodriguez et al. "Structure of the toxic core of α-synuclein from invisible crystals." In: *Nature* 525.7570 (2015), pp. 486–90. DOI: 10.1038/nature15368.

[16] MA Wälti et al. "Atomic-resolution structure of a disease-relevant A β(1-42) amyloid fibril." In: *Proc Natl Acad Sci U S A* 113.34 (2016), E4976–84. DOI: 10.1073/pnas.1600749113.

[17] C Wasmer et al. "Amyloid fibrils of the HET-s(218-289) prion form a beta solenoid with a triangular hydrophobic core." In: *Science* 319.5869 (2008), pp. 1523–6. DOI: 10.1126/science.1151839.

[18] MD Tuttle et al. "Solid-state NMR structure of a pathogenic fibril of full-length human α-synuclein." In: *Nat Struct Mol Biol* 23.5 (2016), pp. 409–15. DOI: 10.1038/nsmb.3194.

[19] MT Colvin et al. "Atomic Resolution Structure of Monomorphic A β42 Amyloid Fibrils." In: *J Am Chem Soc* 138.30 (2016), pp. 9663–74. DOI: 10.1021/jacs.6b05129.

[20] L Gremer et al. "Fibril structure of amyloid- β(1-42) by cryo-electron microscopy." In: *Science* 358.6359 (2017), pp. 116–119. DOI: 10.1126/science.aao2825.

[21] AWP Fitzpatrick et al. "Cryo-EM structures of tau filaments from Alzheimer's disease." In: *Nature* 547.7662 (2017), pp. 185–190. DOI: 10.1038/nature23002.

[22] TP Knowles, M Vendruscolo and CM Dobson. "The amyloid state and its association with protein misfolding diseases." In: *Nat Rev Mol Cell Biol* 15.6 (2014), pp. 384–96. DOI: 10.1038/nrm3810.

[23] CM Dobson. "Protein folding and misfolding." In: *Nature* 426.6968 (2003), pp. 884–90.

[24] CB ANFINSEN et al. "The kinetics of formation of native ribonuclease during oxidation of the reduced polypeptide chain." In: *Proc Natl Acad Sci U S A* 47 (1961), pp. 1309–14.

[25] CM Dobson. "Principles of protein folding, misfolding and aggregation." In: *Semin Cell Dev Biol* 15.1 (2004), pp. 3–16.

[26] M Karplus. "The Levinthal paradox: yesterday and today." In: *Fold Des* 2.4 (1997), S69–75.

[27] FU Hartl and M Hayer-Hartl. "Converging concepts of protein folding in vitro and in vivo." In: *Nat Struct Mol Biol* 16.6 (2009), pp. 574–81. DOI: 10.1038/nsmb.1591.

[28] MM Barnhart and MR Chapman. "Curli biogenesis and function." In: *Annu Rev Microbiol* 60 (2006), pp. 131–47.

[29] IV Baskakov et al. "Folding of prion protein to its native alpha-helical conformation is under kinetic control." In: *J Biol Chem* 276.23 (2001), pp. 19687–90.

[30] E Herczenik and MF Gebbink. "Molecular and cellular aspects of protein misfolding and disease." In: *FASEB J* 22.7 (2008), pp. 2115–33. DOI: 10.1096/fj.07-099671.

[31] M Sunde and C Blake. "The structure of amyloid fibrils by electron microscopy and X-ray diffraction." In: *Adv Protein Chem* 50 (1997), pp. 123–59.

[32] HA Wösten and ML de Vocht. "Hydrophobins, the fungal coat unravelled." In: *Biochim Biophys Acta* 1469.2 (2000), pp. 79–86.

[33] D Claessen et al. "A novel class of secreted hydrophobic proteins is involved in aerial hyphae formation in Streptomyces coelicolor by forming amyloid-like fibrils." In: *Genes Dev* 17.14 (2003), pp. 1714–26.

[34] DM Fowler et al. "Functional amyloid formation within mammalian tissue." In: *PLoS Biol* 4.1 (2006), e6.

[35] DM Fowler et al. "Functional amyloid–from bacteria to humans." In: *Trends Biochem Sci* 32.5 (2007), pp. 217–24.

[36] MR Chapman et al. "Role of Escherichia coli curli operons in directing amyloid fiber formation." In: *Science* 295.5556 (2002), pp. 851–5.

[37] TE Audas et al. "Adaptation to Stressors by Systemic Protein Amyloidogenesis." In: *Dev Cell* 39.2 (2016), pp. 155–168. DOI: 10.1016/j.devcel.2016.09.002.

[38] SK Maji et al. "Functional amyloids as natural storage of peptide hormones in pituitary secretory granules." In: *Science* 325.5938 (2009), pp. 328–32. DOI: 10.1126/science.1173155.

[39] S Whelly et al. "Nonpathological extracellular amyloid is present during normal epididymal sperm maturation." In: *PLoS One* 7.5 (2012), e36394. DOI: 10.1371/journal.pone.0036394.

[40] S Whelly et al. "Cystatin-related epididymal spermatogenic subgroup members are part of an amyloid matrix and associated with extracellular vesicles in the mouse epididymal lumen." In: *Mol Hum Reprod* 22.11 (2016), pp. 729–744.

[41] N Shanmugam et al. "Microbial functional amyloids serve diverse purposes for structure, adhesion and defence." In: *Biophys Rev* 11.3 (2019), pp. 287–302. DOI: 10.1007/s12551-019-00526-1.

[42] N Van Gerven et al. "The Role of Functional Amyloids in Bacterial Virulence." In: *J Mol Biol* 430.20 (2018), pp. 3657–3684. DOI: 10.1016/j.jmb.2018.07.010.

[43] HC Flemming et al. "Biofilms: an emergent form of bacterial life." In: *Nat Rev Microbiol* 14.9 (2016), pp. 563–75. DOI: 10.1038/nrmicro.2016.94.

[44] MS Dueholm et al. "Curli functional amyloid systems are phylogenetically widespread and display large diversity in operon and protein structure." In: *PLoS One* 7.12 (2012), e51274. DOI: 10.1371/journal.pone.0051274.

[45] ML Evans and MR Chapman. "Curli biogenesis: order out of disorder." In: *Biochim Biophys Acta* 1843.8 (2014), pp. 1551–8. DOI: 10.1016/j.bbamcr.2013.09.010.

[46] MS Dueholm et al. "Functional amyloid in Pseudomonas." In: *Mol Microbiol* 77.4 (2010), pp. 1009–20. DOI: 10.1111/j.1365-2958.2010.07269.x.

[47] D Romero et al. "Amyloid fibers provide structural integrity to Bacillus subtilis biofilms." In: *Proc Natl Acad Sci U S A* 107.5 (2010), pp. 2230–4. DOI: 10.1073/pnas.0910560107.

[48] H Vlamakis et al. "Control of cell fate by the formation of an architecturally complex bacterial community." In: *Genes Dev* 22.7 (2008), pp. 945–53. DOI: 10.1101/gad.1645008.

[49] A Taglialegna et al. "Staphylococcal Bap Proteins Build Amyloid Scaffold Biofilm Matrices in Response to Environmental Signals." In: *PLoS Pathog* 12.6 (2016), e1005711. DOI: 10.1371/journal.ppat.1005711.

[50] S Bieler et al. "Amyloid formation modulates the biological activity of a bacterial protein." In: *J Biol Chem* 280.29 (2005), pp. 26880–5.

[51] T Zimaro et al. "The type III protein secretion system contributes to Xanthomonas citri subsp. citri biofilm formation." In: *BMC Microbiol* 14 (2014), p. 96. DOI: 10.1186/1471-2180-14-96.

[52] J Oh et al. "Amyloidogenesis of type III-dependent harpins from plant pathogenic bacteria." In: *J Biol Chem* 282.18 (2007), pp. 13601–9.

[53] K Schwartz et al. "Functional amyloids composed of phenol soluble modulins stabilize Staphylococcus aureus biofilms." In: *PLoS Pathog* 8.6 (2012), e1002744. DOI: 10.1371/journal.ppat.1002744.

[54] E Tayeb-Fligelman et al. "The cytotoxic Staphylococcus aureus PSM$\alpha$3 reveals a cross-$\alpha$ amyloid-like fibril." In: *Science* 355.6327 (2017), pp. 831–833. DOI: 10.1126/science.aaf4901.

[55] M Shahnawaz and C Soto. "Microcin amyloid fibrils A are reservoir of toxic oligomeric species." In: *J Biol Chem* 287.15 (2012), pp. 11665–76. DOI: 10.1074/jbc.M111.282533.

[56] J Li et al. "The RIP1/RIP3 necrosome forms a functional amyloid signaling complex required for programmed necrosis." In: *Cell* 150.2 (2012), pp. 339–50. DOI: 10.1016/j.cell.2012.06.019.

[57] M Mompeán et al. "The Structure of the Necrosome RIPK1-RIPK3 Core, a Human Hetero-Amyloid Signaling Complex." In: *Cell* 173.5 (2018), 1244–1253.e10. DOI: 10.1016/j.cell.2018.03.032.

[58] T Vanden Berghe, B Hassannia and P Vandenabeele. "An outline of necrosome triggers." In: *Cell Mol Life Sci* 73.11-12 (2016), pp. 2137–52. DOI: 10.1007/s00018-016-2189-y.

[59] BL Kagan et al. "Antimicrobial defensin peptides form voltage-dependent ion-permeable channels in planar lipid bilayer membranes." In: *Proc Natl Acad Sci U S A* 87.1 (1990), pp. 210–4.

[60] Y Sokolov et al. "Membrane channel formation by antimicrobial protegrins." In: *Biochim Biophys Acta* 1420.1-2 (1999), pp. 23–9.

[61] NB Last and AD Miranker. "Common mechanism unites membrane poration by amyloid and antimicrobial peptides." In: *Proc Natl Acad Sci U S A* 110.16 (2013), pp. 6382–7. DOI: 10.1073/pnas.1219059110.

[62] J Thundimadathil, RW Roeske and L Guo. "A synthetic peptide forms voltage-gated porin-like ion channels in lipid bilayer membranes." In: *Biochem Biophys Res Commun* 330.2 (2005), pp. 585–90.

[63] J Thundimadathil et al. "Aggregation and porin-like channel activity of a beta sheet peptide." In: *Biochemistry* 44.30 (2005), pp. 10259–70.

[64] R Sood et al. “Binding of LL-37 to model biomembranes: insight into target vs host cell recognition.” In: *Biochim Biophys Acta* 1778.4 (2008), pp. 983–96. DOI: 10.1016/j.bbamem.2007.11.016.

[65] H Jang et al. “Antimicrobial protegrin-1 forms amyloid-like fibrils with rapid kinetics suggesting a functional link.” In: *Biophys J* 100.7 (2011), pp. 1775–83. DOI: 10.1016/j.bpj.2011.01.072.

[66] AK Elias et al. “SEVI, the semen enhancer of HIV infection along with fragments from its central region, form amyloid fibrils that are toxic to neuronal cells.” In: *Biochim Biophys Acta* 1844.9 (2014), pp. 1591–8. DOI: 10.1016/j.bbapap.2014.06.006.

[67] B Watt et al. “PMEL: a pigment cell-specific model for functional amyloid formation.” In: *Pigment Cell Melanoma Res* 26.3 (2013), pp. 300–15. DOI: 10.1111/pcmr.12067.

[68] C Bissig, L Rochin and G van Niel. “PMEL Amyloid Fibril Formation: The Bright Steps of Pigmentation.” In: *Int J Mol Sci* 17.9 (2016).

[69] SJ Soscia et al. “The Alzheimer’s disease-associated amyloid beta-protein is an antimicrobial peptide.” In: *PLoS One* 5.3 (2010), e9505. DOI: 10.1371/journal.pone.0009505.

[70] DK Kumar et al. “Amyloid- β peptide protects against microbial infection in mouse and worm models of Alzheimer’s disease.” In: *Sci Transl Med* 8.340 (2016), 340ra72. DOI: 10.1126/scitranslmed.aaf1059.

[71] P Spitzer et al. “Amyloidogenic amyloid- β-peptide variants induce microbial agglutination and exert antimicrobial activity.” In: *Sci Rep* 6 (2016), p. 32228. DOI: 10.1038/srep32228.

[72] MP Jackson and EW Hewitt. “Why are Functional Amyloids Non-Toxic in Humans?” In: *Biomolecules* 7.4 (2017).

[73] MS Hipp, SH Park and FU Hartl. “Proteostasis impairment in protein-misfolding and -aggregation diseases.” In: *Trends Cell Biol* 24.9 (2014), pp. 506–14. DOI: 10.1016/j.tcb.2014.05.003.

[74] M Bucciantini et al. “Inherent toxicity of aggregates implies a common mechanism for protein misfolding diseases.” In: *Nature* 416.6880 (2002), pp. 507–11.

[75] M Bucciantini et al. “Prefibrillar amyloid protein aggregates share common features of cytotoxicity.” In: *J Biol Chem* 279.30 (2004), pp. 31374–82.

[76] S Baglioni et al. “Prefibrillar amyloid aggregates could be generic toxins in higher organisms.” In: *J Neurosci* 26.31 (2006), pp. 8160–7.

[77] A Alzheimer's. "About a strange, serious disease process of the cerebral cortex". In: *Neurological Centralblatt* 25 (1906), p. 1134.

[78] JD Sipe et al. "Amyloid fibril proteins and amyloidosis: chemical identification and clinical classification International Society of Amyloidosis 2016 Nomenclature Guidelines." In: *Amyloid* 23.4 (2016), pp. 209–213.

[79] R Vassar et al. "Beta-secretase cleavage of Alzheimer's amyloid precursor protein by the transmembrane aspartic protease BACE." In: *Science* 286.5440 (1999), pp. 735–41.

[80] M Goedert et al. "Cloning and sequencing of the cDNA encoding a core protein of the paired helical filament of Alzheimer disease: identification as the microtubule-associated protein tau." In: *Proc Natl Acad Sci U S A* 85.11 (1988), pp. 4051–5.

[81] MC Chartier-Harlin et al. "Alpha-synuclein locus duplication as a cause of familial Parkinson's disease." In: *Lancet* 364.9440 (2004), pp. 1167–9.

[82] SC Warby et al. "CAG expansion in the Huntington disease gene is associated with a specific and targetable predisposing haplogroup." In: *Am J Hum Genet* 84.3 (2009), pp. 351–66. DOI: 10.1016/j.ajhg.2009.02.003.

[83] P Westermark, A Andersson and GT Westermark. "Islet amyloid polypeptide, islet amyloid, and diabetes mellitus." In: *Physiol Rev* 91.3 (2011), pp. 795–826. DOI: 10.1152/physrev.00042.2009.

[84] V Sanchorawala. "Light-chain (AL) amyloidosis: diagnosis and treatment." In: *Clin J Am Soc Nephrol* 1.6 (2006), pp. 1331–41.

[85] KM Koch. "Dialysis-related amyloidosis." In: *Kidney Int* 41.5 (1992), pp. 1416–29.

[86] K Uéda et al. "Molecular cloning of cDNA encoding an unrecognized component of amyloid in Alzheimer disease." In: *Proc Natl Acad Sci U S A* 90.23 (1993), pp. 11282–6.

[87] BI Giasson et al. "Initiation and synergistic fibrillization of tau and alpha-synuclein." In: *Science* 300.5619 (2003), pp. 636–40.

[88] Y Tomidokoro et al. "Familial Danish dementia: co-existence of Danish and Alzheimer amyloid subunits (ADan AND Abeta) in the absence of compact plaques." In: *J Biol Chem* 280.44 (2005), pp. 36883–94.

[89] R Hu et al. "Cross-Seeding Interaction between β-Amyloid and Human Islet Amyloid Polypeptide." In: *ACS Chem Neurosci* 6.10 (2015), pp. 1759–68. DOI: 10.1021/acschemneuro.5b00192.

[90] X Li, D Song and SX Leng. "Link between type 2 diabetes and Alzheimer's disease: from epidemiology to mechanism and treatment." In: *Clin Interv Aging* 10 (2015), pp. 549–60. DOI: 10.2147/CIA.S74042.

[91] C Geula et al. "Aging renders the brain vulnerable to amyloid beta-protein neurotoxicity." In: *Nat Med* 4.7 (1998), pp. 827–31.

[92] J Li, VN Uversky and AL Fink. "Effect of familial Parkinson's disease point mutations A30P and A53T on the structural properties, aggregation, and fibrillation of human alpha-synuclein." In: *Biochemistry* 40.38 (2001), pp. 11604–13.

[93] MG Krone et al. "Effects of familial Alzheimer's disease mutations on the folding nucleation of the amyloid beta-protein." In: *J Mol Biol* 381.1 (2008), pp. 221–8. DOI: 10.1016/j.jmb.2008.05.069.

[94] PP Mangione et al. "Structure, folding dynamics, and amyloidogenesis of D76N β2-microglobulin: roles of shear flow, hydrophobic surfaces, and α-crystallin." In: *J Biol Chem* 288.43 (2013), pp. 30917–30. DOI: 10.1074/jbc.M113.498857.

[95] S Olgiati et al. "Early-onset parkinsonism caused by alpha-synuclein gene triplication: Clinical and genetic findings in a novel family." In: *Parkinsonism Relat Disord* 21.8 (2015), pp. 981–6. DOI: 10.1016/j.parkreldis.2015.06.005.

[96] K Sleegers et al. "APP duplication is sufficient to cause early onset Alzheimer's dementia with cerebral amyloid angiopathy." In: *Brain* 129.Pt 11 (2006), pp. 2977–83.

[97] SF Banani et al. "Biomolecular condensates: organizers of cellular biochemistry." In: *Nat Rev Mol Cell Biol* 18.5 (2017), pp. 285–298. DOI: 10.1038/nrm.2017.7.

[98] S Wegmann et al. "Tau protein liquid-liquid phase separation can initiate tau aggregation." In: *EMBO J* 37.7 (2018).

[99] HT Orr and HY Zoghbi. "Trinucleotide repeat disorders." In: *Annu Rev Neurosci* 30 (2007), pp. 575–621.

[100] HC Fan et al. "Polyglutamine (PolyQ) diseases: genetics to treatments." In: *Cell Transplant* 23.4-5 (2014), pp. 441–58. DOI: 10.3727/096368914X678454.

[101] T Scheuermann et al. "Trinucleotide expansions leading to an extended poly-L-alanine segment in the poly (A) binding protein PABPN1 cause fibril formation." In: *Protein Sci* 12.12 (2003), pp. 2685–92.

[102] B Brais et al. "Short GCG expansions in the PABP2 gene cause oculopharyngeal muscular dystrophy." In: *Nat Genet* 18.2 (1998), pp. 164–7.

[103] RJ O'Brien and PC Wong. "Amyloid precursor protein processing and Alzheimer's disease." In: *Annu Rev Neurosci* 34 (2011), pp. 185–204. DOI: 10.1146/annurev-neuro-061010-113613.

[104] J Wiltfang et al. "Amyloid beta peptide ratio 42/40 but not A beta 42 correlates with phospho-Tau in patients with low- and high-CSF A beta 40 load." In: *J Neurochem* 101.4 (2007), pp. 1053–9.

[105] NA Ramella et al. "Human apolipoprotein A-I-derived amyloid: its association with atherosclerosis." In: *PLoS One* 6.7 (2011), e22532. DOI: 10.1371/journal.pone.0022532.

[106] E Stroo et al. "Cellular Regulation of Amyloid Formation in Aging and Disease." In: *Front Neurosci* 11 (2017), p. 64. DOI: 10.3389/fnins.2017.00064.

[107] J Ellis. "Proteins as molecular chaperones." In: *Nature* 328.6129 (1987), pp. 378–9.

[108] YE Kim et al. "Molecular chaperone functions in protein folding and proteostasis." In: *Annu Rev Biochem* 82 (2013), pp. 323–55. DOI: 10.1146/annurev-biochem-060208-092442.

[109] MP Mayer and B Bukau. "Hsp70 chaperones: cellular functions and molecular mechanism." In: *Cell Mol Life Sci* 62.6 (2005), pp. 670–84.

[110] EA Craig. "Hsp70 at the membrane: driving protein translocation." In: *BMC Biol* 16.1 (2018), p. 11. DOI: 10.1186/s12915-017-0474-3.

[111] AL Schwartz and A Ciechanover. "The ubiquitin-proteasome pathway and pathogenesis of human diseases." In: *Annu Rev Med* 50 (1999), pp. 57–74.

[112] FU Hartl, A Bracher and M Hayer-Hartl. "Molecular chaperones in protein folding and proteostasis." In: *Nature* 475.7356 (2011), pp. 324–32. DOI: 10.1038/nature10317.

[113] C Månsson et al. "DNAJB6 is a peptide-binding chaperone which can suppress amyloid fibrillation of polyglutamine peptides at substoichiometric molar ratios." In: *Cell Stress Chaperones* 19.2 (2014), pp. 227–39. DOI: 10.1007/s12192-013-0448-5.

[114] J Hageman et al. "A DNAJB chaperone subfamily with HDAC-dependent activities suppresses toxic protein aggregation." In: *Mol Cell* 37.3 (2010), pp. 355–69. DOI: 10.1016/j.molcel.2010.01.001.

[115] PK Auluck and NM Bonini. "Pharmacological prevention of Parkinson disease in Drosophila." In: *Nat Med* 8.11 (2002), pp. 1185–6.

[116] J Klucken et al. "Hsp70 Reduces alpha-Synuclein Aggregation and Toxicity." In: *J Biol Chem* 279.24 (2004), pp. 25497–502.

[117] TR Flower et al. "Heat shock prevents alpha-synuclein-induced apoptosis in a yeast model of Parkinson's disease." In: *J Mol Biol* 351.5 (2005), pp. 1081–100.

[118] MM Dedmon et al. "Heat shock protein 70 inhibits alpha-synuclein fibril formation via preferential binding to prefibrillar species." In: *J Biol Chem* 280.15 (2005), pp. 14733–40.

[119] A Pierce et al. "Over-expression of heat shock factor 1 phenocopies the effect of chronic inhibition of TOR by rapamycin and is sufficient to ameliorate Alzheimer's-like deficits in mice modeling the disease." In: *J Neurochem* 124.6 (2013), pp. 880–93. DOI: 10.1111/jnc.12080.

[120] V Kakkar et al. "Barcoding heat shock proteins to human diseases: looking beyond the heat shock response." In: *Dis Model Mech* 7.4 (2014), pp. 421–34. DOI: 10.1242/dmm.014563.

[121] PJ McLean et al. "Geldanamycin induces Hsp70 and prevents alpha-synuclein aggregation and toxicity in vitro." In: *Biochem Biophys Res Commun* 321.3 (2004), pp. 665–9.

[122] FA Aprile et al. "The molecular chaperones DNAJB6 and Hsp70 cooperate to suppress $\alpha$-synuclein aggregation." In: *Sci Rep* 7.1 (2017), p. 9039. DOI: 10.1038/s41598-017-08324-z.

[123] I Rivera et al. "Modulation of Alzheimer's amyloid β peptide oligomerization and toxicity by extracellular Hsp70." In: *Cell Stress Chaperones* 23.2 (2018), pp. 269–279. DOI: 10.1007/s12192-017-0839-0.

[124] PJ Muchowski et al. "Hsp70 and hsp40 chaperones can inhibit self-assembly of polyglutamine proteins into amyloid-like fibrils." In: *Proc Natl Acad Sci U S A* 97.14 (2000), pp. 7841–6.

[125] J Shorter. "The mammalian disaggregase machinery: Hsp110 synergizes with Hsp70 and Hsp40 to catalyze protein disaggregation and reactivation in a cell-free system." In: *PLoS One* 6.10 (2011), e26319. DOI: 10.1371/journal.pone.0026319.

[126] MP Torrente and J Shorter. "The metazoan protein disaggregase and amyloid depolymerase system: Hsp110, Hsp70, Hsp40, and small heat shock proteins." In: *Prion* 7.6 (2013), pp. 457–63.

[127] H Rampelt et al. "Metazoan Hsp70 machines use Hsp110 to power protein disaggregation." In: *EMBO J* 31.21 (2012), pp. 4221–35. DOI: 10.1038/emboj.2012.264.

[128] RU Mattoo et al. "Hsp110 is a bona fide chaperone using ATP to unfold stable misfolded polypeptides and reciprocally collaborate with Hsp70 to solubilize protein aggregates." In: *J Biol Chem* 288.29 (2013), pp. 21399–411. DOI: 10.1074/jbc.M113.479253.

[129] A Scior et al. "Complete suppression of Htt fibrilization and disaggregation of Htt fibrils by a trimeric chaperone complex." In: *EMBO J* 37.2 (2018), pp. 282–299. DOI: 10.15252/embj.201797212.

[130] S DiSalvo et al. "Dominant prion mutants induce curing through pathways that promote chaperone-mediated disaggregation." In: *Nat Struct Mol Biol* 18.4 (2011), pp. 486–92. DOI: 10.1038/nsmb.2031.

[131] DA Parsell et al. "Protein disaggregation mediated by heat-shock protein Hsp104." In: *Nature* 372.6505 (1994), pp. 475–8.

[132] J Shorter and S Lindquist. "Hsp104 catalyzes formation and elimination of self-replicating Sup35 prion conformers." In: *Science* 304.5678 (2004), pp. 1793–7.

[133] J Winkler et al. "Hsp70 targets Hsp100 chaperones to substrates for protein disaggregation and prion fragmentation." In: *J Cell Biol* 198.3 (2012), pp. 387–404. DOI: 10.1083/jcb.201201074.

[134] P Tessarz, A Mogk and B Bukau. "Substrate threading through the central pore of the Hsp104 chaperone as a common mechanism for protein disaggregation and prion propagation." In: *Mol Microbiol* 68.1 (2008), pp. 87–97. DOI: 10.1111/j.1365-2958.2008.06135.x.

[135] ME DeSantis et al. "Operational plasticity enables hsp104 to disaggregate diverse amyloid and nonamyloid clients." In: *Cell* 151.4 (2012), pp. 778–793. DOI: 10.1016/j.cell.2012.09.038.

[136] SS Cao and RJ Kaufman. "Unfolded protein response." In: *Curr Biol* 22.16 (2012), R622–6. DOI: 10.1016/j.cub.2012.07.004.

[137] M Schröder and RJ Kaufman. "The mammalian unfolded protein response." In: *Annu Rev Biochem* 74 (2005), pp. 739–89.

[138] Y Kozutsumi et al. "The presence of malfolded proteins in the endoplasmic reticulum signals the induction of glucose-regulated proteins." In: *Nature* 332.6163 (1988), pp. 462–4.

[139] HP Harding, Y Zhang and D Ron. "Protein translation and folding are coupled by an endoplasmic-reticulum-resident kinase." In: *Nature* 397.6716 (1999), pp. 271–4.

[140] KJ Travers et al. "Functional and genomic analyses reveal an essential coordination between the unfolded protein response and ER-associated degradation." In: *Cell* 101.3 (2000), pp. 249–58.

[141] M Halliday and GR Mallucci. "Review: Modulating the unfolded protein response to prevent neurodegeneration and enhance memory." In: *Neuropathol Appl Neurobiol* 41.4 (2015), pp. 414–27. DOI: 10.1111/nan.12211.

[142] JJ Hoozemans et al. "The unfolded protein response is activated in Alzheimer's disease." In: *Acta Neuropathol* 110.2 (2005), pp. 165–72.

[143] U Unterberger et al. "Endoplasmic reticulum stress features are prominent in Alzheimer disease but not in prion diseases in vivo." In: *J Neuropathol Exp Neurol* 65.4 (2006), pp. 348–57.

[144] JJ Hoozemans et al. "Activation of the unfolded protein response in Parkinson's disease." In: *Biochem Biophys Res Commun* 354.3 (2007), pp. 707–11.

[145] H Lee et al. "IRE1 plays an essential role in ER stress-mediated aggregation of mutant huntingtin via the inhibition of autophagy flux." In: *Hum Mol Genet* 21.1 (2012), pp. 101–14. DOI: 10.1093/hmg/ddr445.

[146] D Kaganovich, R Kopito and J Frydman. "Misfolded proteins partition between two distinct quality control compartments." In: *Nature* 454.7208 (2008), pp. 1088–95. DOI: 10.1038/nature07195.

[147] S Escusa-Toret, WI Vonk and J Frydman. "Spatial sequestration of misfolded proteins by a dynamic chaperone pathway enhances cellular fitness during stress." In: *Nat Cell Biol* 15.10 (2013), pp. 1231–43. DOI: 10.1038/ncb2838.

[148] JA Johnston, CL Ward and RR Kopito. "Aggresomes: a cellular response to misfolded proteins." In: *J Cell Biol* 143.7 (1998), pp. 1883–98.

[149] R Kumar, PP Nawroth and J Tyedmers. "Prion Aggregates Are Recruited to the Insoluble Protein Deposit (IPOD) via Myosin 2-Based Vesicular Transport." In: *PLoS Genet* 12.9 (2016), e1006324. DOI: 10.1371/journal.pgen.1006324.

[150] MA Rujano et al. "Polarised asymmetric inheritance of accumulated protein damage in higher eukaryotes." In: *PLoS Biol* 4.12 (2006), e417.

[151] A Ciechanover and YT Kwon. "Degradation of misfolded proteins in neurodegenerative diseases: therapeutic targets and strategies." In: *Exp Mol Med* 47 (2015), e147. DOI: 10.1038/emm.2014.117.

[152] A Ciechanover, A Orian and AL Schwartz. "Ubiquitin-mediated proteolysis: biological regulation via destruction." In: *Bioessays* 22.5 (2000), pp. 442–51.

[153] R Kiffin et al. "Activation of chaperone-mediated autophagy during oxidative stress." In: *Mol Biol Cell* 15.11 (2004), pp. 4829–40.

[154] C Rothenberg et al. "Ubiquilin functions in autophagy and is degraded by chaperone-mediated autophagy." In: *Hum Mol Genet* 19.16 (2010), pp. 3219–32. DOI: 10.1093/hmg/ddq231.

[155] H Koga and AM Cuervo. "Chaperone-mediated autophagy dysfunction in the pathogenesis of neurodegeneration." In: *Neurobiol Dis* 43.1 (2011), pp. 29–37. DOI: 10.1016/j.nbd.2010.07.006.

[156] L Alvarez-Erviti et al. "Chaperone-mediated autophagy markers in Parkinson disease brains." In: *Arch Neurol* 67.12 (2010), pp. 1464–72. DOI: 10.1001/archneurol.2010.198.

[157] KS McNaught and P Jenner. "Proteasomal function is impaired in substantia nigra in Parkinson's disease." In: *Neurosci Lett* 297.3 (2001), pp. 191–4.

[158] JS Park, DH Kim and SY Yoon. "Regulation of amyloid precursor protein processing by its KFERQ motif." In: *BMB Rep* 49.6 (2016), pp. 337–42.

[159] Y Wang et al. "Tau fragmentation, aggregation and clearance: the dual role of lysosomal processing." In: *Hum Mol Genet* 18.21 (2009), pp. 4153–70. DOI: 10.1093/hmg/ddp367.

[160] KS McNaught et al. "Systemic exposure to proteasome inhibitors causes a progressive model of Parkinson's disease." In: *Ann Neurol* 56.1 (2004), pp. 149–62.

[161] AH Schapira et al. "Proteasomal inhibition causes loss of nigral tyrosine hydroxylase neurons." In: *Ann Neurol* 60.2 (2006), pp. 253–5.

[162] F Chiti and CM Dobson. "Protein misfolding, functional amyloid, and human disease." In: *Annu Rev Biochem* 75 (2006), pp. 333–66.

[163] J Fargnoli et al. "Decreased expression of heat shock protein 70 mRNA and protein after heat treatment in cells of aged rats." In: *Proc Natl Acad Sci U S A* 87.2 (1990), pp. 846–50.

[164] MA Pahlavani et al. "The expression of heat shock protein 70 decreases with age in lymphocytes from rats and rhesus monkeys." In: *Exp Cell Res* 218.1 (1995), pp. 310–8.

[165] DM Hall et al. "Aging reduces adaptive capacity and stress protein expression in the liver after heat stress." In: *J Appl Physiol (1985)* 89.2 (2000), pp. 749–59.

[166] JE Nuss et al. "Decreased enzyme activities of chaperones PDI and BiP in aged mouse livers." In: *Biochem Biophys Res Commun* 365.2 (2008), pp. 355–61.

[167] JP Rabek, 3rd Boylston WH and J Papaconstantinou. "Carbonylation of ER chaperone proteins in aged mouse liver." In: *Biochem Biophys Res Commun* 305.3 (2003), pp. 566–72.

[168] N Naidoo et al. "Aging impairs the unfolded protein response to sleep deprivation and leads to proapoptotic signaling." In: *J Neurosci* 28.26 (2008), pp. 6539–48. DOI: 10.1523/JNEUROSCI.5685-07.2008.

[169] Y Ma and J Li. "Metabolic shifts during aging and pathology." In: *Compr Physiol* 5.2 (2015), pp. 667–86. DOI: 10.1002/cphy.c140041.

[170] P Ritz and G Berrut. "Mitochondrial function, energy expenditure, aging and insulin resistance." In: *Diabetes Metab* 31 Spec No 2 (2005), 5S67–5S73.

[171] S Kaushik and AM Cuervo. "Proteostasis and aging." In: *Nat Med* 21.12 (2015), pp. 1406–15. DOI: 10.1038/nm.4001.

[172] M Brehme et al. "A chaperome subnetwork safeguards proteostasis in aging and neurodegenerative disease." In: *Cell Rep* 9.3 (2014), pp. 1135–50. DOI: 10.1016/j.celrep.2014.09.042.

[173] M Paz Gavilán et al. "Cellular environment facilitates protein accumulation in aged rat hippocampus." In: *Neurobiol Aging* 27.7 (2006), pp. 973–82.

[174] RC Taylor and A Dillin. "XBP-1 is a cell-nonautonomous regulator of stress resistance and longevity." In: *Cell* 153.7 (2013), pp. 1435–47. DOI: 10.1016/j.cell.2013.05.042.

[175] LM de Lau and MM Breteler. "Epidemiology of Parkinson's disease." In: *Lancet Neurol* 5.6 (2006), pp. 525–35.

[176] J Parkinson. "An essay on the shaking palsy. 1817." In: *J Neuropsychiatry Clin Neurosci* 14.2 (2002), 223–36, discussion 222.

[177] CG Goetz. "The history of Parkinson's disease: early clinical descriptions and neurological therapies." In: *Cold Spring Harb Perspect Med* 1.1 (2011), a008862. DOI: 10.1101/cshperspect.a008862.

[178] WR Gibb and AJ Lees. "The relevance of the Lewy body to the pathogenesis of idiopathic Parkinson's disease." In: *J Neurol Neurosurg Psychiatry* 51.6 (1988), pp. 745–52.

[179] TK Khoo et al. "The spectrum of nonmotor symptoms in early Parkinson disease." In: *Neurology* 80.3 (2013), pp. 276–81. DOI: 10.1212/WNL.0b013e31827deb74.

[180] RB Postuma et al. "Identifying prodromal Parkinson's disease: pre-motor disorders in Parkinson's disease." In: *Mov Disord* 27.5 (2012), pp. 617–26. DOI: 10.1002/mds.24996.

[181] IG McKeith. "Consensus guidelines for the clinical and pathologic diagnosis of dementia with Lewy bodies (DLB): report of the Consortium on DLB International Workshop." In: *J Alzheimers Dis* 9.3 Suppl (2006), pp. 417–23.

[182] JM Fearnley and AJ Lees. "Ageing and Parkinson's disease: substantia nigra regional selectivity." In: *Brain* 114 ( Pt 5) (1991), pp. 2283–301.

[183] S Greffard et al. "Motor score of the Unified Parkinson Disease Rating Scale as a good predictor of Lewy body-associated neuronal loss in the substantia nigra." In: *Arch Neurol* 63.4 (2006), pp. 584–8.

[184] JH Kordower et al. "Disease duration and the integrity of the nigrostriatal system in Parkinson's disease." In: *Brain* 136.Pt 8 (2013), pp. 2419–31. DOI: 10.1093/brain/awt192.

[185] TJ Ferman and BF Boeve. "Dementia with Lewy bodies." In: *Neurol Clin* 25.3 (2007), pp. 741–60, vii.

[186] NP Visanji et al. "The prion hypothesis in Parkinson's disease: Braak to the future." In: *Acta Neuropathol Commun* 1 (2013), p. 2. DOI: 10.1186/2051-5960-1-2.

[187] H Braak et al. "Staging of brain pathology related to sporadic Parkinson's disease." In: *Neurobiol Aging* 24.2 (2003), pp. 197–211.

[188] DJ Irwin et al. "Neuropathologic substrates of Parkinson disease dementia." In: *Ann Neurol* 72.4 (2012), pp. 587–98. DOI: 10.1002/ana.23659.

[189] D Iacono et al. "Parkinson disease and incidental Lewy body disease: Just a question of time?" In: *Neurology* 85.19 (2015), pp. 1670–9. DOI: 10.1212/WNL.0000000000002102.

[190] JH Power, OL Barnes and F Chegini. "Lewy Bodies and the Mechanisms of Neuronal Cell Death in Parkinson's Disease and Dementia with Lewy Bodies." In: *Brain Pathol* 27.1 (2017), pp. 3–12. DOI: 10.1111/bpa.12344.

[191] MG Spillantini et al. "Alpha-synuclein in Lewy bodies." In: *Nature* 388.6645 (1997), pp. 839–40.

[192] MG Spillantini et al. "alpha-Synuclein in filamentous inclusions of Lewy bodies from Parkinson's disease and dementia with lewy bodies." In: *Proc Natl Acad Sci U S A* 95.11 (1998), pp. 6469–73.

[193] A Iwai et al. "The precursor protein of non-A beta component of Alzheimer's disease amyloid is a presynaptic protein of the central nervous system." In: *Neuron* 14.2 (1995), pp. 467–75.

[194] R Borghi et al. "Full length alpha-synuclein is present in cerebrospinal fluid from Parkinson's disease and normal subjects." In: *Neurosci Lett* 287.1 (2000), pp. 65–7.

[195] Jr Bussell R and D Eliezer. "A structural and functional role for 11-mer repeats in alpha-synuclein and other exchangeable lipid binding proteins." In: *J Mol Biol* 329.4 (2003), pp. 763–78.

[196] DL Fortin et al. "Lipid rafts mediate the synaptic localization of alpha-synuclein." In: *J Neurosci* 24.30 (2004), pp. 6715–23.

[197] L Maroteaux, JT Campanelli and RH Scheller. "Synuclein: a neuron-specific protein localized to the nucleus and presynaptic nerve terminal." In: *J Neurosci* 8.8 (1988), pp. 2804–15.

[198] BG Wilhelm et al. "Composition of isolated synaptic boutons reveals the amounts of vesicle trafficking proteins." In: *Science* 344.6187 (2014), pp. 1023–8. DOI: 10.1126/science.1252884.

[199] J Burré et al. "Alpha-synuclein promotes SNARE-complex assembly in vivo and in vitro." In: *Science* 329.5999 (2010), pp. 1663–7. DOI: 10.1126/science.1195227.

[200] DE Cabin et al. "Synaptic vesicle depletion correlates with attenuated synaptic responses to prolonged repetitive stimulation in mice lacking alpha-synuclein." In: *J Neurosci* 22.20 (2002), pp. 8797–807.

[201] VM Nemani et al. "Increased expression of alpha-synuclein reduces neurotransmitter release by inhibiting synaptic vesicle reclustering after endocytosis." In: *Neuron* 65.1 (2010), pp. 66–79. DOI: 10.1016/j.neuron.2009.12.023.

[202] DD Murphy et al. "Synucleins are developmentally expressed, and alpha-synuclein regulates the size of the presynaptic vesicular pool in primary hippocampal neurons." In: *J Neurosci* 20.9 (2000), pp. 3214–20.

[203] R Jahn and RH Scheller. "SNAREs–engines for membrane fusion." In: *Nat Rev Mol Cell Biol* 7.9 (2006), pp. 631–43.

[204] S Chandra et al. "Alpha-synuclein cooperates with CSPalpha in preventing neurodegeneration." In: *Cell* 123.3 (2005), pp. 383–96.

[205] J Burré, M Sharma and TC Südhof. "$\alpha$-Synuclein assembles into higher-order multimers upon membrane binding to promote SNARE complex formation." In: *Proc Natl Acad Sci U S A* 111.40 (2014), E4274–83. DOI: 10.1073/pnas.1416598111.

[206] W Zhou et al. "Overexpression of human alpha-synuclein causes dopamine neuron death in rat primary culture and immortalized mesencephalon-derived cells." In: *Brain Res* 866.1-2 (2000), pp. 33–43.

[207] Y Chu and JH Kordower. "Age-associated increases of alpha-synuclein in monkeys and humans are associated with nigrostriatal dopamine depletion: Is this the target for Parkinson's disease?" In: *Neurobiol Dis* 25.1 (2007), pp. 134–49.

[208] PH Weinreb et al. "NACP, a protein implicated in Alzheimer's disease and learning, is natively unfolded." In: *Biochemistry* 35.43 (1996), pp. 13709–15.

[209] D Eliezer et al. "Conformational properties of alpha-synuclein in its free and lipid-associated states." In: *J Mol Biol* 307.4 (2001), pp. 1061–73.

[210] WS Davidson et al. "Stabilization of alpha-synuclein secondary structure upon binding to synthetic membranes." In: *J Biol Chem* 273.16 (1998), pp. 9443–9.

[211] TS Ulmer et al. "Structure and dynamics of micelle-bound human alpha-synuclein." In: *J Biol Chem* 280.10 (2005), pp. 9595–603.

[212] T Bartels, JG Choi and DJ Selkoe. "$\alpha$-Synuclein occurs physiologically as a helically folded tetramer that resists aggregation." In: *Nature* 477.7362 (2011), pp. 107–10. DOI: 10.1038/nature10324.

[213] W Wang et al. "A soluble $\alpha$-synuclein construct forms a dynamic tetramer." In: *Proc Natl Acad Sci U S A* 108.43 (2011), pp. 17797–802. DOI: 10.1073/pnas.1113260108.

[214] U Dettmer et al. "In vivo cross-linking reveals principally oligomeric forms of $\alpha$-synuclein and β-synuclein in neurons and non-neural cells." In: *J Biol Chem* 288.9 (2013), pp. 6371–85. DOI: 10.1074/jbc.M112.403311.

[215] TK Kerppola. "Design and implementation of bimolecular fluorescence complementation (BiFC) assays for the visualization of protein interactions in living cells." In: *Nat Protoc* 1.3 (2006), pp. 1278–86.

[216] L Wang et al. "$\alpha$-synuclein multimers cluster synaptic vesicles and attenuate recycling." In: *Curr Biol* 24.19 (2014), pp. 2319–26. DOI: 10.1016/j.cub.2014.08.027.

[217] B Fauvet et al. "$\alpha$-Synuclein in central nervous system and from erythrocytes, mammalian cells, and Escherichia coli exists predominantly as disordered monomer." In: *J Biol Chem* 287.19 (2012), pp. 15345–64. DOI: 10.1074/jbc.M111.318949.

[218] FX Theillet et al. "Structural disorder of monomeric $\alpha$-synuclein persists in mammalian cells." In: *Nature* 530.7588 (2016), pp. 45–50. DOI: 10.1038/nature16531.

[219] U Dettmer et al. "KTKEGV repeat motifs are key mediators of normal $\alpha$-synuclein tetramerization: Their mutation causes excess monomers and neurotoxicity." In: *Proc Natl Acad Sci U S A* 112.31 (2015), pp. 9596–601. DOI: 10.1073/pnas.1505953112.

[220] P Ciryam et al. "Widespread aggregation and neurodegenerative diseases are associated with supersaturated proteins." In: *Cell Rep* 5.3 (2013), pp. 781–90. DOI: 10.1016/j.celrep.2013.09.043.

[221] C Galvagnion et al. "Lipid vesicles trigger $\alpha$-synuclein aggregation by stimulating primary nucleation." In: *Nat Chem Biol* 11.3 (2015), pp. 229–34. DOI: 10.1038/nchembio.1750.

[222] AM Cuervo et al. "Impaired degradation of mutant alpha-synuclein by chaperone-mediated autophagy." In: *Science* 305.5688 (2004), pp. 1292–5.

[223] M Xilouri et al. "Abberant alpha-synuclein confers toxicity to neurons in part through inhibition of chaperone-mediated autophagy." In: *PLoS One* 4.5 (2009), e5515. DOI: 10.1371/journal.pone.0005515.

[224] LC Serpell et al. "Fiber diffraction of synthetic alpha-synuclein filaments shows amyloid-like cross-beta conformation." In: *Proc Natl Acad Sci U S A* 97.9 (2000), pp. 4897–902.

[225] BI Giasson et al. "A hydrophobic stretch of 12 amino acid residues in the middle of alpha-synuclein is essential for filament assembly." In: *J Biol Chem* 276.4 (2001), pp. 2380–6.

[226] JT Jarrett and Jr Lansbury PT. "Amyloid fibril formation requires a chemically discriminating nucleation event: studies of an amyloidogenic sequence from the bacterial protein OsmB." In: *Biochemistry* 31.49 (1992), pp. 12345–52.

[227] AK Buell et al. "Solution conditions determine the relative importance of nucleation and growth processes in $\alpha$-synuclein aggregation." In: *Proc Natl Acad Sci U S A* 111.21 (2014), pp. 7671–6. DOI: 10.1073/pnas.1315346111.

[228] SJ Wood et al. "alpha-synuclein fibrillogenesis is nucleation-dependent. Implications for the pathogenesis of Parkinson's disease." In: *J Biol Chem* 274.28 (1999), pp. 19509–12.

[229] I Horvath et al. "Mechanisms of protein oligomerization: inhibitor of functional amyloids templates $\alpha$-synuclein fibrillation." In: *J Am Chem Soc* 134.7 (2012), pp. 3439–44. DOI: 10.1021/ja209829m.

[230] N Cremades et al. "Direct observation of the interconversion of normal and toxic forms of $\alpha$-synuclein." In: *Cell* 149.5 (2012), pp. 1048–59. DOI: 10.1016/j.cell.2012.03.037.

[231] KA Conway et al. "Acceleration of oligomerization, not fibrillization, is a shared property of both alpha-synuclein mutations linked to early-onset Parkinson's disease: implications for pathogenesis and therapy." In: *Proc Natl Acad Sci U S A* 97.2 (2000), pp. 571–6.

[232] B Li et al. "Cryo-EM of full-length $\alpha$-synuclein reveals fibril polymorphs with a common structural kernel." In: *Nat Commun* 9.1 (2018), p. 3609. DOI: 10.1038/s41467-018-05971-2.

[233] R Guerrero-Ferreira et al. "Cryo-EM structure of alpha-synuclein fibrils." In: *Elife* 7 (2018).

[234] R Guerrero-Ferreira et al. "Two new polymorphic structures of human full-length alpha-synuclein fibrils solved by cryo-electron microscopy." In: *Elife* 8 (2019).

[235] RA Crowther, SE Daniel and M Goedert. "Characterisation of isolated alpha-synuclein filaments from substantia nigra of Parkinson's disease brain." In: *Neurosci Lett* 292.2 (2000), pp. 128–30.

[236] T Strohäker et al. "Structural heterogeneity of $\alpha$-synuclein fibrils amplified from patient brain extracts." In: *Nat Commun* 10.1 (2019), p. 5535. DOI: 10.1038/s41467-019-13564-w.

[237] DA Scott et al. "A pathologic cascade leading to synaptic dysfunction in alpha-synuclein-induced neurodegeneration." In: *J Neurosci* 30.24 (2010), pp. 8083–95. DOI: 10.1523/JNEUROSCI.1091-10.2010.

[238] AA Cooper et al. "Alpha-synuclein blocks ER-Golgi traffic and Rab1 rescues neuron loss in Parkinson's models." In: *Science* 313.5785 (2006), pp. 324–8.

[239] E Colla et al. "Accumulation of toxic $\alpha$-synuclein oligomer within endoplasmic reticulum occurs in $\alpha$-synucleinopathy in vivo." In: *J Neurosci* 32.10 (2012), pp. 3301–5. DOI: 10.1523/JNEUROSCI.5368-11.2012.

[240] J Sikkema, JA de Bont and B Poolman. "Mechanisms of membrane toxicity of hydrocarbons." In: *Microbiol Rev* 59.2 (1995), pp. 201–22.

[241] SW Chen et al. "Structural characterization of toxic oligomers that are kinetically trapped during $\alpha$-synuclein fibril formation." In: *Proc Natl Acad Sci U S A* 112.16 (2015), E1994–2003. DOI: 10.1073/pnas.1421204112.

[242] MJ Volles et al. "Vesicle permeabilization by protofibrillar alpha-synuclein: implications for the pathogenesis and treatment of Parkinson's disease." In: *Biochemistry* 40.26 (2001), pp. 7812–9.

[243] B Winner et al. "In vivo demonstration that alpha-synuclein oligomers are toxic." In: *Proc Natl Acad Sci U S A* 108.10 (2011), pp. 4194–9. DOI: 10.1073/pnas.1100976108.

[244] KA Conway et al. "Kinetic stabilization of the alpha-synuclein protofibril by a dopamine-alpha-synuclein adduct." In: *Science* 294.5545 (2001), pp. 1346–9.

[245] L Pieri et al. "Fibrillar $\alpha$-synuclein and huntingtin exon 1 assemblies are toxic to the cells." In: *Biophys J* 102.12 (2012), pp. 2894–905. DOI: 10.1016/j.bpj.2012.04.050.

[246] WF Xue et al. "Fibril fragmentation enhances amyloid cytotoxicity." In: *J Biol Chem* 284.49 (2009), pp. 34272–82. DOI: 10.1074/jbc.M109.049809.

[247] L Bousset et al. "Structural and functional characterization of two alpha-synuclein strains." In: *Nat Commun* 4 (2013), p. 2575. DOI: 10.1038/ncomms3575.

[248] G Taschenberger et al. "Aggregation of $\alpha$Synuclein promotes progressive in vivo neurotoxicity in adult rat dopaminergic neurons." In: *Acta Neuropathol* 123.5 (2012), pp. 671–83. DOI: 10.1007/s00401-011-0926-8.

[249] DP Karpinar et al. "Pre-fibrillar alpha-synuclein variants with impaired beta-structure increase neurotoxicity in Parkinson's disease models." In: *EMBO J* 28.20 (2009), pp. 3256–68. DOI: 10.1038/emboj.2009.257.

[250] A Jan et al. "Abeta42 neurotoxicity is mediated by ongoing nucleated polymerization process rather than by discrete Abeta42 species." In: *J Biol Chem* 286.10 (2011), pp. 8585–96. DOI: 10.1074/jbc.M110.172411.

[251] JY Li et al. "Lewy bodies in grafted neurons in subjects with Parkinson's disease suggest host-to-graft disease propagation." In: *Nat Med* 14.5 (2008), pp. 501–3. DOI: 10.1038/nm1746.

[252] JH Kordower et al. "Lewy body-like pathology in long-term embryonic nigral transplants in Parkinson's disease." In: *Nat Med* 14.5 (2008), pp. 504–6. DOI: 10.1038/nm1747.

[253] P Desplats et al. "Inclusion formation and neuronal cell death through neuron-to-neuron transmission of alpha-synuclein." In: *Proc Natl Acad Sci U S A* 106.31 (2009), pp. 13010–5. DOI: 10.1073/pnas.0903691106.

[254] KC Luk et al. "Intracerebral inoculation of pathological $\alpha$-synuclein initiates a rapidly progressive neurodegenerative $\alpha$-synucleinopathy in mice." In: *J Exp Med* 209.5 (2012), pp. 975–86. DOI: 10.1084/jem.20112457.

[255] A Jang et al. "Non-classical exocytosis of alpha-synuclein is sensitive to folding states and promoted under stress conditions." In: *J Neurochem* 113.5 (2010), pp. 1263–74. DOI: 10.1111/j.1471-4159.2010.06695.x.

[256] L Alvarez-Erviti et al. "Lysosomal dysfunction increases exosome-mediated alpha-synuclein release and transmission." In: *Neurobiol Dis* 42.3 (2011), pp. 360–7. DOI: 10.1016/j.nbd.2011.01.029.

[257] E Emmanouilidou et al. "Cell-produced alpha-synuclein is secreted in a calcium-dependent manner by exosomes and impacts neuronal survival." In: *J Neurosci* 30.20 (2010), pp. 6838–51. DOI: 10.1523/JNEUROSCI.5699-09.2010.

[258] HJ Lee, S Patel and SJ Lee. "Intravesicular localization and exocytosis of alpha-synuclein and its aggregates." In: *J Neurosci* 25.25 (2005), pp. 6016–24.

[259] HJ Lee et al. "Assembly-dependent endocytosis and clearance of extracellular alpha-synuclein." In: *Int J Biochem Cell Biol* 40.9 (2008), pp. 1835–49. DOI: 10.1016/j.biocel.2008.01.017.

[260] X Mao et al. "Pathological $\alpha$-synuclein transmission initiated by binding lymphocyte-activation gene 3." In: *Science* 353.6307 (2016).

[261] S Abounit et al. "Tunneling nanotubes spread fibrillar $\alpha$-synuclein by intercellular trafficking of lysosomes." In: *EMBO J* 35.19 (2016), pp. 2120–2138.

[262] LA Volpicelli-Daley et al. "Exogenous $\alpha$-synuclein fibrils induce Lewy body pathology leading to synaptic dysfunction and neuron death." In: *Neuron* 72.1 (2011), pp. 57–71. DOI: 10.1016/j.neuron.2011.08.033.

[263] KC Luk et al. "Exogenous alpha-synuclein fibrils seed the formation of Lewy body-like intracellular inclusions in cultured cells." In: *Proc Natl Acad Sci U S A* 106.47 (2009), pp. 20051–6. DOI: 10.1073/pnas.0908005106.

[264] T Jakhria et al. " β2-microglobulin amyloid fibrils are nanoparticles that disrupt lysosomal membrane protein trafficking and inhibit protein degradation by lysosomes." In: *J Biol Chem* 289.52 (2014), pp. 35781–94. DOI: 10.1074/jbc.M114.586222.

[265] VC Wasinger et al. "Progress with gene-product mapping of the Mollicutes: Mycoplasma genitalium." In: *Electrophoresis* 16.7 (1995), pp. 1090–4.

[266] H Fujiwara et al. "alpha-Synuclein is phosphorylated in synucleinopathy lesions." In: *Nat Cell Biol* 4.2 (2002), pp. 160–4.

[267] YE Kim et al. "Soluble Oligomers of PolyQ-Expanded Huntingtin Target a Multiplicity of Key Cellular Factors." In: *Mol Cell* 63.6 (2016), pp. 951–64. DOI: PMID:27570076.

[268] T Ratovitski et al. "Huntingtin protein interactions altered by polyglutamine expansion as determined by quantitative proteomic analysis." In: *Cell Cycle* 11.10 (2012), pp. 2006–21. DOI: 10.4161/cc.20423.

[269] N Pappireddi, L Martin and M Wühr. "A Review on Quantitative Multiplexed Proteomics." In: *Chembiochem* 20.10 (2019), pp. 1210–1224. DOI: 10.1002/cbic.201800650.

[270] Y Zhang et al. "Protein analysis by shotgun/bottom-up proteomics." In: *Chem Rev* 113.4 (2013), pp. 2343–94. DOI: 10.1021/cr3003533.

[271] RL Gundry et al. "Preparation of proteins and peptides for mass spectrometry analysis in a bottom-up proteomics workflow." In: *Curr Protoc Mol Biol* Chapter 10 (2009), Unit10.25. DOI: 10.1002/0471142727.mb1025s88.

[272] JB Fenn et al. "Electrospray ionization for mass spectrometry of large biomolecules." In: *Science* 246.4926 (1989), pp. 64–71.

[273] J Muntel et al. "Abundance-based classifier for the prediction of mass spectrometric peptide detectability upon enrichment (PPA)." In: *Mol Cell Proteomics* 14.2 (2015), pp. 430–40. DOI: 10.1074/mcp.M114.044321.

[274] DF Hunt et al. "Protein sequencing by tandem mass spectrometry." In: *Proc Natl Acad Sci U S A* 83.17 (1986), pp. 6233–7.

[275] P Roepstorff and J Fohlman. "Proposal for a common nomenclature for sequence ions in mass spectra of peptides." In: *Biomed Mass Spectrom* 11.11 (1984), p. 601.

[276] JK Eng, AL McCormack and JR Yates. "An approach to correlate tandem mass spectral data of peptides with amino acid sequences in a protein database." In: *J Am Soc Mass Spectrom* 5.11 (1994), pp. 976–89. DOI: 10.1016/1044-0305.

[277] DN Perkins et al. "Probability-based protein identification by searching sequence databases using mass spectrometry data." In: *Electrophoresis* 20.18 (1999), pp. 3551–67.

[278] J Cox et al. "Andromeda: a peptide search engine integrated into the MaxQuant environment." In: *J Proteome Res* 10.4 (2011), pp. 1794–805. DOI: 10.1021/pr101065j.

[279] JK Eng, TA Jahan and MR Hoopmann. "Comet: an open-source MS/MS sequence database search tool." In: *Proteomics* 13.1 (2013), pp. 22–4. DOI: 10.1002/pmic.201200439.

[280] AI Nesvizhskii et al. "A statistical model for identifying proteins by tandem mass spectrometry." In: *Anal Chem* 75.17 (2003), pp. 4646–58.

[281] RD Voyksner and H Lee. "Investigating the use of an octupole ion guide for ion storage and high-pass mass filtering to improve the quantitative performance of electrospray ion trap mass spectrometry." In: *Rapid Commun Mass Spectrom* 13.14 (1999), pp. 1427–37.

[282] D Chelius and PV Bondarenko. "Quantitative profiling of proteins in complex mixtures using liquid chromatography and mass spectrometry." In: *J Proteome Res* 1.4 (2002), pp. 317–23.

[283] W Wang et al. "Quantification of proteins and metabolites by mass spectrometry without isotopic labeling or spiked standards." In: *Anal Chem* 75.18 (2003), pp. 4818–26.

[284] C Müller et al. "Ion suppression effects in liquid chromatography-electrospray-ionisation transport-region collision induced dissociation mass spectrometry with different serum extraction methods for systematic toxicological analysis with mass spectra libraries." In: *J Chromatogr B Analyt Technol Biomed Life Sci* 773.1 (2002), pp. 47–52.

[285] SA Gerber et al. "Absolute quantification of proteins and phosphoproteins from cell lysates by tandem MS." In: *Proc Natl Acad Sci U S A* 100.12 (2003), pp. 6940–5.

[286] C Ludwig et al. "Estimation of absolute protein quantities of unlabeled samples by selected reaction monitoring mass spectrometry." In: *Mol Cell Proteomics* 11.3 (2012), p. M111.013987. DOI: 10.1074/mcp.M111.013987.

[287] M Wühr et al. "Deep proteomics of the Xenopus laevis egg using an mRNA-derived reference database." In: *Curr Biol* 24.13 (2014), pp. 1467–1475. DOI: 10.1016/j.cub.2014.05.044.

[288] M Bantscheff et al. "Quantitative mass spectrometry in proteomics: a critical review." In: *Anal Bioanal Chem* 389.4 (2007), pp. 1017–31.

[289] PV Bondarenko, D Chelius and TA Shaler. "Identification and relative quantitation of protein mixtures by enzymatic digestion followed by capillary reversed-phase liquid chromatography-tandem mass spectrometry." In: *Anal Chem* 74.18 (2002), pp. 4741–9.

[290] MC Wiener et al. "Differential mass spectrometry: a label-free LC-MS method for finding significant differences in complex peptide and protein mixtures." In: *Anal Chem* 76.20 (2004), pp. 6085–96.

[291] RE Higgs et al. "Comprehensive label-free method for the relative quantification of proteins from biological samples." In: *J Proteome Res* 4.4 (2005), pp. 1442–50.

[292] MP Washburn, D Wolters and 3rd Yates JR. "Large-scale analysis of the yeast proteome by multidimensional protein identification technology." In: *Nat Biotechnol* 19.3 (2001), pp. 242–7.

[293] H Liu, RG Sadygov and 3rd Yates JR. "A model for random sampling and estimation of relative protein abundance in shotgun proteomics." In: *Anal Chem* 76.14 (2004), pp. 4193–201.

[294] MQ Dong et al. "Quantitative mass spectrometry identifies insulin signaling targets in C. elegans." In: *Science* 317.5838 (2007), pp. 660–3.

[295] B Zybailov et al. "Statistical analysis of membrane proteome expression changes in Saccharomyces cerevisiae." In: *J Proteome Res* 5.9 (2006), pp. 2339–47.

[296] M Stepath et al. "Systematic Comparison of Label-Free, SILAC, and TMT Techniques to Study Early Adaption toward Inhibition of EGFR Signaling in the Colorectal Cancer Cell Line DiFi." In: *J Proteome Res* 19.2 (2020), pp. 926–937. DOI: 10.1021/acs.jproteome.9b00701.

[297] DA Megger et al. "Comparison of label-free and label-based strategies for proteome analysis of hepatoma cell lines." In: *Biochim Biophys Acta* 1844.5 (2014), pp. 967–76. DOI: 10.1016/j.bbapap.2013.07.017.

[298] Z Li et al. "Systematic comparison of label-free, metabolic labeling, and isobaric chemical labeling for quantitative proteomics on LTQ Orbitrap Velos." In: *J Proteome Res* 11.3 (2012), pp. 1582–90. DOI: 10.1021/pr200748h.

[299] J Cox et al. "Accurate proteome-wide label-free quantification by delayed normalization and maximal peptide ratio extraction, termed MaxLFQ." In: *Mol Cell Proteomics* 13.9 (2014), pp. 2513–26. DOI: 10.1074/mcp.M113.031591.

[300] SE Ong et al. "Stable isotope labeling by amino acids in cell culture, SILAC, as a simple and accurate approach to expression proteomics." In: *Mol Cell Proteomics* 1.5 (2002), pp. 376–86.

[301] SP Gygi et al. "Quantitative analysis of complex protein mixtures using isotope-coded affinity tags." In: *Nat Biotechnol* 17.10 (1999), pp. 994–9.

[302] H Zhou et al. "Quantitative proteome analysis by solid-phase isotope tagging and mass spectrometry." In: *Nat Biotechnol* 20.5 (2002), pp. 512–5.

[303] AE Merrill et al. "NeuCode labels for relative protein quantification." In: *Mol Cell Proteomics* 13.9 (2014), pp. 2503–12. DOI: 10.1074/mcp.M114.040287.

[304] A Thompson et al. "Tandem mass tags: a novel quantification strategy for comparative analysis of complex protein mixtures by MS/MS." In: *Anal Chem* 75.8 (2003), pp. 1895–904.

[305] PL Ross et al. "Multiplexed protein quantitation in Saccharomyces cerevisiae using amine-reactive isobaric tagging reagents." In: *Mol Cell Proteomics* 3.12 (2004), pp. 1154–69.

[306] MK Lee et al. "Human alpha-synuclein-harboring familial Parkinson's disease-linked Ala-53; Thr mutation causes neurodegenerative disease with alpha-synuclein aggregation in transgenic mice." In: *Proc Natl Acad Sci U S A* 99.13 (2002), pp. 8968–73.

[307] BI Giasson et al. "Oxidative damage linked to neurodegeneration by selective alpha-synuclein nitration in synucleinopathy lesions." In: *Science* 290.5493 (2000), pp. 985–9.

[308] Y Liu et al. "A novel molecular mechanism for nitrated alpha-synuclein-induced cell death." In: *J Mol Cell Biol* 3.4 (2011), pp. 239–49. DOI: 10.1093/jmcb/mjr011.

[309] Z Yu et al. "Nitrated alpha-synuclein induces the loss of dopaminergic neurons in the substantia nigra of rats." In: *PLoS One* 5.4 (2010), e9956. DOI: 10.1371/journal.pone.0009956.

[310] Y Saito et al. "Accumulation of phosphorylated alpha-synuclein in aging human brain." In: *J Neuropathol Exp Neurol* 62.6 (2003), pp. 644–54.

[311] JF Kellie et al. "Quantitative measurement of intact alpha-synuclein proteoforms from post-mortem control and Parkinson's disease brain tissue by intact protein mass spectrometry." In: *Sci Rep* 4 (2014), p. 5797. DOI: 10.1038/srep05797.

[312] H Olzscha et al. "Amyloid-like aggregates sequester numerous metastable proteins with essential cellular functions." In: *Cell* 144.1 (2011), pp. 67–78. DOI: 10.1016/j.cell.2010.11.050.

[313] KF Winklhofer, J Tatzelt and C Haass. "The two faces of protein misfolding: gain- and loss-of-function in neurodegenerative diseases." In: *EMBO J* 27.2 (2008), pp. 336–49. DOI: 10.1038/sj.emboj.7601930.

[314] S Calabretta and S Richard. "Emerging Roles of Disordered Sequences in RNA-Binding Proteins." In: *Trends Biochem Sci* 40.11 (2015), pp. 662–672. DOI: 10.1016/j.tibs.2015.08.012.

[315] AC Woerner et al. "Cytoplasmic protein aggregates interfere with nucleocytoplasmic transport of protein and RNA." In: *Science* 351.6269 (2016), pp. 173–6. DOI: 10.1126/science.aad2033.

[316] AJ Williams and HL Paulson. "Polyglutamine neurodegeneration: protein misfolding revisited." In: *Trends Neurosci* 31.10 (2008), pp. 521–8. DOI: 10.1016/j.tins.2008.07.004.

[317] E Scherzinger et al. "Huntingtin-encoded polyglutamine expansions form amyloid-like protein aggregates in vitro and in vivo." In: *Cell* 90.3 (1997), pp. 549–58.

[318] S Chen, FA Ferrone and R Wetzel. "Huntington's disease age-of-onset linked to polyglutamine aggregation nucleation." In: *Proc Natl Acad Sci U S A* 99.18 (2002), pp. 11884–9.

[319] G Rigaut et al. "A generic protein purification method for protein complex characterization and proteome exploration." In: *Nat Biotechnol* 17.10 (1999), pp. 1030–2.

[320] DK Kim et al. "Molecular and functional signatures in a novel Alzheimer's disease mouse model assessed by quantitative proteomics." In: *Mol Neurodegener* 13.1 (2018), p. 2. DOI: 10.1186/s13024-017-0234-4.

[321] A Brückner et al. "Yeast two-hybrid, a powerful tool for systems biology." In: *Int J Mol Sci* 10.6 (2009), pp. 2763–88. DOI: 10.3390/ijms10062763.

[322] S Fields and O Song. "A novel genetic system to detect protein-protein interactions." In: *Nature* 340.6230 (1989), pp. 245–6. DOI: 10.1038/340245a0.

[323] B Popova et al. "Identification of Two Novel Peptides That Inhibit $\alpha$-Synuclein Toxicity and Aggregation." In: *Front Mol Neurosci* 14 (2021), p. 659926. DOI: 10.3389/fnmol.2021.659926.

[324] C Haenig et al. "Interactome Mapping Provides a Network of Neurodegenerative Disease Proteins and Uncovers Widespread Protein Aggregation in Affected Brains." In: *Cell Rep* 32.7 (2020), p. 108050. DOI: 10.1016/j.celrep.2020.108050.

[325] Yoav Benjamini and Yosef Hochberg. "Controlling the false discovery rate: a practical and powerful approach to multiple testing". In: *Journal of the Royal statistical society: series B (Methodological)* 57.1 (1995), pp. 289–300.

[326] S Maere, K Heymans and M Kuiper. "BiNGO: a Cytoscape plugin to assess overrepresentation of gene ontology categories in biological networks." In: *Bioinformatics* 21.16 (2005), pp. 3448–9.

[327] G Bindea et al. "ClueGO: a Cytoscape plug-in to decipher functionally grouped gene ontology and pathway annotation networks." In: *Bioinformatics* 25.8 (2009), pp. 1091–3. DOI: 10.1093/bioinformatics/btp101.

[328] P Sormanni, FA Aprile and M Vendruscolo. "The CamSol method of rational design of protein mutants with enhanced solubility." In: *J Mol Biol* 427.2 (2015), pp. 478–90. DOI: 10.1016/j.jmb.2014.09.026.

[329] PM Harrison. "fLPS: Fast discovery of compositional biases for the protein universe." In: *BMC Bioinformatics* 18.1 (2017), p. 476. DOI: PMID:29132292.

[330] M Iljina et al. "Kinetic model of the aggregation of alpha-synuclein provides insights into prion-like spreading." In: *Proc Natl Acad Sci U S A* 113.9 (2016), E1206–15. DOI: 10.1073/pnas.1524128113.

[331] W Hoyer et al. "Dependence of alpha-synuclein aggregate morphology on solution conditions." In: *J Mol Biol* 322.2 (2002), pp. 383–93.

[332] KM Danzer et al. "Different species of alpha-synuclein oligomers induce calcium influx and seeding." In: *J Neurosci* 27.34 (2007), pp. 9220–32.

[333] MHR Ludtmann et al. "$\alpha$-synuclein oligomers interact with ATP synthase and open the permeability transition pore in Parkinson's disease." In: *Nat Commun* 9.1 (2018), p. 2293. DOI: 10.1038/s41467-018-04422-2.

[334] J Narkiewicz, G Giachin and G Legname. "In vitro aggregation assays for the characterization of $\alpha$-synuclein prion-like properties." In: *Prion* 8.1 (2014), pp. 19–32.

[335] ME van Raaij et al. "Concentration dependence of alpha-synuclein fibril length assessed by quantitative atomic force microscopy and statistical-mechanical theory." In: *Biophys J* 95.10 (2008), pp. 4871–8. DOI: 10.1529/biophysj.107.127464.

[336] ET Powers and DL Powers. "The kinetics of nucleated polymerizations at high concentrations: amyloid fibril formation near and above the "supercritical concentration"." In: *Biophys J* 91.1 (2006), pp. 122–32.

[337] D Pinotsi et al. "Nanoscopic insights into seeding mechanisms and toxicity of $\alpha$-synuclein species in neurons." In: *Proc Natl Acad Sci U S A* 113.14 (2016), pp. 3815–9. DOI: 10.1073/pnas.1516546113.

[338] KA Conway, JD Harper and PT Lansbury. "Accelerated in vitro fibril formation by a mutant alpha-synuclein linked to early-onset Parkinson disease." In: *Nat Med* 4.11 (1998), pp. 1318–20.

[339] S Campioni et al. "The presence of an air-water interface affects formation and elongation of $\alpha$-Synuclein fibrils." In: *J Am Chem Soc* 136.7 (2014), pp. 2866–75. DOI: 10.1021/ja412105t.

[340] WF Xue and SE Radford. "An imaging and systems modeling approach to fibril breakage enables prediction of amyloid behavior." In: *Biophys J* 105.12 (2013), pp. 2811–9. DOI: 10.1016/j.bpj.2013.10.034.

[341] VV Shvadchak, MM Claessens and V Subramaniam. "Fibril breaking accelerates $\alpha$-synuclein fibrillization." In: *J Phys Chem B* 119.5 (2015), pp. 1912–8. DOI: 10.1021/jp5111604.

[342] D Pinotsi et al. "Direct observation of heterogeneous amyloid fibril growth kinetics via two-color super-resolution microscopy." In: *Nano Lett* 14.1 (2014), pp. 339–45. DOI: 10.1021/nl4041093.

[343] L Giehm and DE Otzen. "Strategies to increase the reproducibility of protein fibrillization in plate reader assays." In: *Anal Biochem* 400.2 (2010), pp. 270–81. DOI: 10.1016/j.ab.2010.02.001.

[344] VN Uversky, J Li and AL Fink. "Evidence for a partially folded intermediate in alpha-synuclein fibril formation." In: *J Biol Chem* 276.14 (2001), pp. 10737–44.

[345] JL Biedler, L Helson and BA Spengler. "Morphology and growth, tumorigenicity, and cytogenetics of human neuroblastoma cells in continuous culture." In: *Cancer Res* 33.11 (1973), pp. 2643–52.

[346] JL Biedler et al. "Multiple neurotransmitter synthesis by human neuroblastoma cell lines and clones." In: *Cancer Res* 38.11 Pt 1 (1978), pp. 3751–7.

[347] H Xicoy, B Wieringa and GJ Martens. "The SH-SY5Y cell line in Parkinson's disease research: a systematic review." In: *Mol Neurodegener* 12.1 (2017), p. 10. DOI: 10.1186/s13024-017-0149-0.

[348] RA Ross and JL Biedler. "Presence and regulation of tyrosinase activity in human neuroblastoma cell variants in vitro." In: *Cancer Res* 45.4 (1985), pp. 1628–32.

[349] A Krishna et al. "Systems genomics evaluation of the SH-SY5Y neuroblastoma cell line as a model for Parkinson's disease." In: *BMC Genomics* 15 (2014), p. 1154. DOI: 10.1186/1471-2164-15-1154.

[350] LA Volpicelli-Daley et al. "Formation of $\alpha$-synuclein Lewy neurite-like aggregates in axons impedes the transport of distinct endosomes." In: *Mol Biol Cell* 25.25 (2014), pp. 4010–23. DOI: 10.1091/mbc.E14-02-0741.

[351] BM Kohli et al. "Interactome of the amyloid precursor protein APP in brain reveals a protein network involved in synaptic vesicle turnover and a close association with Synaptotagmin-1." In: *J Proteome Res* 11.8 (2012), pp. 4075–90. DOI: 10.1021/pr300123g.

[352] PC Weber et al. "Structural origins of high-affinity biotin binding to streptavidin." In: *Science* 243.4887 (1989), pp. 85–8.

[353] A Makky et al. "Nanomechanical properties of distinct fibrillar polymorphs of the protein $\alpha$-synuclein." In: *Sci Rep* 6 (2016), p. 37970. DOI: 10.1038/srep37970.

[354] L Fernandes et al. "An ortho-Iminoquinone Compound Reacts with Lysine Inhibiting Aggregation while Remodeling Mature Amyloid Fibrils." In: *ACS Chem Neurosci* 8.8 (2017), pp. 1704–1712. DOI: 10.1021/acschemneuro.7b00017.

[355] MG Iadanza et al. "MpUL-multi: Software for Calculation of Amyloid Fibril Mass per Unit Length from TB-TEM Images." In: *Sci Rep* 6 (2016), p. 21078. DOI: 10.1038/srep21078.

[356] Y Li et al. "Amyloid fibril structure of $\alpha$-synuclein determined by cryo-electron microscopy." In: *Cell Res* 28.9 (2018), pp. 897–903. DOI: 10.1038/s41422-018-0075-x.

[357] W Li et al. "Aggregation promoting C-terminal truncation of alpha-synuclein is a normal cellular process and is enhanced by the familial Parkinson's disease-linked mutations." In: *Proc Natl Acad Sci U S A* 102.6 (2005), pp. 2162–7.

[358] E de Cecco and G Legname. "The role of the prion protein in the internalization of $\alpha$-synuclein amyloids." In: *Prion* 12.1 (2018), pp. 23–27. DOI: 10.1080/19336896.2017.1423186.

[359] S Aulić et al. "α-Synuclein Amyloids Hijack Prion Protein to Gain Cell Entry, Facilitate Cell-to-Cell Spreading and Block Prion Replication." In: *Sci Rep* 7.1 (2017), p. 10050. DOI: 10.1038/s41598-017-10236-x.

[360] AC Hoffmann et al. "Extracellular aggregated alpha synuclein primarily triggers lysosomal dysfunction in neural cells prevented by trehalose." In: *Sci Rep* 9.1 (2019), p. 544. DOI: 10.1038/s41598-018-35811-8.

[361] VV Shvadchak, K Afitska and DA Yushchenko. "Inhibition of α-Synuclein Amyloid Fibril Elongation by Blocking Fibril Ends." In: *Angew Chem Int Ed Engl* 57.20 (2018), pp. 5690–5694. DOI: 10.1002/anie.201801071.

[362] G Suzuki et al. "α-synuclein strains that cause distinct pathologies differentially inhibit proteasome." In: *Elife* 9 (2020).

[363] CL Masters et al. "Amyloid plaque core protein in Alzheimer disease and Down syndrome." In: *Proc Natl Acad Sci U S A* 82.12 (1985), pp. 4245–9.

[364] MH Polymeropoulos et al. "Mutation in the alpha-synuclein gene identified in families with Parkinson's disease." In: *Science* 276.5321 (1997), pp. 2045–7.

[365] AB Singleton et al. "alpha-Synuclein locus triplication causes Parkinson's disease." In: *Science* 302.5646 (2003), p. 841.

[366] JJ Zarranz et al. "The new mutation, E46K, of alpha-synuclein causes Parkinson and Lewy body dementia." In: *Ann Neurol* 55.2 (2004), pp. 164–73.

[367] K Lunnon et al. "Methylomic profiling implicates cortical deregulation of ANK1 in Alzheimer's disease." In: *Nat Neurosci* 17.9 (2014), pp. 1164–70. DOI: 10.1038/nn.3782.

[368] BW Kunkle et al. "Genetic meta-analysis of diagnosed Alzheimer's disease identifies new risk loci and implicates A β, tau, immunity and lipid processing." In: *Nat Genet* 51.3 (2019), pp. 414–430. DOI: 10.1038/s41588-019-0358-2.

[369] J Cox and M Mann. "Quantitative, high-resolution proteomics for data-driven systems biology." In: *Annu Rev Biochem* 80 (2011), pp. 273–99. DOI: 10.1146/annurev-biochem-061308-093216.

[370] NT Seyfried et al. "A Multi-network Approach Identifies Protein-Specific Co-expression in Asymptomatic and Symptomatic Alzheimer's Disease." In: *Cell Syst* 4.1 (2017), 60–72.e4. DOI: 10.1016/j.cels.2016.11.006.

[371] AL Mahul-Mellier et al. "The process of Lewy body formation, rather than simply α-synuclein fibrillization, is one of the major drivers of neurodegeneration." In: *Proc Natl Acad Sci U S A* 117.9 (2020), pp. 4971–4982. DOI: 10.1073/pnas.1913904117.

[372] ECB Johnson et al. "Deep proteomic network analysis of Alzheimer's disease brain reveals alterations in RNA binding proteins and RNA splicing associated with disease." In: *Mol Neurodegener* 13.1 (2018), p. 52. DOI: 10.1186/s13024-018-0282-4.

[373] CM Hales et al. "Changes in the detergent-insoluble brain proteome linked to amyloid and tau in Alzheimer's Disease progression." In: *Proteomics* 16.23 (2016), pp. 3042–3053. DOI: 10.1002/pmic.201600057.

[374] M Ashburner et al. "Gene ontology: tool for the unification of biology. The Gene Ontology Consortium." In: *Nat Genet* 25.1 (2000), pp. 25–9.

[375] Consortium. Gene Ontology. "The Gene Ontology resource: enriching a GOld mine." In: *Nucleic Acids Res* 49.D1 (2021), pp. D325–D334. DOI: 10.1093/nar/gkaa1113.

[376] B Snel et al. "STRING: a web-server to retrieve and display the repeatedly occurring neighbourhood of a gene." In: *Nucleic Acids Res* 28.18 (2000), pp. 3442–4.

[377] PD Thomas et al. "Applications for protein sequence-function evolution data: mRNA/protein expression analysis and coding SNP scoring tools." In: *Nucleic Acids Res* 34.Web Server issue (2006), W645–50.

[378] H Mi et al. "PANTHER version 14: more genomes, a new PANTHER GO-slim and improvements in enrichment analysis tools." In: *Nucleic Acids Res* 47.D1 (2019), pp. D419–D426. DOI: 10.1093/nar/gky1038.

[379] Jr Dennis G et al. "DAVID: Database for Annotation, Visualization, and Integrated Discovery." In: *Genome Biol* 4.5 (2003), P3.

[380] KG Calderón-González et al. "Bioinformatics Tools for Proteomics Data Interpretation." In: *Adv Exp Med Biol* 919 (2016), pp. 281–341.

[381] Consortium. Gene Ontology. "The Gene Ontology project in 2008." In: *Nucleic Acids Res* 36.Database issue (2008), pp. D440–4.

[382] M Kanehisa and S Goto. "KEGG: kyoto encyclopedia of genes and genomes." In: *Nucleic Acids Res* 28.1 (2000), pp. 27–30. DOI: 10.1093/nar/28.1.27.

[383] M Kanehisa. "Toward understanding the origin and evolution of cellular organisms." In: *Protein Sci* 28.11 (2019), pp. 1947–1951. DOI: 10.1002/pro.3715.

[384] M Kanehisa et al. "KEGG: integrating viruses and cellular organisms." In: *Nucleic Acids Res* 49.D1 (2021), pp. D545–D551. DOI: 10.1093/nar/gkaa970.

[385] Minoru Kanehisa. *Post-genome informatics*. OUP Oxford, 2000.

[386] D Szklarczyk et al. “STRING v11: protein-protein association networks with increased coverage, supporting functional discovery in genome-wide experimental datasets.” In: *Nucleic Acids Res* 47.D1 (2019), pp. D607–D613. DOI: 10.1093/nar/gky1131.

[387] J Barretina et al. “The Cancer Cell Line Encyclopedia enables predictive modelling of anticancer drug sensitivity.” In: *Nature* 483.7391 (2012), pp. 603–7. DOI: 10.1038/nature11003.

[388] Stijn Marinus Van Dongen. “Graph clustering by flow simulation”. PhD thesis. 2000.

[389] JB Leverenz et al. “Proteomic identification of novel proteins in cortical lewy bodies.” In: *Brain Pathol* 17.2 (2007), pp. 139–45.

[390] J Huerta-Cepas et al. “PhylomeDB v4: zooming into the plurality of evolutionary histories of a genome.” In: *Nucleic Acids Res* 42.Database issue (2014), pp. D897–902. DOI: 10.1093/nar/gkt1177.

[391] C Betzer et al. “Identification of synaptosomal proteins binding to monomeric and oligomeric $\alpha$-synuclein.” In: *PLoS One* 10.2 (2015), e0116473. DOI: 10.1371/journal.pone.0116473.

[392] AD Humphries et al. “Dissection of the mitochondrial import and assembly pathway for human Tom40.” In: *J Biol Chem* 280.12 (2005), pp. 11535–43.

[393] M Kato et al. “Cell-free formation of RNA granules: low complexity sequence domains form dynamic fibers within hydrogels.” In: *Cell* 149.4 (2012), pp. 753–67. DOI: 10.1016/j.cell.2012.04.017.

[394] A Patel et al. “A Liquid-to-Solid Phase Transition of the ALS Protein FUS Accelerated by Disease Mutation.” In: *Cell* 162.5 (2015), pp. 1066–77. DOI: 10.1016/j.cell.2015.07.047.

[395] GM Castillo et al. “The sulfate moieties of glycosaminoglycans are critical for the enhancement of beta-amyloid protein fibril formation.” In: *J Neurochem* 72.4 (1999), pp. 1681–7.

[396] GM Castillo et al. “Perlecan binds to the beta-amyloid proteins (A beta) of Alzheimer’s disease, accelerates A beta fibril formation, and maintains A beta fibril stability.” In: *J Neurochem* 69.6 (1997), pp. 2452–65.

[397] SL Cotman, W Halfter and GJ Cole. “Agrin binds to beta-amyloid (Abeta), accelerates abeta fibril formation, and is localized to Abeta deposits in Alzheimer’s disease brain.” In: *Mol Cell Neurosci* 15.2 (2000), pp. 183–98.

[398] SD Ginsberg et al. “RNA sequestration to pathological lesions of neurodegenerative diseases.” In: *Acta Neuropathol* 96.5 (1998), pp. 487–94.

[399] MA Bradley-Whitman et al. "Nucleic acid oxidation: an early feature of Alzheimer's disease." In: *J Neurochem* 128.2 (2014), pp. 294–304. DOI: 10.1111/jnc.12444.

[400] DJ Watson, AD Lander and DJ Selkoe. "Heparin-binding properties of the amyloidogenic peptides Abeta and amylin. Dependence on aggregation state and inhibition by Congo red." In: *J Biol Chem* 272.50 (1997), pp. 31617–24.

[401] S Jha et al. "Mechanism of amylin fibrillization enhancement by heparin." In: *J Biol Chem* 286.26 (2011), pp. 22894–904. DOI: 10.1074/jbc.M110.215814.

[402] S Bourgault et al. "Sulfated glycosaminoglycans accelerate transthyretin amyloidogenesis by quaternary structural conversion." In: *Biochemistry* 50.6 (2011), pp. 1001–15. DOI: 10.1021/bi101822y.

[403] AJ Borysik et al. "Specific glycosaminoglycans promote unseeded amyloid formation from beta2-microglobulin under physiological conditions." In: *Kidney Int* 72.2 (2007), pp. 174–81.

[404] M Goedert et al. "Assembly of microtubule-associated protein tau into Alzheimer-like filaments induced by sulphated glycosaminoglycans." In: *Nature* 383.6600 (1996), pp. 550–3.

[405] J McLaurin et al. "Interactions of Alzheimer amyloid-beta peptides with glycosaminoglycans effects on fibril nucleation and growth." In: *Eur J Biochem* 266.3 (1999), pp. 1101–10.

[406] Y Fichou et al. "Cofactors are essential constituents of stable and seeding-active tau fibrils." In: *Proc Natl Acad Sci U S A* 115.52 (2018), pp. 13234–13239. DOI: 10.1073/pnas.1810058115.

[407] FJB Bäuerlein et al. "In Situ Architecture and Cellular Interactions of PolyQ Inclusions." In: *Cell* 171.1 (2017), 179–187.e10. DOI: 10.1016/j.cell.2017.08.009.

[408] E Mutez et al. "Involvement of the immune system, endocytosis and EIF2 signaling in both genetically determined and sporadic forms of Parkinson's disease." In: *Neurobiol Dis* 63 (2014), pp. 165–70. DOI: 10.1016/j.nbd.2013.11.007.

[409] JA Moreno et al. "Sustained translational repression by eIF2$\alpha$-P mediates prion neurodegeneration." In: *Nature* 485.7399 (2012), pp. 507–11. DOI: 10.1038/nature11058.

[410] A Jan et al. "Activity of translation regulator eukaryotic elongation factor-2 kinase is increased in Parkinson disease brain and its inhibition reduces alpha synuclein toxicity." In: *Acta Neuropathol Commun* 6.1 (2018), p. 54. DOI: 10.1186/s40478-018-0554-9.

[411] J Creus-Muncunill et al. "Increased translation as a novel pathogenic mechanism in Huntington's disease." In: *Brain* 142.10 (2019), pp. 3158–3175. DOI: 10.1093/brain/awz230.

[412] CG Gkogkas et al. "Autism-related deficits via dysregulated eIF4E-dependent translational control." In: *Nature* 493.7432 (2013), pp. 371–7. DOI: 10.1038/nature11628.

[413] SG Dastidar et al. "4E-BP1 Protects Neurons from Misfolded Protein Stress and Parkinson's Disease Toxicity by Inducing the Mitochondrial Unfolded Protein Response." In: *J Neurosci* 40.45 (2020), pp. 8734–8745. DOI: 10.1523/JNEUROSCI.0940-20.2020.

[414] I Martin et al. "Ribosomal protein s15 phosphorylation mediates LRRK2 neurodegeneration in Parkinson's disease." In: *Cell* 157.2 (2014), pp. 472–485. DOI: 10.1016/j.cell.2014.01.064.

[415] P Deshpande et al. "Protein synthesis is suppressed in sporadic and familial Parkinson's disease by LRRK2." In: *FASEB J* 34.11 (2020), pp. 14217–14233. DOI: 10.1096/fj.202001046R.

[416] S Banerjee et al. "Tau protein- induced sequestration of the eukaryotic ribosome: Implications in neurodegenerative disease." In: *Sci Rep* 10.1 (2020), p. 5225. DOI: 10.1038/s41598-020-61777-7.

[417] AE Dahlberg. "The functional role of ribosomal RNA in protein synthesis." In: *Cell* 57.4 (1989), pp. 525–9.

[418] SJ Watkins and CJ Norbury. "Translation initiation and its deregulation during tumorigenesis." In: *Br J Cancer* 86.7 (2002), pp. 1023–7.

[419] M Sokabe and CS Fraser. "Human eukaryotic initiation factor 2 (eIF2)-GTP-Met-tRNAi ternary complex and eIF3 stabilize the 43 S preinitiation complex." In: *J Biol Chem* 289.46 (2014), pp. 31827–36. DOI: 10.1074/jbc.M114.602870.

[420] D Brina et al. "Translational control by 80S formation and 60S availability: the central role of eIF6, a rate limiting factor in cell cycle progression and tumorigenesis." In: *Cell Cycle* 10.20 (2011), pp. 3441–6. DOI: 10.4161/cc.10.20.17796.

[421] G Kaul, G Pattan and T Rafeequi. "Eukaryotic elongation factor-2 (eEF2): its regulation and peptide chain elongation." In: *Cell Biochem Funct* 29.3 (2011), pp. 227–34. DOI: 10.1002/cbf.1740.

[422] J Frank et al. "The process of mRNA-tRNA translocation." In: *Proc Natl Acad Sci U S A* 104.50 (2007), pp. 19671–8.

[423] EM Rocha, B de Miranda and LH Sanders. "Alpha-synuclein: Pathology, mitochondrial dysfunction and neuroinflammation in Parkinson's disease." In: *Neurobiol Dis* 109.Pt B (2018), pp. 249–257. DOI: 10.1016/j.nbd.2017.04.004.

[424] AH Schapira et al. "Mitochondrial complex I deficiency in Parkinson's disease." In: *J Neurochem* 54.3 (1990), pp. 823–7.

[425] Jr Parker WD, SJ Boyson and JK Parks. "Abnormalities of the electron transport chain in idiopathic Parkinson's disease." In: *Ann Neurol* 26.6 (1989), pp. 719–23.

[426] R Betarbet et al. "Chronic systemic pesticide exposure reproduces features of Parkinson's disease." In: *Nat Neurosci* 3.12 (2000), pp. 1301–6.

[427] Y Kotake and S Ohta. "MPP+ analogs acting on mitochondria and inducing neuro-degeneration." In: *Curr Med Chem* 10.23 (2003), pp. 2507–16.

[428] SJ Chinta et al. "Mitochondrial $\alpha$-synuclein accumulation impairs complex I function in dopaminergic neurons and results in increased mitophagy in vivo." In: *Neurosci Lett* 486.3 (2010), pp. 235–9. DOI: 10.1016/j.neulet.2010.09.061.

[429] L Devi et al. "Mitochondrial import and accumulation of alpha-synuclein impair complex I in human dopaminergic neuronal cultures and Parkinson disease brain." In: *J Biol Chem* 283.14 (2008), pp. 9089–100. DOI: 10.1074/jbc.M710012200.

[430] D Grassi et al. "Identification of a highly neurotoxic $\alpha$-synuclein species inducing mitochondrial damage and mitophagy in Parkinson's disease." In: *Proc Natl Acad Sci U S A* 115.11 (2018), E2634–E2643. DOI: 10.1073/pnas.1713849115.

[431] ES Luth et al. "Soluble, prefibrillar $\alpha$-synuclein oligomers promote complex I-dependent, Ca2+-induced mitochondrial dysfunction." In: *J Biol Chem* 289.31 (2014), pp. 21490–507. DOI: 10.1074/jbc.M113.545749.

[432] A Bender et al. "TOM40 mediates mitochondrial dysfunction induced by $\alpha$-synuclein accumulation in Parkinson's disease." In: *PLoS One* 8.4 (2013), e62277. DOI: 10.1371/journal.pone.0062277.

[433] R Di Maio et al. "α-Synuclein binds to TOM20 and inhibits mitochondrial protein import in Parkinson's disease." In: *Sci Transl Med* 8.342 (2016), 342ra78. DOI: 10.1126/scitranslmed.aaf3634.

[434] H Yano et al. "Inhibition of mitochondrial protein import by mutant huntingtin." In: *Nat Neurosci* 17.6 (2014), pp. 822–31. DOI: 10.1038/nn.3721.

[435] BV Dieriks et al. "α-synuclein transfer through tunneling nanotubes occurs in SH-SY5Y cells and primary brain pericytes from Parkinson's disease patients." In: *Sci Rep* 7 (2017), p. 42984. DOI: 10.1038/srep42984.

[436] S Tortorella and TC Karagiannis. "Transferrin receptor-mediated endocytosis: a useful target for cancer therapy." In: *J Membr Biol* 247.4 (2014), pp. 291–307. DOI: 10.1007/s00232-014-9637-0.

[437] BB Holmes et al. "Heparan sulfate proteoglycans mediate internalization and propagation of specific proteopathic seeds." In: *Proc Natl Acad Sci U S A* 110.33 (2013), E3138–47. DOI: 10.1073/pnas.1301440110.

[438] RJ Jr Karpowicz et al. "Selective imaging of internalized proteopathic α-synuclein seeds in primary neurons reveals mechanistic insight into transmission of synucleinopathies." In: *J Biol Chem* 292.32 (2017), pp. 13482–13497. DOI: 10.1074/jbc.M117.780296.

[439] TE Hansen and T Johansen. "Following autophagy step by step." In: *BMC Biol* 9 (2011), p. 39. DOI: 10.1186/1741-7007-9-39.

[440] P Jiang et al. "Impaired endo-lysosomal membrane integrity accelerates the seeding progression of α-synuclein aggregates." In: *Sci Rep* 7.1 (2017), p. 7690. DOI: 10.1038/s41598-017-08149-w.

[441] D Freeman et al. "Alpha-synuclein induces lysosomal rupture and cathepsin dependent reactive oxygen species following endocytosis." In: *PLoS One* 8.4 (2013), e62143. DOI: 10.1371/journal.pone.0062143.

[442] AL Mahul-Mellier et al. "Fibril growth and seeding capacity play key roles in α-synuclein-mediated apoptotic cell death." In: *Cell Death Differ* 22.12 (2015), pp. 2107–22. DOI: 10.1038/cdd.2015.79.

[443] SJ Rodman and A Wandinger-Ness. "Rab GTPases coordinate endocytosis." In: *J Cell Sci* 113 Pt 2 (2000), pp. 183–92.

[444] MF López-Aranda et al. "Role of a Galphai2 protein splice variant in the formation of an intracellular dopamine D2 receptor pool." In: *J Cell Sci* 120.Pt 13 (2007), pp. 2171–8. DOI: 10.1242/jcs.005611.

[445] "UniProt: The universal protein knowledgebase in 2021". In: *Nucleic Acids Research* 49.D1 (2021), pp. D480–D489.

[446] JB Pereira-Leal and MC Seabra. "Evolution of the Rab family of small GTP-binding proteins." In: *J Mol Biol* 313.4 (2001), pp. 889–901. DOI: 10.1006/jmbi.2001.5072.

[447] B Binotti, R Jahn and JJ Chua. "Functions of Rab Proteins at Presynaptic Sites." In: *Cells* 5.1 (2016). DOI: 10.3390/cells5010007.

[448] AH Hutagalung and PJ Novick. "Role of Rab GTPases in membrane traffic and cell physiology." In: *Physiol Rev* 91.1 (2011), pp. 119–49. DOI: 10.1152/physrev.00059.2009.

[449] I Kouranti et al. "Rab35 regulates an endocytic recycling pathway essential for the terminal steps of cytokinesis." In: *Curr Biol* 16.17 (2006), pp. 1719–25. DOI: 10.1016/j.cub.2006.07.020.

[450] C Bucci et al. "Rab7: a key to lysosome biogenesis." In: *Mol Biol Cell* 11.2 (2000), pp. 467–80. DOI: 10.1091/mbc.11.2.467.

[451] C Bucci et al. "The small GTPase rab5 functions as a regulatory factor in the early endocytic pathway." In: *Cell* 70.5 (1992), pp. 715–28. DOI: 10.1016/0092-8674(92)90306-w.

[452] H McLauchlan et al. "A novel role for Rab5-GDI in ligand sequestration into clathrin-coated pits." In: *Curr Biol* 8.1 (1998), pp. 34–45. DOI: 10.1016/s0960-9822(98)70018-1.

[453] K Klinkert and A Echard. "Rab35 GTPase: A Central Regulator of Phosphoinositides and F-actin in Endocytic Recycling and Beyond." In: *Traffic* 17.10 (2016), pp. 1063–77. DOI: 10.1111/tra.12422.

[454] JS Bonifacino and BS Glick. "The mechanisms of vesicle budding and fusion." In: *Cell* 116.2 (2004), pp. 153–66. DOI: 10.1016/s0092-8674(03)01079-1.

[455] MC Lee et al. "Bi-directional protein transport between the ER and Golgi." In: *Annu Rev Cell Dev Biol* 20 (2004), pp. 87–123. DOI: 10.1146/annurev.cellbio.20.010403.105307.

[456] P Lőrincz et al. "Rab2 promotes autophagic and endocytic lysosomal degradation." In: *J Cell Biol* 216.7 (2017), pp. 1937–1947. DOI: 10.1083/jcb.201611027.

[457] OM Schlüter et al. "Rab3 superprimes synaptic vesicles for release: implications for short-term synaptic plasticity." In: *J Neurosci* 26.4 (2006), pp. 1239–46. DOI: 10.1523/JNEUROSCI.3553-05.2006.

[458] FR Kiral et al. "Rab GTPases and Membrane Trafficking in Neurodegeneration." In: *Curr Biol* 28.8 (2018), R471–R486. DOI: 10.1016/j.cub.2018.02.010.

[459] MM Shi, CH Shi and YM Xu. "Rab GTPases: The Key Players in the Molecular Pathway of Parkinson's Disease." In: *Front Cell Neurosci* 11 (2017), p. 81. DOI: 10.3389/fncel.2017.00081.

[460] CC Chiu et al. "Increased Rab35 expression is a potential biomarker and implicated in the pathogenesis of Parkinson's disease." In: *Oncotarget* 7.34 (2016), pp. 54215–54227. DOI: 10.18632/oncotarget.11090.

[461] C Masaracchia et al. "Membrane binding, internalization, and sorting of alpha-synuclein in the cell." In: *Acta Neuropathol Commun* 6.1 (2018), p. 79. DOI: 10.1186/s40478-018-0578-1.

[462] RHC Chen et al. "$\alpha$-Synuclein membrane association is regulated by the Rab3a recycling machinery and presynaptic activity." In: *J Biol Chem* 288.11 (2013), pp. 7438–7449. DOI: 10.1074/jbc.M112.439497.

[463] SR Wente and MP Rout. "The nuclear pore complex and nuclear transport." In: *Cold Spring Harb Perspect Biol* 2.10 (2010), a000562. DOI: 10.1101/cshperspect.a000562.

[464] A Kulkarni and DM 3rd Wilson. "The involvement of DNA-damage and -repair defects in neurological dysfunction." In: *Am J Hum Genet* 82.3 (2008), pp. 539–66. DOI: 10.1016/j.ajhg.2008.01.009.

[465] JH Hoeijmakers. "DNA damage, aging, and cancer." In: *N Engl J Med* 361.15 (2009), pp. 1475–85. DOI: 10.1056/NEJMra0804615.

[466] G Bitetto and Fonzo A Di. "Nucleo-cytoplasmic transport defects and protein aggregates in neurodegeneration." In: *Transl Neurodegener* 9.1 (2020), p. 25. DOI: 10.1186/s40035-020-00205-2.

[467] K Weis. "Regulating access to the genome: nucleocytoplasmic transport throughout the cell cycle." In: *Cell* 112.4 (2003), pp. 441–51. DOI: 10.1016/s0092-8674(03)00082-5.

[468] H Cheng et al. "Human mRNA export machinery recruited to the 5' end of mRNA." In: *Cell* 127.7 (2006), pp. 1389–400. DOI: 10.1016/j.cell.2006.10.044.

[469] CC Chou et al. "TDP-43 pathology disrupts nuclear pore complexes and nucleocytoplasmic transport in ALS/FTD." In: *Nat Neurosci* 21.2 (2018), pp. 228–239. DOI: 10.1038/s41593-017-0047-3.

[470] JC Grima et al. "Mutant Huntingtin Disrupts the Nuclear Pore Complex." In: *Neuron* 94.1 (2017), 93–107.e6. DOI: 10.1016/j.neuron.2017.03.023.

[471] J Cornett et al. "Polyglutamine expansion of huntingtin impairs its nuclear export." In: *Nat Genet* 37.2 (2005), pp. 198–204. DOI: 10.1038/ng1503.

[472] S Hunot et al. "Nuclear translocation of NF-kappaB is increased in dopaminergic neurons of patients with parkinson disease." In: *Proc Natl Acad Sci U S A* 94.14 (1997), pp. 7531–6. DOI: 10.1073/pnas.94.14.7531.

[473] EM Chalovich et al. "Functional repression of cAMP response element in 6-hydroxydopamine-treated neuronal cells." In: *J Biol Chem* 281.26 (2006), pp. 17870–81. DOI: 10.1074/jbc.M602632200.

[474] E Kontopoulos, JD Parvin and MB Feany. "Alpha-synuclein acts in the nucleus to inhibit histone acetylation and promote neurotoxicity." In: *Hum Mol Genet* 15.20 (2006), pp. 3012–23. DOI: 10.1093/hmg/ddl243.

[475] Seungjin Ryu, Inkyung Baek and Hyunjeong Liew. "Sumoylated $\alpha$-synuclein translocates into the nucleus by karyopherin $\alpha$6". In: *Molecular & Cellular Toxicology* 15.1 (2019), pp. 103–109.

[476] WM Rosencrans et al. "$\alpha$-Synuclein emerges as a potent regulator of VDAC-facilitated calcium transport." In: *Cell Calcium* 95 (2021), p. 102355. DOI: 10.1016/j.ceca.2021.102355.

[477] T Rostovtseva and M Colombini. "ATP flux is controlled by a voltage-gated channel from the mitochondrial outer membrane." In: *J Biol Chem* 271.45 (1996), pp. 28006–8. DOI: 10.1074/jbc.271.45.28006.

[478] TK Rostovtseva et al. "$\alpha$-Synuclein Shows High Affinity Interaction with Voltage-dependent Anion Channel, Suggesting Mechanisms of Mitochondrial Regulation and Toxicity in Parkinson Disease." In: *J Biol Chem* 290.30 (2015), pp. 18467–77. DOI: 10.1074/jbc.M115.641746.

[479] J Saraste. "Spatial and Functional Aspects of ER-Golgi Rabs and Tethers." In: *Front Cell Dev Biol* 4 (2016), p. 28. DOI: 10.3389/fcell.2016.00028.

[480] PK Mishra et al. "Photo-crosslinking: An Emerging Chemical Tool for Investigating Molecular Networks in Live Cells." In: *Chembiochem* 21.7 (2020), pp. 924–932. DOI: 10.1002/cbic.201900600.

[481] JE Horne et al. "Rapid Mapping of Protein Interactions Using Tag-Transfer Photocrosslinkers." In: *Angew Chem Int Ed Engl* 57.51 (2018), pp. 16688–16692. DOI: 10.1002/anie.201809149.